HYDROGEOLOGY, SIMULATED GROUND-WATER FLOW, AND GROUND-WATER QUALITY, WRIGHT-PATTERSON AIR FORCE BASE, OHIO

By Denise H. Dumouchelle, Charles W. Schalk, Gary L. Rowe, and Jeffery T. de Roche

U.S. GEOLOGICAL SURVEY
Water-Resources Investigations Report 93-4047

Prepared in Cooperation with
WRIGHT-PATTERSON AIR FORCE BASE

Columbus, Ohio
1993

U. S. DEPARTMENT OF THE INTERIOR

BRUCE BABBIT, Secretary

U.S. GEOLOGICAL SURVEY

Dallas L. Peck, Director

For additional information
write to:

District Chief
Water Resources Division
U.S. Geological Survey
975 W. Third Avenue
Columbus, OH 43212-3192

Copies of this report can
be purchased from:

U.S. Geological Survey
Books and Open-File Reports
Section
Box 25425
Denver Federal Center
Denver, CO 80225

CONTENTS

CONTENTS--Continued

ILLUSTRATIONS

ILLUSTRATIONS--Continued

ILLUSTRATIONS--Continued

TABLES

CONVERSION FACTORS, VERTICAL DATUM, AND ABBREVIATED WATER-QUALITY UNITS

Multiply	By	To obtain
	Length	
inch (in.)	25.4	millimeter
foot (ft)	0.3048	meter
mile (mi)	1.609	kilometer
	Area	
square foot (ft^2)	0.09290	square meter
square mile (mi^2)	2.590	square kilometer
acre	0.4047	square hectometer
	Volume	
gallon (gal)	3.785	liter
	Flow	
cubic foot per second (ft^3/s)	0.02832	cubic meter per second
gallon per day (gal/d)	3.785	liter per day
gallon per day per mile [(gal/d)/mi]	2.352	liter per day per kilometer
million gallons per day (Mgal/d)	0.04381	cubic meter per second
	Rate of accumulation	
inch per hour (in/h)	25.4	millimeter per hour
inch per year (in/yr)	25.4	millimeter per year
	Slope	
foot per mile (ft/mi)	0.1894	meter per kilometer
	Hydraulic conductivity	
foot per day (ft/d)	0.3048	meter per day
	Transmissivity	
foot squared per day (ft^2/d)	0.09290	meter squared per day

Temperature is given in degrees Celsius (°C), which can be converted to degrees Fahrenheit (°F) by use of the following equation:

$$F = 1.8(°C) + 32$$

Sea level: In this report "sea level" refers to the National Geodetic Vertical Datum of 1929 (NGVD of 1929)—a geodetic datum derived from a general adjustment of the first-order level nets of both the United States and Canada, formerly called Sea Level Datum of 1929.

Abbreviated water-quality units used in this report: Chemical concentration is given in milligrams per liter (mg/L). This unit expresses the concentration of chemical constituents in solution as weight (milligrams) of solute per unit volume (liter) of solvent (water). For concentrations less than 7,000 mg/L, the numerical value is the same as for concentrations in parts per million. Concentration of tritium, a radioisotope of hydrogen, is given in tritium units (TU). Volumes of water-quality samples are given in liters (L) or milliliters (mL). Pore sizes of membrane filters are given in micrometers (µm).

Specific conductance of water is expressed in microsiemens per centimeter at 25 degrees Celsius (µS/cm). This unit is equivalent to micromhos per centimeter at 25 degrees Celsius (µmho/cm), formerly used by the U.S. Geological Survey.

Hydrogeology, Simulated Ground-Water Flow, and Ground-Water Quality, Wright-Patterson Air Force Base, Ohio

By Denise H. Dumouchelle, Charles W. Schalk, Gary L. Rowe, and Jeffrey T. de Roche

ABSTRACT

Ground water is the primary source of water in the Wright-Patterson Air Force Base area. The aquifer consists of glacial sands and gravels that fill a buried bedrock-valley system. Consolidated rocks in the area consist of poorly permeable Ordovician shales of the Richmondian stage, in the upland areas, the Brassfield Limestone of Silurian age. The valleys are filled with glacial sediments of Wisconsinan age consisting of clay-rich tills and coarse-grained outwash deposits. Estimates of hydraulic conductivity of the shales based on results of displacement/recovery tests range from 0.0016 to 12 feet per day; estimates for the glacial sediments range from less than 1 foot per day to more than 1,000 feet per day.

Ground water flows from the uplands towards the valleys and the major rivers in the region, the Great Miami and the Mad Rivers. Hydraulic-head data indicate that ground water flows between the bedrock and unconsolidated deposits; however, the volume of water is negligible compared to flow within the unconsolidated deposits. Data from a gain/loss study of the Mad River system and hydrographs from nearby wells reveal that the reach of the river next to Wright-Patterson Air Force Base is a ground-water discharge area.

A steady-state, three-dimensional ground-water-flow model was developed to simulate ground-water flow in the region. The model contains three layers and encompasses about 100 square miles centered on Wright-Patterson Air Force Base. Ground water enters the modeled area primarily by river leakage and underflow at the model boundary. Ground water exits the modeled area primarily by flow through the valleys at the model boundaries and through production wells. A model sensitivity analysis involving systematic changes in values of hydrologic parameters in the model indicates that the model is most sensitive to decreases in riverbed conductance and vertical conductance between the upper two layers. The analysis also indicates that the contribution of water to the buried-valley aquifer from the bedrock that forms the valley walls is about 2 to 4 percent of the total ground-water flow in the study area.

Ground waters in the vicinity of Wright-Patterson Air Force Base can be classified into two compositional groups on the basis of their chemical composition: calcium magnesium bicarbonate-type and sodium chloride-type waters. Calcium magnesium bicarbonate-type waters are found in the glacial deposits and the Brassfield Limestone, whereas the sodium chloride waters are exclusively associated with the shales. Equilibrium speciation calculations indicate that ground water of the glacial drift aquifer is in equilibrium with calcite, dolomite, and chalcedony, but is undersaturated with respect to gypsum and fluorite. Waters from the shales are slightly supersaturated with respect to calcite, dolomite, and siderite but are undersaturated with respect to chalcedony. Simple-mass balance calculations treating boron as a conservative species indicate that little (< 5 percent) or no recharge from the shales to the glacial drift aquifer takes place.

Data on the stable isotopes of oxygen and hydrogen indicate a meteoric origin for all ground water beneath Wright-Patterson Air Force Base, but the data were inconclusive with respect to identification of distinct isotopic differences between water collected from the glacial drift and bedrock aquifers. Tritium concentrations, used to distinguish waters having a pre- and post-1953 recharge component, indicate that most water entered the glacial drift aquifer after 1953. This finding indicates that recharge from shallow to deep parts (greater than 150 feet) of the aquifer takes place over time intervals of a few years or decades. However, the fact that some deep parts of the glacial aquifer did not contain measurable tritium indicates that ground-water flow from recharge zones to these parts of the aquifer takes decades or longer.

INTRODUCTION

Since the early 1900's, the area where Clark, Greene, and Montgomery Counties join in southwestern Ohio has been used for airfield activities. Huffman Prairie, where the Wright brothers tested early aircraft, is in northwestern Greene County. During World War I, military installations were established in the area. In 1948, the area was designated Wright-Patterson Air Force Base (WPAFB or Base). WPAFB encompasses about 8,500 acreas of Montgomery and Greene Counties (fig. 1). The Base is divided into three administrative areas: A, B, and C. The main part of the Base comprises Areas A and C. Area B is southwest of Areas A and C. WPAFB employs about 35,000 civilian and military personnel. In 1990, the population of the three counties was 859,702 (Hoffman, 1990).

Ground water is an important source of water in the area. WPAFB overlies a highly productive aquifer in the glacial deposits of the Mad River Valley. The aquifer consists of sands and gravels that fill a buried bedrock-valley system. Wells in the aquifer commonly yield more than 1,000 gal/min. This aquifer is the source of drinking water in Clark and Greene Counties. All of Montgomery County's public-water supply is from ground water, and the county withdraws more ground water than any other county in Ohio (R.J. Veley, 1993).

Research and development pursuits and ordinary Base operations produced numerous waste products. Early waste-disposal practices rarely considered environmental effects. As a result, many sites of known or potential ground-water contamination exist on the Base.

With the promulgation of the Comprehensvie Environmental Response, Compensation, and Liability Act of 1980 (CERCLA), the Department of Defense initiated the Installation Restoration Program (IRP) to guide environmental activities at Department of Defense facilities. The goal of the IRP is to identify and control migration of environmental contamination that may have resulted from past disposal practices. At WPAFB, the IRP is administered by the Base host, the 645th Air Base Wing, Air Force Materiel Command, through their Environmental Management Office. In 1987, the U.S. Geological Survey (USGS) began a cooperative program with WPAFB to conduct hydrogeologic studies in support of the Base IRP. The USGS studies have concentrated on Base property; however, parts of the surrounding area also have been investigated to assist in determining regional hydrogeology.

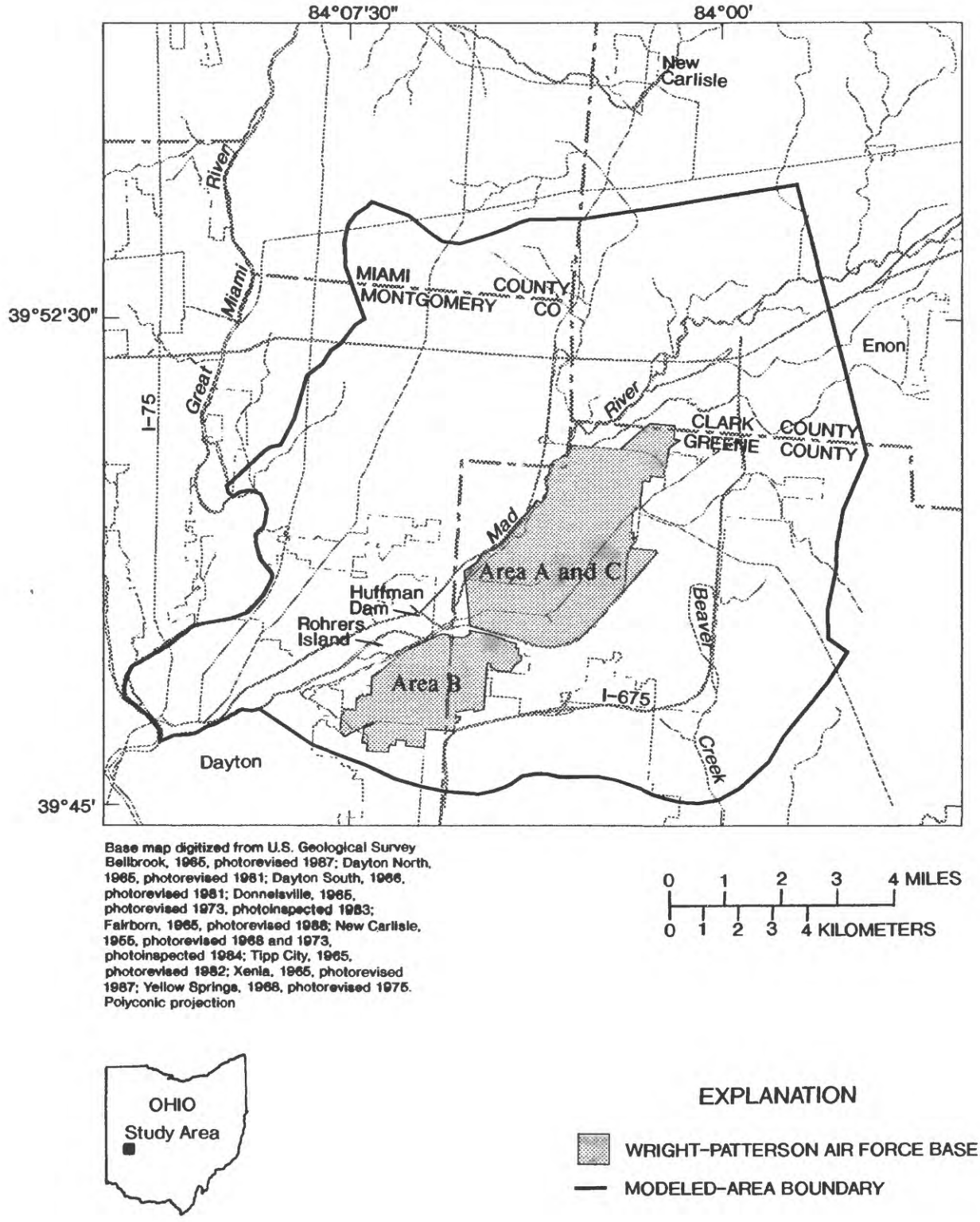

Figure 1.--Location of Wright-Patterson Air Force Base.

Purpose and Scope

The purpose of this report is to describe the hydrogeology and the simulated flow and quality of ground water at WPAFB and the surrounding area (fig. 1). Thirty-five wells were drilled on the Base to collect data on ground-water conditions. Water levels were measured three times in more than 200 wells in a network including both on- and off-Base wells. Streambed-permeability data were collected on several streams and lakes, and a stream gain/loss study was done to determine the relations between surface and ground water. Samples of ground water were collected from 28 wells on the Base and one well off-Base to assess (1) the effects of recharge on ground-water quality in the glacial-outwash deposits, (2) geochemical controls on water quality, and (3) the importance of recharge through the bedrock-valley walls. A numerical model was used to simulate ground-water flow in the study area, with special emphasis on ground-water sources and sinks, aquifer characteristics, and hydrologic interdependency of the buried valleys and upland areas.

Environmental Setting

Southwestern Ohio is in the north temperate climate zone. The average annual temperature in the WPAFB study area is 52.5°F. Data collected at two Dayton area weather stations during 1951-80 indicate that July is the warmest month (mean temperature of 76°F) and January is the coldest month (mean temperature of 28°F) (Harstine, 1991; National Oceanic and Atmospheric Administration, 1982). The maximum recorded temperature of 102°F occurred in June 1988; the minimum recorded temperature of -24°F occurred in January 1984 (Gale Research Company, 1989). The average annual precipitation is 38 in. The mean snowfall in the study area during 1936-65 ranged from 20 to 30 in. Data from the two weather stations indicate that precipitation is evenly distributed throughout the whole year. In June, the wettest month, precipitation ranges from 3.8 to 4.4 in.; in October, the driest month, precipitation ranges from 2.0 to 2.2 in. (Harstine, 1991; National Oceanic and Atmospheric Administration, 1982).

The study area is in the Till Plains section of the Central Lowlands physiographic province. The topography of the Till Plains is the result of continental glaciation. Bedrock features formed by preglacial drainage systems were buried under glacial deposits. The result is a land surface that is flat to gently rolling (Fenneman, 1938). The area between the Mad and Great Miami Rivers (fig. 1), west of WPAFB, is an upland area that ranges from about 800 ft above sea level along both of the rivers to more than 1,000 ft. The slopes of this upland area are generally steep and are dissected by small intermittent streams.

Much of the Base is on the broad flood plain of the Mad River (fig. 1). Areas A and C range from about 820 ft above sea level along the north boundary of the Base to 790 ft near Huffman Dam. The flood plain slopes to the southwest at about 6 ft/mi. Huffman Dam, located where the flood plain narrows from more than 2 mi wide to about 0.5 mi wide, is a flood-control structure that does not affect normal flow of the Mad River. Area B is downstream from Huffman Dam. The western half of Area B is in a valley, where the land-surface altitude ranges from 785 to 800 ft above sea level. The eastern half is on a ridge. The highest point on the Base, at an altitude of 980 ft, is in the southeast corner of Area B.

Previous Investigations

During 1948-52, three comprehensive studies of the water resources of Montgomery, Greene, and Clark Counties were done. These reports (Norris and others, 1948, 1950, and 1952) describe the geography, ground- and surface-water resources, and the chemical quality of the water in the counties. The hydrogeology of the consolidated and unconsolidated deposits is discussed. Ground-water conditions in specific areas, including Dayton, WPAFB, and the Fairborn area, also are discussed. These reports also include well records and maps showing the altitude and configuration of the bedrock surface and the distribution of the consolidated and glacial deposits.

Walton and Scudder (1960) describe the ground-water resources of the Fairborn area. The geology and aquifer properties are discussed. Data from aquifer tests at WPAFB and Southwestern Portland Cement (southeast of Fairborn) are presented. Additionally, the report includes a ground-water budget, well records, and contour maps of the water table and the bedrock surface.

Norris and Spieker (1966) describe the ground-water resources of the Dayton area. Detailed sections on the geology and hydrology of the valley-fill deposits around Dayton are presented. The results of several aquifer tests at well fields in Dayton are discussed. Data on the chemical quality of the surface and ground waters also are presented. Maps showing the geology, bedrock contours, and potentiometric surface are included in the report.

Evans (1977) presents water-quality data for the glacial-outwash aquifer of the Great Miami River basin. Data on major and selected minor chemical constituents in water from 98 wells sampled in 1976 are presented. Areal distributions for concentrations of dissolved solids, total organic carbon, iron, and manganese in the glacial-outwash aquifer are given; however, none of the wells reported in Evans (1977) study are in the current study area.

Geraghty & Miller, Incorporated (1987), prepared a report on the Mad River well field for the city of Dayton. The well field is on Rohrer's Island in the Mad River downstream from Huffman Dam. The report describes the water quality and the hydrologic conditions of the well field. The results of a digital ground-water-flow model are presented. Well-field management, development, and environmental programs also are discussed.

A number of studies have been done at WPAFB as part of the IRP process. The initial phase of the IRP is a problem identification and records search investigation (Engineering-Science, Incorporated, 1982). Investigators interviewed Base employees, examined aerial photographs, and reviewed Base records. As a result of their investigation, 24 past waste disposal or storage sites were identified. Fourteen of the sites were recommended for monitoring in the next phase of the IRP.

Weston, Incorporated (1983) outlined the initial approach for the investigations of 21 sites at WPAFB, and field investigations were initiated. Twenty-seven monitoring wells were installed and sampled. Samples of surface water, sediment, and leachate were collected and analyzed. Results of the initial field investigations were reported in 1985 (Weston). Two landfills were recommended for immediate remediation, and further site characterization was recommended for the other sites.

Dames & Moore, Incorporated (1986a, 1986b), investigated three landfills at WPAFB. Monitoring wells were installed, water samples were collected and analyzed, and aquifer tests were done at several wells. The landfill covers were investigated to determine their quality and integrity. Air monitoring was done to measure concentrations of gases released by the landfills. The two reports include data on lithology, hydrogeology, permeability tests, and analytical results.

Weston, Incorporated (1989), did additional site investigations at 27 sites at WPAFB. A multivolume report presents the results of the investigations. The report details past disposal activities, recent environmental investigations, types of contaminants found on the Base, field investigations, and site-specific work. Much of the work concentrated on identification and investigation of specific waste sites. The report includes logs of borings and wells; results of aquifer tests; results of surface geophysical surveys; and analytical results from sediment, surface-water, and ground-water samples.

IT Corporation (1990) assessed the nature and extent of contamination near the southwestern boundary of Area C (near Huffman Dam) and the western boundary of Area B. An initial assessment was made from existing information, and a field investigation was designed. The report contains information and data on water resources, ground-water use and quality, and the results of the field investigation program.

Engineering-Science, Incorporated (1991), presented a work plan and Standard Operating Procedures for remedial actions at WPAFB. Detailed descriptions and specific procedures for all sampling and related activities are presented.

Three reports have been published as part of the work the USGS has done at WPAFB. The first report describes the well-construction methods, lists lithologic and soil-sample data, and presents the final well-construction details for 35 wells installed by the USGS (Dumouchelle and de Roche, 1991). Another report consists of a map showing ground-water levels in the study area during autumn 1987 (Schalk, 1992). The third report is a map showing the altitude and configuration of the bedrock surface in the study area (Dumouchelle, 1992).

Acknowledgments

The authors thank personnel of the city of Dayton for assistance in collecting water-level data in city-owned wells, Paul Plummer of the Miami Conservancy District for his assistance in collecting water-level and geologic data, and the Ohio Department of Natural Resources, Division of Water, for providing well-log data. The authors also thank the numerous individual well owners who allowed water levels in their wells to be measured and the communities and industries who provided data on ground-water withdrawals.

METHODS OF INVESTIGATION

The hydrogeology of the study area was investigated according to methods described in this section. Data were collected that describe well-construction details, water levels, streambed permeability, and stream discharge. Samples of ground water were collected and analyzed for major ions, selected trace elements, and oxygen and hydrogen isotopes.

Ground-Water Data

Ground-water resources of WPAFB were investigated by installation of new wells and by collection of water-level, water-quality, and aquifer-test data. Examination of existing data indicated that new wells were needed to obtain additional data on regional water levels and vertical-head distributions. Water-level and water-quality recorders were installed at selected wells to gather data over an extended time period. Slug tests, sometimes called displacement/recovery aquifer tests, were done to obtain data on aquifer characteristics.

Well Installation

The USGS installed 35 wells at 13 sites (fig. 2) on WPAFB (Dumouchelle and de Roche, 1991). Fourteen wells were completed in bedrock, and the remaining wells were completed at various depths in the unconsolidated sediments. A site at which more than one well was constructed is referred to in this report as a "well cluster" or "cluster". Most clusters consist of one well completed in bedrock and one to three wells completed in the unconsolidated sediments.

The bedrock wells were the first wells installed at each site. Geologic data collected from these wells were used to determine if the installation of additional wells in the unconsolidated sediments was necessary. Double- or triple-cased well completions were used in wells that penetrate clay layers in the unconsolidated deposits. The drilling procedures were conducted in a manner to minimize personnel exposure to potential toxic chemicals and to minimize the potential for cross-contamination of wells.

Split-spoon samples of the unconsolidated materials were collected at 5-ft intervals during the drilling of the deepest well in each cluster. A total of four Shelby-tube samples were collected from clay-rich units. Three-inch-diameter rock cores totaling 20 ft in length were collected from each bedrock well. The cores are stored with the Ohio Department of Natural Resources (ODNR), Division of Geological Survey.

All of the wells were constructed by use of a drive casing larger than the final well casing. When the target depth was reached, the final well casing was installed through the drive casing, which was then pulled back, and the annulus was grouted to the land surface.

All but three of the bedrock wells (GR-308, GR-309, and GR-312) were screened rather than finished with an open interval. The annular space around the screens was packed with silica sand. In all but two of the wells (GR-316 and GR-326) completed in the unconsolidated materials, the formation at the screened depth was relatively free of clay. As the drive casing was pulled back, the formation material was allowed to collapse around the screen to create a natural gravel pack. At GR-316 and GR-326, the annular space around the screen was packed with clean silica sand before the drive casing was pulled back. A granular bentonite seal was placed above all sand packs to prevent infiltration of the grout into the screened interval.

The bedrock wells are constructed of black steel water-well casing. The remainder of the wells are constructed of stainless-steel casing. The screens in all of the wells are constructed of stainless steel.

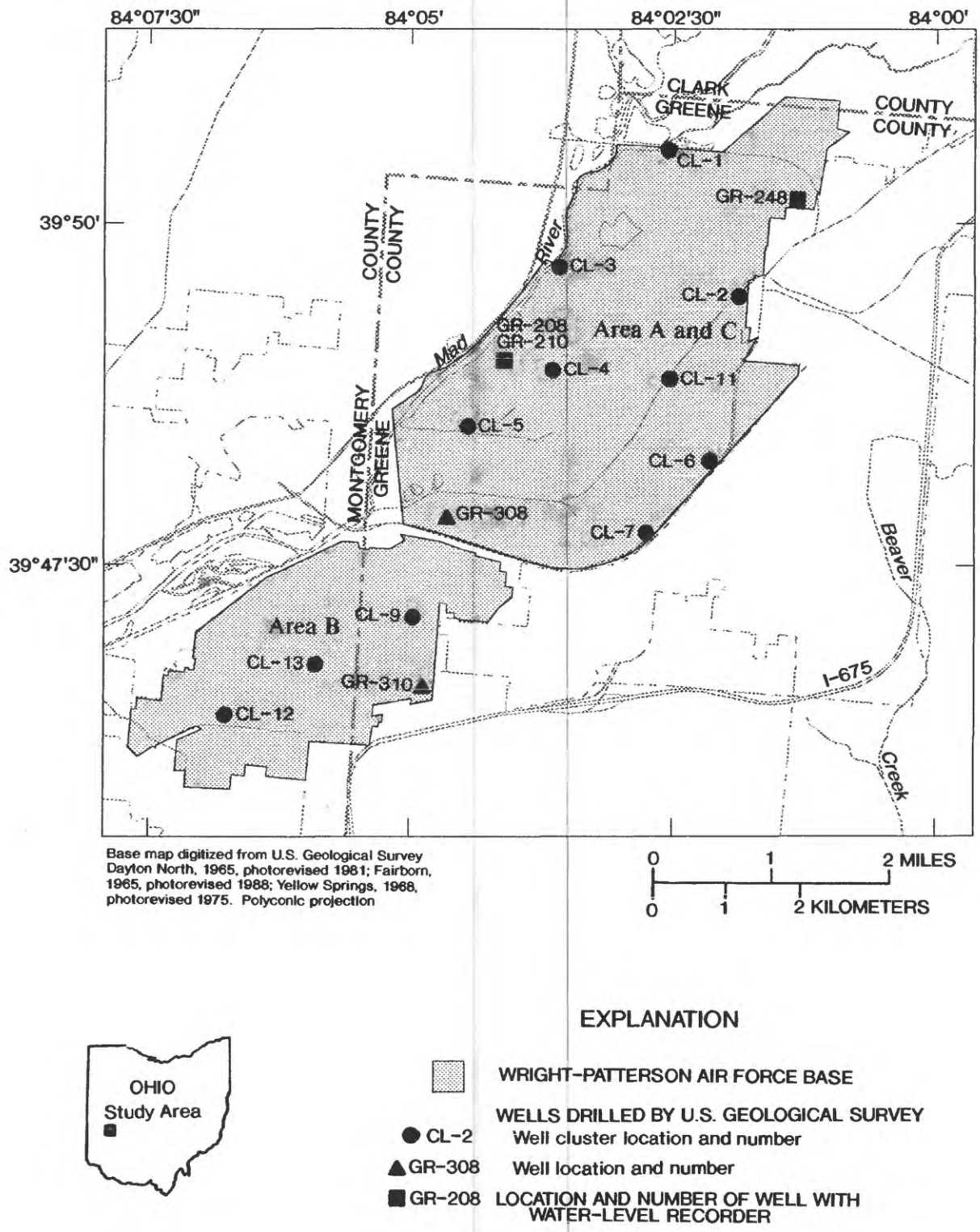

Figure 2.--Locations of wells drilled by U.S. Geological Survey and wells equipped with water-level recorders.

The altitude of the land surface at each cluster was surveyed by USGS personnel. The altitude of the top of the casing for each well also was surveyed. The altitudes are within $\pm$ 0.03 ft.

Data Collection

Water levels were measured monthly in all of the wells installed by the USGS (fig. 2). Measurements began upon completion of drilling and continued during the study. The water levels were measured with either an electric or a chalked steel tape. The electric tapes were marked in 1-ft increments; a ruler was used to measure the water level to 0.01 ft. The steel tapes were marked in 0.01-ft increments. Measurements were accurate to 0.01 ft. The top of each well casing was used as the measuring point. Equipment was cleaned with methanol and rinsed with deionized water after each measurement to prevent cross-contamination between wells.

In addition, the water levels in more than 200 wells on and off the Base were measured three times between autumn 1987 and summer 1989. Monitoring wells on WPAFB were measured in the manner described above. Off-Base wells included domestic water wells and observation wells at the Mad River well field. Well-log records from the ODNR were searched to locate domestic wells in the area. Water levels in off-Base wells were measured with chalked steel tapes. The tapes were cleaned in a chlorine-bleach rinse between measurements.

In the summer of 1989, water-level recorders were installed on three wells (fig. 2). Two wells (GR-208 and GR-210) are within 900 ft of the Mad River. The recorders were installed to examine the interaction between ground water and the Mad River. The third recorder (on well GR-248) was installed as a control. Water levels were recorded at hourly intervals. The recorders were serviced and checked monthly; the recorded water levels are considered accurate to 0.01 ft.

Data describing the well characteristics (such as well-construction methods, materials, and completion depths) and ground-water levels discussed in this report are stored in and can be accessed through the USGS Ground-Water Site Inventory (GWSI) computer data base, a data base maintained by the USGS as part of the National Water Information System (NWIS). Data from routine measurements of ground-water levels in the study area were published in the USGS annual water-data reports for Ohio (Shindel and others, 1989-92).

In April 1991, five wells at four clusters were equipped with sensors that record the water temperature and specific conductance to determine if there were seasonal variations in these two water-quality characteristics. The sensors were calibrated before installation, and the specific-conductance sensor was recalibrated periodically in the field. At least three well volumes were purged from the wells before installation of the sensors. Data were recorded hourly. Pressure transducers were also installed at two of the five wells to record water-level fluctuations. Monthly water-level measurements confirmed the accuracy of the pressure transducers.

Aquifer Tests

Aquifer tests were not done using pumped wells because of concerns about the containment, sampling, and disposal of potentially contaminated ground water. The volume of water expected from a long-term pumped-well aquifer test made the containment procedure prohibitive in terms of logistics and expenses. Thus, slug tests, which do not involve pumping water, were done.

A slug test is a type of aquifer test that can be used to derive a point estimate of the horizontal hydraulic conductivity of the aquifer. Slug tests consist of creating an instantaneous change in the water level in a well and observing the water-level recovery over time. As the water in the well recovers to its original level, frequent water-level measurements are made. The time and water-level data can be used to calculate horizontal hydraulic conductivity.

Forty-five wells were tested, of which all but four were completed in the unconsolidated sediments. Those completed in the unconsolidated deposits include 21 of the wells installed by the USGS and 20 monitoring wells installed during previous investigations. The tested wells that were completed in the bedrock were installed by the USGS.

The wells were selected for slug testing on the basis of three criteria: location, water quality, and well design and construction methods. A uniform areal distribution of hydraulic conductivities was desired so that the areal variation of hydraulic conductivity within the study area could be defined. Access to the wells also was considered; some monitoring wells are within landfill boundaries and are difficult to access. When available, the results of water-quality analyses were checked so that wells containing contaminated water could be avoided. Well records were checked to ensure that the depth of the well was sufficient for testing. Where possible, wells at the same location but screened at different depths were tested to define any vertical variation in hydraulic conductivity.

The water in the wells was displaced by use of a 6.42-foot-long section of 2-inch-diameter (nominal inside diameter) stainless-steel well casing that was capped on both ends. The slug was raised and lowered on a length of Teflon[1]-coated stainless steel cable. The water level in the well was measured before testing. The changes in the water level as the slug was injected or withdrawn were measured with a pressure transducer. The tests were complete when the water level in the well stabilized at or near the original level.

Except for one well in which the water level did not recover during the test, each well was tested with at least one injection (falling head) and one withdrawal (rising head) test. When the testing was finished at a well, all the equipment that came into contact with the ground water was cleaned with methanol and rinsed with deionized water.

---

1. Use of trade or company names is for identification purposes only and does not constitute endorsement by the U.S. Geological Survey.

The method described by Bouwer and Rice (1976) was used to analyze the slug-test data because this method can be used with partially penetrating wells and with confined or unconfined aquifers. All of the wells tested at WPAFB were partially penetrating, and some were screened below silty-clayey layers and may reflect semiconfined conditions. In the Bouwer and Rice method, the change in water level is plotted on semi-log graph paper as a function of time. Part of the data curve should form a straight line from which a value of the water-level change at a given time can be obtained. These values are used in equations to compute the hydraulic conductivity. Other variables needed for the computation are the radius of the well casing, the distance from the center of the well to undisturbed aquifer material, the length of the screen, the depth of the well, and the saturated thickness of the aquifer.

Data for most of the variables were taken from well-construction records. The thickness of the aquifer at each site was determined from well logs. If the well logs did not indicate any clay layers above or below the well screen, then the entire saturated thickness of the aquifer was used. Depths to the bedrock were estimated from the bedrock altitude map by Dumouchelle (1992). Bouwer and Rice (1976) noted that small errors in estimating the aquifer thickness do not have measurable effects on the results if the thickness of the aquifer is much greater than the portion of the aquifer that the well penetrates. Any overestimation of the aquifer thickness would not greatly affect the results because the wells were partially penetrating.

Surface-Water Data

The surface-water resources of WPAFB were investigated through use of streambed-permeability measurements and a gain/loss study. Measurements of streambed permeability were needed to estimate how easily water could flow through the streambed. A gain/loss study was done on the Mad River and its tributaries to quantify the gain or loss of water in the streams as they flow through the study area.

Streambed-Permeability Measurements

Eight sites on and around WPAFB were chosen for determination of streambed permeability by use of a seepage meter. Sites on the Mad River, Hebble and Trout Creeks, and Gravel and Bass Lakes were tested. A seepage meter measures the flux between ground-water and surface-water bodies by isolating an area of the streambed and measuring the change in water volume in a bag connected to the container during a known time period. The meter was constructed from the end section of a 55-gal drum (fig. 3). A rubber stopper with an outlet tube connected to a flexible collection bag was fitted in the bunghole of the drum. A piezometer was installed in the streambed near the seepage meter to determine the difference in hydraulic head between the stream and shallow ground water. The piezometer consisted of a 1.25-inch-diameter galvanized pipe with an 18-in. wire-wrapped stainless-steel screened drive point. The center of the screen was placed 23 in. below the streambed. A manometer was used to measure the difference in head between the stream and water within the piezometer.

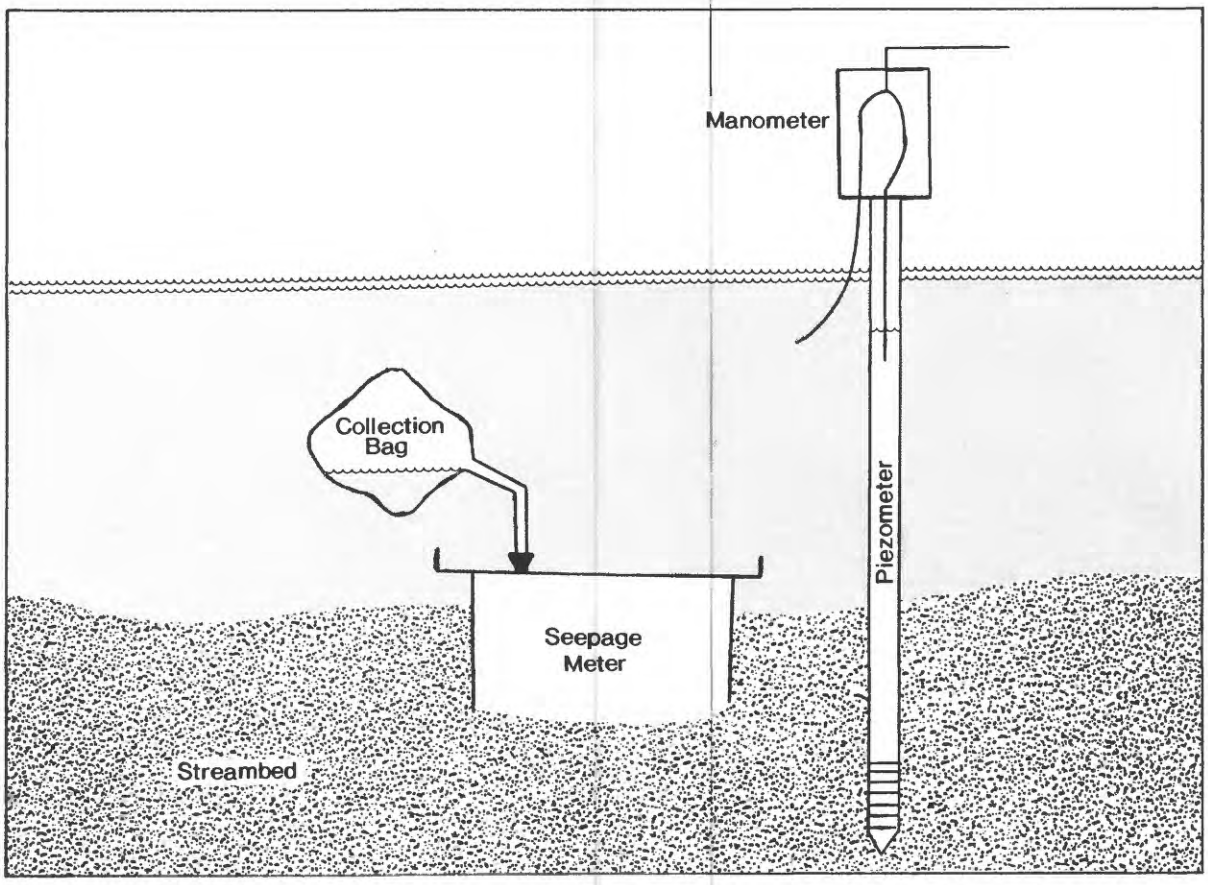

Figure 3.--Seepage meter and piezometer. (Modified from Cunningham, 1992.)

The seepage meter was installed by allowing the trapped air to escape and driving the open end of the drum into the streambed. Then a collection bag containing a known volume of water was attached to the meter. At a later time the amount of water in the collection bag was measured. If the volume of water in the bag had increased, the stream was gaining ground water; if the volume had decreased, the stream was losing water to the aquifer. The permeability of the streambed can then be calculated by use of Darcy's law, as follows:

$$Q = - K A \, dh/dl, \qquad (1)$$

where Q is the discharge or the change in water volume in the collection bag
K is the hydraulic conductivity (permeability of the streambed),
A is the cross-sectional area of the seepage meter, and
dh/dl is the hydraulic gradient between the aquifer and the stream.

Samples of the streambed material also were collected at the eight seepage-test sites. The samples were collected in a plastic container about 6 in. in length. The container was driven into the streambed, the material around the outside of the container was dug out, and a cap was slipped under the top of the container. The hole was cleaned out, and the procedure was repeated to collect a second sample from the 6- to 12-in. depth. Grain-size distributions were determined for each sample by dry-sieve analysis.

The permeability of the streambed was estimated from the grain-size data according to the methods described by Hazen (1911) and Masch and Denny (1966). These methods relate grain-size diameters to hydraulic conductivity. The Hazen method uses an equation and the d_{10} grain size; d_{10} is the maximum diameter of the smallest 10 percent of the grains in the sample. The Masch and Denny method uses a set of empirically derived curves that relate grain sizes to hydraulic conductivity to determine the hydraulic conductivity; five effective diameters (d_5, d_{16}, d_{50}, d_{84}, and d_{95}) are needed.

Gain/Loss Study

On July 23, 1991, a gain/loss study was done on the Mad River, Hebble Creek, Trout Creek, and several other small tributaries to the Mad River. The study was done during a period of low flow (75 percent of the Mad River flow-duration curve) to minimize any input from precipitation or surface runoff. The study consisted of a series of discharge measurements along the streams; in all, 28 sites were measured. Before the study, a reconnaissance was made to identify sites at which the channel was stable and to establish a reference point for measuring stage. Discharge measurements were made according to methods outlined by Rantz and others (1982).

Water-Quality Sampling and Analytical Procedures

Water from 29 wells was sampled for major ions, selected trace elements, dissolved organic carbon (DOC), tritium, and stable isotopes of oxygen and hydrogen in late June and early July 1991. Twenty-eight of the wells were on WPAFB; one well east of the Base in Fairborn also was sampled for comparative purposes. Of the 29 wells, 21 were completed in unconsolidated glacial outwash deposits of Pleistocene age, 2 were completed in the Brassfield Limestone of Silurian age, and 6 wells were completed in shales of Ordovician age. During sampling of the wells, water temperature, specific conductance, dissolved oxygen (DO), pH, and alkalinity were measured. Sampling procedures used in the field followed guidelines prepared by WPAFB and Engineering-Science, Incorporated (1991). Detailed descriptions of sampling procedures are given below.

Ground water was pumped with a centrifugal pump through polypropylene tubing to the sampling containers. During pumping, pH, temperature, specific conductance, and DO concentrations were monitored by use of a closed flowthrough cell attached to a four-parameter probe. The purpose of the flowthrough cell was to prevent degassing of CO_2 and other dissolved gases, which could affect measurement of sample pH, and to prevent contact with atmospheric gases, particularly oxygen, which could affect the redox status of the ground water and thereby affect determinations of dissolved iron and manganese concentrations. Samples were collected only after the equivalent of three borehole volumes of water had been removed and temperature, pH, and specific-conductance readings (taken every 5-10 minutes) had stabilized within instrumental error ($\pm$ 5 percent).

Specific conductance and pH probes were calibrated daily by use of specific conductance and pH standard solutions prepared by the National Water Quality Laboratory of the USGS. The accuracy of the temperature probe was checked with a mercury thermometer certified by the National Institute of Standards and Technology. The DO probe was calibrated by measuring the dissolved oxygen concentration of distilled water equilibrated with atmospheric oxygen under field conditions. Alkalinity titrations in the field were done on unfiltered samples collected directly from the well. Alkalinity was determined by titration of 50 mlL of sample to a pH of 4.5 with a standardized sulfuric acid solution. The endpoint pH was determined with a portable pH meter and electrode.

Samples collected for determination of major-ion and of trace-metal concentrations were collected by use of a polypropylene tube attached to the flowthrough cell into a 1-L polypropylene bottle. Samples for determination of major-cation and trace-element concentrations were then filtered through 0.45-µm membrane filters (142-mm diameter) mounted in a plastic filter holder. Major cation and trace metal samples were acidified to an approximate pH of 1.0 with 1 to 2 mL of ultrapure concentrated nitric acid. Filtered samples for major-anion determinations were not acidified. Samples collected for DOC analysis were filtered with 0.45-µm silver membrane filters by use of a stainless-steel, nitrogen-pressurized filter chamber and then stored in 250-mL amber glass bottles. For tritium analysis, 1L of unfiltered sample water was placed in a glass container. For analysis of hydrogen and oxygen stable isotopes, 125 mL of unfiltered sample water was placed in a polypropylene bottle with a polyseal cap. Samples were placed in insulated, ice-filled containers, chilled to 4°C, and then shipped to the appropriate analytical facility.

A five-step process was used to clean all sampling equipment before each well was sampled. First, all exterior pump parts, tubing, and filter-holder parts were washed with a detergent solution. Second, all parts were rinsed with local tap water. Third, all parts were rinsed successively with 5 percent HNO_3 and 10 percent HCl. Each acid rinse was followed by a thorough rinsing with deionized water. The interior of the pump and the inside of the tubing were cleaned by successively pumping the three cleaning solutions through the pump and attached tubing.

Laboratory analyses for major ions, trace elements, pH, alkalinity, dissolved solids, specific conductance, and DOC were done by the Rocky Mountain Analytical Laboratory, operated by Enseco, Incorporated. Descriptions of analytical and standardization techniques, analytical equipment used, and the precision and reliability of analytical results reported by Enseco regarding data for WPAFB ground-water samples are described in the data reports (Enseco, Incorporated, 1991). Tritium analyses were done at the USGS Tritium Laboratory in Reston, Va., and hydrogen- and oxygen-isotope samples were analyzed at the USGS Stable Isotope Laboratory, also in Reston, Va. Documentation of quality-assurance/quality-control procedures used to validate the stable-isotope and tritium data is available from the USGS National Water Quality Laboratory.

HYDROGEOLOGY

During most of the Paleozoic Era, 570 to 240 million years ago, the study area was submerged beneath a shallow sea. The rocks in the study area originated from the bottom sediments of this sea. Near the end of the Paleozoic Era, the sea regressed from what is now western Ohio, and erosion by surface streams began to remove the sediments. During the late Tertiary Period, about 10 to 15 million years ago, this area was uplifted, and, as a result, streams began to erode deep valleys (Norris and Spieker, 1966).

The major bedrock valleys in the study area (fig. 4) were formed during the time of the Teays River system, which existed from the late Tertiary Period to the Pleistocene Epoch. The main stem of the Teays River flowed northwestward across Ohio and into Indiana, passing about 30 mi northeast of Dayton. The streams in the valleys shown on figure 4 could have flowed southwestward toward a preglacial Ohio River (Norris and Spieker, 1966; R.A. Sheets, U.S. Geological Survey, oral commun., 1991).

The Teays drainage system was modified greatly over a period of thousands of years with the advance of the Pleistocene continental glaciers. Glaciers blocked the Teays drainage system, filling the valleys with sediments. Over time, another drainage system developed, and erosion removed some sediments, deepened the bedrock valleys, and formed new valleys. This drainage system, called the Deep Stage, cut the bedrock valleys to their present depths. Outwash from the Illinoian and Wisconsinan glaciers filled the bedrock valleys with as much as 260 ft of unconsolidated sediments in the study area. The current drainage system developed after the advance of the Illinoian ice sheet disrupted the Deep State system. The current stream system is similar to the Deep Stage system. The current topography is the result of deposits left by the continental glaciers and modern stream erosion (Norris and Spieker, 1966).

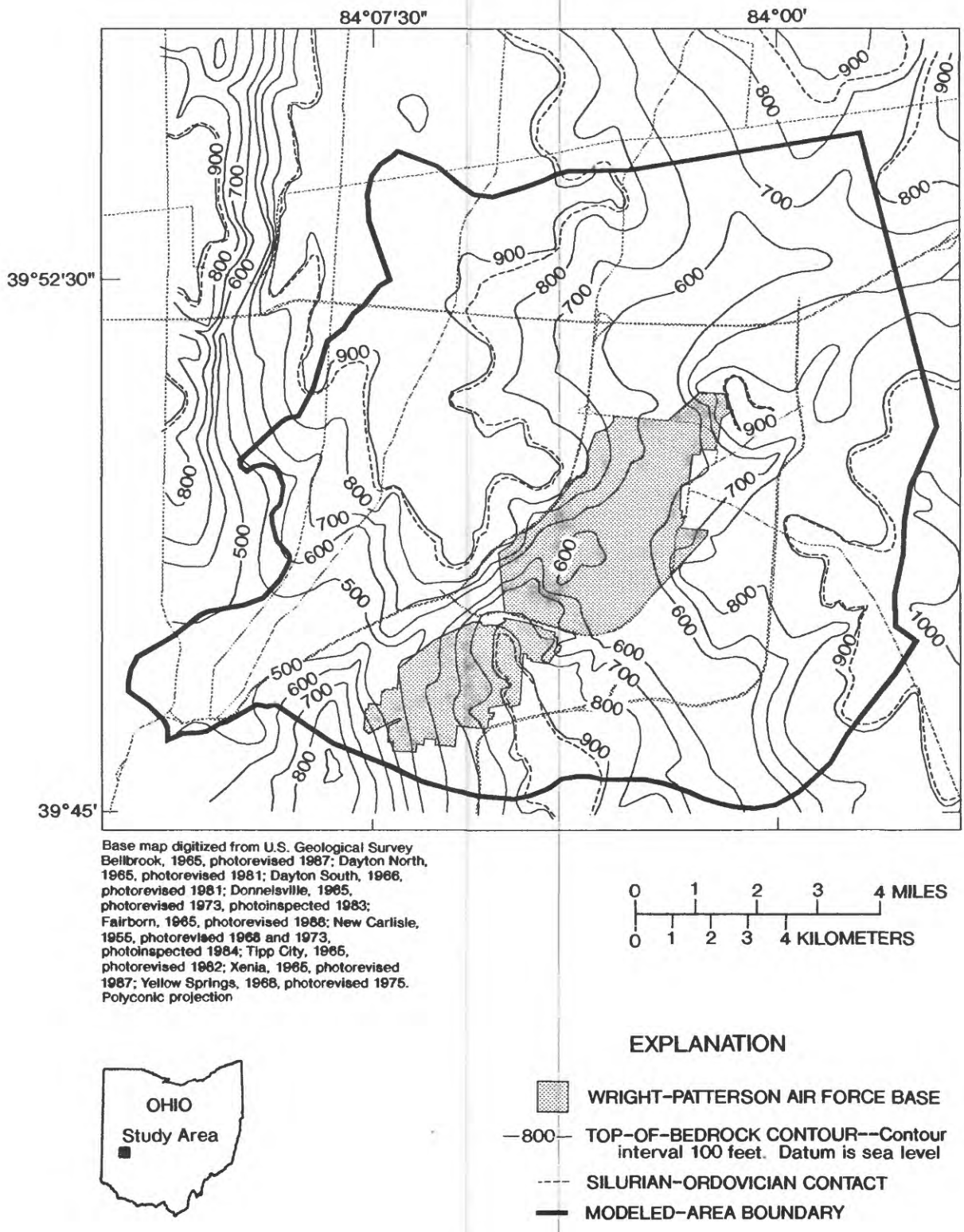

Figure 4.--Bedrock topography in the study area. (Modified from Dumouchelle, 1992.)

Geologic Characteristics and Ground-Water Availability

The unconsolidated glacial deposits consist of fine-grained tills and sand and gravel outwash deposits. The tills are poorly permeable and yield little water to wells. The outwash deposits are much more permeable, and most water-supply wells in the region are completed in these deposits. Most of the bedrock in the study area consists of poorly permeable shales. In upland areas, carbonate bedrock overlies the shales and can yield sufficient water for domestic uses.

Unconsolidated Deposits

Wisconsinan glacial deposits cover much of the bedrock in the study area. Illinoian glacial deposits may underlie the Wisconsinan deposits in the deepest areas of the buried valleys. The deposits can be separated into ground moraine or till and outwash or valley-train deposits. Modern stream valleys in the area contain thin deposits of alluvium.

Till consists of a mixture of unstratified, poorly sorted sediments ranging in size from clay and silt to boulders. Clay-rich till covers most of the upland areas. The till ranges from less than 1 ft to more than 80 ft in thickness and can contain sand and gravel stringers (Walton and Scudder, 1960).

The clay-rich tills are poorly permeable compared to coarse-grained deposits. Wells completed in tills in Montgomery County yield 2 to 10 gal/min. Wells that yield more than 10 gal/min are probably partially screened in a sand and gravel lens within the till (Norris and others, 1948, p. 32-33). In Greene County, wells completed in thick till deposits yield an average of 12 gal/min (Norris and others, 1950, p. 15). The hydraulic conductivity of till samples in the Dayton area, as determined by permeameter tests, ranges from 0.0013 to 0.067 ft/d. The vertical hydraulic conductivity of the till layer near Rohrer's Island, as determined from aquifer tests, ranges from 0.004 to 0.017 ft/d (Norris and Spieker, 1966, p. 52-58). The vertical hydraulic conductivity of samples from four clay layers at WPAFB, as determined by permeameter test, ranged from 7.7×10^{-6} to 1.0×10^{-4} ft/d (Dumouchelle and de Roche, 1991, p. 6).

The bedrock valleys are filled with stratified valley-train deposits which range from fine-grained sands to gravels. The stratification of the deposits results in horizontal hydraulic conductivities that are generally larger than the vertical hydraulic conductivities. Lenses of till are present within these deposits. Downstream from Huffman Dam, the valley-train deposits are separated into two aquifers by buried till sheets. These sheets may extend almost completely across the valley. For example, two sand and gravel aquifers separated by a low-permeability clay-rich layer have been identified at Rohrer's Island. In other areas, the till layers consist of irregular lenses. The till may be absent locally (Norris and Spieker, 1966).

The coarse sands and gravels of the valley-train deposits are among the most productive aquifers in the study area, yielding as much as 2,000 gal/min to wells. Production wells completed in the outwash deposits on WPAFB and around Fairborn yield 500 to 1,500 gal/min (Norris, and others, 1950). In 1987, about 50 Mgal/d was pumped from well fields in the valley-train deposits in the Dayton-WPAFB area (Schalk, 1992).

Well logs from WPAFB indicate that the unconsolidated deposits consist of clay-rich tills and silty, fine- to coarse-grained sand and gravel (outwash) deposits. The clay layers are discontinuous and range in thickness from a few inches to more than 40 ft. The silty, fine-grained sand deposits are well sorted and can be as much as 25 ft thick. The poorly sorted outwash deposits consist of very fine to very coarse sand, gravel, and cobbles with some silt and clay. In some places, these deposits are more than 200 ft thick (Dumouchelle and de Roche, 1991).

The variability in lithologies and the discontinuous nature of layers makes mapping any specific unit at a regional scale difficult. The location lines of three geologic sections through the region are shown in figure 5. The geologic sections are shown on figures 6, 7 and 8. The types of deposits logged at each well used to construct the section are shown, but, because of the heterogeneity of the unconsolidated deposits, no attempt was made to interpolate the stratigraphy between the wells. It may be possible to collect sufficient data over small distances (tens to hundreds of feet) to map units with distinct lithologic changes[2]; however, it is difficult to collect such data over greater distances. The heterogeneity of the unconsolidated deposits can be seen on figure 7; the four ODNR wells on the left side of the figure show different deposits at a given depth. Similar variations in the lithologies between wells can be seen on the other sections. The gross lithology in any of these wells is similar but the proportions of clay, silt, sand, and gravel differ greatly from well to well. At a regional scale, many units probably grade gradually from one specific lithologic unit into another.

Consolidated Deposits

Most of the consolidated rocks in the region are from the Richmondian Stage of the Late Ordovician Period (table 1). These rocks consist of fossiliferous interbedded shales and limestones. The shale is fine-grained, soft, fissile, and contains thin layers of limestone. Shale layers are as thick as 20 ft. The limestone is hard and dense and consists of thin layers that range from a few inches to 2 ft thick (Walton and Scudder, 1960). Limestone can form 25 to 50 percent of the sequence. The rocks are greenish or blue gray; however, in the upper part of the unit, noticeably reddish zones also are present (Norris and Spieker, 1966). The upper part of the sequence is exposed in a railroad cut at the southern end of Huffman Dam.

---

2. During a remedial investigation of a site along the northeastern boundary of Areas A and C at WPAFB, it was found that lithologies can change markedly over very short distances. For example, a clay layer was found from 33.5 to 39 ft below land surface in well MW9-1D; in a second well, MW9-2I, drilled less than 10 ft from the first well and coarse sand and gravel was found from 33 to 39 ft. Logs from other wells drilled at the site also show this extreme heterogeneity (Michael Jackson, Engineering-Science, Inc., oral commun., 1992). These ata indicate that, in some areas, it may not be possible to map lithologies over even small distances.

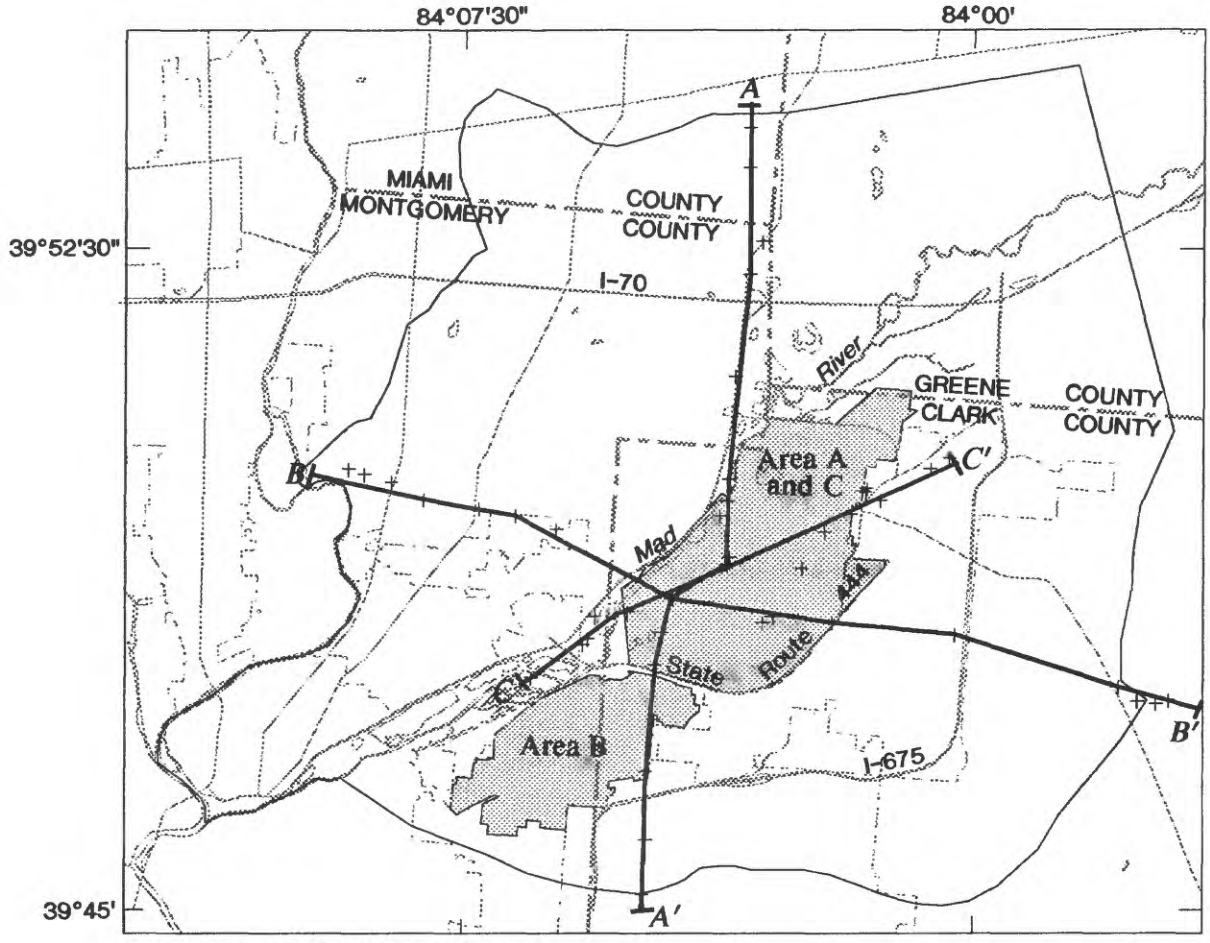

Figure 5.--Location of geologic sections.

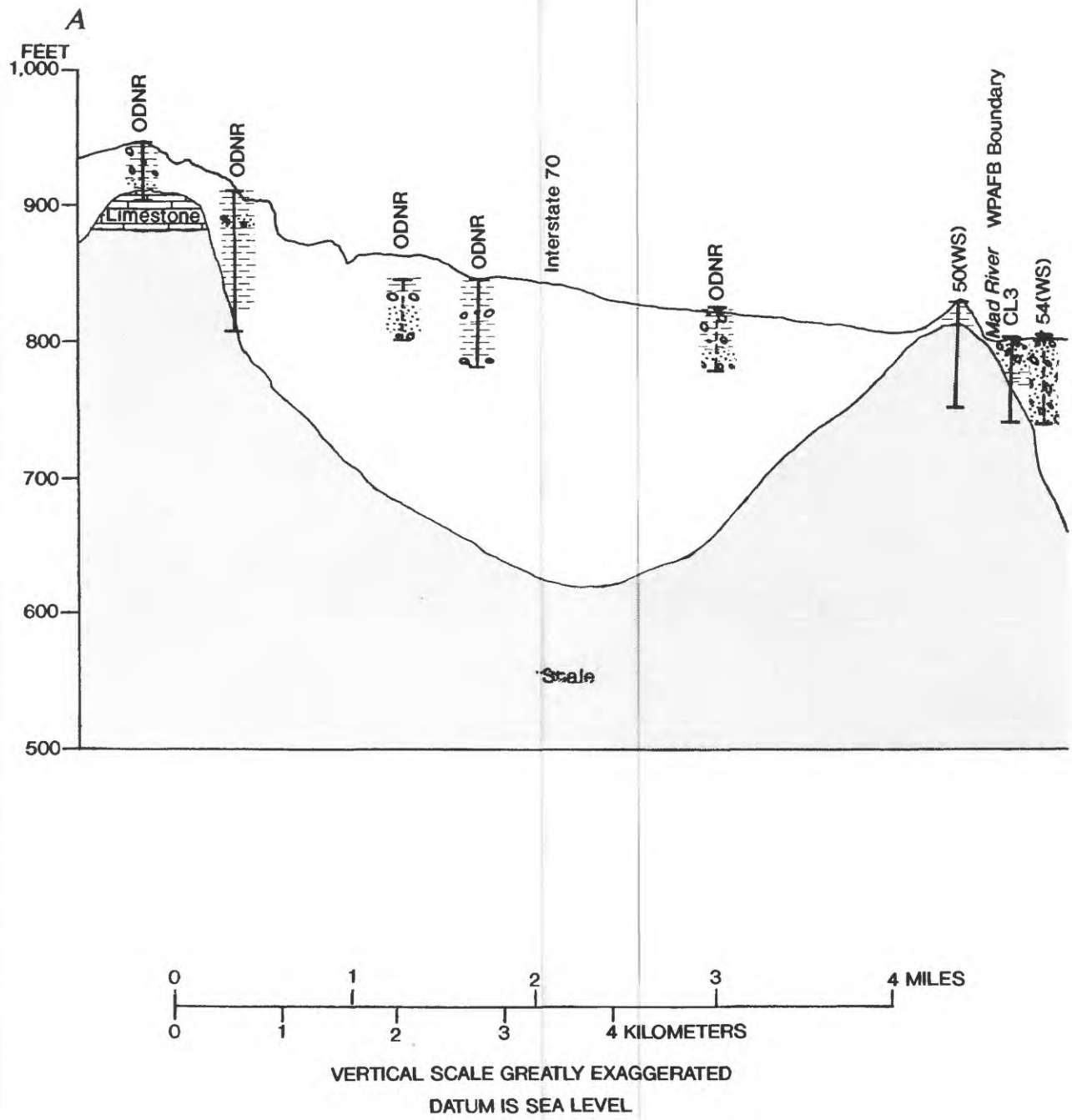

Figure 6.--Geologic section $A-A'$ (section trace shown in figure 5).

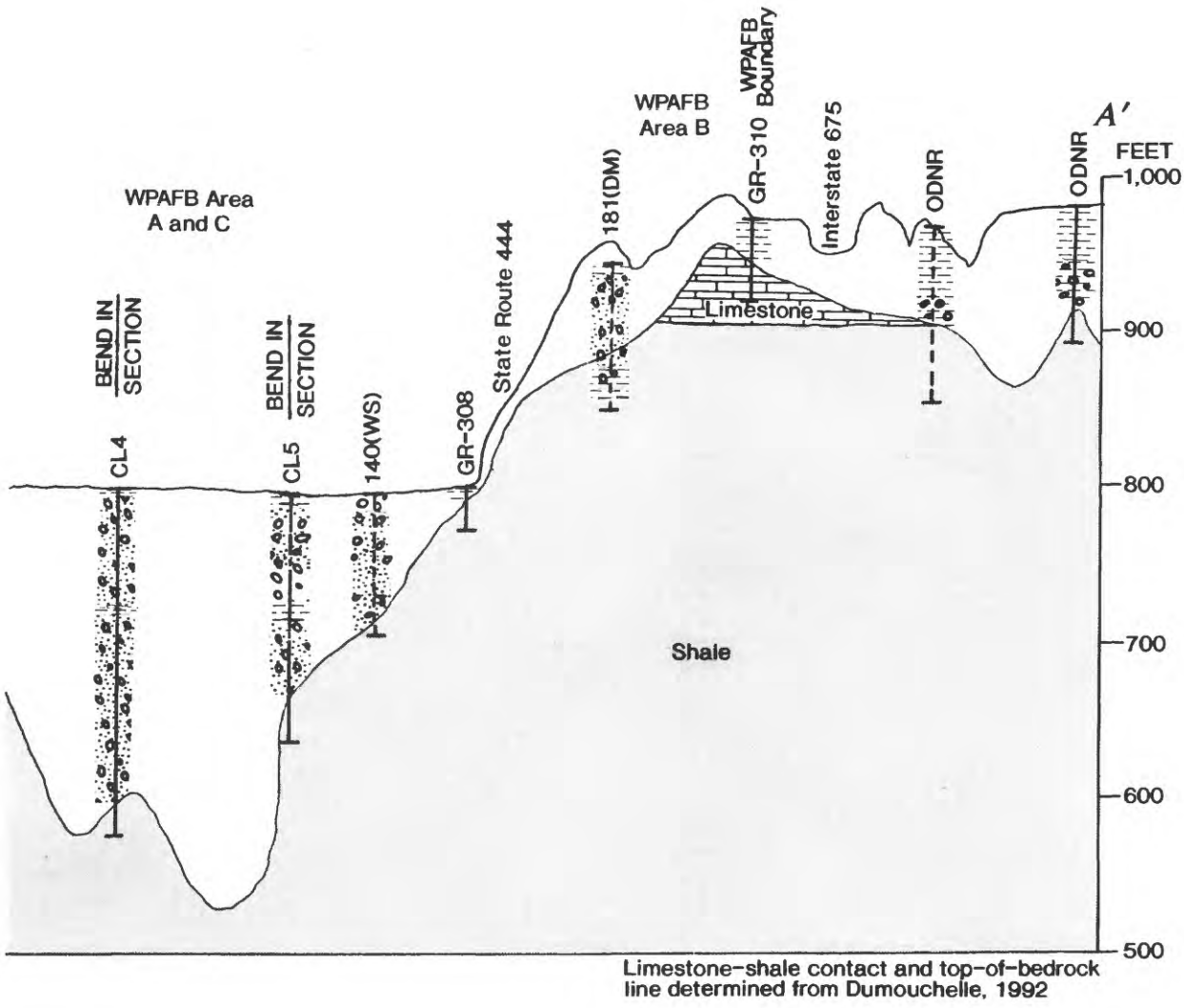

EXPLANATION

CLAY AND (OR) SILT

SAND

GRAVEL

WELL ON GEOLOGIC-SECTION LINE

WELL PROJECTED TO GEOLOGIC-SECTION LINE--All within 1,000 feet of section line

WELL IDENTIFICATION

140(WS)	Log number in Walton and Scudder (1960)
CL5	Well-cluster number, wells drilled by U.S. Geological Survey. Location in figure 2 (Dumouchelle and deRoche, 1991)
ODNR	Well log on file with the Ohio Department of Natural Resources, Division of Water
GR-308	Well drilled by U.S. Geological Survey. Location shown in figure 2 (Dumouchelle and deRoche, 1991)
181(DM)	Monitoring well number, well installed by Dames & Moore, Inc. (1986a)

Figure 6.--Geologic section *A*-*A'* (section trace shown in figure 5)--Continued.

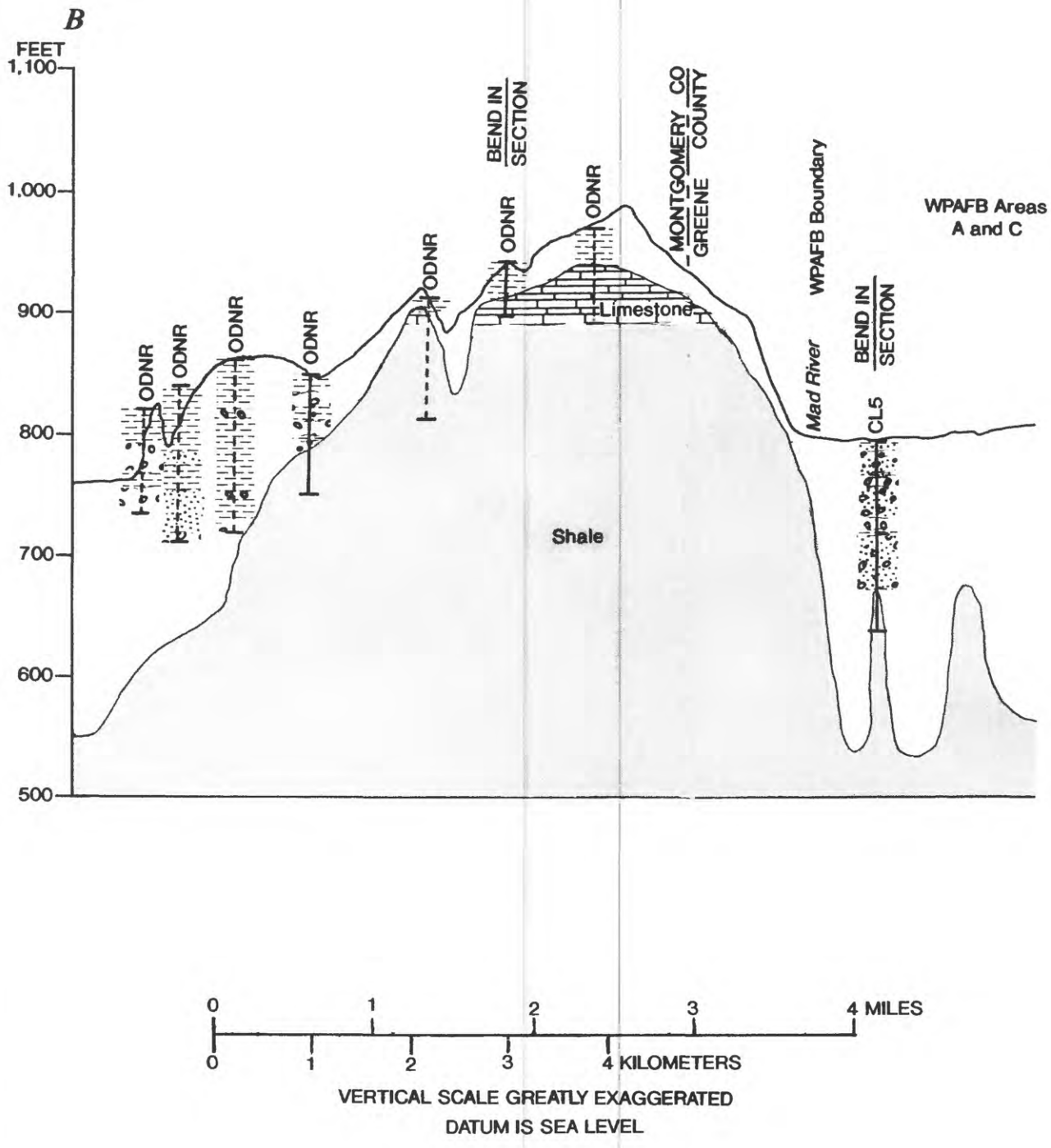

Figure 7.--Geologic section *B*–*B′* (section trace shown in figure 5).

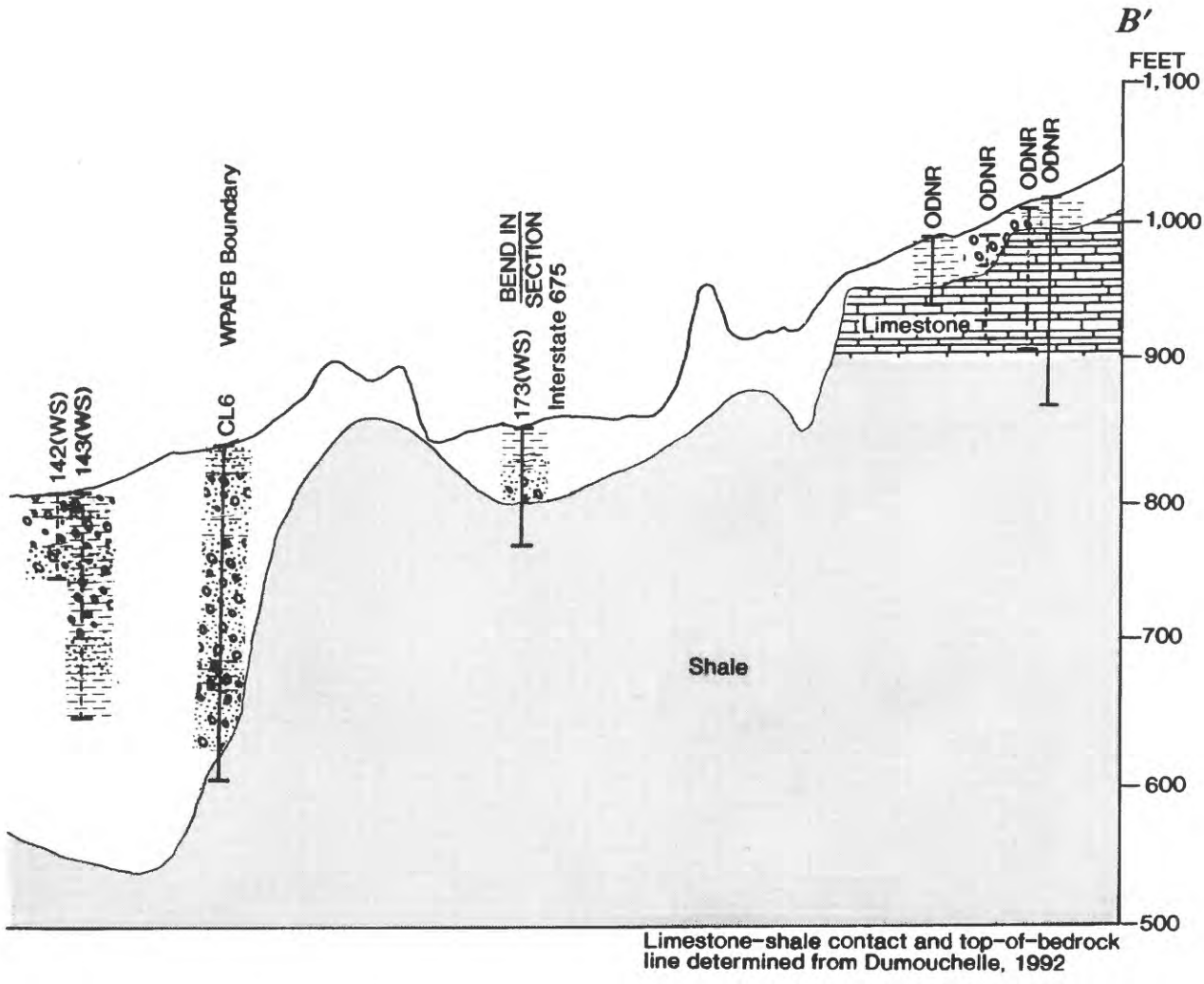

EXPLANATION

CLAY AND (OR) SILT

SAND

GRAVEL

WELL ON GEOLOGIC–SECTION LINE

WELL PROJECTED TO GEOLOGIC–SECTION LINE––All within 1,000 feet of section line

WELL IDENTIFICATION

142(WS)	Log number in Walton and Scudder (1960)
CL6	Well–cluster number, wells drilled by U.S. Geological Survey. Location in figure 2 (Dumouchelle and deRoche, 1991)
ODNR	Well log on file with the Ohio Department of Natural Resources, Division of Water

Figure 7.––Geologic section *B–B′* (section trace shown in figure 5)––Continued.

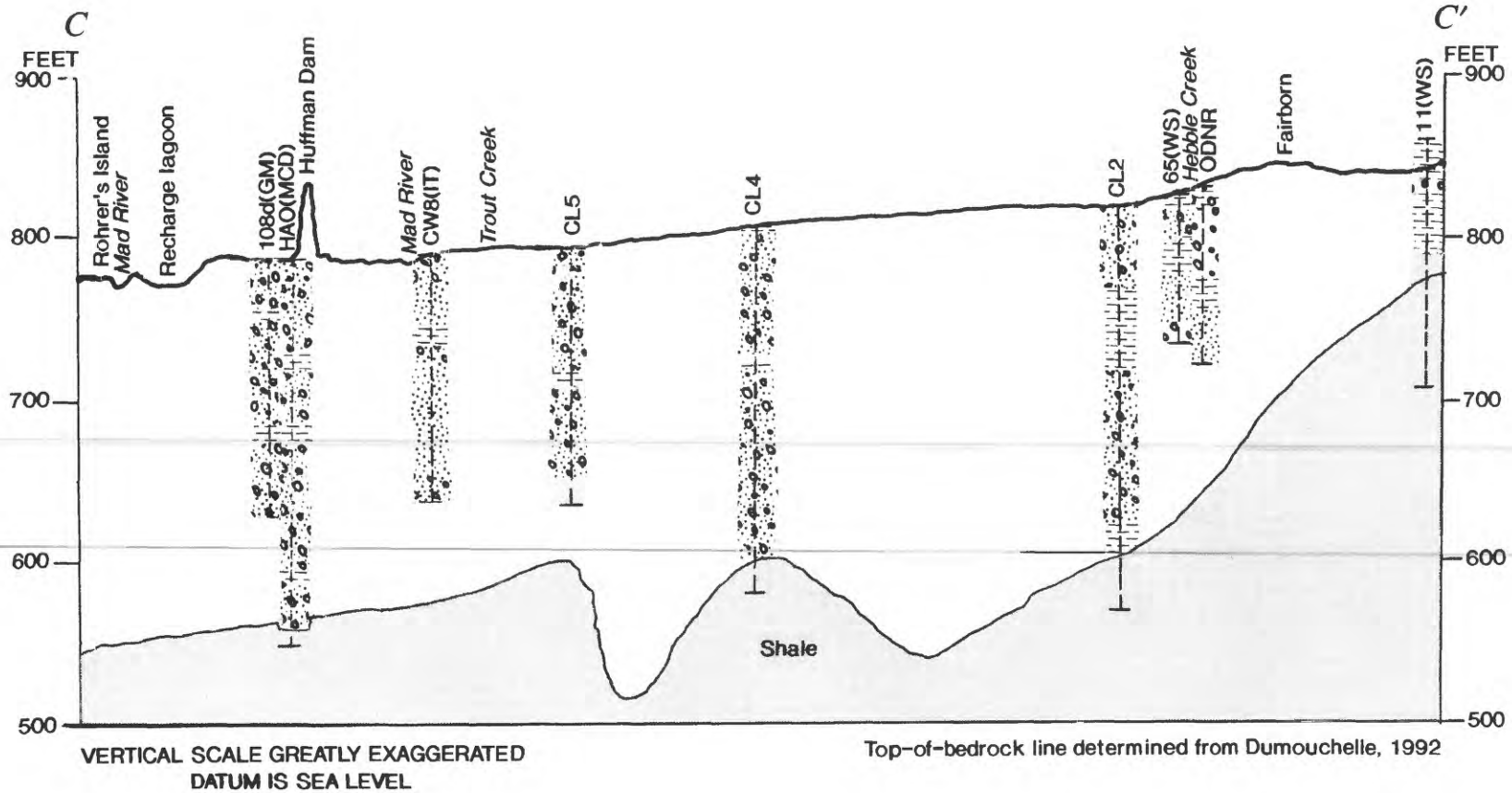
C
C′
FEET
900
800
700
600
500
Rohrer's Island
Mad River
Recharge lagoon
108d(GM)
HAO(MCD)
Huffman Dam
Mad River
CW8(IT)
Trout Creek
CL5
CL4
CL2
65(WS)
Hebble Creek
ODNR
Fairborn
11(WS)
Shale
VERTICAL SCALE GREATLY EXAGGERATED
DATUM IS SEA LEVEL
Top-of-bedrock line determined from Dumouchelle, 1992

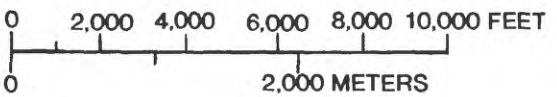

EXPLANATION

CLAY AND (OR) SILT

SAND

GRAVEL

WELL PROJECTED TO GEOLOGIC-SECTION LINE--All within 1,000 feet of section line. The unusual bedrock position in wells HAO, CL5 and 11 are due to the projection of these wells to the line of section

WELL IDENTIFICATION

65(WS)	Log number in Walton and Scudder (1960)
CL5	Well-cluster number, wells drilled by U.S. Geological Survey. Location in figure 2 (Dumouchelle and deRoche, 1991)
ODNR	Well log on file with the Ohio Department of Natural Resources, Division of Water
108D(GM)	Well number in Geraghty & Miller, Inc. (1987)--Clay at approximately 750 feet was not found in 108s, a nearby well
HAO(MCD)	Well number in Miami Conservancy District files
CW8(IT)	Well cluster in IT Corporation (1990)

Figure 8.--Geologic section *C*–*C′* (section trace shown in figure 5).

Table 1.—Generalized geologic column for section of the Wright-Patterson Air Force Base area

[Modified from Walton and Scudder, 1960, table 1]

System or Period	Series or Epoch	Stage or Formation	Thickness (feet)	Character of material
	Holocene		5 +	Flood-plain deposits, chiefly silt and clay.
Quaternary	Pleistocene	Wisconsinan stage	260 +	Outwash sand and gravel (deposited as kames and valley train by meltwaters from the glacier); and (or) till, a heterogeneous mixture of clay, sand, gravel, and boulders in which clay predominates (deposited directly by the glacier).
		Pre-Illinoian stage	unknown	Sand and gravel or till in the deepest part of the buried valleys beneath the Wisconsinan deposits.
Silurian	Middle Silurian		55 +	Massive and porous to well-bedded and dense dolomites and limestones. Calcareous shales with limestone layers.
	Lower (or Early) Silurian	Brassfield Limestone	30 +	Limestone in layers ranging from thick and massive layers near the base to thin near the top.
Ordovician	Upper (or Late) Ordovician	Richmondian, Maysvillian, and Edenian Stages, undivided	1,000+	Shale, soft, calcareous, interbedded with thin layers of hard limestone.

The Ordovician shales are virtually impermeable. The limestone layers are dense and not very porous, and the fine-grained shales are generally less permeable. Most wells drilled into these rocks are effectively dry; when such wells are pumped, yields are not more than 1 gal/min, drawdowns are large, and recoveries are slow. Significant, but small, amounts of water can be found only near the top of the unit in weathered zones where the water is present in fractures and solution openings (Norris and others, 1950). In general, the horizontal hydraulic conductivity of these rocks is greater than the vertical hydraulic conductivity because of bedding-plane separations in the shales and between the shale and limestone layers.

Fourteen of the wells installed by the USGS at WPAFB were completed in the bedrock. Twelve of these wells were completed in the Ordovician shales, one well was completed in the Brassfield Limestone, and one well was completed in both units. Recovery times for three wells on which aquifer tests were done are listed in table 2 (see section on "Hydraulic Conductivity and Transmissivity"). The recovery times ranged from less than a minute to an hour. However, several wells were virtually dry; recovery times from drilling or pumping range from several weeks to years (table 2).

On the basis of aquifer tests, the hydraulic conductivity of the shales is estimated to range from 0.0016 to 12 ft/d (see section on "Hydraulic Conductivity and Transmissivity"). Walton and Scudder (1960) estimated the flow through the bedrock-valley walls (shale) to be 160,000 gal/d. Depending on the hydraulic gradient and cross-sectional area chosen, 160,000 gal/d translates to a hydraulic conductivity in the range of tenths of feet per day to a few feet per day.

The Brassfield Limestone of Early Silurian age is present in the upland areas (altitudes 850 ft above sea level). The Brassfield Limestone is massive and evenly bedded near the base of the formation but forms thin and irregular beds near the top. At some locations, the base of the unit consists of a granular limestone. The limestone contains abundant crinoid fossils in the upper beds; however, few fossils are present in the massive lower section. The Brassfield ranges from dark gray to pink (Norris and others, 1948).

Most wells completed in the Brassfield Limestone yield sufficient water for domestic purposes. Most yields are as much as 15 gal/min, and a few wells yield as much as 100 gal/min, but wells with more than 100-gal/min yields are possible. The contact between the Brassfield Limestone and the less permeable Ordovician shales is often a zone of springs, particularly in northern Montgomery County (Norris and others, 1948).

In some places in the region, other Silurian rocks consisting of two calcareous shale formations and several formations of dolomite and limestone, overlie the Brassfield Limestone. The carbonates range from massive and porous to well bedded and dense. The average yields to wells completed in these rocks is about 16 gal/min. Some wells yield as much as 50 gal/min, and exceptional wells can yield 150 gal/min (Norris and others, 1948).

Table 2.—Water-level recoveries in selected bedrock wells

[Except for well GR-309, all of these wells are completed in the Ordovician shales; GR-309 has 60 feet of open hole, of which the first 20 feet is completed in the Brassfield Limestone and the last 40 feet is completed in the shales. --, slug test not done.]

Well	Date	Elapsed time [1] (minutes: seconds)	Water level [2] (feet below land surface)
GR-314	08-15-90	00:00	20.24
		00:01	22.60
		01:23	22.24
		05:59	21.88
		09:40	21.58
		16:42	21.22
		57:31	20.66
GR-303	09-25-90	00:00	10.93
		00:01	12.98
		03:05	12.63
		07:36	12.23
		12:25	11.90
		21:33	11.54
		39:36	11.15
GR-309	11-08-90	00:00	27.73
		00:01	28.54
		00:05	28.53
		00:09	28.20
		00:14	28.05
		00:21	27.93
		00:34	27.78
GR-315	01-18-89	--	259
	06-16-89	--	232
	12-13-89	--	207
	06-08-90	--	187
	12-17-90	--	168
	06-18-91	--	151
	12-30-91	--	138
GR-306	03-19-89	--	209
	05-18-89	--	126
	07-12-89	--	70
	09-13-89	--	44
	12-07-89	--	34

Table 2.—Water-level recoveries in selected bedrock wells—Continued

Well	Date	Elapsed time [1] (minutes: seconds)	Water level [2] (feet below land surface)
GR-306	06-27-91	--	172
	08-29-91	--	78
	10-23-91	--	52
	12-30-91	--	40
	02-25-92	--	36
GR-307	07-18-91	--	121
	09-27-91	--	83
	11-26-91	--	66
	01-31-92	--	55
	03-31-92	--	49
GR-311	04-12-89	--	266
	10-24-89	--	159
	04-16-90	--	105
	10-12-90	--	71
	04-24-91	--	49
	10-23-91	--	37
GR-312	07-18-91	--	106
	10-23-91	--	103
	01-31-92	--	101
	04-29-92	--	99
	07-29-92	--	98
MT-133	03-26-89	--	233
	03-30-89	--	80
	04-12-89	--	33

1 Recovery time from a slug test.

2 Water levels for GR-315, GR-306, GR-307, GR-311, GR-312, and MT-133 were rounded to the nearest foot.

The axis of the Cincinnati Arch trends in a north-south direction through western Ohio. Generally, the strata along the flank of the arch dip to the northeast at about 5 ft/mi. In Montgomery County, the rocks dip to the northeast at less than 1 ft/mi. In Clark County, the rocks dip about 15 ft/mi (Norris and others, 1948, 1952). In the Fairborn area, the dip of the rocks is affected by a small fold about 0.5 mi east of the Base. The fold extends from southwestern Greene County to southwestern Clark County. About 4 mi east of WPAFB the rocks are almost horizontal. Northwest of the Base the rocks dip to the northwest at about 15 ft/mi (Walton and Scudder, 1960).

Hydraulic Conductivity and Transmissivity

Hydraulic conductivity is a measure of the rate at which water can move through a porous media under a unit hydraulic gradient. Transmissivity is the rate at which water moves through a unit width of aquifer and is equal to the hydraulic conductivity multiplied by the saturated thickness of the aquifer.

Hydraulic conductivity is a function of the properties of the fluid and those of the porous material through which the fluid is moving. Except for unusual conditions, such as saline or high-temperature fluids, the properties of the fluid (viscosity and density) in an aquifer can be assumed to be constant. As a result, hydraulic conductivity can be thought of as a property of the porous media itself. In sediments, the degree of sorting, grain shape, and orientation affects hydraulic conductivity. Well-sorted sediments and coarse materials generally have greater hydraulic conductivities than do poorly sorted, fine-grained materials.

Hydraulic conductivities can be estimated by use of many methods, including laboratory permeameter tests, grain-size analysis, slug tests, and pumped-well aquifer tests. Bradbury and Muldoon (1990) found that the scale of the area considered (regional compared to site-specific compared to laboratory tests) influences estimates of hydraulic conductivity in glacial deposits. Measured hydraulic conductivities tend to increase with the size of test sample. For example, laboratory tests produce hydraulic conductivities that are one to two orders of magnitude lower than hydraulic conductivities derived from field tests (Bradbury and Muldoon, 1990).

Several common field methods are used to measure hydraulic conductivity. In unconfined aquifers, the most accurate field-scale estimates are obtained from pumped-well aquifer tests that last for several days and include water level measurements at several observation wells. Pumped-well tests produce large volumes of water that, because of concerns about the quality of ground-water at WPAFB, would have to have been contained and sampled; therefore, no pumped-well tests were done at WPAFB. Results from previous pumped-well tests at WPAFB and elsewhere in the study area were compiled. USGS personnel did slug tests instead of pumped-well tests at WPAFB. Hydraulic conductivities obtained from slug tests represent a smaller volume of the aquifer than those from pumped-well tests. As a result, the hydraulic conductivities estimated from slug tests tend to be lower than values estimated from pumped-well tests (Bradbury and Muldoon, 1990).

Results of Pumped-Well Aquifer Tests

Hydraulic conductivities and transmissivities from pumped-well tests in and around the study area are listed in table 3. The locations of the tests are shown on figure 9. All of these tests were done in unconsolidated deposits. Hydraulic conductivities range from 0.004 to 2,500 ft/d. Fewer transmissivity values are reported, probably because the saturated thickness of the aquifer was commonly unknown. The transmissivity values range from 2,140 to 37,400 ft^2/d.

At WPAFB, the range of horizontal hydraulic conductivities reported from pumped-well tests is 0.95 to 1,893 ft/d. Around Dayton, reported horizontal hydraulic conductivities are 134 to 334 ft/d for the sands and gravels. Transmissivities in the lower aquifer in the Dayton area range from about 16,700 ft^2/d at Rohrer's Island to greater than 33,000 ft^2/d south of Dayton. The maximum estimated transmissivity of the sands and gravels in the Dayton area is about 66,800 ft^2/d (Norris and Spieker, 1966).

Results of Slug Tests

Slug tests (displacement/recovery tests) were done at 45 wells at WPAFB. The locations of the test sites are shown on figure 10. Many of the sites are clusters at which two or more wells, with different screened intervals, were tested. Forty-one of the wells were completed in the unconsolidated deposits and four in the bedrock. Multiple tests were done on most of the wells. The slug-test data were analyzed according to the Bouwer and Rice (1976) method. Estimates of the horizontal hydraulic conductivity of the deposits, based on the slug-test data, are listed in table 4.

Although the actual thickness of the Ordovician shales was not known at any of the test sites, the Bouwer and Rice (1976) method was considered appropriate for estimating the hydraulic conductivity. The wells completed in the shale were assumed to be fully penetrating (in other words, the shale unit was assumed to be only 20 to 30 ft thick). Estimates of the hydraulic conductivity will decrease as the saturated thickness of the aquifer increases; thus, the result of the assumption is that the values shown on table 4 are the largest estimates of the hydraulic-conductivity for the shale, based on the slug-test data. Although the water level in well GR-309 recovered from the slug test in less than a minute (table 2), the estimated hydraulic conductivity is not much greater than those for the other three bedrock wells tested. Recovery was faster in GR-309 because the open interval and borehole diameter are larger than those of the other wells. These factors reduce the change in the water level during the test and thus reduce the recovery time. The higher hydraulic conductivity for GR-309 may also be an effect of the rock at the top few feet of the borehole, which consists of the more permeable Brassfield limestone.

Table 3. — Summary of horizontal hydraulic conductivities and transmissivities reported from pumped-well tests in the unconsolidated deposits at Wright-Patterson Air Force Base (WPAFB) and surrounding area

[--, data not available]

Test location	Data source	Site number in figure 9	Hydraulic conductivity (feet per day)	Transmissivity (feet squared per day)
WPAFB	Weston, Inc. (1989)	1	1.3[a]	--
WPAFB	Weston, Inc. (1989)	1	3.1 - 3.7	--
WPAFB	Weston, Inc. (1989)	2	18 - 274	--
WPAFB	Weston, Inc. (1989)	3	4.8[a]	--
WPAFB	Weston, Inc. (1989)	3	225	--
WPAFB	Weston, Inc. (1989)	4	111 - 310	--
WPAFB	Weston, Inc. (1989)	5	22.5[a]	--
WPAFB	Weston, Inc. (1989)	5	31.7 - 48.9	--
WPAFB	Weston, Inc. (1989)	6	69.1	--
WPAFB	Weston, Inc. (1989)	7	22.1	--
WPAFB	Weston, Inc. (1989)	8	61.0	--
WPAFB	Weston, Inc. (1989)	9	372	--
WPAFB	Weston, Inc. (1989)	10	28.3 - 273	--
WPAFB	Dames & Moore, Inc. (1986)	2	1,893[a]	--
WPAFB	Dames & Moore, Inc. (1986)	2	0.95[a]	--
WPAFB	Dames & Moore, Inc. (1986)	1	1.25 - 3.69[a]	--
WPAFB	Walton and Scudder (1960)	11	468	37,400
Rohrer's Island	Norris and Spieker (1966)	12	334	16,700
Rohrer's Island	Norris and Spieker (1966)	12	.004 - .017[b]	--
Rohrer's Island	Geraghty & Miller, Inc. (1987)	12	11 - 2,500	--
Rohrer's Island	U.S. Geological Survey files	12	--	19,500
Huffman Dam	U.S. Geological Survey files	13	--	34,500
SW Portland Cement	Walton and Scudder (1960)	14	308	2,140
Miami River well field	Norris and Spieker (1966)	15	308	--
Beardshear Road	U.S. Geological Survey files	16	221	30,100
Vandalia	U.S. Geological Survey files	17	--	10,200
Tait Station	Norris and Spieker (1966)	18	267	33,400
Frigidaire Plant 1	Norris and Spieker (1966)	19	134	5,350
Dryden Road	Norris and Spieker (1966)	20	214	32,100
Lamme Road	Norris and Spieker (1966)	21	267-334	--

[a] Value is from a slug test.

[b] Vertical hydraulic conductivity in a clay-rich unit.

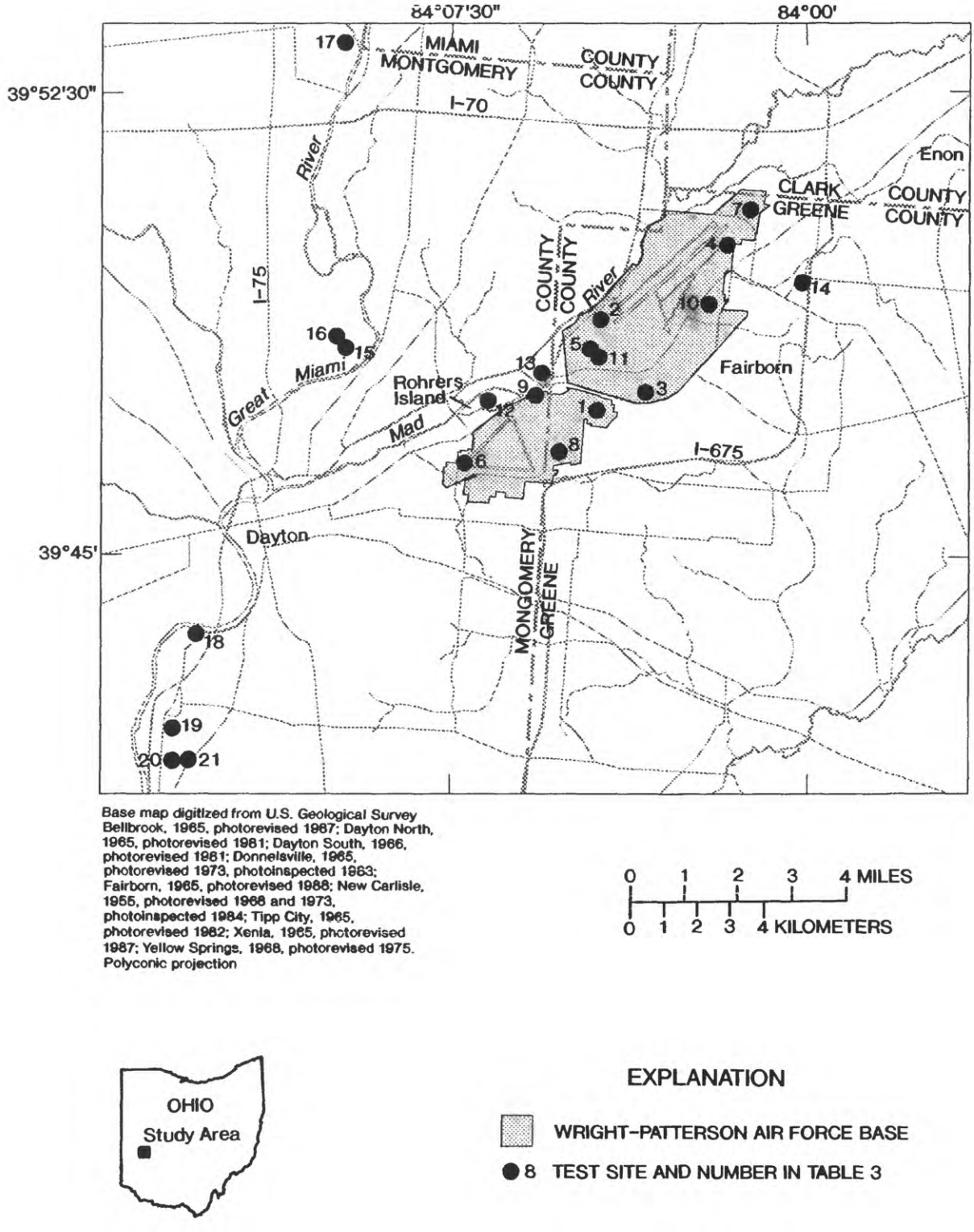

Figure 9.--Locations of pumped-well aquifer tests.

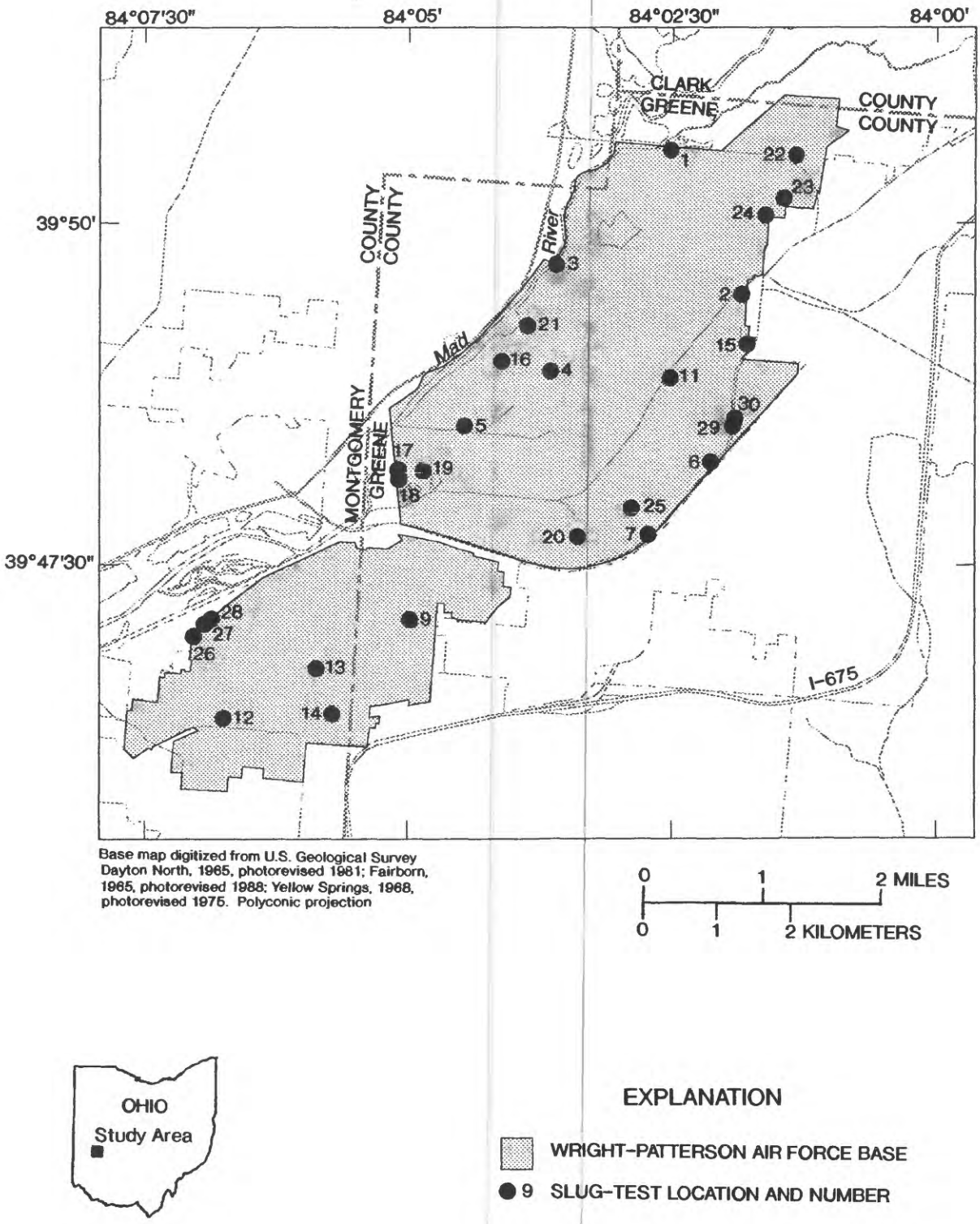

Figure 10.--Locations of slug-test sites.

Table 4.—Ranges of hydraulic conductivity determined from slug-test data for wells at Wright-Patterson Air Force Base

[h.c., horizontal hydraulic conductivity]

Well number	Site number in figure 10	Depth of screened interval[1] (feet)	Ranges of horizontal hydraulic conductivity (feet per day)	Number slug of tests done	Comments
GR-316	1	48-53	275-1002	4	median h.c. was 425
GR-317	1	126-131	2-36	4	
GR-318	2	43-48	79-901	3	median h.c. was 225
GR-319	2	151-161	87-202	4	median h.c. was 167
GR-314	2	233-243	.282, .329	2	bedrock well, screened
GR-320	3	17-22	330-888	5	median h.c. was 639
GR-303	3	51-61	.386, .393	2	bedrock well, screened
GR-321	4	38-43	375-564	4	median h.c. was 470
GR-322	4	137-147	155-232	4	median h.c. was 200
GR-323	5	46-51	61-100	4	
GR-324	5	118-128	112-536	6	median h.c. was 211
GR-330	6	40-50	212-469	4	median h.c. was 297
GR-331	6	105-115	112-184	4	
GR-332	6	186-196	26-31	3	
GR-326	7	34-39	107-131	4	
GR-327	7	144-154	142-301	6	median h.c. was 163
GR-328	7	240-245	116-125	3	
GR-309	9	44-104	9-12	4	bedrock well, 60 ft open hole-no screen
GR-312	9	116-136	.0016	1	bedrock well, 20 ft open hole-no screen
GR-333	11	25-35	27-35	4	
GR-334	11	145-155	67-99	4	
GR-335	11	225-235	30-85	6	
MT-152	12	26-36	72-130	6	
MT-153	12	80-90	17-34	4	
GR-329	13	45-55	210-771	3	median h.c. was 541
00-501	14	5-20	.036, .04	2	screened predominately in silt
00-600	15	80-90	14-20	4	
07-608	16	51-61	147-622	6	median h.c. was 184
08-020	17	11-21	35-55	6	
08-021	18	13-23	35-48	6	

Table 4.—Ranges of hydraulic conductivity determined from slug-test data for wells at Wright-Patterson Air Force Base—Continued

Well number	Site number in figure 10	Depth of screened interval[1] (feet)	Ranges of hydraulic conductivity (feet per day)	Number slug of tests done	Comments
08-022	19	26-36	338-393	4	
11-540	20	10-20	8-18	4	
11-618	20	55-65	86-105	4	
12-621	21	40-50	251-322	4	
13-551	22	12-22	83-282	3	median h.c. was 163
14-017	23	6-16	135-161	4	
14-625	23	50-60	9-11	4	
14-553	24	8-18	106-177	6	
14-626	24	65-75	25-27	4	
15-555	25	30-40	.33, .80	2	screened predominately in silt/fine sand
18-559	26	23-33	156-306	6	median h.c. was 265
18-560	27	25-35	230-582	6	median h.c. was 409
18-561	28	26-36	89-584	4	median h.c. was 228
23-577	29	30-40	132-280	6	median h.c. was 169
23-578	30	32-42	11-15	4	

1 Depths are in feet below land surface; all depths are rounded to the nearest foot.

The hydraulic conductivities of the unconsolidated deposits estimated from the slug tests are within the published ranges for sands and gravels (table 5). Most of the wells that were tested are screened in sands and gravels. A few of the wells are screened in very fine sands or silt. The hydraulic conductivities estimated from the tests at these wells are also within published ranges (table 5).

Table 5.—Horizontal hydraulic conductivities for selected types of unconsolidated deposits

[modified from Bouwer, 1978]

Type of deposit	Horizontal hydraulic conductivity (feet per day)
Clay	3.3×10^{-8} - .65
Sand	3 - 3×10^{2}
Gravel	3 - 3×10^{3}
Sand and gravel	16 - 3×10^{2}
Clay, sand, and gravel (till)	3.3×10^{-3} - .3

Ground-Water Recharge and Flow

The ultimate source of recharge to an aquifer is precipitation. Only some of the precipitation that falls in any area will infiltrate the soils and recharge an aquifer. Some proportion of precipitation will run off to surface-water bodies. The amount and pattern of runoff differs with storm intensity and basin characteristics such as topography, soil type and moisture content, geology, plant cover, and land use. Generally, runoff is greatest in areas of sloping terrain, with short intense storms, with saturated soil conditions, and in paved or urban areas (Freeze and Cherry, 1979; Fetter 1988).

The amount of precipitation that reaches an aquifer depends on many factors, including the soil type. In general, infiltration rates of coarse soils are greater than those of fine-grained soils. Most of the soils in the study area are silt loams with a moderate permeability of 0.6 to 2.0 in./hr. A silt loam is a soil consisting of 50 to 88 percent silt, 0 to 27 percent clay, and 0 to 50 percent sand (Garner and others, 1978; Davis and others, 1976; Lehman and Bottrell, 1978; Ohio Soil Survey, 1969; Petro, 1958).

In a ground-water budget for the valley-train deposits in the vicinity of WPAFB, Walton and Scudder (1960) estimated a net ground-water recharge rate of 12.4 in./yr from precipitation. Using a ground-water recession curve, J.T. de Roche (U.S. Geological Survey, written commun., 1990) estimated the recharge from precipitation at 12.4 to 15.8 in./yr. Ground-water recharge in the uplands is probably lower because of the predominance of clay-rich deposits and the proximity of the poorly permeable bedrock to the land surface.

Other sources of recharge to the unconsolidated deposits are subsurface flow from the bedrock-valley walls and infiltration from streams. Walton and Scudder (1960) estimated rates for subsurface flow from the valley walls to be 160,000 (gal/d)/mi of wall. They also estimated a total infiltration rate from both Hebble Creek and Mud Run of 2.68 Mgal/d.

Ground water flows from areas of high hydraulic head to areas of low hydraulic head. The contours on a potentiometric-surface map represent lines of equal hydraulic head (equipotential lines). Ground-water flow is perpendicular to potentiometric contours. The slope of the potentiometric surface, or change in head per unit of distance, is called the hydraulic gradient. In autumn 1987, USGS personnel measured water levels in more than 200 wells in the Dayton-WPAFB area. These data, combined with static water levels from driller's logs, were used to contour the water-level surface (Schalk, 1992). Wells in the study area are screened at many depths; thus, the ground-water surface represents neither semi-confined nor water-table conditions exclusively. Figure 11 is a smaller, modified version of the map by Schalk (1992).

Northwest of Areas A and C (WPAFB) is a regional ground-water divide. East of the divide, ground water flows toward the Mad River; west of the divide ground water flows toward the Great Miami River. North and east of Areas A and C, ground water flows toward the Mad River. Ground water flows both east and west from the ridge southeast of Area B. West of the ridge, flow is toward the Mad River, and, east of the ridge, flow is toward the Mad River or Beaver Creek. Ground water in the southeastern part of the study area flows to the south.

The hydraulic gradients in the uplands are generally 100 to 500 ft/mi (0.019 to 0.095). The hydraulic gradients in the valleys are lower, in the range of 5 to 50 ft/mi (0.00095 to 0.0095). The lower gradients reflect the flatter topography and the higher transmissivity of the valley-train deposits. The hydraulic gradient at WPAFB in Areas A and C is less than 10 ft/mi (0.0019), and the gradient in Area B is approximately 330 ft/mi (0.063) on the ridge and approximately 50 ft/mi in the valley west of the ridge.

Ground-water flow directions can be determined graphically with a flow net. A flow net is constructed by drawing equipotential lines based on water-level data and then drawing flowlines perpendicular to the equipotential lines. Water-level data collected from the well clusters provided data on vertical head gradients at WPAFB. A cross-sectional flow net was constructed along a horizontal flow line to determine vertical ground-water-flow directions, particularly between bedrock and valley-train deposits. The flow net is shown in figure 12. The line of section is the same as for the geologic section C-C′ and is shown on figure 5.

The flow net (fig. 12) shows that ground water is being recharged in the uplands northeast of WPAFB. Shallow ground water flows slightly downwards toward the center of the bedrock valley and then begins to flow upward; some ground water may discharge to surface-water bodies. Southwest of Huffman Dam, a steep downward gradient has formed in response to the pumping at Rohrer's Island. Deep ground water flows downward into the valley and then horizontally beneath WPAFB. The effects of pumping at Rohrer's Island can also be seen in the deeper ground-water-flow system.

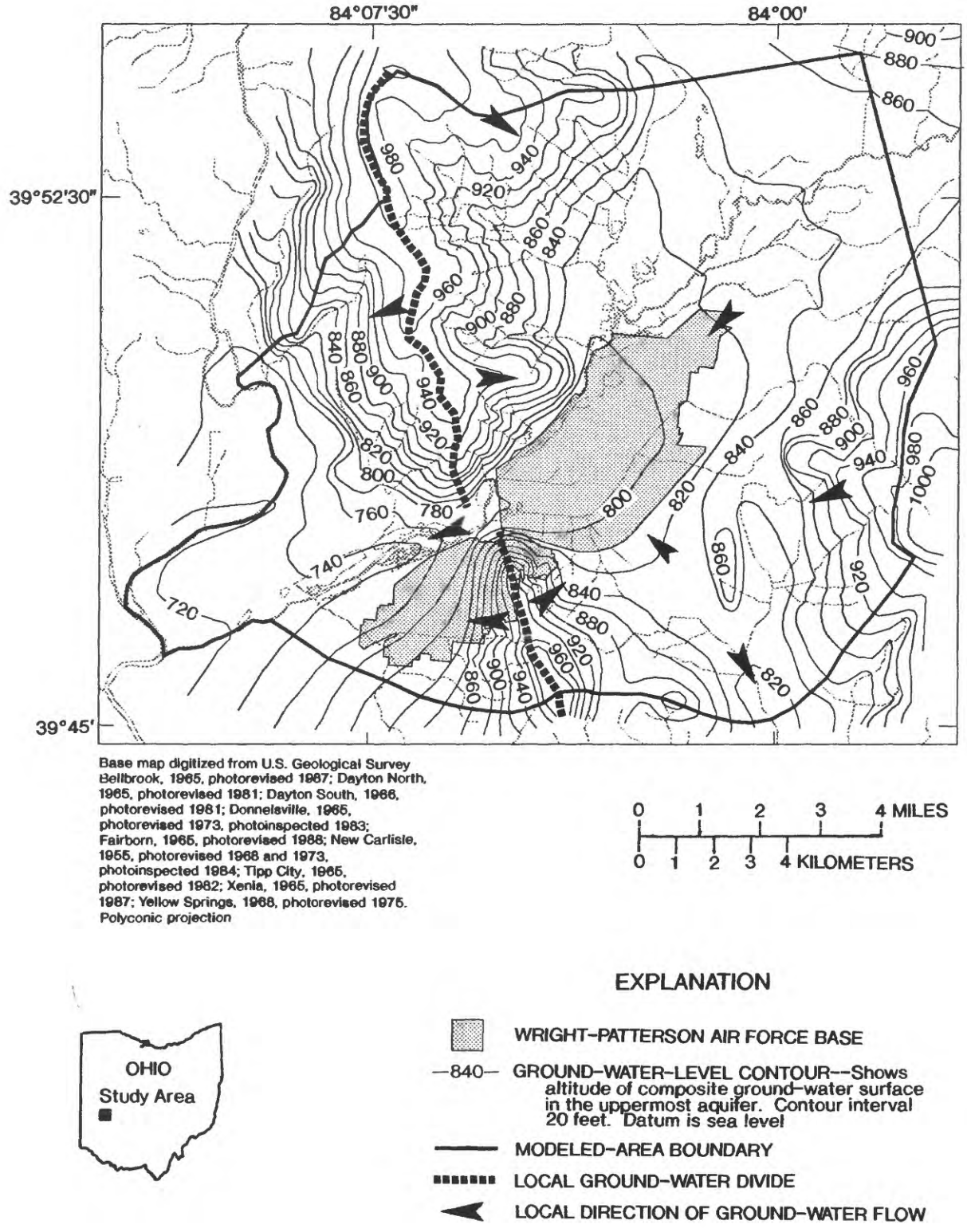

Figure 11.--Ground-water levels in the region. (Modified from Schalk, 1992.)

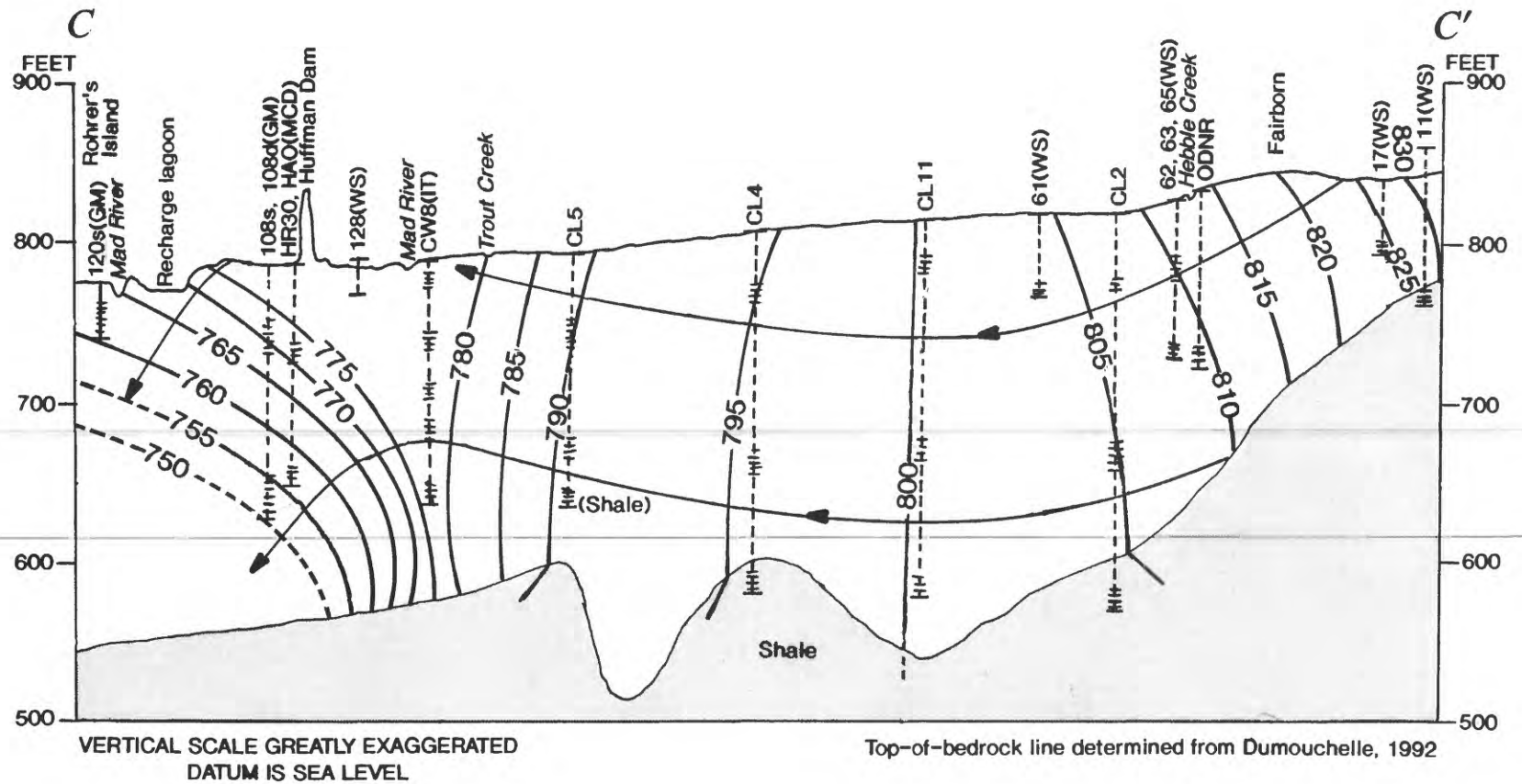
C
C′
FEET
900
800
700
600
500
120s(GM) Mad River
Rohrer's Island
Recharge lagoon
108s, 108d(GM) HR30, HAO(MCD) Huffman Dam
128(WS)
Mad River CW8(IT)
Trout Creek
CL5
CL4
CL11
61(WS)
CL2
62, 63, 65(WS) Hebble Creek
ODNR
Fairborn
17(WS)
11(WS)
765
760
755
750
775
770
780
785
790
795
800
805
810
815
820
825
830
(Shale)
Shale
VERTICAL SCALE GREATLY EXAGGERATED
DATUM IS SEA LEVEL
Top-of-bedrock line determined from Dumouchelle, 1992

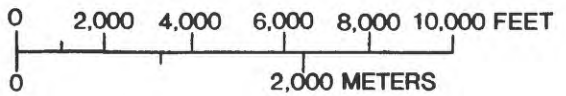

EXPLANATION

700 — POTENTIOMETRIC LINE--based on measured or reported water levels. Shows altitude at which water-level stands in tightly cased wells

GENERALIZED DIRECTION OF FLOW

WELL ON SECTION LINE

WELL PROJECTED TO SECTION LINE--All well except cluster 11 are within 1,000 feet of section line. Cluster 11 is 2,200 feet from the section line

WELL IDENTIFICATION

62(WS)	Log number in Walton and Scudder (1960)
CL5	Well-cluster number, wells drilled by U.S. Geological Survey. Location in figure 2 (Dumouchelle and deRoche, 1991)
ODNR	Well log on file with the Ohio Department of Natural Resources, Division of Water
120s(GM)	Well number in Geraghty & Miller, Inc. (1987)
HR30(MCD)	Well number in Miami Conservancy District files
CW8(IT)	Well cluster in IT Corporation (1960)

Figure 12.--Generalized vertical-section ground-water flow net. (Trace of section shown in figure 5.)

At well cluster 2, the hydraulic head in the bedrock is lower than in the valley-train deposits. Thus, in this area on the edge of the valley, ground water should move from the sands and gravels into the bedrock. In the center of the valley, at clusters 4 and 5, the hydraulic heads in the bedrock are higher than in the valley-train deposits, indicating flow from the bedrock into the sands and gravels. Data from other well clusters also show differences in the vertical hydraulic heads (table 6) between the bedrock and the valley-train deposits. However, given the difference in hydraulic conductivities between the shales and the sands and gravels, the volume of water flowing into or out of the bedrock is negligible compared to the flow within the valley-train deposits.

Surface-Water and Streambed Characteristics

The Mad River and its tributaries drain most of the region. Tributaries to the Mad River include Hebble, Mud, and Trout Creeks, Mud Run, and unnamed intermittent streams (fig. 13). Beaver Creek (fig. 1), which flows south to the Little Miami River (outside the study area), drains the south-central part of the study area. The western half of the uplands northwest of WPAFB drain to the Great Miami River (fig. 1). The Great Miami and Mad Rivers form the southeastern border of the study area. There are many small lakes in the region, most of which were created by gravel-mining operations.

The permeabilities of streambeds were estimated by use of data from seepage-meter tests and grain-size analyses. The locations of the test sites are shown on figure 13. Two sites on the Mad River, three sites on Hebble Creek, one site on Trout Creek, and one site each in Bass and Gravel Lakes were tested. Two samples for grain-size analysis also were collected at each of these sites. The hydraulic conductivities estimated from the seepage-meter and grain-size data are listed in table 7.

Two methods of analysis were used to estimate the hydraulic conductivity from the grain-size data. The first method (Hazen, 1911) requires the d_{10} effective grain-size diameter. At sites 4 and 8, the d_{10} fraction was too small to be determined with dry sieves, and thus the Hazen method could not be used. The second method (Masch and Denny, 1966) requires values for d_{16} and values of 1.5 mm or less for the d_{50} fraction. Only the samples from site 3 and the top sample from site 2 met these requirements. The hydraulic conductivities estimated with the grain-size data are of limited value because only one sample was collected at each site.

There are several orders of magnitude difference in streambed hydraulic conductivities determined by the three methods (table 7). Grain-size methods are used to determine horizontal hydraulic conductivities, whereas the seepage meter is used to determine vertical hydraulic conductivities. Vertical hydraulic conductivities are generally lower than horizontal hydraulic conductivities. Furthermore, the relation between grain-size distributions and hydraulic conductivities is proportional to grading uniformity. At site 3, the grain-size distribution was more uniform that at any of the other sites, and agreement between methods was the best for this site. The high values determined in the Hazen method reflect the greater variability in the grain-size distributions of those samples.

Table 6.—Vertical hydraulic gradients between the bedrock and the valley-train deposits at Wright-Patterson Air Force Base

[Well-screen midpoint depths are in feet below land surface; B refers to the bedrock well in each set; U refers to an upward gradient; D refers to a downward gradient, -- not applicable]

Well number	Site number in figure 10	Midpoint of well screen	Gradient on November 13, 1990	Gradient on February 21, 1991	Gradient on June 19-28, 1991
GR-314 B	2	238	--	--	--
GR-318		45	0.019 D	0.023 D	0.017 D
GR-319		156	.0094 D	.005 D	.0013 U
GR-303 B	3	55	--	--	--
GR-320		19	.024 U	.020 U	.029 U
GR-304 B	4	221	--	--	--
GR-321		40	.0095 U	.0086 U	.0067 U
GR-322		142	.009 U	.0054 U	.014 U
GR-305 B	5	153	--	--	--
GR-323		48	.018 U	.021 U	.020 U
GR-324		123	.037 U	.038 U	.034 U
GR-306 B	6	233	--	--	--
GR-330		45	.008 U	.0078 U	.010 U[1]
GR-331		110	.011 U	.011 U	.014 U[1]
GR-332		191	.023 D	.025 D	.017 D[1]

Table 6.—Vertical hydraulic gradients between the bedrock and the valley-train deposits at Wright-Patterson Air Force Base—Continued

Well number	Site number in figure 10	Midpoint of well screen	Gradient on November 13, 1990	Gradient on February 21, 1991	Gradient on June 19-28, 1991
GR-307 B	7	273	--	--	--
GR-326		36	0.022 D	0.026 D	0.026 D[1]
GR-327		149	.042 D	.051 D	.050 D[1]
GR-328		242	.028 D	.056 D	.053 D[1]
MT-133 B	12	237	--	--	--
MT-152		31	.037 D	.039 D	.036 D
MT-153		85	.05 D	.052 D	.052 D
GR-313 B	13	89	--	--	--
GR-329		50	.031 D	.029 D	.033 D

[1] Gradient on May 21, 1991.

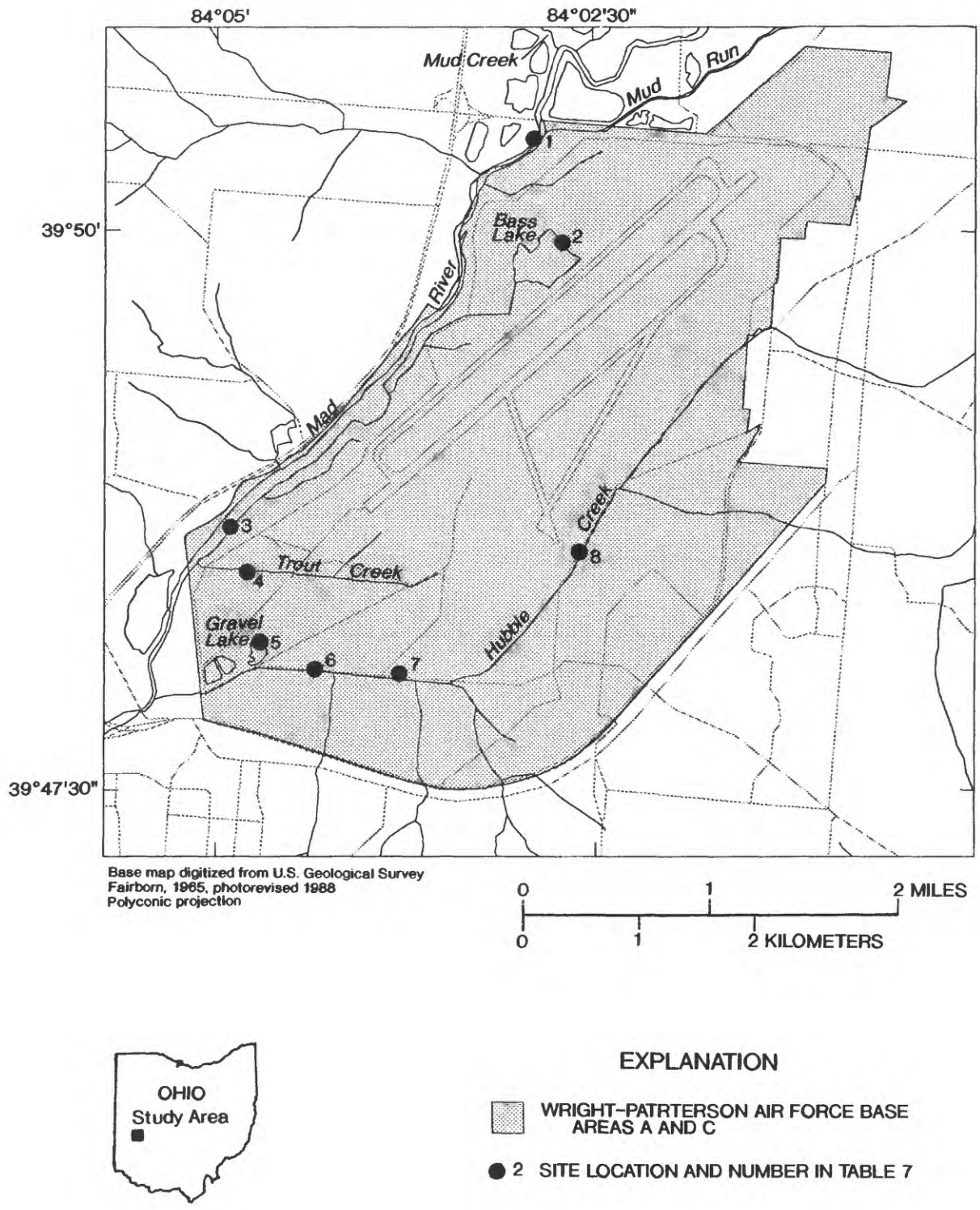

Figure 13.--Locations of sites for seepage-meter tests and streambed grain-size sampling.

Table 7.—Estimates of streambed hydraulic conductivity

[(T) refers to the sediment sample from 0 to 6 inches below the streambed; (B) refers to the sample from 6 to 12 inches. Two seepage-meter tests were done at each site except at site 8, where only one test was done. --, hydraulic conductivity not computed.]

Site number in figure 13	Location	Hydraulic conductivity (feet per day)			
		Seepage meter		Hazen[1]	Masch and Denny[2]
1	Mad River	13.6 - 18.7	(T)	5,560	--
			(B)	13,750	--
2	Bass Lake	5.9 - 7.6	(T)	400	12.6
			(B)	400	--
3	Mad River	10.9 - 13.7	(T)	92	46.9
			(B)	92	57
4	Trout Creek	.01 - .02		--	--
5	Gravel Lake	.56 - .84	(T)	12,500	--
			(B)	4,080	--
6	Hebble Creek	.02 - .1		1,310	--
7	Hebble Creek	.006 - .0007		500	--
8	Hebble Creek	.024		--	--

[1] Hydraulic conductivity determined from the grain-size data by use of the method described by Hazen (1911).

[2] Hydraulic conductivity determined from the grain-size data by use of the method described by Masch and Denny (1966).

Ground-Water/Surface-Water Relations

Gaining streams are streams in which the base flow increases downstream regardless of the inflow of tributaries. Along gaining streams, the water table is higher than the streambed, and ground water seeps through the streambed and banks into the stream. Losing streams, decrease in base flow downstream. Along losing streams, the water table is lower than the streambed, and water seeps through the streambed and banks, recharging the aquifer. During the year, as the water table fluctuates, a stream may change from one type to the other.

Whether a stream is gaining or losing in any given reach can be determined by a gain/loss study. This kind of study consists of a series of discharge measurements along a stream and its tributaries. When the input from tributaries is accounted for, changes in discharge between any two points must be due to the gain from or loss to ground water. On July 23, 1991, the USGS personnel made a series of discharge measurements along the Mad River from northeast of the study area to downstream of Rohrer's Island. The measurement sites and measured discharges for the Mad River within the study area are shown on figure 14.

The discharge measurements on the Mad River were rated as fair to good; these ratings mean the estimated error of the measurements was from 5 to 8 percent. These ratings and similar ratings for measurements on tributaries indicate that, for the reach of the Mad River from I-70 to Huffman Dam, the gain or loss of water cannot be reliably determined. The data suggest that the Mad River is gaining water from I-70 to Huffman Dam. From Huffman Dam to downstream of Harshman Road, the changes in discharge exceed the estimated errors in the measurements. In this reach, the Mad River lost 80 ft^3/s. The loss is due to diversion of the Mad River to lagoons used to recharge the aquifer beneath the Mad River well field.

The gain or loss of Hebble Creek also was measured (fig. 15). The discharge measurements on Hebble Creek were all rated as good (estimated errors of 5 percent), and the changes in discharge exceeded the 5-percent estimated error. From I-675 to the WPAFB boundary, the creek lost 0.62 ft^3/s, a loss of about 0.48 $(ft^3/s)/mi$. From the Base boundary to Skeel Avenue, the creek runs underground in a storm sewer. Discharges from drains were not measured. From Skeel Avenue to Hebble Creek Road, 0.16 ft^3/s was lost (about 0.129 $(ft^3/s)/mi$). Along Hebble Creek Road to near Twin Lakes, the creek lost 0.55 ft^3/s (0.39 $(ft^3/s)/mi$). The measurements on Trout Creek were within the estimated errors; thus, the gain or loss of water in the creek could not be determined.

Water-level measurements in three piezometers set in Hebble Creek confirmed that the creek recharged the aquifer over most of the measurement period. The three piezometers were set in Hebble Creek, near seepage-meter sites 6, 7, and 8 (fig. 13). The water level in the piezometer near site 8 was measured about every month for 2 years. The water level in the piezometer was always lower than the level of the creek, indicating that the stream was recharging the aquifer (fig. 16). The piezometer near site 7 was measured about once a month for 9 months. The water level in the piezometer was generally lower than the level of the creek. The measurements at the third piezometer were considered unusable because of scouring around the pipe. Piezometers also were set in Bass, Gravel, and south Twin Lakes. The data from these piezometers indicate that in all of

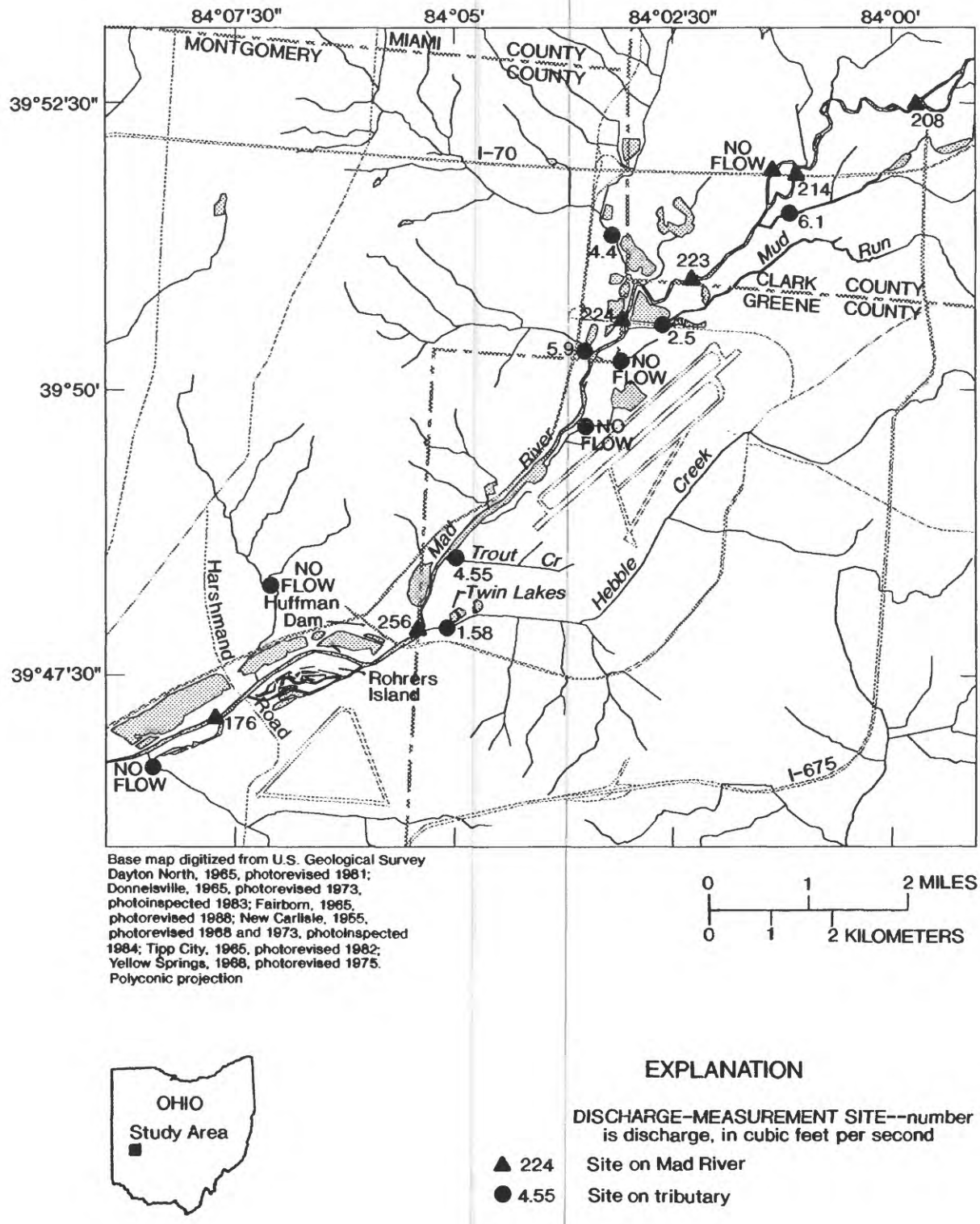

Figure 14.--Location of discharge-measurement sites and discharge on Mad River and tributaries, July 23,1991.

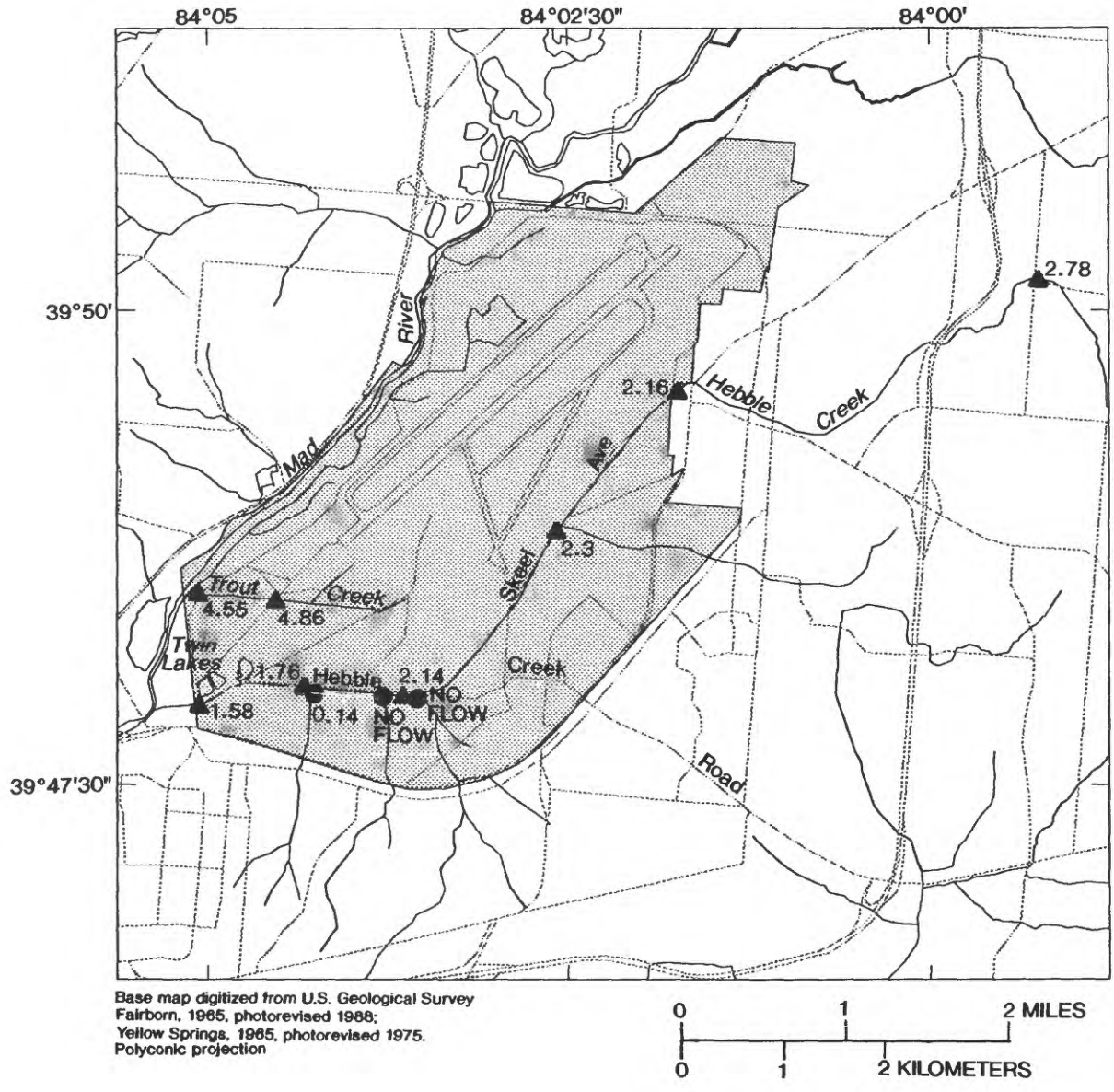

EXPLANATION

DISCHARGE-MEASUREMENT SITE--Number is discharge, in cubic feet per second

▲ 2.14 Site on Mad River

● 0.14 Site on tributary

Figure 15.--Discharge-measurement locations on Hebble Creek, Trout Creek, and tributaries.

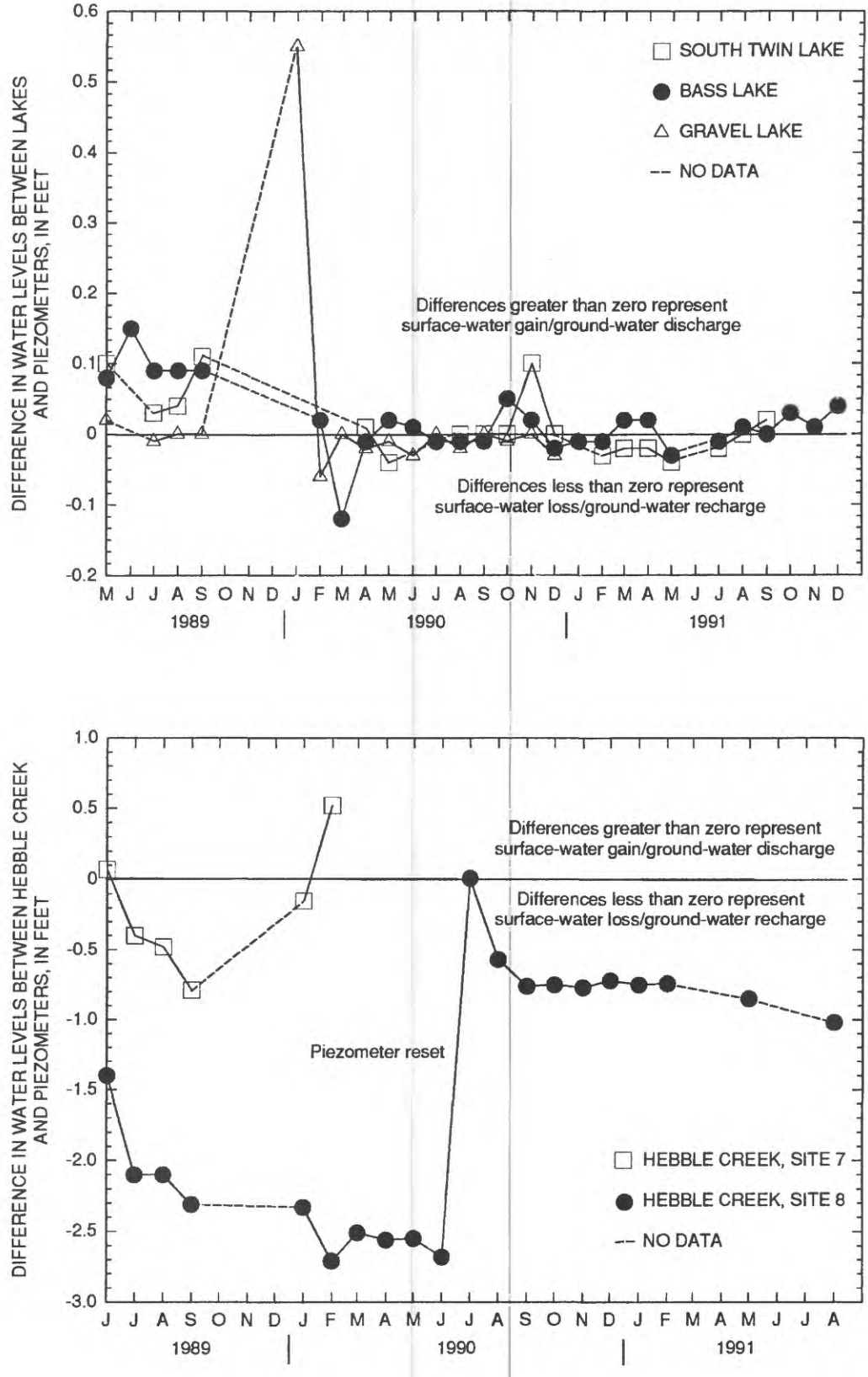

Figure 16.--Hydrographs of piezometer data.

the lakes, gains and losses fluctuated with no apparent relation to season (fig. 16). During summer 1989, Bass and south Twin Lakes were gaining ground water. In Gravel Lake, the water levels in the piezometer and the lake were either equal or indicated the loss of water. From April 1990 through December 1991, the water level in each lake was about the same as the level in the piezometer at that lake, with both gains and losses indicated.

The interaction of ground water and surface water also can be examined by comparing water-level records for wells near a river and discharge records for the river. A discharge hydrograph for the Mad River, a precipitation record from the National Weather Service's station in Dayton, and hydrographs from four wells near the river are shown in figure 17. The streamflow-gaging station on the Mad River is just upstream from Huffman Dam. Wells GR-208 and GR-210 (fig. 2) are screened in the unconsolidated deposits from 4.5 to 19.5 and 33 to 38 ft below the land surface, respectively. Well GR-320 is screened from 16.8 to 21.8 ft below land surface in the unconsolidated deposits, and GR-303 is screened from 51.4 to 61.4 ft below land surface in the Ordovician shales. These wells are at site CL-3 on figure 2.

The water-level hydrographs from wells GR-208 and GR-210 (fig. 17C) show that water levels in these wells respond quickly to precipitation events (fig. 17B) and drop fairly quickly after the events. The similarity of the water-level records and the river hydrograph (fig. 17A) indicate that the aquifer is in hydraulic connection with the river. The water levels in well GR-210 are about 1 ft higher than in the shallower well, GR-208 (fig. 17C). This consistent upward gradient indicates that this is a discharge area for the aquifer. The gain/loss data from the Mad River also indicate that the river is gaining ground water along the reach near these wells.

The water levels in wells GR-210 and GR-208 were measured hourly, whereas the water levels for wells GR-303 and GR-320 were measured monthly. The effect of the less frequent measurements can be seen in the less detailed hydrographs (fig. 17D). GR-303 and GR-320 probably respond in a similar manner to GR-210. This can be seen in the peaks of February and July 1990, which correspond closely to precipitation events and peaks in the other ground-water hydrographs. The monthly measurements missed the peaks in 1991; however, the general rise in water levels during the winter months of 1991 corresponds closely with the peaks and higher levels seen in the other hydrographs.

Water-level differences between the wells GR-303 and GR-320 also indicate a consistent upward gradient. The response of the bedrock well, GR-303, indicates that the bedrock in this area may be fractured or weathered enough to respond like shallower wells screened in unconsolidated deposits. The bottom of the Mad River is probably within 10 ft of bedrock in this area. The integrity of the well casing was tested with a packer test after drilling. The well casing and surface seals were intact, so the response could not be attributed to faulty well construction.

In addition to providing data for determining streambed conductivity, the data from the seepage-meter tests can indicate flow directions. The tests were done on the Mad River, Trout and Hebble Creeks, and Bass and Gravel Lakes (fig. 13) in August 1988. The Mad River and Bass Lake sites gained ground water. Trout Creek and Gravel Lake lost water to the aquifer. All of the Hebble Creek sites lost water. The piezometer data (fig. 16) showed that Hebble Creek gained

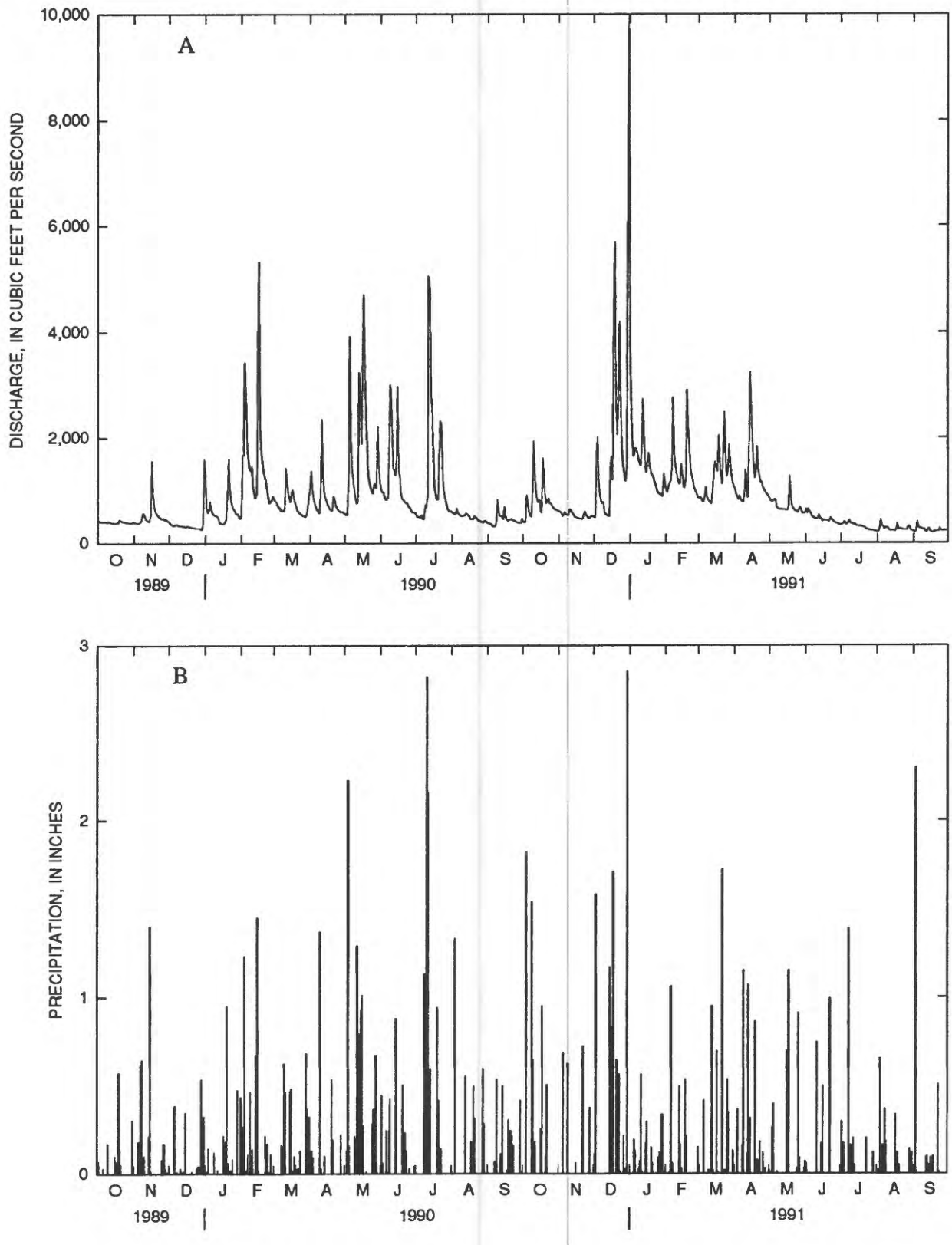

Figure 17.--Hydrographs of (A) daily mean discharge of Mad River near Dayton, (B) precipitation at Dayton, (C) water levels in wells GR-208 and GR-210, and (D) water levels in GR-320 and GR-303.

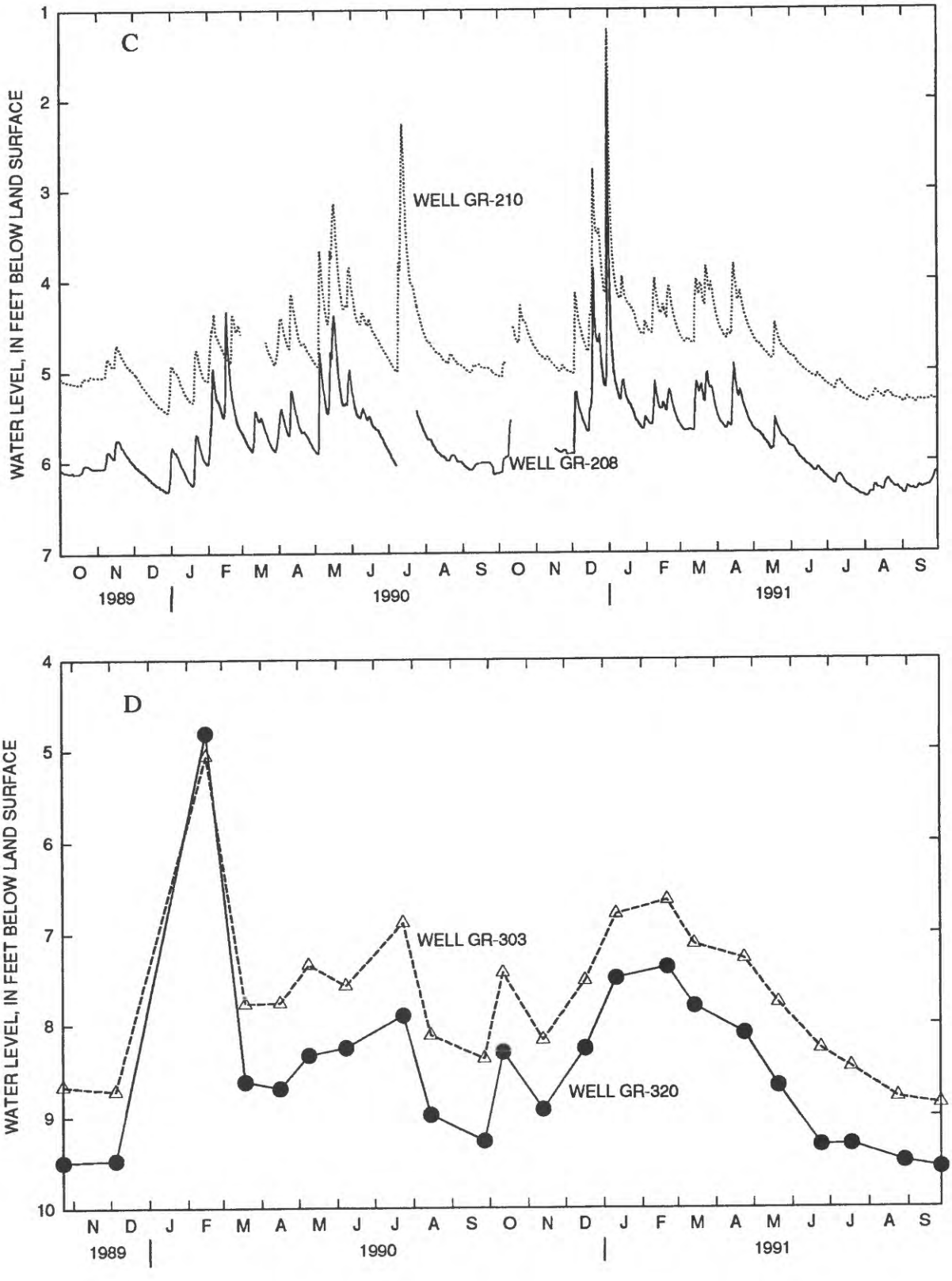

Figure 17.--Hydrographs of (A) daily mean discharge of Mad River near Dayton, (B) precipitation at Dayton, (C) water levels in wells GR-208 and GR-210, and (D) water levels in GR-320 and GR-303--Continued.

ground water. Together, the two sets of data show that the creek can alternate between gaining and losing water in response to changes in ground-water levels.

The gain/loss, piezometer, ground-water level, and seepage-meter data define the interaction of surface and ground water in Areas A and C. Trout and Hebble Creeks and Bass and Gravel Lakes alternated between ground-water gains and losses. The Mad River gains ground water. These data and the data on the hydrogeology were used to develop and refine the conceptual and numerical models of ground-water flow.

SIMULATED REGIONAL GROUND-WATER FLOW

The modular, finite-difference digital computer program of the USGS (McDonald and Harbaugh, 1988), hereafter referred to as "MODFLOW", was used to construct a regional, three-dimensional, steady-state model of ground-water flow. This program solves the ground-water-flow equations (see section on "Description of the Numerical Model") at discrete and regularly arranged points, or nodes, by an iterative algorithm. Because of the nature of finite-difference formulations, the solution is approximate in several respects (McDonald and Harbaugh, 1988; Wang and Anderson, 1982). First, most of the input data (such as hydraulic conductivity and recharge) must be estimated spatially and (or) quantitatively. These estimates are constrained by the range of what is hydrologically reasonable, on the basis of measured data. Second, the formulations are solved discretely rather than continuously in the modeled area. Solutions at the nodes can be used to estimate the nature of the flow system between the nodes. Third, because its solution method is iterative, MODFLOW requires a user-defined tolerance to instruct it when to stop the computation. The solution of the current iteration is compared with that of the previous iteration; if the solutions are with the tolerance, computation ceases.

A user-defined grid divides the modeled area into rectangular, prismatic cells that represent discrete volumes of the flow system. The node of each cell, located at the center of the cell, is assigned hydrologic parametric values representative of conditions in its cell. Grid spacing and orientation commonly are chosen to balance the level of detail with the computational requirements. Hydraulic heads at nodes and volumetric fluxes between cells are calculated by MODFLOW. Calibration is the process whereby parameter values are changed subjectively, one at a time and within reasonable ranges, until heads (water levels) and fluxes (flow rates) calculated by the model are acceptable. When head and flux values obtained from the model match approximately those measured or estimated from field data, the model is assumed to represent adequately the ground-water-flow system within the limitations of the available data and computational method.

Most of the input data sets for this ground-water-flow model were generated and processed in ARC/Info, a vector-based geographic information system (GIS) (Environmental Systems Research Institute, 1987). Information stored in GIS data layers was converted into data sets for MODFLOW. ARC/Info's TIN (triangulated irregular network) package, which was used to draw the contour lines in several figures of this report, is based on a linear interpolation method and the assumption that the feature surface is constant between data points.

The purpose of this modeling study is threefold: (1) to determine and evaluate sources and sinks of ground-water flow in the area centered on WPAFB; (2) to use the ground-water-flow model as a tool for understanding the hydrogeologic aspects of the flow system, including recharge and hydraulic conductivity; and (3) to evaluate the hydrologic interdependency of the valley-train aquifer and the bedrock upon which it lies. The sections that follow describe in turn the conceptualization of the flow system; the assumptions, hydrogeologic framework, and boundary conditions that support the conceptualization; the parameters used to define the numerical model; and analyses of the simulations made using the numerical model.

Description of the Conceptual Model

The nature of the flow system must be evaluated before MODFLOW is implemented. Particularly important to the modeling effort are model configuration, boundary conditions, sources and sinks of water, and general flow directions. Field-based data, including, for example, water levels, aquifer characteristics, and precipitation records, are used to create a conceptual model—a clear, qualitative, mental and physical picture of the natural system. The validity of the solution returned by MODFLOW must be assessed in light of the conceptual model. The conceptual flow system discussed in this section is based on the data and interpretations described in the "Hydrogeology" section of this report.

The project area was, for the most part, limited to the 12 mi^2 within the boundaries of WPAFB. The modeled area, however, encompassed a larger area centered on WPAFB; thus, this report describes a regional model. The model boundaries were extended beyond the Base boundaries for two reasons. First, actual hydrogeologic boundaries, such as streamlines and (or) ground-water divides, should be used in the model wherever possible. Most of the northwestern and southeastern boundaries of the model are actual hydrogeologic boundaries. Second, artificial hydrogeologic boundaries, such as estimated water fluxes, that are set at sufficient distance from the Base should not significantly affect flow simulation near or on the Base. For this reason, the northeastern and southwestern boundaries of the model stretch from Enon to Dayton, although the model was not designed to simulate conditions at either extreme. (See section on "Boundary Conditions" for a discussion of types of boundary conditions used in this model.)

Two distinct flow regimes exist near WPAFB. The unconsolidated deposits in buried valleys near WPAFB are permeable and extensive; most of the ground-water flow in the region occurs in these buried valleys. The shale bedrock underlying the valleys is dense and virtually impermeable and does not contribute greatly to regional ground-water flow. Thus, the shale is considered the lower no-flow boundary throughout the modeled area. Thus limestone bedrock in upland areas is more permeable than the shale that underlies it; ground water discharges from the limestone at the limestone-shale contact in the form of springs and seeps that contribute to surface flow.

A map of water levels in 1987 (Schalk, 1992), reproduced in figure 11, was used to conceptualize flow conditions at lateral boundaries. Ground-water divides form no-flow boundaries in the uplands; streamlines form no-flow boundaries elsewhere. Generally, shallow flow in the buried valleys underlying WPAFB is toward the Mad River, but a deeper component of flow is toward the southwest, along the axis of the buried valley beneath WPAFB. Because of this deep flow component, some flow occurs across the model boundaries where the boundaries

transect the buried valleys. Schalk (1992) presented evidence that the flow system near WPAFB is relatively constant with time; thus, the system was modeled as steady state.

The Mad River interacts closely with the valley-train aquifer. North of Huffman Dam, the river gains water from the aquifer, which is supplied by precipitation and, to a lesser extent, by discharge from the valley walls. The flow of the Mad River is the most sustained streamflow of all major streams in Ohio, even during periods of drought (Norris and others, 1952; Cross and Feulner, 1964). River leakage, especially near the Mad River well field south of Huffman Dam, is a source of water to the aquifer. Artificial recharge lagoons on Rohrer's Island allow increased infiltration from the river to the aquifer. Smaller streams, such as Hebble Creek, do not interact closely with the regional flow system.

Description of the Numerical Model

The numerical model is created from the conceptual model by converting idealizations of the flow system into data sets and parameters for MODFLOW. The partial differential equation governing steady-state ground-water flow is a combined form of Darcy's law and the continuity equation (Wang and Anderson, 1982), written as

$$\frac{\partial}{\partial x}(-K_x\frac{\partial h}{\partial x}) + \frac{\partial}{\partial y}(-K_y\frac{\partial h}{\partial y}) + \frac{\partial}{\partial z}(-K_z\frac{\partial h}{\partial z}) = 0, \qquad (2)$$

where x, y, and z are the three directional variables; K_x, K_y, and K_z are the hydraulic conductivities of the aquifer media in the x-, y-, and z-directions, respectively; and h is the hydraulic head in the aquifer at the point (or node) where the equation is being solved. A finite-difference form of equation 2 is

$$- K_{x_{(i-1),j,k}}\Delta y\Delta z\frac{(h_{i,j,k} - h_{(i-1),j,k})}{\Delta x} - K_{y_{i,(j-1),k}}\Delta x\Delta z\frac{(h_{i,j,k} - h_{i,(j-1),k})}{\Delta y}$$

$$- K_{z_{i,j,(k-1)}}\Delta x\Delta y\frac{(h_{i,j,k} - h_{i,j,(k-1)})}{\Delta z} + K_{x_{(i+1),j,k}}\Delta y\Delta z\frac{(h_{(i+1),j,k} - h_{i,j,k})}{\Delta x}$$

$$+ K_{y_{i,(j+1),k}}\Delta x\Delta z\frac{(h_{i,(j+1),k} - h_{i,j,k})}{\Delta y} + K_{z_{i,j,(k+1)}}\Delta x\Delta y\frac{(h_{i,j,(k+1)} - h_{i,j,k})}{\Delta z} = 0, \qquad (3)$$

where Δx, Δy, and Δz are distances between nodes in the x-, y-, and z-directions, respectively, and subscripts (i -1) and (i +1), for example, are coordinates that refer to nodes on either side of node i, j, k in the x direction (fig. 18). Columns, rows, and layers correspond to x-, y-, and z-directions and i-, j-, and k-coordinates, respectively, in MODFLOW.

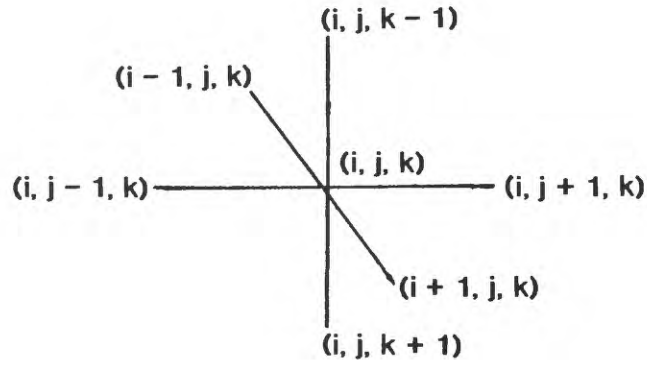

Figure 18.--Orthogonal seven-point star representing three-dimensional finite-difference approximation in MODFLOW.

Simplifying assumptions commonly are needed to satisfy equation 3 in the mathematical code. The following sections describe the assumptions, boundary conditions, and parameters used to construct and calibrate the model.

Assumptions

The following assumptions and simplifications were incorporated into the ground-water-flow model:

1. The shale bedrock is not an aquifer; therefore, it is not included as an active layer (see next section) in the model except where it is the uppermost saturated medium in layer 1. The limestone bedrock is not modeled as a separate layer because it is isolated from the buried valleys and is present only locally throughout the modeled area.
2. Ground-water levels in the last three months of 1987 approximate average annual water levels in the modeled area. The ground-water system is at steady state; that is, no net gain or loss of water occurs in the modeled area.
3. Confining clays in the buried valleys are continuous southwest of Huffman Dam and discontinuous northeast of the dam. Two aquifers in the valley train deposits, separated by the confining clay, are present southwest of the dam. One aquifer in valley train is present northeast of the dam.
4. The shallow part of the buried-valley aquifer is in close hydraulic connection with the Mad and Great Miami Rivers.
5. The streambed thickness of all rivers and surface drains is 1 ft.
6. Each well fully penetrates the layer in which it is completed.
7. Horizontal hydraulic conductivity in each layer is uniform with depth in that layer but is variable areally.

Discrete Hydrogeologic Framework

The arrangement of cells used in a finite-difference model is called a grid. Grid spacing, orientation, and layering are chosen to accommodate all aspects of the modeling effort: natural boundaries and flow conditions, amount of field data, limitations of numerical modeling, and desired use of the flow model.

Grid spacing and orientation

The grid pattern used to create the flow model is displayed in figure 19. Grid spacing is variable; the smallest, most refined cells are in the vicinity of pumping centers (Rohrer's Island and WPAFB production wells) and steep hydraulic gradients (near Huffman Dam). Closely spaced cells help to increase detail, model stability, and computational accuracy in these areas. The model grid is 102 rows by 110 columns; cell dimensions are 500, 750, or 1,000 ft per side. Grid orientation is 46.5 degrees east of north, which was chosen to ensure that ground-water flow is parallel to the cell axis i (see figure 18), which also is parallel to the primary flow direction of the Mad River through the modeled area.

Grid layering

The ground-water-flow model has three layers (figures 20 and 21). The first layer (shallowest) has 6,132 active cells and encompasses 101 mi^2. Layer 1 was defined as the upper 20 to 200 ft of saturated media. The thicker areas of layer 1 correspond to the uplands, primarily shale bedrock, in the modeled area. Active in layer 1 are upland areas and valley-train deposits. Ground-water flow between the two regimes is modeled only at the interface of the uplands and the valley-train deposits in layer 1, as shown in figure 21. This interface is rather thin, consisting of an average of 56 ft of shale and unconsolidated deposits. In this numerical model, flow from the shale to the valley-train deposits was simulated only along the thin interface, not along the entire depth of the valley wall. The lower boundary of layer 1 in the upland areas is at an elevation approximately equal to that of the bottom of layer 1 in the valley-train deposits. This assignment of the lower boundary causes the thickness of layer 1 to increase with distance from the buried valleys because the top of the zone of saturation rises away from the valleys. Because the vertical hydraulic conductivity of the shale is small, the bottom of layer 1 in the uplands is modeled as a no-flow boundary. Hence, the assignment of elevation to the bottom of layer 1 in the uplands is somewhat arbitrary. The scheme presented here was chosen so that the thickness of layer 1 would be great enough to ensure numerical stability.

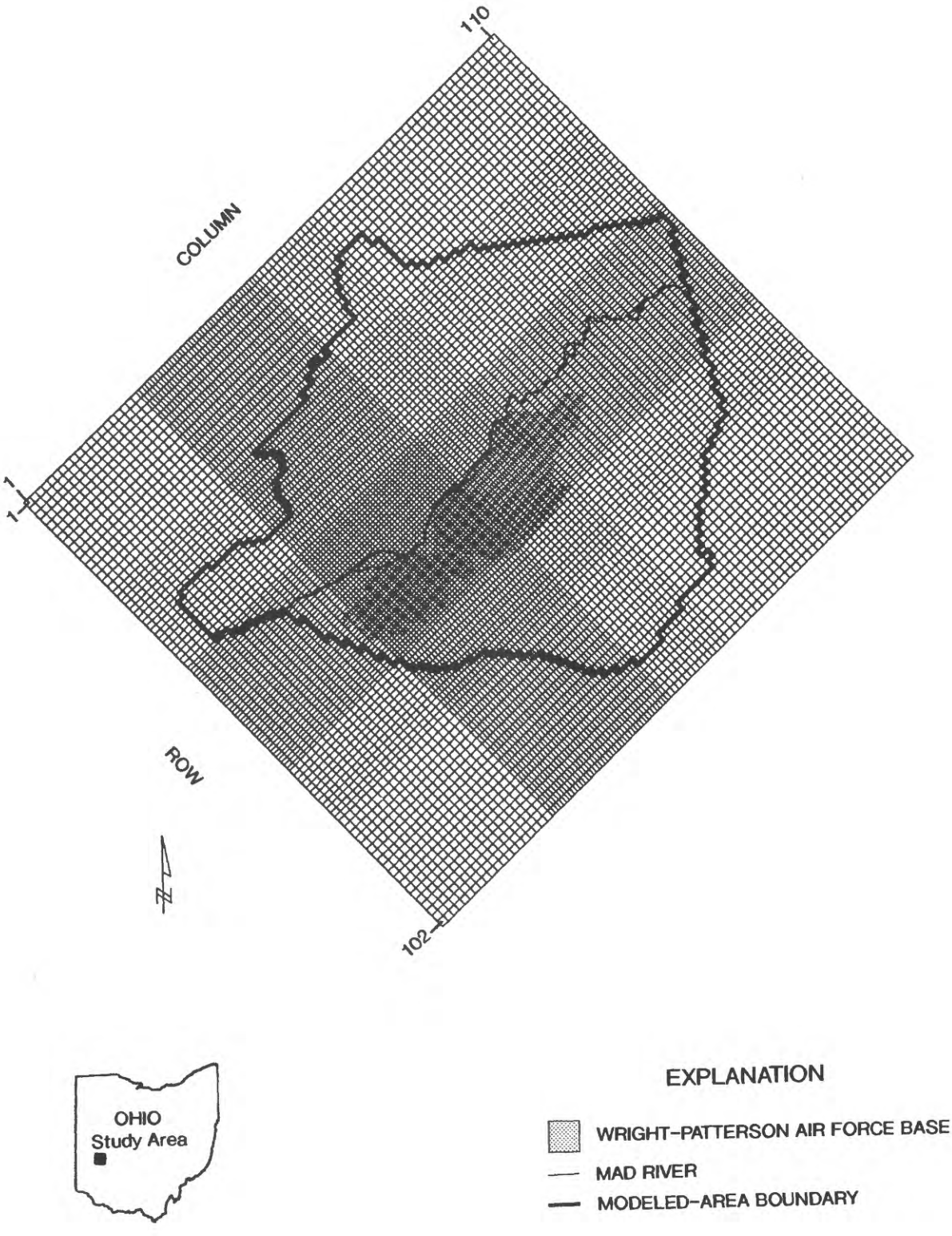

Figure 19.--Model grid in relation to modeled area.

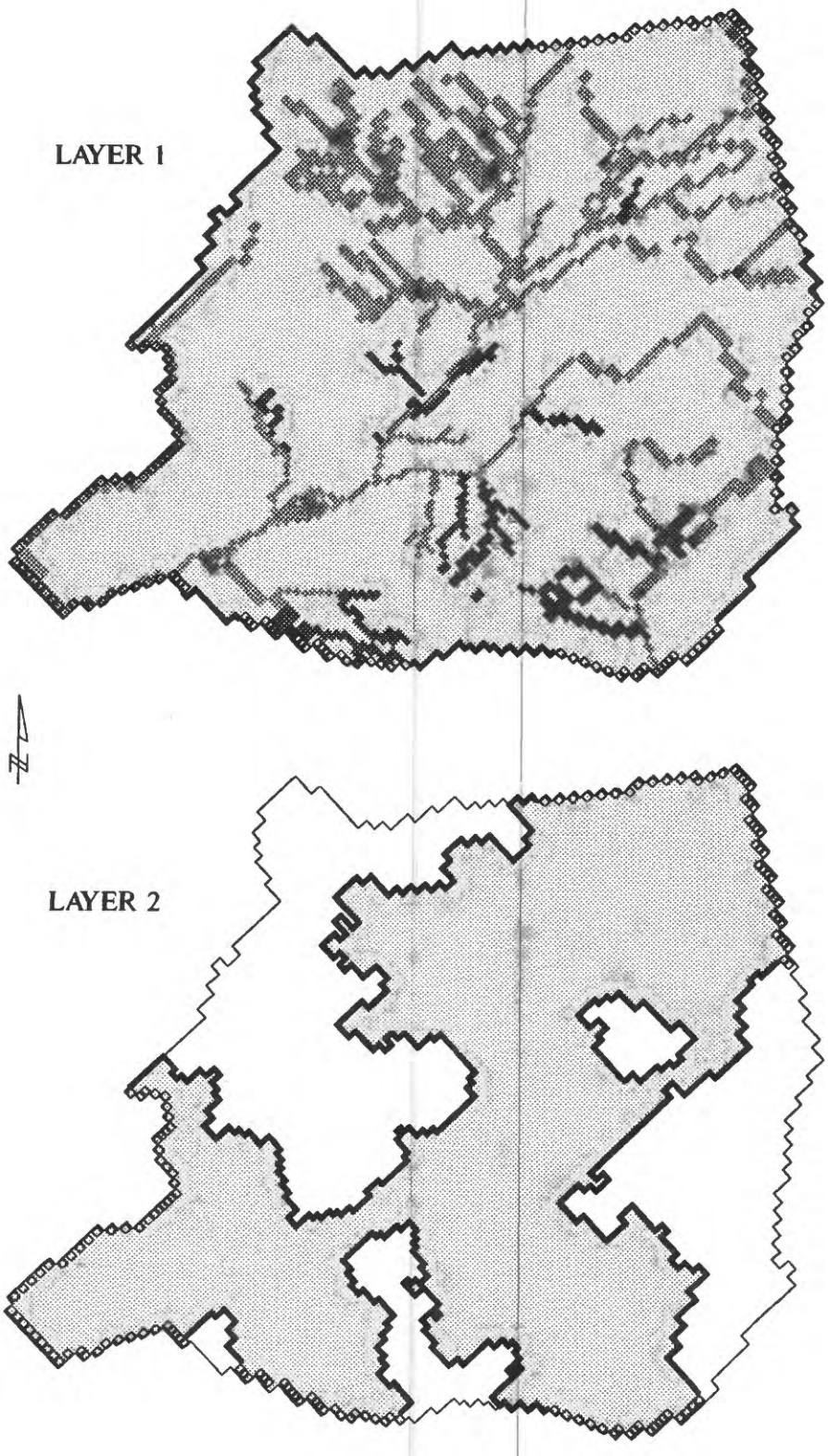

Figure 20.--Boundary conditions in model layers 1, 2, and 3.

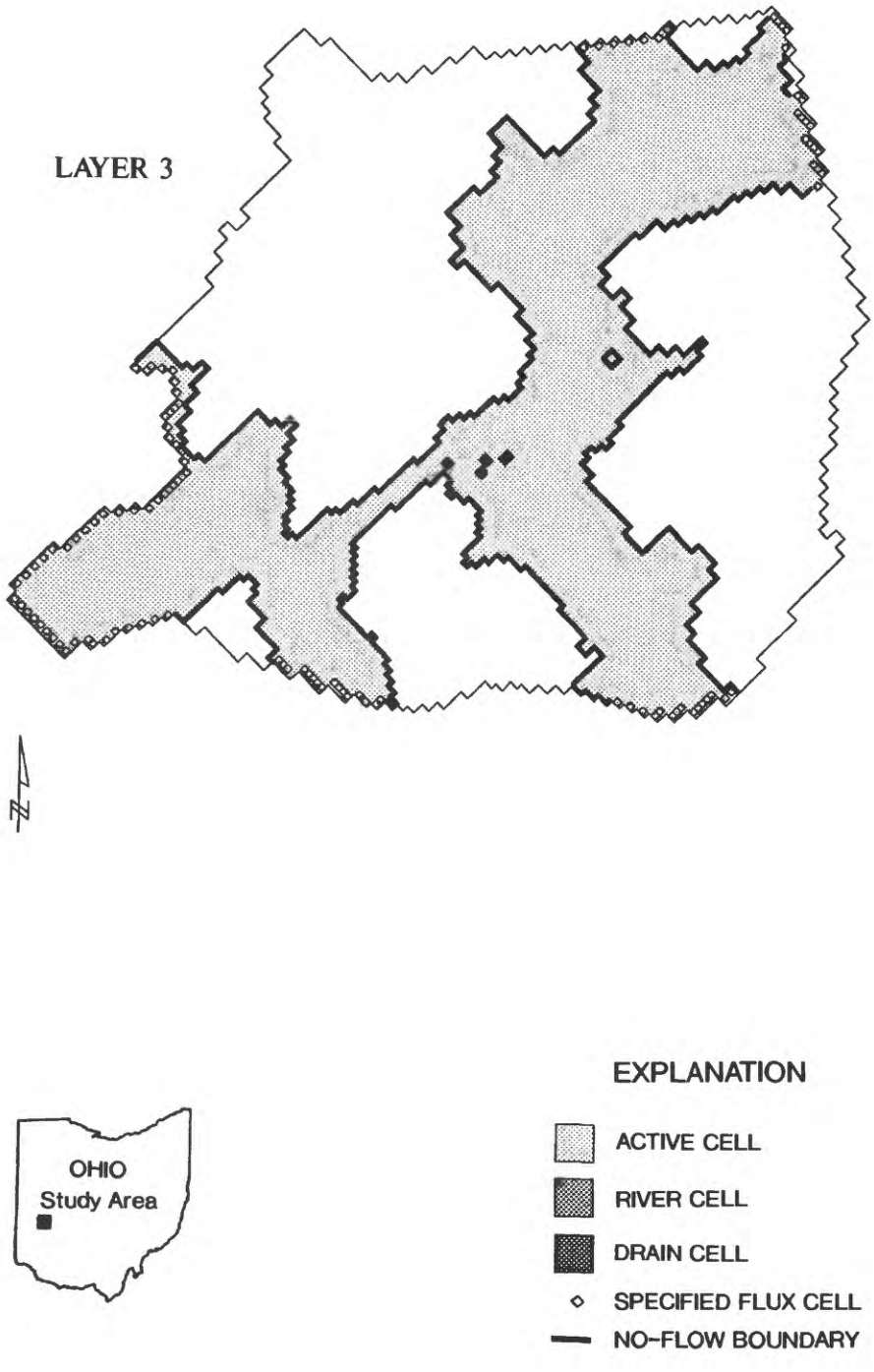

Figure 20.--Boundary conditions in model layers 1, 2, and 3--Continued.

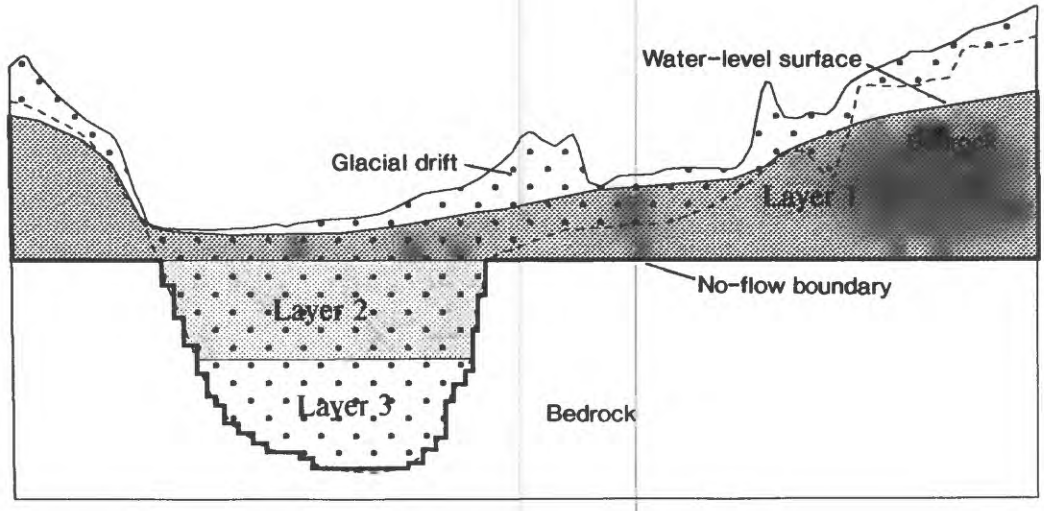

Figure 21.--A sectional view of the three layers in the model.

The second layer has 4,047 active cells and encompasses 64 mi^2. Layer 2 was assigned a thickness of as much as 90 ft in the buried-valley aquifer to ensure that most of the production wells that penetrate layer 2 were screened entirely in this layer; that is, this thickness was chosen to prevent modeling any production wells in layer 3 for which hydrogeologic data were limited. The third layer has 2,650 active cells and encompasses 41 mi^2. The thickness of layer 3 in the buried-valley aquifer was calculated as the difference between the altitudes of the bottom of layer 2 and the top of bedrock. Maximum thickness of layer 3 is about 200 ft in the buried valleys underlying Beaver Creek southeast of WPAFB and the Mad River northeast of WPAFB. The thicknesses of model layers 1, 2, and 3, contoured in ARC/Info by linear interpolation between data points, are shown in figures 22 through 24.

MODFLOW documentation (McDonald and Harbaugh, 1988) defines an unconfined layer as one for which transmissivity depends upon the altitude of the water table. Confined layers are those having constant transmissivity. By these definitions, layer 1 was modeled as unconfined, whereas layers 2 and 3 were modeled as confined.

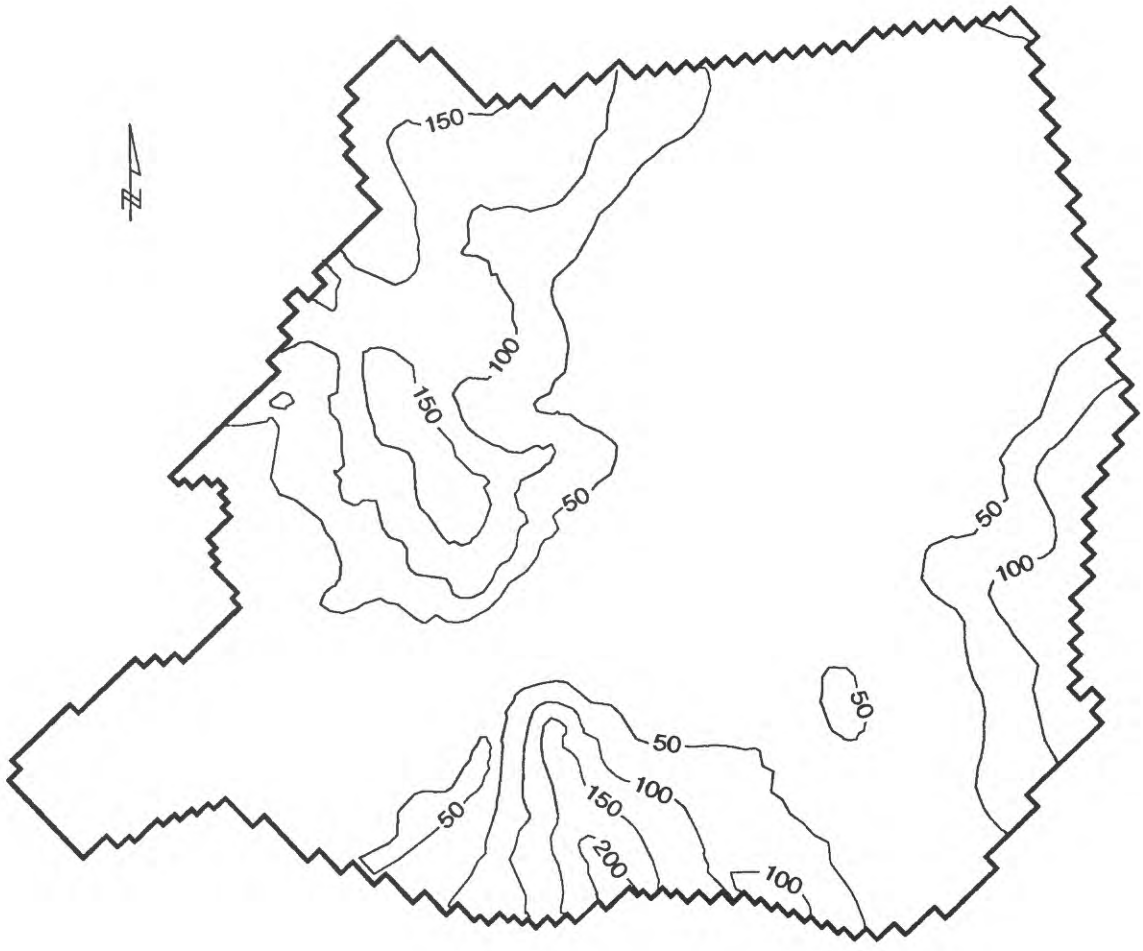

EXPLANATION

LAYER 1 MODEL BOUNDARY

—50— LINE OF EQUAL THICKNESS OF LAYER 1--Interval 50 feet

Figure 22.--Thickness of model layer 1.

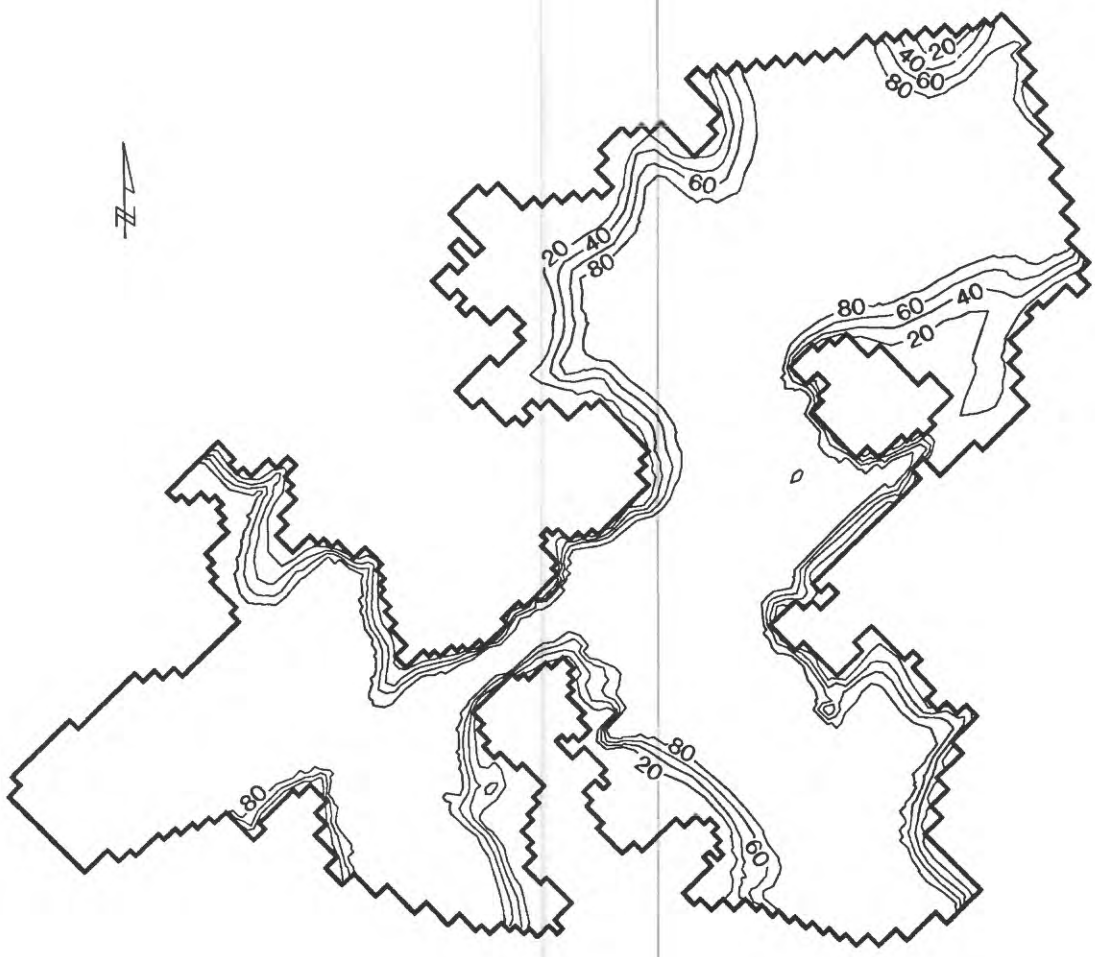

EXPLANATION

LAYER 2 MODEL BOUNDARY

—40— LINE OF EQUAL THICKNESS OF LAYER 2--Interval 20 feet

Figure 23.--Thickness of model layer 2.

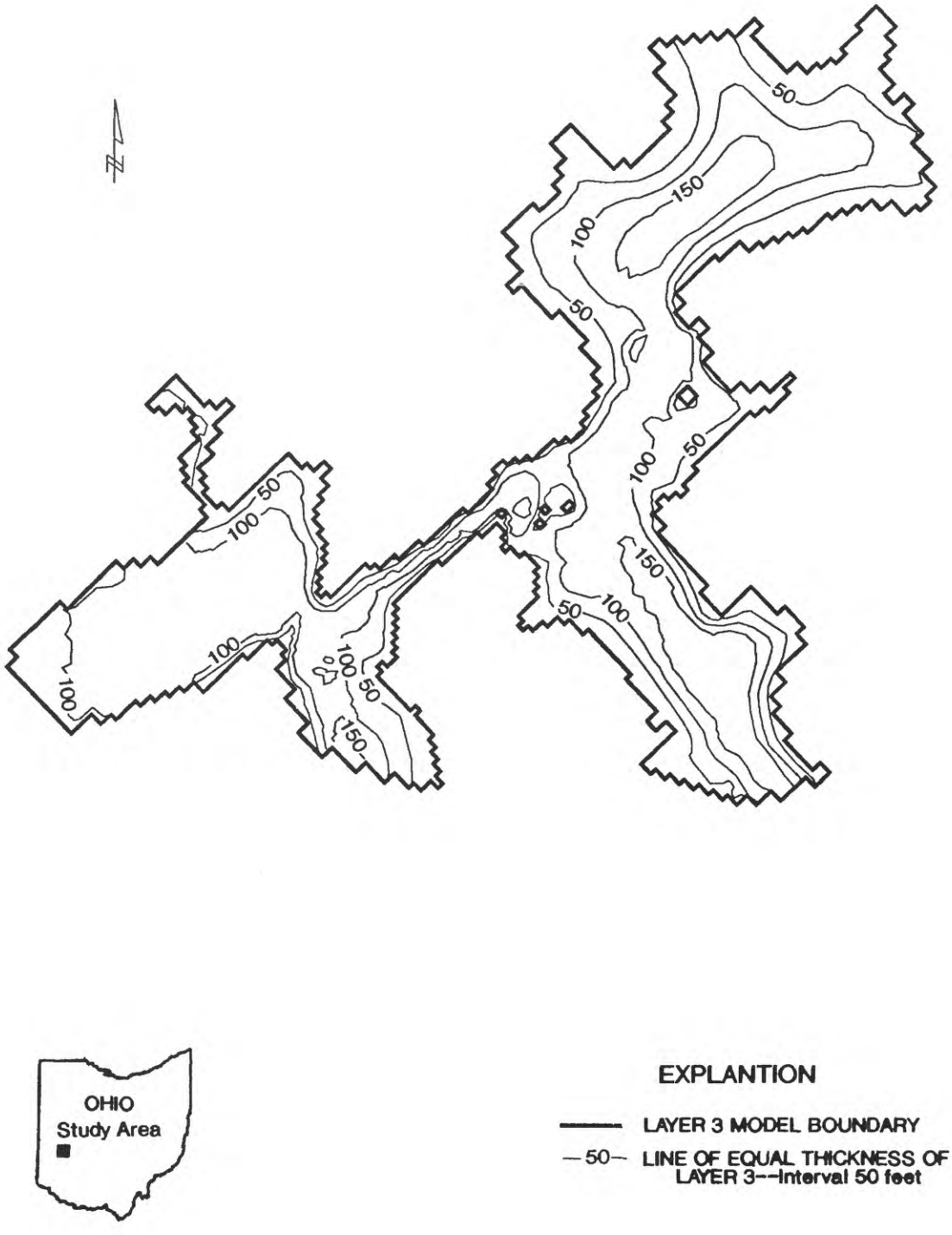

Figure 24.--Thickness of model layer 3.

Boundary Conditions

Equation 3 is a general solution to steady-state, three-dimensional ground-water flow. The solution to the equation becomes specific as boundary conditions or constraints are applied to the problem. Seven types of boundary conditions used in MODFLOW and other ground-water-flow models (Franke and others, 1987) are defined briefly below:

Streamline — flow is parallel to the flow-velocity vectors at every point along the boundary; thus, no water can cross the boundary.

Specified-flux — flux across the boundary surface is specified with time. No-flow is a specified-flux boundary for which the flux is zero.

Constant-head — hydraulic head is uniform at all points along the boundary surface and through time.

Head-dependent flux — flux across the boundary surface depends upon head within the aquifer adjacent to the boundary.

Specified-head — head is specified as a function of location and time over part of the boundary surface.

Free-surface — the position of the boundary may fluctuate with time; the water table is a free-surface boundary.

Seepage-face — a boundary between the aquifer and the atmosphere along which water discharges, usually in response to gravity and (or) evaporation.

Boundaries can be external or internal. External boundary conditions are those at the lateral edges of the modeled area. Internal boundaries are used within a model to simulate production wells, rivers, the water table. Any of the seven types of boundaries can be assigned externally or internally.

No-flow lateral boundaries were delineated along ground-water divides and streamlines, primarily along the southern and northwestern edges of the model (fig. 20). The top of the shale bedrock is a no-flow boundary in the buried valleys. Analysis of aquifer-test data indicated horizontal hydraulic conductivity, K_h, of the shale ranges from 0.0016 to 0.393 ft/d (table 4, GR-303, GR-309, GR-312, and GR-314); vertical hydraulic conductivity, K_v, is expected to be several orders of magnitude less. The amount of water entering the valley-train deposits from the shale is negligible relative to the flux of water within and through the buried valleys.

Specified-flux cells were defined where the flow-model boundaries transect the buried valleys and in the uplands along the eastern edge of the region. Magnitudes of flux (Q, in cubic feet per day) were calculated from Darcy's law,

$$Q = -K_h A \frac{dh}{dl} ,$$

where A is the cross-sectional area (square feet) of the cell through which flow occurs, and $\frac{dh}{dl}$ is the hydraulic gradient (feet/feet) in the cell. The hydraulic gradients for these cells were estimated from the water-level map (fig. 11). The negative sign indicates that flow is in the direction of decreasing hydraulic head. Cross-sectional area A is the product of the width (in feet)

of the cell perpendicular to flow and the saturated thickness (in feet). Determination of K_h is discussed in "Hydraulic conductivity and transmissivity."

The southwestern boundary of the flow model coincides with the Great Miami River. Along this boundary, specified flux out of the modeled area was assigned in layers 2 and 3 because of the depth of the valley and the presence of clay layers that restrict upward flow to the river. The boundary was modeled as a series of river nodes in layer 1, forcing the river to be either gaining water from or losing water to the aquifer. No data were obtained to estimate recharge from or discharge to the Great Miami River; however, water levels in late 1987 were below the bottom of the river (Schalk, 1992), indicating that the aquifer was gaining water from the river.

Input Parameters

Input parameters to MODFLOW include horizontal and vertical hydraulic conductivities (K_h and K_v, respectively) and (or) transmissivities (T) in each layer, recharge to and pumping from each layer, and vertical conductance of streambeds and drains. This section describes these parameter values and how they were obtained or estimated.

Hydraulic conductivity and transmissivity

Aquifer-test data were used to estimate spatial variations in K_h. Pumped-well-test values were obtained from the literature (table 3). Slug tests provided additional data on K_h of the buried-valley unconsolidated deposits and the shale and limestone bedrock (table 4). K_h was estimated from lithologies recorded in well logs for areas where no aquifer-test data were available; initial estimates, based on aquifer-test data for similar hydrogeologic media, ranged from 0.001 ft/d in the shale to 1,000 ft/d in the valley-train deposits. K_h distributions were compiled for each layer and were refined during calibration. K_h of the limestone bedrock did not enter the calculations directly because of the relative thinness and the small areal distribution of that rock in the modeled area.

The shale bedrock in upland areas is the same geologic unit as that underlying the buried valleys; therefore, K_h of shale in the uplands was assumed to be equal to that of shale underlying the buried valleys, for which aquifer-test data were available. Thickness of layer 1 in the uplands was determined previously (see discussion in the section on "Grid Layering"). An effective transmissivity, T_e (ft^2/d), was determined for one cell in the upland areas as

$$T_e = K_h b_c,$$

where b_c is the saturated thickness of the cell, in feet. K_h estimates for the rest of the cells in the upland areas were obtained by assigning the constant T_e to all upland cells and dividing T_e by the thickness of each cell. T_e was adjusted until an acceptable match between observed and measured heads was obtained. By this method, K_h in the uplands ranged from 0.06 to 17 ft/d.

The presence of clay in glacial outwash decreases K_h and K_v. Clay-rich sediments were most evident along the buried-valley walls northeast of Huffman Dam and throughout the buried valley southwest of the dam. Geraghty and Miller (1987) defined a confining unit of clay in the vicinity of Rohrer's Island that is as much as 80 ft thick at a depth of 30 to 50 ft below land surface; this

clay is not continuous northeast of Huffman Dam. Thin alluvial silts and clays were found at depths of as much as 20 ft along the reach of the Mad River near instrumented wells GR-208 and GR-210 (Dames and Moore, 1986b). In areas along the buried-valley walls, where the transition from low- to high-permeability deposits is gradual, values of K_h were increased gradually from low (uplands) to high (valley train) because of the likely presence of clay-rich units along the walls. The range of K_h values for layer 1 in the valley train is 0.2 to 210 ft/d. Distribution of K_h in layer 1 is shown in figure 25.

Because of their discontinuity in the buried valleys, low-permeability clays and silts were not modeled as distinct layers but as vertical leakance (Vcont, day^{-1}) terms. Vcont describes flow between model layers without explicitly modeling the clays as layers. Vertical leakance between layers was calculated as

$$Vcont_{i,j,(k+\frac{1}{2})} = \frac{1}{VCF\left(\frac{\Delta z_k}{K_{h_k}} + \frac{\Delta z_{k+1}}{K_{h_{k+1}}}\right)}, \qquad (4)$$

where VCF is an anisotropy factor, Δz is the distance between nodes, and the subscript $(k+\frac{1}{2})$ denotes that Vcont is calculated between nodes in the vertical direction. For this model, VCF ranged from 2,000 to about 1. The extreme values were "backed out" of equation 4 during calibration as Vcont was adjusted directly to obtain acceptable matches between simulated and observed hydraulic gradients and river discharges. The areal distribution of VCF between layers 1 and 2 and layers 2 and 3, respectively, is shown in figures 26 and 27. The areas around Rohrer's Island and along the eastern wall of the buried valley under WPAFB contain the lowest vertical conductance in the modeled area.

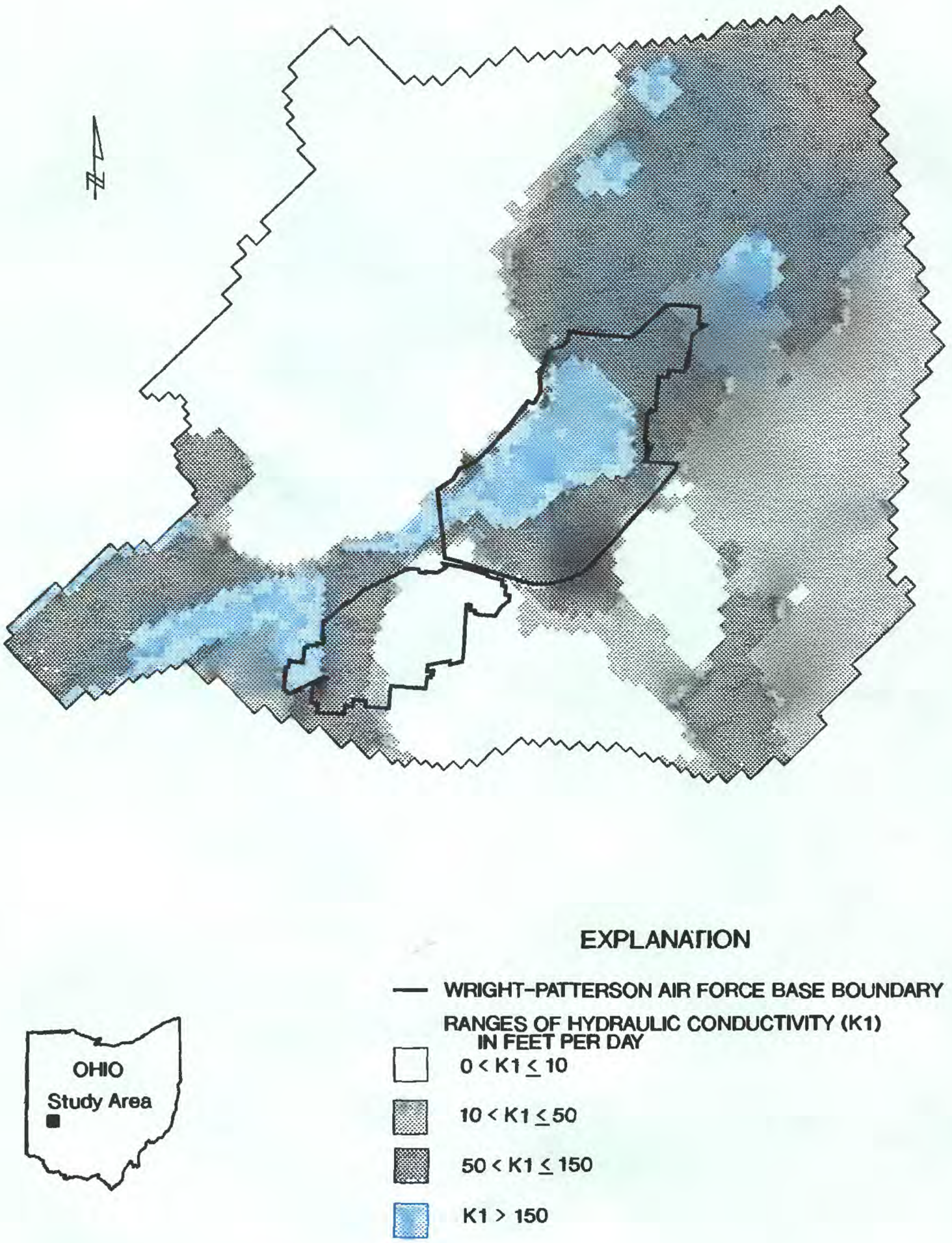

Figure 25.--Hydraulic-conductivity distribution of layer 1.

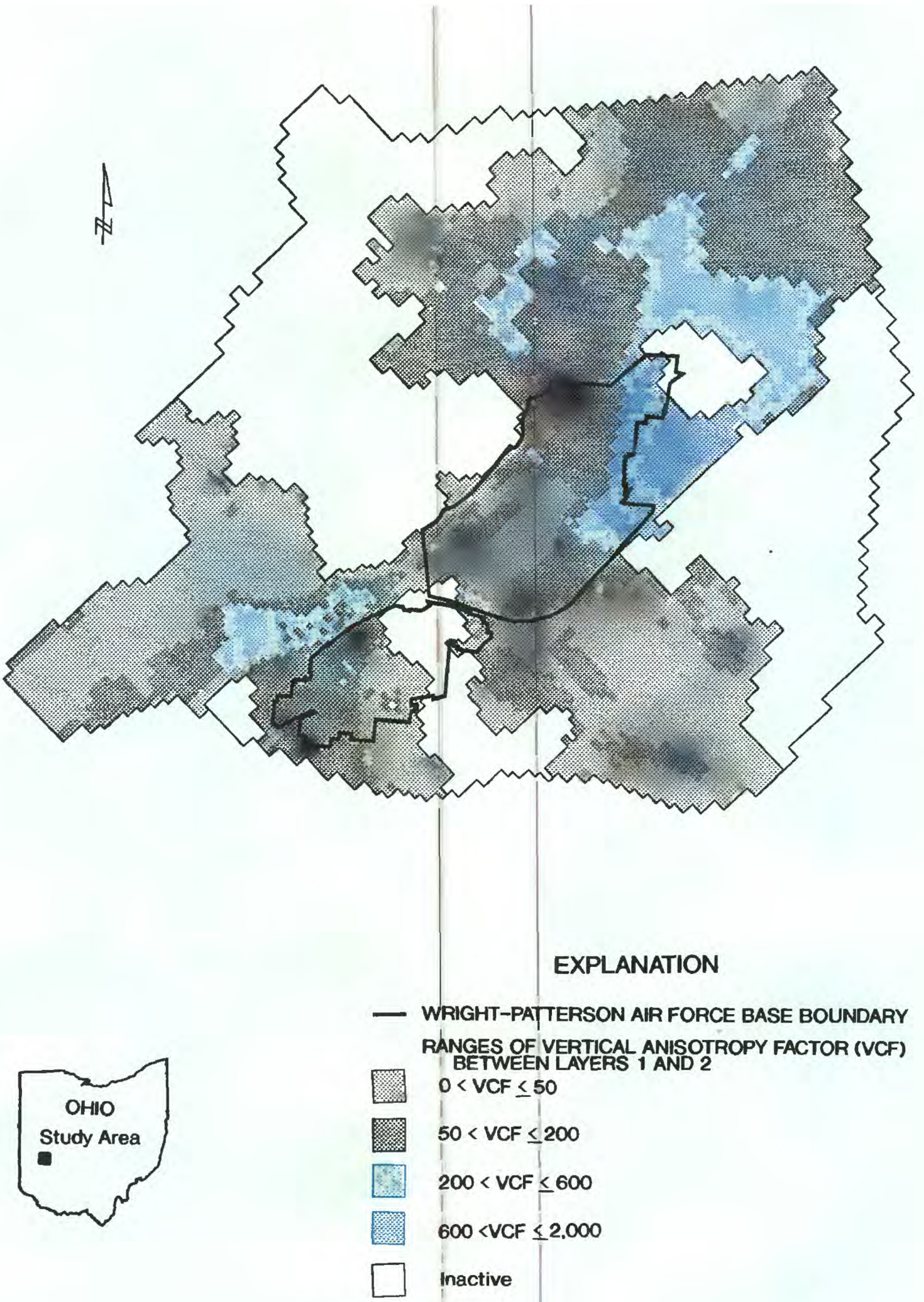

Figure 26.--Distribution of vertical anisotropy factor, layer 1 and 2.

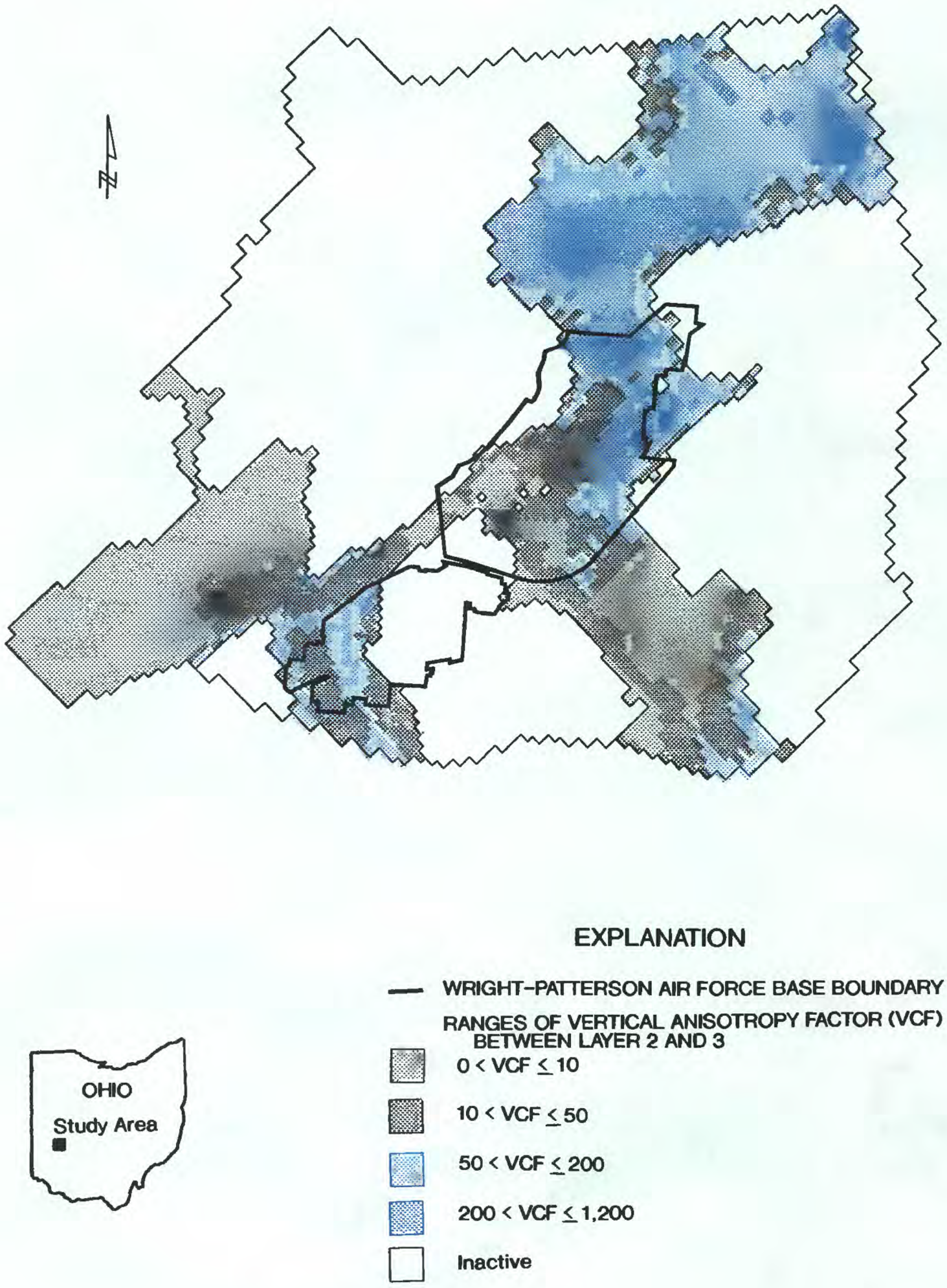

Figure 27.--Distribution of vertical anisotropy factor, layers 2 and 3.

Transmissivity is required as an input parameter for simulation of confined aquifers. Layers 2 and 3 were modeled as confined (in the sense of maintaining constant T). Values of T in layers 2 and 3, derived from aquifer-test data and calibration, range from 4 to 76,600 ft^2/d. Thickness of the layers was discussed in the section on "Grid Layering." The distribution of T in layers 2 and 3 is shown in figures 28 and 29.

Recharge

Recharge is the amount of precipitation that reaches the water table after runoff, soil-moisture replenishment, and evapotranspiration have been deducted. Surficial geology maps of Clark, Greene, and Montgomery Counties (Norris and others, 1948, 1950, and 1952) were used to delineate permeable deposits, such as glacial outwash and alluvium, from less permeable deposits, such as till. Generally, higher recharge rates were assigned to areas of more permeable glacial deposits than to areas of till. Published estimates of recharge from precipitation range from 7.5 to 12 in./yr in the valley-fill deposits near Fairborn (Fidler, 1975; Walton and Scudder, 1960); these values represent average recharge over the entire basin. Recharge to the valley-train aquifer was calculated as 12.4 to 15.8 in./yr by use of a recession curve of water levels in a well in unconsolidated deposits. Estimates of recharge were decreased for urban and high-till-content areas, where one expects more runoff because of the less permeable surficial material. On the basis of these estimates, recharge values of 3 to 12 in./yr were assigned to layer 1 in areas overlying valley train.

Many of the upland areas around WPAFB contain well-developed surface-drainage systems in the form of intermittent streams and gullies. The presence of these intermittent streams is indicative of the impermeability of the till and bedrock in the uplands. Recharge of about 2 in./yr was assigned to layer 1 in the upland areas. The areal distribution of recharge from precipitation in the calibrated model is shown in figure 30.

Pumping rates

Volumes of pumpage were determined from pumping records of municipalities, corporations, Wright State University, and WPAFB. Well field locations and pumping rates used in the model are listed in table 8. It should be noted that these were the active non-residential pumping centers in late 1987, which was the calibration target date. Some of these well fields may have altered pumping rates or ceased operation since 1987, and other well fields may have become active since then. The western production wells of WPAFB Area B, for example, were not pumping during the last three months of 1987. Several corporations that mine gravel from the aquifer north of WPAFB pump water from shallow wells. This pumpage is not included in the model because the water is returned to the shallow aquifer by way of lagoons after mining operations.

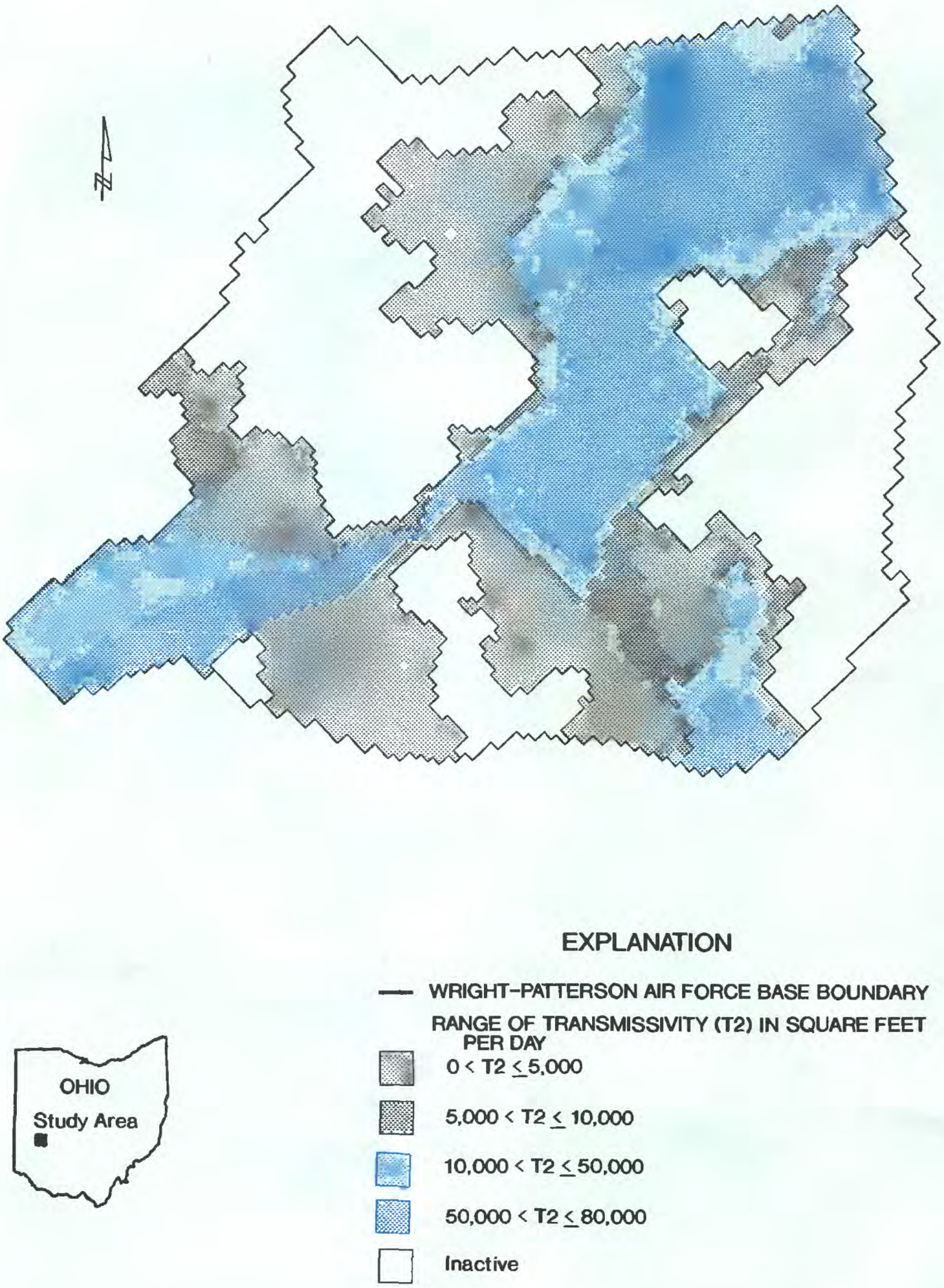

Figure 28.--Distribution of transmissivity, layer 2.

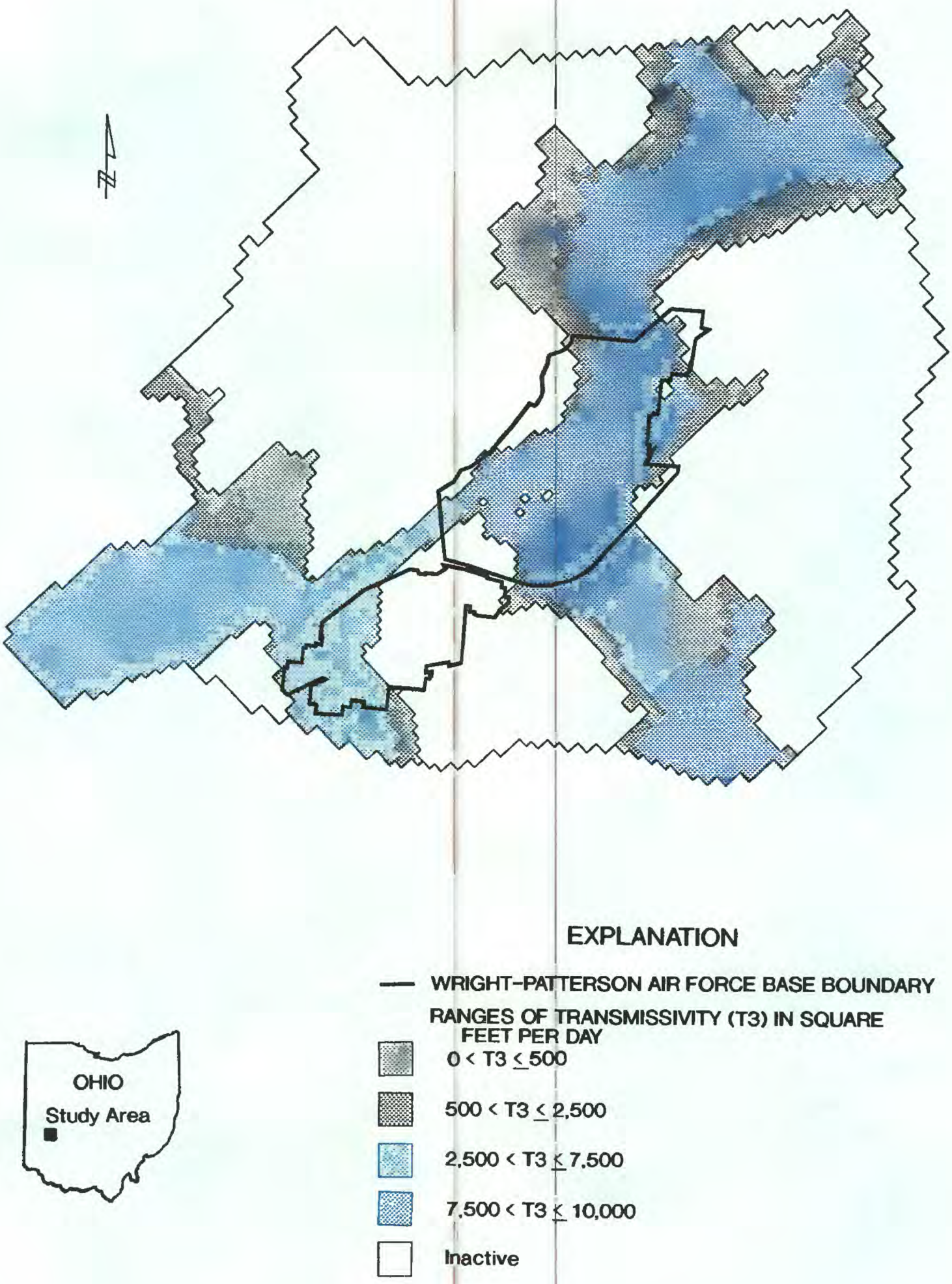

Figure 29.--Distribution of transmissivity, layer 3.

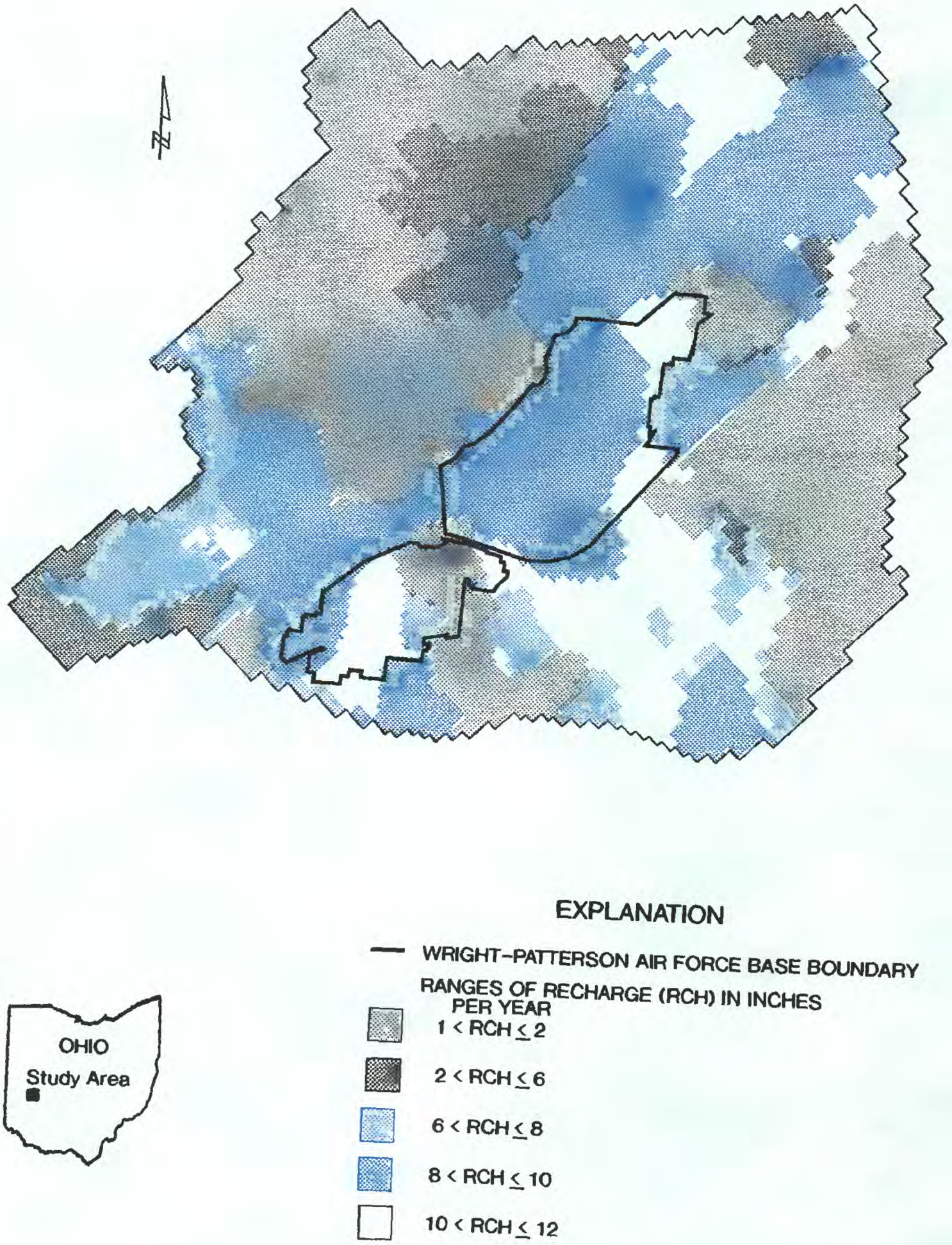

Figure 30.--Distribution of recharge to layer 1.

Table 8.—Locations of and pumping rates at well fields simulated in the regional ground-water-flow model

[ft^3/d, cubic feet per day; pumping rate is assumed average, October-December 1987. —, not applicable.]

Well field	Model location (layer, row, column)	Pumping rate (ft^3/d)	Model location (layer, row, column)	Pumping rate (ft^3/d)
Dayton-Mad River Well Field	1, 39, 10	133,690	2, 44, 19	267,380
	1, 40, 13	133,690	2, 44, 28	133,690
	1, 42, 16	133,690	2, 45, 28	133,690
	1, 43, 16	133,690	2, 46, 28	133,690
	1, 44, 20	133,690	2, 47, 28	133,690
	1, 45, 24	133,690	2, 47, 29	133,690
	1, 46, 27	133,690	2, 48, 29	267,380
	1, 46, 30	133,690	2, 48, 31	171,120
	1, 48, 30	342,240	2, 48, 32	342,240
	1, 48, 33	342,240	2, 49, 31	342,240
	1, 49, 32	342,240	2, 49, 32	342,240
	1, 49, 33	171,120	2, 49, 34	171,120
	1, 49, 34	171,120	2, 49, 36	171,120
	1, 49, 35	171,120	2, 50, 34	171,120
	1, 50, 35	171,120	2, 50, 37	171,120
	1, 50, 37	171,120	2, 51, 33	171,120
	2, 43, 17	133,690	2, 51, 34	171,120
	2, 44, 17	133,690	2, 51, 37	171,120
WPAFB-Skeel Road	1, 63, 72	38,450	1, 65, 68	38,450
	1, 63, 74	76,900	2, 65, 69	38,450
	1, 63, 75	38,450	2, 67, 64	38,450
WPAFB -Commissary	1, 71, 74	38,450	—	—
WPAFB-Marl Road	2, 57, 54	39,740	2, 59, 54	39,740
	2, 57, 55	39,740	2, 59, 56	40,110
	2, 58, 55	39,740	—	—
Southwestern Portland Cement	1, 71, 80	66,850	—	—
Valley Water Works	2, 45, 76	13,120	—	—
Fairborn-Medway Road	2, 47, 83	73,530	2, 48, 83	73,530
Wright State University	2, 73, 57	30,080	—	—

Some explanation of the distribution of pumping at Mad River well field is warranted. Records of pumpage from individual wells at the Mad River well field are not kept. Forty-four wells in operation at Mad River well field produced about 51 Mgal/d in late 1987 (George Crosby, City of Dayton, oral commun., 1992); 28 of these wells are on Rohrer's Island. For the purpose of this model, it was assumed that the wells on Rohrer's Island produced most of the water in the Mad River well field because of the recharge lagoons on the island that are designed to induce infiltration to the aquifer. Model row and column were assigned to each well on the basis of its actual location; however, the pumping rates of the wells and the model layer to which pumping was assigned were estimated. The specific capacity of the deep aquifer (simulated in model layers 2 and 3) is greater than that of the upper aquifer (Geraghty and Miller, 1987); thus, more water was assumed to be pumped from wells completed in layer 2 than from those in layer 1. The amount of pumping from layer 2 was 1.3 times greater than the pumpage from layer 1 in the calibrated model.

Rivers and Drains

Streambed conductance was based on seepage-meter measurements for the Mad River and Hebble Creek. Streambed conductance (C_{riv}, in ft^2/d) is calculated as

$$C_{riv} = \frac{K_{riv} A_{riv}}{M},$$

where K_{riv} is the vertical hydraulic conductivity (feet/day) of the streambed medium, A_{riv} is the surface area (square feet) of the stream in the cell, and M is the thickness (feet) of the streambed. Measurements of K_{riv} yielded a range of 10.8 to 18.7 ft/d in the Mad River and 0.006 to 0.024 ft/d in Hebble Creek. On the basis of these measurements, the Mad River north of Huffman Dam and the recharge lagoons on Rohrer's Island were assigned K_{riv} values of 13 ft/d. The Mad River south of Huffman Dam and the Great Miami River were assigned K_{riv} values of 0.4 ft/d to allow the recharge lagoons on Rohrer's Island to provide most of the induced infiltration to the aquifer. Small streams crossing the glacial outwash, such as Hebble Creek, were assigned K_{riv} values of 0.03 ft/d, which is approximately equal to the measured values. Streams in upland areas were assumed to be less conductive than those overlying valley train, and were assigned K_{riv} values of about 0.002 ft/d.

The surface areas of the Great Miami and Mad Rivers and parts of smaller streams were calculated by use of ARC/Info, on the basis of digitized USGS 1:24,000-scale topographic quadrangle maps. Surface areas of all other streams were calculated as the product of length (also determined by ARC/Info) and width, assumed to be 5 ft. All rivers and streams were assumed to have streambed thicknesses of 1 ft.

Water discharges from the aquifer into rivers and drains when the hydraulic head in the aquifer adjacent to the river or drain is greater than the hydraulic head in the river or drain. For surface drains, the hydraulic head is assumed to be equal to the altitude of the bottom of the drain. Drains, unlike rivers, do not allow flow to the aquifer when the head in the aquifer is lower than the head in the drain. Surface drains were simulated in areas where deep gullies are known to exist

and in low-lying areas where the water table is high. Streambed conductance of the drains was estimated to be equal to that of streams in similar geologic materials. Cells containing simulated rivers and drains are shown in figure 20.

Slope-area measurements after the flood of January 1959 were used to estimate streambed altitudes of the Mad and Great Miami Rivers (data from ODNR, Division of Water, 1959, on file with USGS, Columbus, Ohio). Streambed altitudes of other rivers and surface drains were estimated from USGS 1:24,000 topographic quadrangle maps.

Steady-State Calibration

The model was calibrated against assumed steady-state conditions for late 1987. Calibration of the model was based on best-fit analyses of simulated and measured hydraulic heads in the aquifer, gains to and losses from several rivers and streams, and vertical hydraulic gradients at well clusters. Calculation of summary statistics, such as root-mean-square error (RMSE), average absolute head difference (AAHD), and average head difference (AHD) were also used in the calibration process.

The RMSE accounts for variance and bias of the compared data, and is calculated as

$$RMSE = \sqrt{\frac{\sum_{i=1}^{N} (h_{cal_i} - h_{m_i})^2}{N}},$$

where h_{cal} is the simulated head, h_m is the measured head, and N is the number of well points used in error computations. The term "$h_{cal} - h_m$" is known as the head difference or residual head. The variance of the compared data is indicated by AAHD also, which is calculated as

$$AAHD = \frac{\sum_{i=1}^{N} abs\,(h_{cal_i} - h_{m_i})}{N},$$

where 'abs' indicates the absolute value of the expression in parentheses. Low values of RMSE and AAHD indicate low variance and, therefore, high correlation.

The degree of skewness in the compared data is reflected in AHD, which is calculated as

$$AHD = \frac{\sum_{i=1}^{N} (h_{cal_i} - h_{m_i})}{N}.$$

A low absolute value of AHD indicates an even spread of simulated results around the measured-head data. As simulated heads approach measured heads, all of these statistical values approach zero. Statistics are reported in table 9.

Table 9.—Results of statistical analyses of simulated and measured heads in the vicinity of Wright-Patterson Air Force Base

[RMSE, root-mean-square error; AAHD, average absolute difference between measured and simulated heads; AHD, average difference between measured and simulated heads; ft, feet]

	Number of observations	RMSE (feet)	AAHD (feet)	AHD (feet)
Layer 1, all	330	09.3	7.3	-1.4
Layer 1, uplands	88	12.1	9.7	-1.2
Layer 1, valley train	242	8.1	6.5	-2.3

Values of hydraulic head in layers 2 and 3 of the model were not considered during calibration because most of the wells at which water levels were measured are completed in the shallow (layer 1) parts of the ground-water system. Vertical hydraulic gradients at well clusters, which are presented later in this section, were used rather than hydraulic head to include the deeper parts of the glacial aquifer in the calibration process.

Contours on the simulated water-level surface are shown in figure 31, which was generated in ARC/Info from MODFLOW head output. In most of the areas, the simulated heads match the measured heads. Heads in the upland areas are simulated reasonably well, as indicated by RMSE = 12.1 ft and AAHD = 9.7 ft at well points in upland areas. In several upland areas, the steep hydraulic gradients were difficult to simulate because of the large cell sizes in the model. Low RMSE and AAHD are not critical in upland areas because (1) the data inputs, such as the altitude-estimation error of water levels and the number of wells, are not as precise in those areas as those in the buried valleys; and (2) the contribution of the uplands to flow in the modeled area is small.

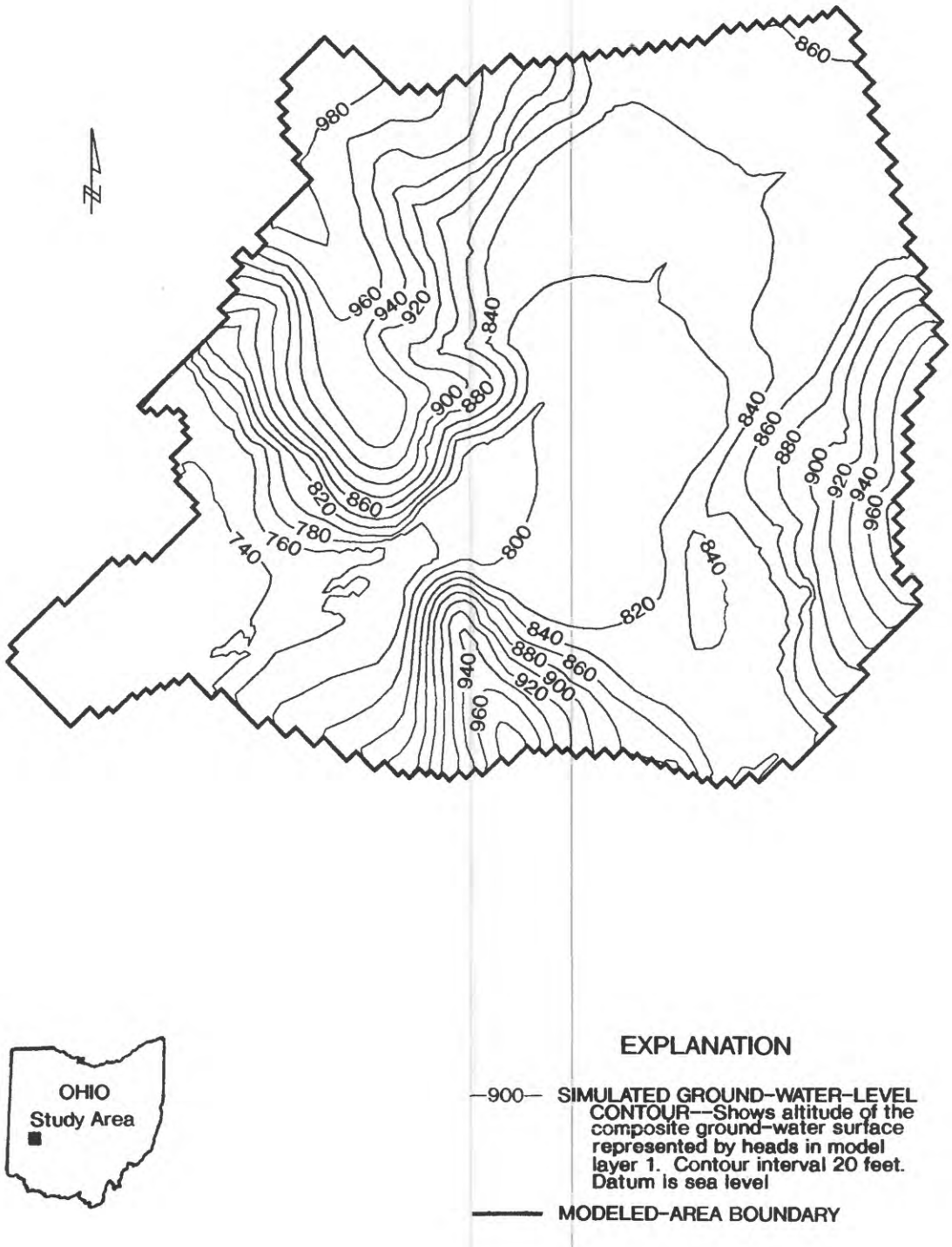

Figure 31.--Simulated water-level surface.

The measurements of error are less when observed water levels in the valley train are used in the calculations. For wells completed in the valley-train deposits, RMSE = 8.1 ft and AAHD = 6.5 ft. Differences between measured and simulated heads in the buried valleys are greatest along the buried-valley walls, where hydraulic conductivities are highly diverse and hydraulic gradients are steep, and at Rohrer's Island, where the water-level surface was difficult to simulate because of its interaction with the Mad River. Correlations between measured and simulated water levels in all wells and in wells completed in valley train and upland areas are shown in figure 32. Maximum difference between measured and simulated water levels is 30 ft at a well in the upland area east of WPAFB. Water levels in the upland areas were simulated better at lower water-level altitudes (750 - 825 ft) than at higher (875 - 925 ft) altitudes. Maximum difference between measured and simulated heads in the valley train is 22 ft in an area along the buried-valley wall. Agreement between measured and simulated heads in the valley-train wells is best at water-level altitudes of 775 to 850 ft. Most of the wells on WPAFB are completed at water-level altitudes within this last range.

Gains from and losses to rivers and streams in the vicinity of WPAFB were examined during calibration. Measured and simulated discharges could not be compared directly because base flow of rivers and streams in the vicinity of WPAFB was measured in July 1991, not in late 1987. Simulated and observed gains and losses along reaches of several streams in the vicinity of WPAFB are listed in table 10.

Table 10.—Simulated and observed losses of flow along reaches of selected streams in the vicinity of Wright-Patterson Air Force Base

[ft^3/s, cubic feet per second. Negative losses are gains to the stream from the aquifer; observed losses are from discharge measurements in July 1991]

Stream reach	Loss of flow (ft^3/s)	
	Simulated	Observed
Trout Creek, from Prairie Road to outfall at Mad River	0.011	0.31
Hebble Creek, from Skeel Avenue to Twin Lakes	-.057	.72
Mad River, from WPAFB boundary to Huffman Dam	-13.3	-17.47
Mad River, from Huffman Dam to below Harshman Road	50.5	80.0

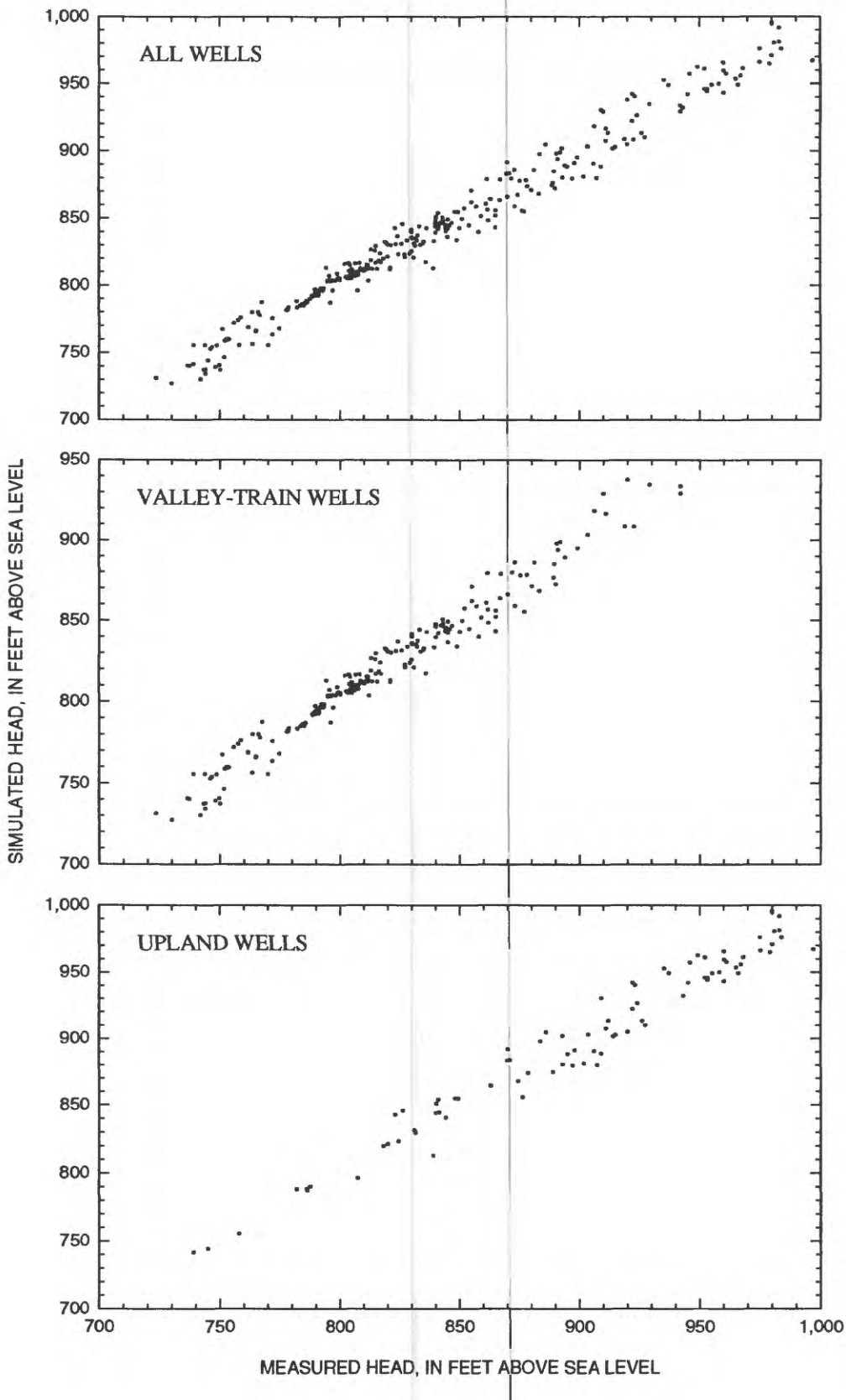

Figure 32.--Scatter plots of measured and simulated head in wells in the modeled area.

Differences in hydrologic conditions between late 1987 and July 1991 and uncertainty of the distribution of pumping at Mad River well field limit the comparability of measured and simulated gains and losses. Pumping at Mad River well field was approximately 51 Mgal/d in late 1987, but it was approximately 56 Mgal/d in July 1991 (George Crosby, City of Dayton, oral commun., 1992). The higher pumping rate in July 1991 was probably due to the high summer demand compounded by drought conditions. As a result, more water was lost to the aquifer from the Mad River in July 1991 than in late 1987. In addition, the modeled system south of Huffman Dam represents a more equal distribution of pumping at Mad River well field than may exist.

Simulated gains to the Mad River north of Huffman Dam are on the same order as those measured in 1991. Between the northern boundary of WPAFB and Huffman Dam, the Mad River gains 13.3 ft^3/s, or 8.6 Mgal/d. In contrast, ground-water flow under Huffman Dam, discussed more fully in the next section, is about 2.8 Mgal/d. Thus, about three times more water discharges to the Mad River north of Huffman Dam along the western WPAFB boundary than flows under the dam. Although sources of water flowing to the Mad River and under Huffman Dam cannot be ascertained with certainty, a reasonable inference is that the area contributing to flow to the Mad River along this reach is larger than the area contributing to flow under Huffman Dam. Implications concerning advectively transported chemicals should not rely solely upon these general "contributing area" statements; the phenomena could be evaluated with the aid of particle-tracking software.

Except for Hebble Creek, simulated streams were gaining water along reaches that were gaining in 1991. Trout Creek was simulated and observed to be losing water, although Hebble and Trout Creeks may gain or lose seasonally in response to the rise and fall of the water table, as shown previously in the hydrogeology section of this report. Differences between measured and simulated gains in both creeks were less than 1 ft^3/s.

Vertical hydraulic gradients at several well clusters also were used to calibrate the flow model. The wells were chosen on the basis of their location (recharge or discharge areas), screened depths, and data availability. Pertinent well information and measured and simulated head gradients between the well screens are listed in table 11.

Table 11.—Simulated and measured vertical hydraulic gradients at well clusters in the vicinity of Wright-Patterson Air Force Base

[ft, feet. Measured gradients based on 1987 water-level measurements; simulated heads are those in the grid cells (layers 1 and 2) where the well is located]

	Well	Location	Depth (ft)	Vertical gradient	
				Simulated	Measured
		Recharge areas			
1.	MT-125	Southwest Area B	27		
	MT-129	Southwest Area B	54	-0.02	-0.09
2.	GR-288	Near north end of Skeel Road	32		
	GR-289	Near north end of Skeel Road	90	-.02	-.03
3.	GR-257	Near north end of main runway	18		
	GR-256	Near north end of main runway	75	-.02	-.08
		Discharge areas			
1.	GR-221	Mad River	15		
	GR-223	Mad River	55	+0.09	+0.06
2.	GR-281	Mad River	21		
	GR-282	Mad River	50	+.003	+.04
3.	GR-277	Mad River	35		
	GR-278	Mad River	50	+.02	+.07

Magnitudes of most of the simulated gradients listed in table 11 are smaller than those measured, but simulated directions are the same as those measured in all cases. A positive vertical gradient indicates a discharge area, commonly near a gaining stream or a production well. The wells in table 11 that are in areas simulated as discharging (positive gradients) are near the Mad River, which, according to analysis of discharge measurements, is gaining. Likewise, wells in recharge areas (negative gradients) are at higher land-surface altitudes, away from the rivers.

A water budget was calculated by use of the calibrated ground-water-flow model (table 12). The budget indicates that the sources of water entering the modeled ground-water system are boundary flux (especially along the northeastern corner), recharge from precipitation, and river leakage (approximately 35 percent of the river leakage occurs at Rohrer's Island).

Table 12.—Ground-water budget for the modeled area as calculated by use of the calibrated ground-water-flow model

[Data are in cubic feet per day.]

Budget component	Input	Output
Specified flux	6,278,800	9,705,000
Wells	0	7,582,000
Drains	0	26,200
Recharge	4,234,100	0
River leakage	11,343,000	4,353,400
Total	21,855,900	21,666,600

Percent discrepancy = 0.87 = 100 x (Total in - total out) / [(Total in + total out) / 2]

One aspect of the hydrologic budget that is worthy of note is the flow of water from the shale to the buried valleys along the thin interface between the valley-train deposits and uplands bedrock (see "Grid layering" section). Walton and Scudder (1960) estimated flow from the shale to be about 0.16 Mgal/d per mile of valley wall, though they did not verify that amount by field or modeling methods. In this model, cell-by-cell flows were calculated along two 1-mi lengths of the interface between the uplands and the valley train. The first line, labeled "hill 1" in figure 33, is along the bedrock hill west of WPAFB Areas A & C and just north of Huffman Dam. Hill 1 contributed about 0.057 Mgal/d through the interface to the buried-valley aquifer; or approximately 37 percent of Walton and Scudder's estimate. The second line, "hill 2" in figure 33, is along the bedrock hill east of WPAFB Areas A & C in Fairborn. Hill 2 contributed about 0.15 Mgal/d to the buried-valley aquifer; approximately equal to Walton and Scudder's estimate. Assuming these values to be representative of flow from the bedrock to the buried valley everywhere along the length of its wall, the bedrock contributes from 2 to 4 percent of the total ground-water flow in this area. Additional discussion of the contribution of bedrock to ground-water flow in the buried valleys is presented in the next section.

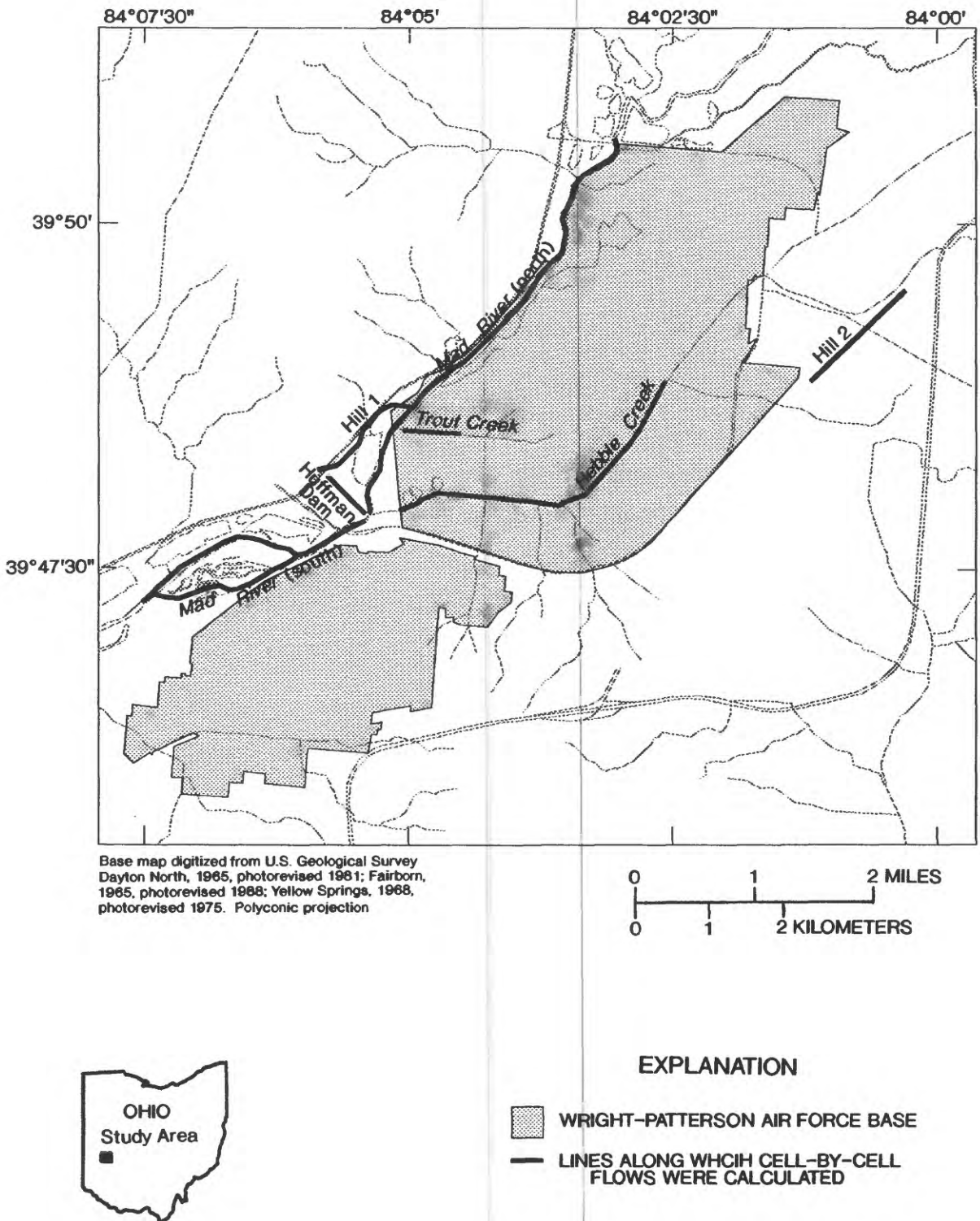

Figure 33.--Locations of lines along which cell-by-cell flows were calculated.

Sensitivity Analysis

An analysis was done to assess the sensitivity of the calibrated model to systematic changes in values of input parameters. Each change in parameter value was incorporated into a separate run of the model; sensitivity of the model could be greatly different for combinations of changes. The purpose of this analysis was to determine which parameters have the greatest effect upon the ability of the model to simulate natural conditions, and to determine the interdependency of the uplands and buried valleys.

Parameters that were varied in the sensitivity analysis included vertical hydraulic conductance between layers 1 and 2 and between layers 2 and 3 (V1 and V2, respectively), horizontal hydraulic conductivity of layer 1 (K1) in the uplands and the valley train, transmissivity of layers 2 and 3 (T2 and T3, respectively), recharge (RCH) to the uplands and the valley train, and riverbed conductance (K_{riv}). Parameters V1, V2, and K1 were varied by ±1 order of magnitude. Parameters T2, T3, RCH, and K_{riv} were varied from ±5 to ±50 percent. The sensitivity analysis required 96 model runs.

Simulated hydraulic heads at well points, determined in the same manner as those described in the previous section, were compared statistically to heads measured at the wells in the last three months of 1987. Head responses are reported as the RMSE of residuals in uplands, valley-train, and all wells. Results of the sensitivity analysis in terms of percent changes of RMSE are shown in figures 34-38. This method was used to standardize the presentation of the model sensitivity to changes in input parameters. A negative-percent change in RMSE, which is equivalent to a decrease in RMSE, indicates that the match between observed and simulated water levels from a sensitivity-analysis run is better than that of the calibrated model presented in the "Steady-state Calibration" section. A positive-percent change in RMSE indicates that the match between observed and simulated water levels from a sensitivity-analysis run is worse than that of the calibrated model. RMSE improved with increases in T3 (fig. 35) and K_{riv} (fig. 34) during the sensitivity analysis. In both of these cases, the improvements are negligible (about 1 percent) and are evident only in upland areas. Sensitivity of head residuals to changes in V3 is not presented because changes in V3 within the ±50-percent range had no effect on hydraulic heads at well points.

Model sensitivity also was analyzed by studying three responses to changes in input parameters: river discharges to the Mad River and Trout and Hebble Creeks, cell-by-cell flows from the uplands to the buried valleys and under Huffman Dam, and hydraulic heads in the uplands and buried valleys. Lines along which discharges were analyzed are shown in figure 33. River reaches hereafter are called Hebble Creek, Mad River North, Mad River South, and Trout Creek. Lines along which cell-by-cell flows were calculated are hereafter called hill 1, along the western uplands; hill 2, along the eastern uplands; and Huffman Dam. Flow responses are presented in figures 36-38. Results presented in the figures are those that show at least 5-percent variability during the sensitivity analysis. Flows to Trout Creek were affected only by changes in K_{riv}; the relation is linear (decreased flow with decreased K_{riv}) and is not represented in any figure.

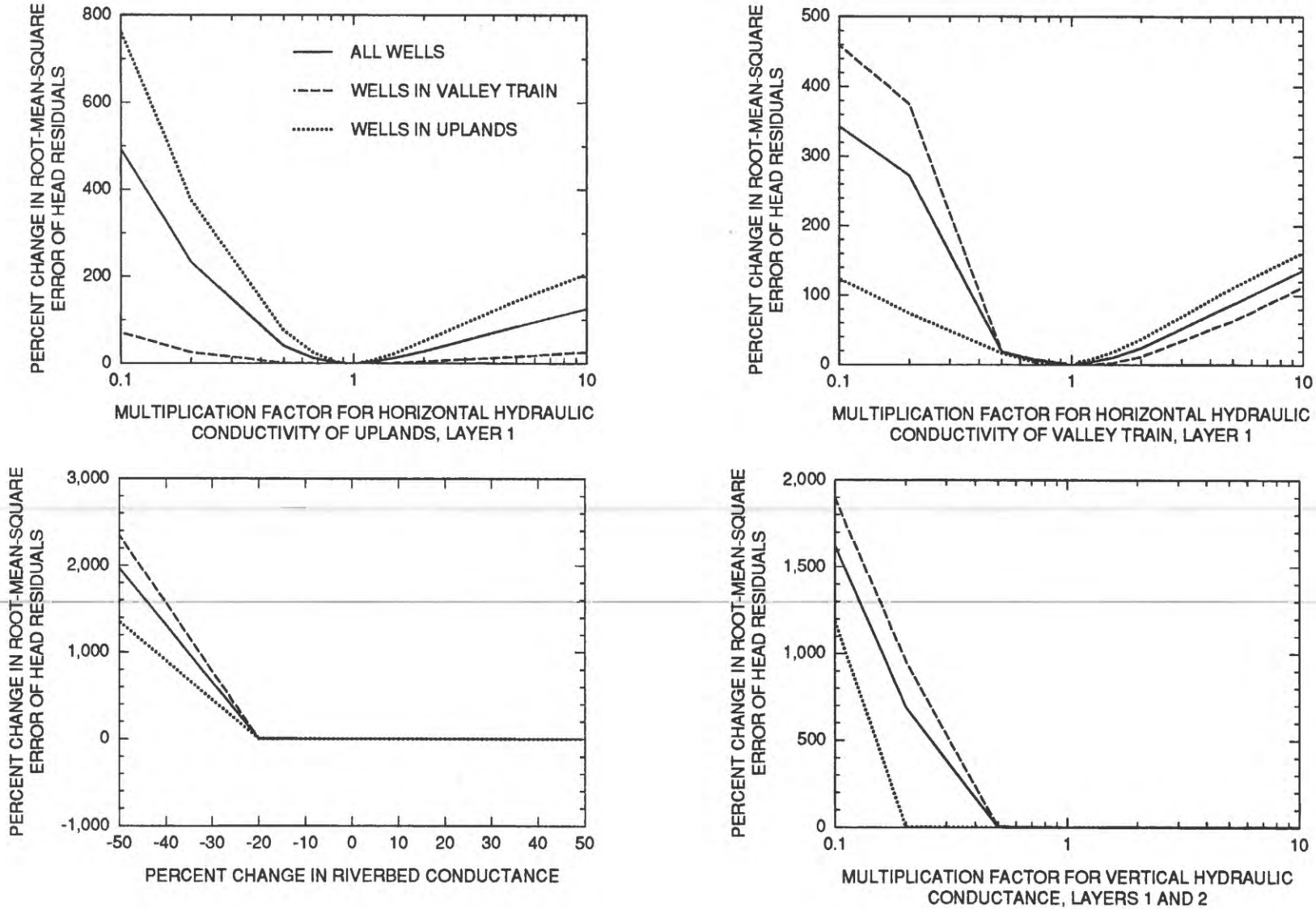

Figure 34.--Sensitivity of simulated heads to changes in horizontal hydraulic conductivity, riverbed conductance, and vertical hydraulic conductance in model of ground-water-flow system, Wright-Patterson Air Force Base and vicinity.

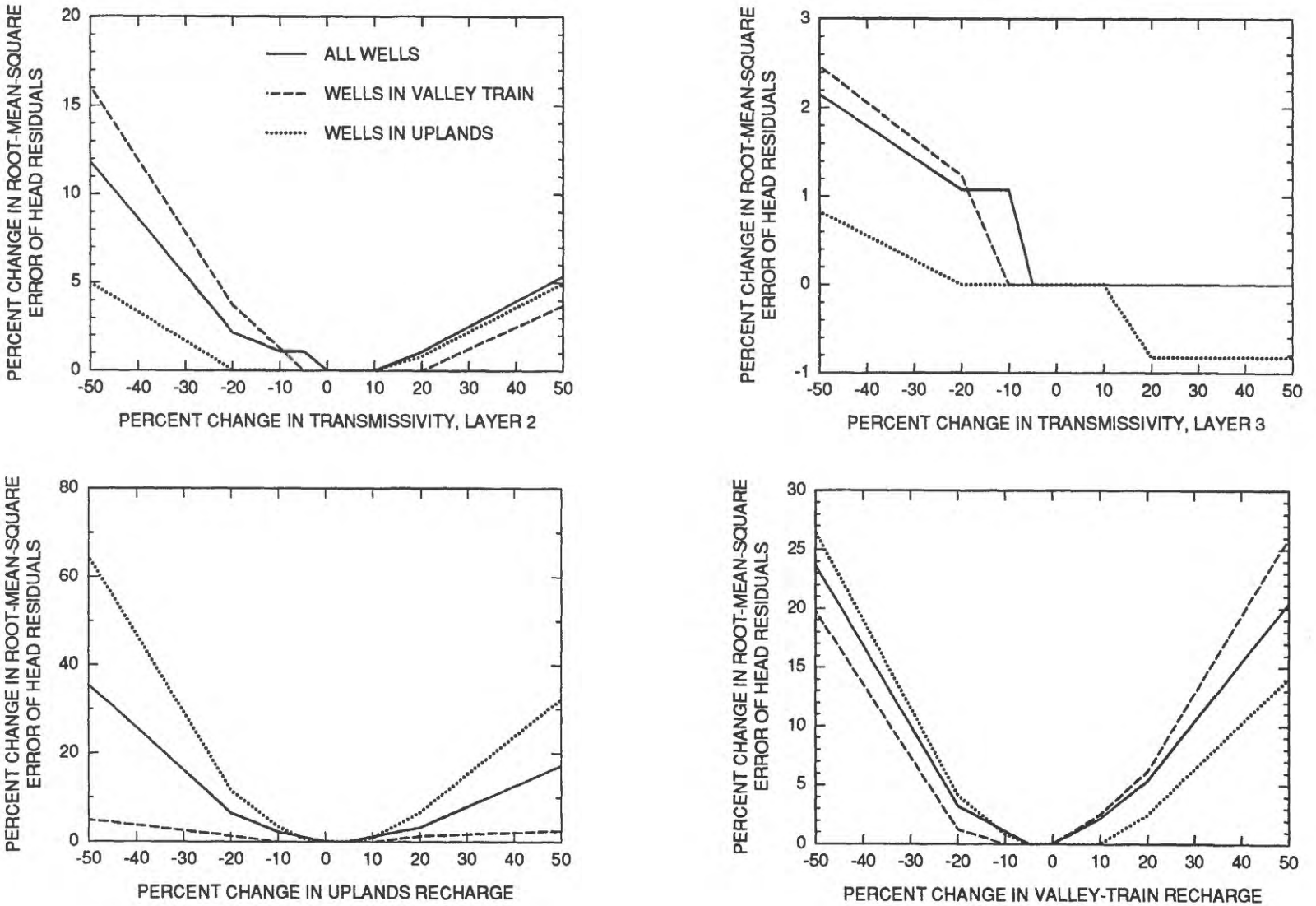

Figure 35.--Sensitivity of simulated heads to changes in transmissivity and recharge in model of ground-water-flow system, Wright-Patterson Air Force Base and vicinity.

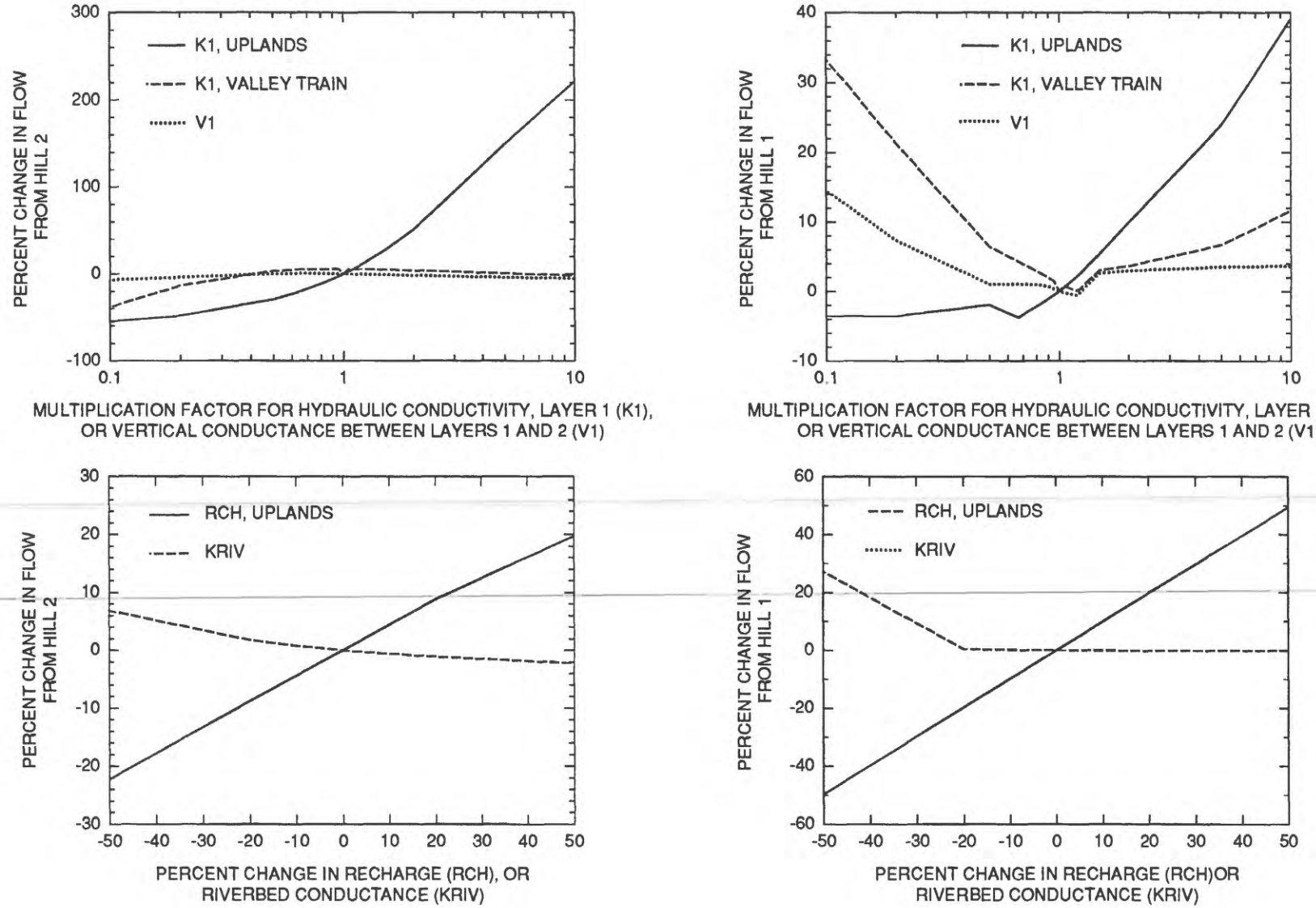

Figure 36.--Sensitivity of simulated flows from hill 1 and hill 2 to changes in hydrogeologic parameters in model of ground-water-flow system, Wright-Patterson Air Force Base and vicinity.

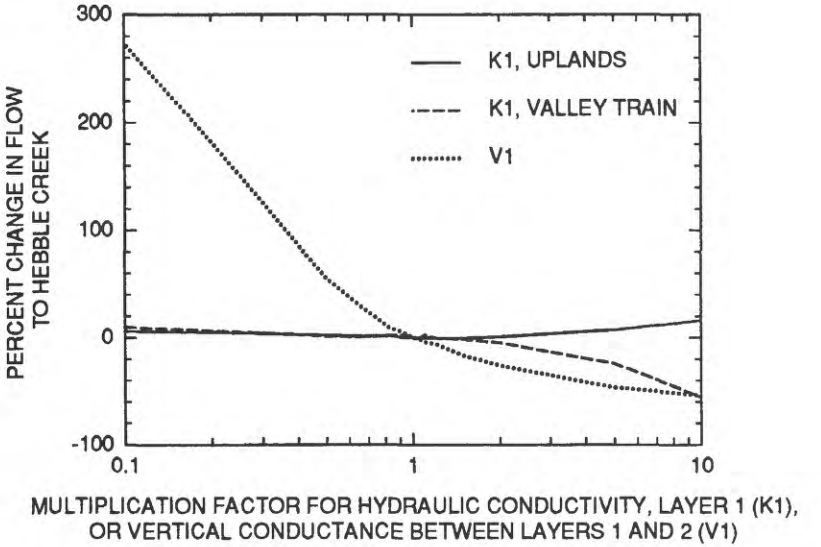

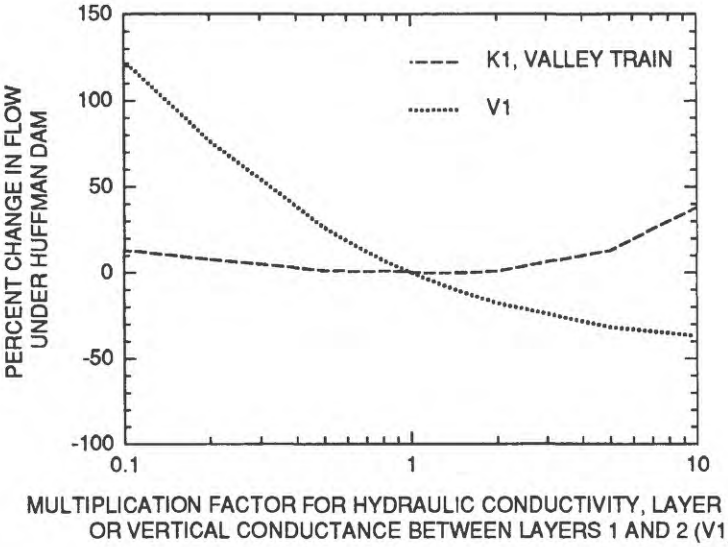

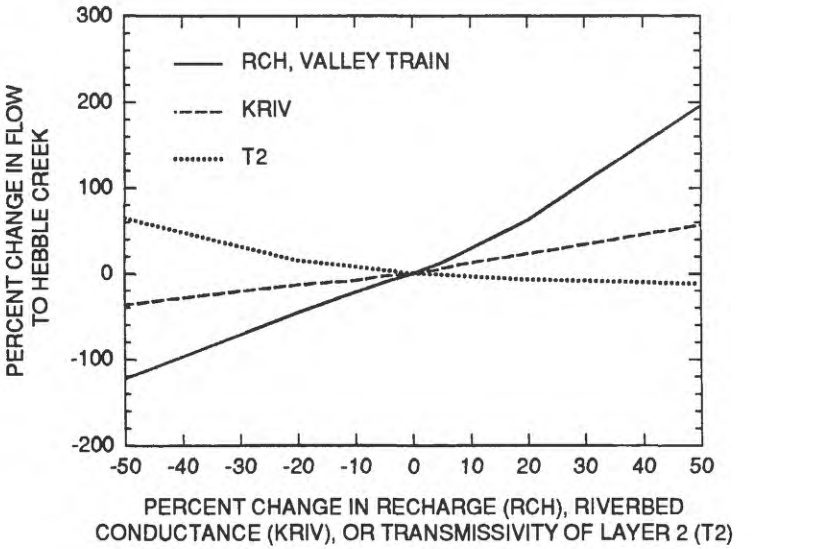

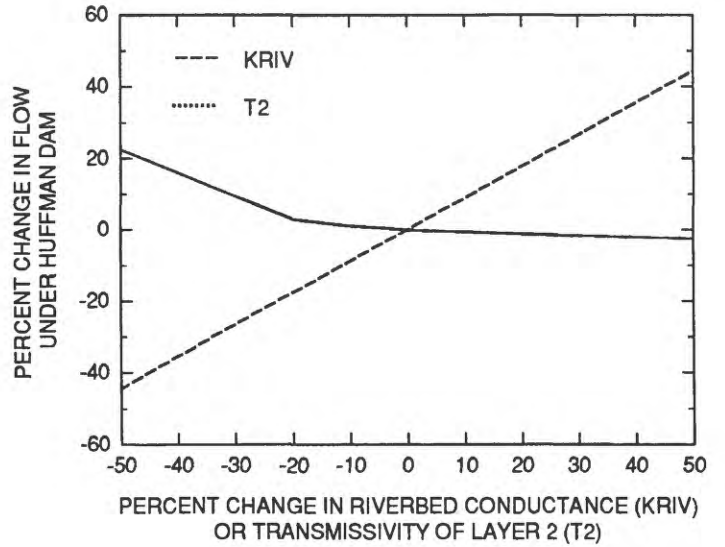

Figure 37.--Sensitivity of simulated flows under Huffmand Dam or to Hebble Creek to changes in hydrogeologic parameters in model of ground-water-flow system, Wright-Patterson Air Force Base and vicinity.

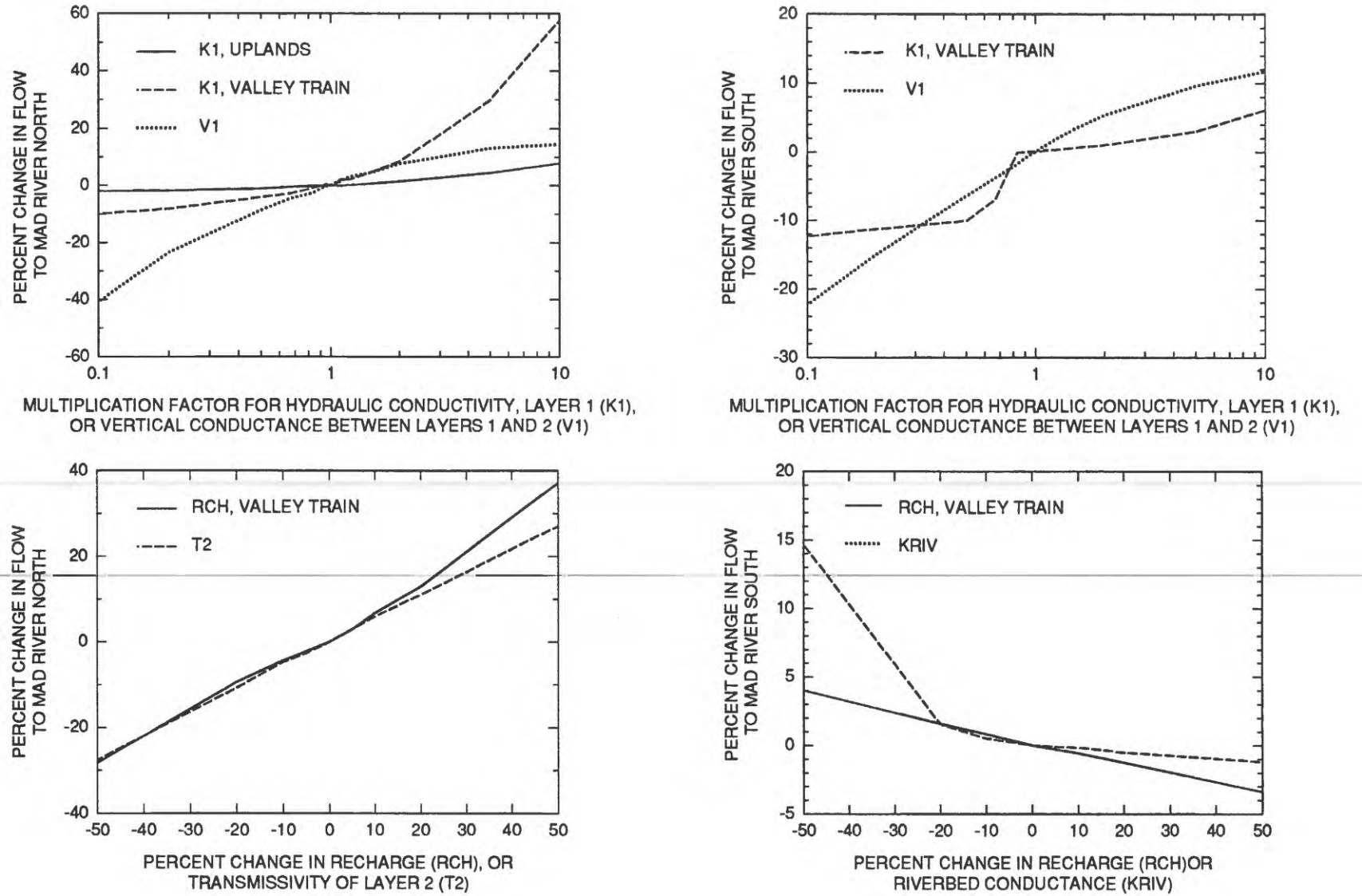

Figure 38.--Sensitivity of simulated flows to Mad River (north) and Mad River (south) to changes in hydrogeologic parameters in model of the ground-water-flow system, Wright-Patterson Air Force Base and vicinity.

Head residuals are highly sensitive to changes in K1, as expected. Most of the wells used during the calibration and sensitivity analysis of the model are completed in layer 1, and hydrogeologic data are the most numerous for this layer. The sensitivity of heads to K1 indicates that K1 cannot vary greatly from those values to which the model was calibrated without introducing gross errors to the model. The range of K1 values in the model adequately reflects the regional hydrogeologic conditions of the study area.

Hydraulic heads simulated by the model are more sensitive to changes of recharge and K1 in the upland areas than it is in the valley train, for two reasons. First, the model is two-dimensional in upland areas; that is, it has one active layer in the uplands. Recharge and K1 are the only hydrologic parameters that define layer 1 in the uplands. Simulation of the buried valleys, however, includes three layers that are highly transmissive and interactive, and neither K1 nor recharge dominate the flow regime. Second, the values of recharge and K1 in the upland areas of the calibrated model are small; changes in these values, however small, have a larger effect on the predicted heads than a similar change does in the valley train. Because K1 is small in the upland areas, ground water cannot be distributed rapidly, and steep gradients result.

Simulated hydraulic heads are most sensitive to decreases in V1 and K_{riv}, particularly in the valley-train deposits. RMSE increased rapidly when V1 decreased by more than 50 percent, indicating the importance of vertical flow to recharge and discharge, and when K_{riv} decreased by more than 20 percent, indicating the close interaction of rivers and the aquifer (discussed further below).

Increases in V1 increased flows to Mad River South and decreased flow under Huffman Dam without affecting the RMSE in the uplands or the valley train; however, increases in V1 also decreased the vertical gradients between wells at the well clusters listed in table 11. A new "calibrated" model incorporating increased values of V1 to reflect the slight improvements in simulated flows is not justified because of the increased error in the simulation of vertical gradients.

The results of the sensitivity analysis on K_{riv} verify evidence that has already been presented concerning the connection between the aquifer and the streams that cross it. The Mad River receives most of the discharge from the aquifer north of Huffman Dam; decreasing the riverbed conductance of the Mad River causes an increase of hydraulic heads north of the dam and an increase in flow beneath Huffman Dam. The same decrease in K_{riv} limits the amount of water available to recharge the aquifer by induced infiltration south of Huffman Dam at Rohrer's Island (fig. 38), resulting in increased drawdown. Several model nodes in layer 2 near Rohrer's Island went dry when K_{riv} was decreased by 20 percent, which violates the assumption that layer 2 was always confined and further emphasizes the sensitivity of the model to decreased K_{riv}. Except for increased flows to Hebble and Trout Creeks, the model displays little sensitivity to increases in K_{riv}.

Hydraulic heads and flows in the buried valleys southwest of Huffman Dam are sensitive to hydrogeologic conditions in the vicinity of Mad River well field. Although the distribution and volume of pumpage at Mad River well field were not included as parameters in the sensitivity analysis, they probably can significantly affect the model results in that area.

The sensitivity analysis indicates that the flow system could have been simulated with two layers instead of three. The model is negligibly sensitive to changes in the parameters defining layer 3, T3, and V2. All flows were affected by changes in V1, but not by changes in V2. Ground-water flows responded to changes in T3 and T2 similarly; that is, in most cases the directions of the responses were the same, but the magnitude of response was larger for changes in T2 than for changes in T3. An exception to this relation is the simulated discharge to Hebble Creek, which increases slightly with larger T3 (not shown in figure 37) but decreases with larger T2. This effect may be attributed to the presence of deep as opposed to shallow flow paths. Increased T2 enables a greater percentage of shallow flow to discharge to the Mad River, whereas decreased T2 forces more flow to Hebble Creek. Because this effect is not seen with changes in T3, it is concluded that Hebble Creek is not part of the deep flow system in the region.

The upland areas do not contribute greatly to flow in the buried valleys. A 20-percent increase of recharge in the upland areas, which is about 0.4 in., increases flow in Hebble Creek (which is near the wall of the Mad River backwater plain along part of its reach) by 5 percent, Mad River North by 3 percent, and Mad River South not at all. Flows under Huffman Dam and heads in the valley train are not affected by changes in K1 or recharge in the uplands. Similarly, the upland areas are not greatly sensitive to changes in the valley-train parameters.

Flow from the uplands, which include shale bedrock and a veneer of glacial drift, to the buried valleys is small. Discharge along hill 1 varied from 0.078 to 0.028 (Mgal/d)/mi, whereas discharge along hill 2 varied from 0.459 to 0.064 (Mgal/d)/mi. Although only the topmost part of the valley walls was simulated (the uplands and valley-train interface in layer 1, see fig. 21), the values of discharge reported are probably realistic because of the method used to calculate K1 in the uplands. Had more of the slope of the wall been simulated as available for discharge to the valleys, the thickness of layer 1 would have been greater, and K1 would have decreased. In either instance, the effective transmissivity of the upland areas is small, and the shale forming the uplands and the sides of the buried valleys contributes little to the total ground-water system.

Applications of the Model

The calibrated ground-water-flow model was used to delineate recharge-discharge areas and to estimate flow paths in the valley-train deposits along several transects. Recharge and discharge areas, shown in figure 39, are determined from head differences between model layers. Cells in layer 1 containing higher hydraulic head than those in underlying layers are shown as recharge (downward gradient) areas, whereas cells in layer 1 containing lower hydraulic head than those in underlying layers are shown as discharge (upward gradient) areas. Cells in layer 1 that overlie areas of small or no vertical hydraulic gradient are shown as neutral areas.

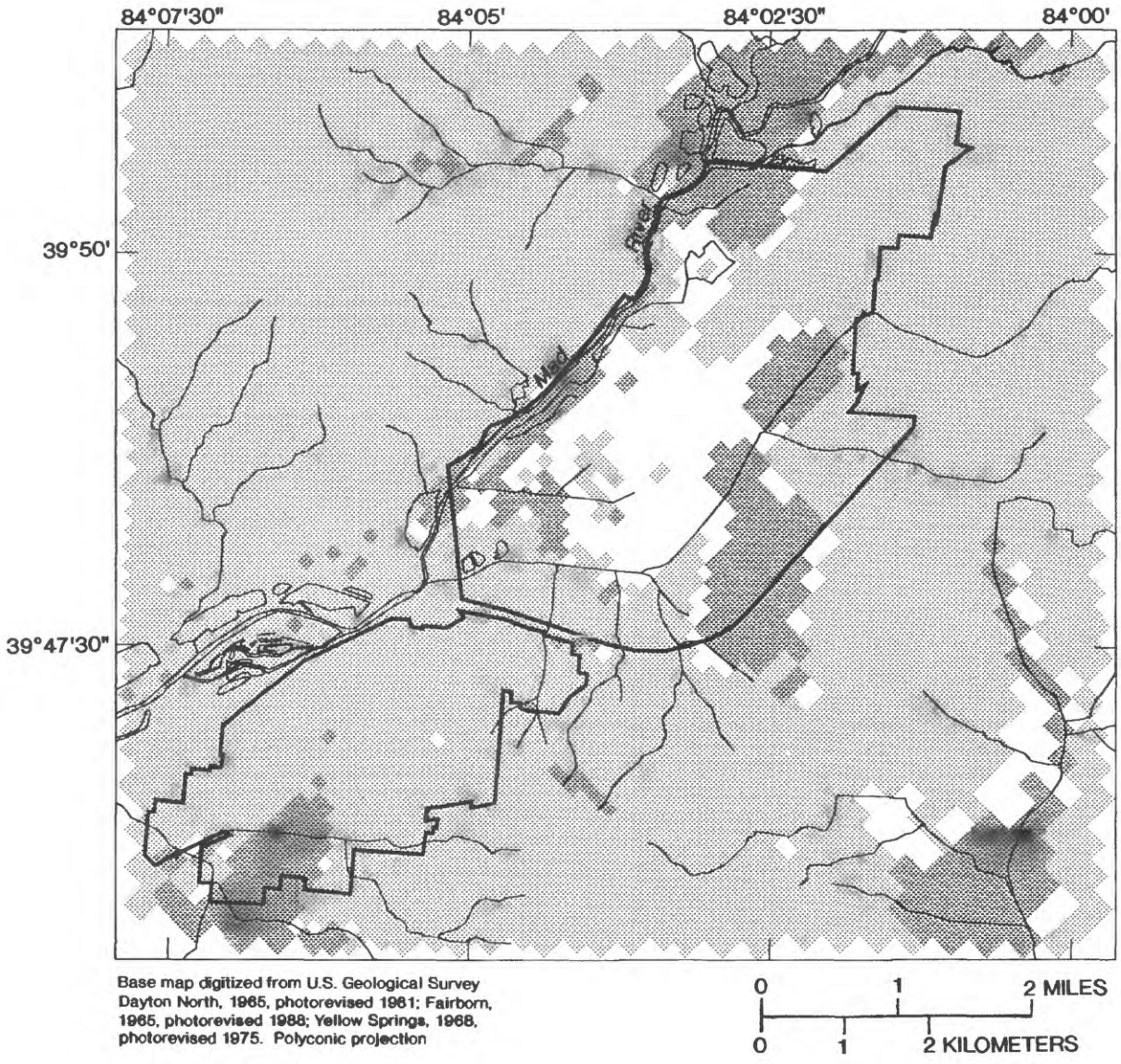

Figure 39.--Simulated discharge and recharge areas in the vicinity of Wright-Patterson Air Force Base.

During artificially unstressed conditions (that is, no pumping or other anthropogenic influence), ground water is expected to flow from upland (recharge) areas to low-lying (discharge) areas, where the heads are lower than those in the uplands. In the area surrounding WPAFB, natural discharge areas are centered on rivers that cross the valley-train deposits, including Mad River, Beaver Creek, and Hebble Creek. Pumping stress at production wells, however, changes the natural regional pattern of recharge and discharge. For example, the Mad River southwest of Huffman Dam is a recharge area (downward hydraulic gradients) because of the effect of pumping at Mad River well field. Figure 39 can be compared with the flow net shown in figure 12, which also depicts downward flow in the vicinity of Mad River well field. Upward flow in the south-eastern part of WPAFB Areas A and C is probably due to constriction of flow in the smaller buried valley that underlies that part of the Base.

Figure 39 indicates areas of recharge and discharge, but does not give any indication of amounts of recharge or discharge. Flow volumes between recharge and discharge areas depend not only on the head gradient but also on the transmissivity of the media and the area of contact shared by the media. A discussion of flow volumes was presented in the previous section.

The water-level surface predicted by the ground-water-flow model (fig. 31) is shown in three dimensions in figure 40; upland and valley-train areas are readily differentiated. As stated earlier, ground-water flow in the region is primarily in the valley-train deposits. Generally, areas of higher altitude serve as recharge sources for areas of lower altitude. Figure 40 also shows several lines of vertical sections through the valley-train deposits. Flow patterns calculated along these transects through WPAFB, shown in figure 41, are not necessarily primary flow paths, but do illustrate the general trends of flow in the region. The Mad River is the central discharge area for ground-water flow; however, some of the deeper water in the buried valleys flows under Huffman Dam rather than to the Mad River. The flow lines in figure 41 are typical of prevailing flow patterns in the vicinity of WPAFB; flow is mostly horizontal and includes only a slight vertical component.

Limitations of the Model

Because the ground-water-flow model is a numerical representation of the natural flow system, the model has inherent limitations. Some of these limitations were discussed earlier; numerical approximations and convergence tolerances that are defined by the user can produce models that simulate the natural system but never completely mimic it.

The model user should be wary of scale limitations of the model. Some aspects of the hydrologic regime, such as flow in some of the smaller rivers and streams (Hebble and Trout Creeks, for example), are difficult to simulate because of the regional nature of the model. Large and extensive hydrologic features, such as the Mad River and the buried-valley aquifer, can be modeled confidently on a regional scale. However, should the user require detailed information on a relatively small hydrologic feature, a more site-specific model would be required. Emphasis should not be placed on the simulation of small features on a regional scale. Determining the effects of changes in the system due to natural or anthropogenic causes is one such problem of

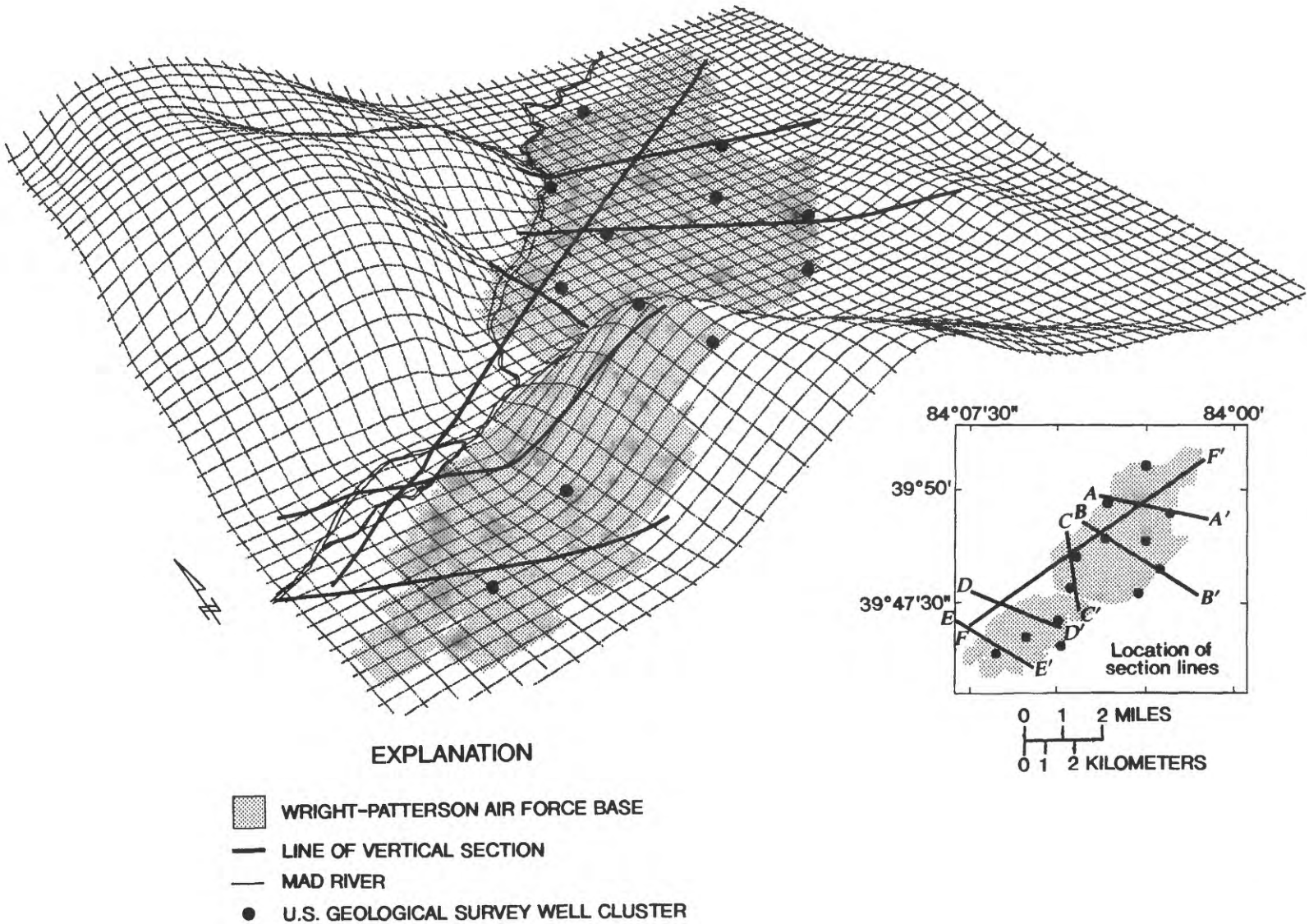

Figure 40.--Three-dimensional representation of the simulated water-level surface at Wright-Patterson Air Force Base.

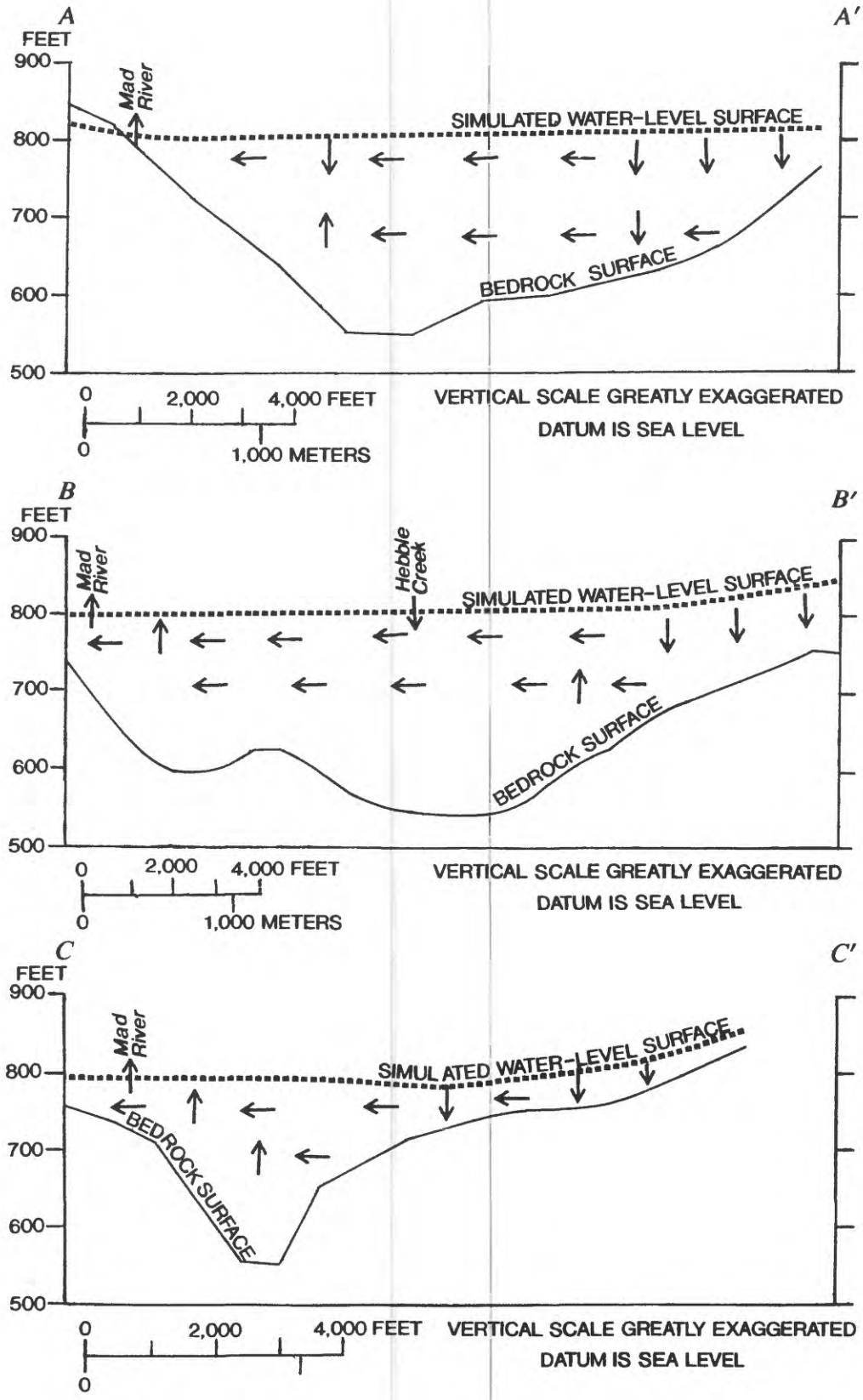

Figure 41.--Vertical-section ground-water flow nets derived from model results. (Arrows show flow direction based on head values in model cells. Location of section shown in figure 40.)

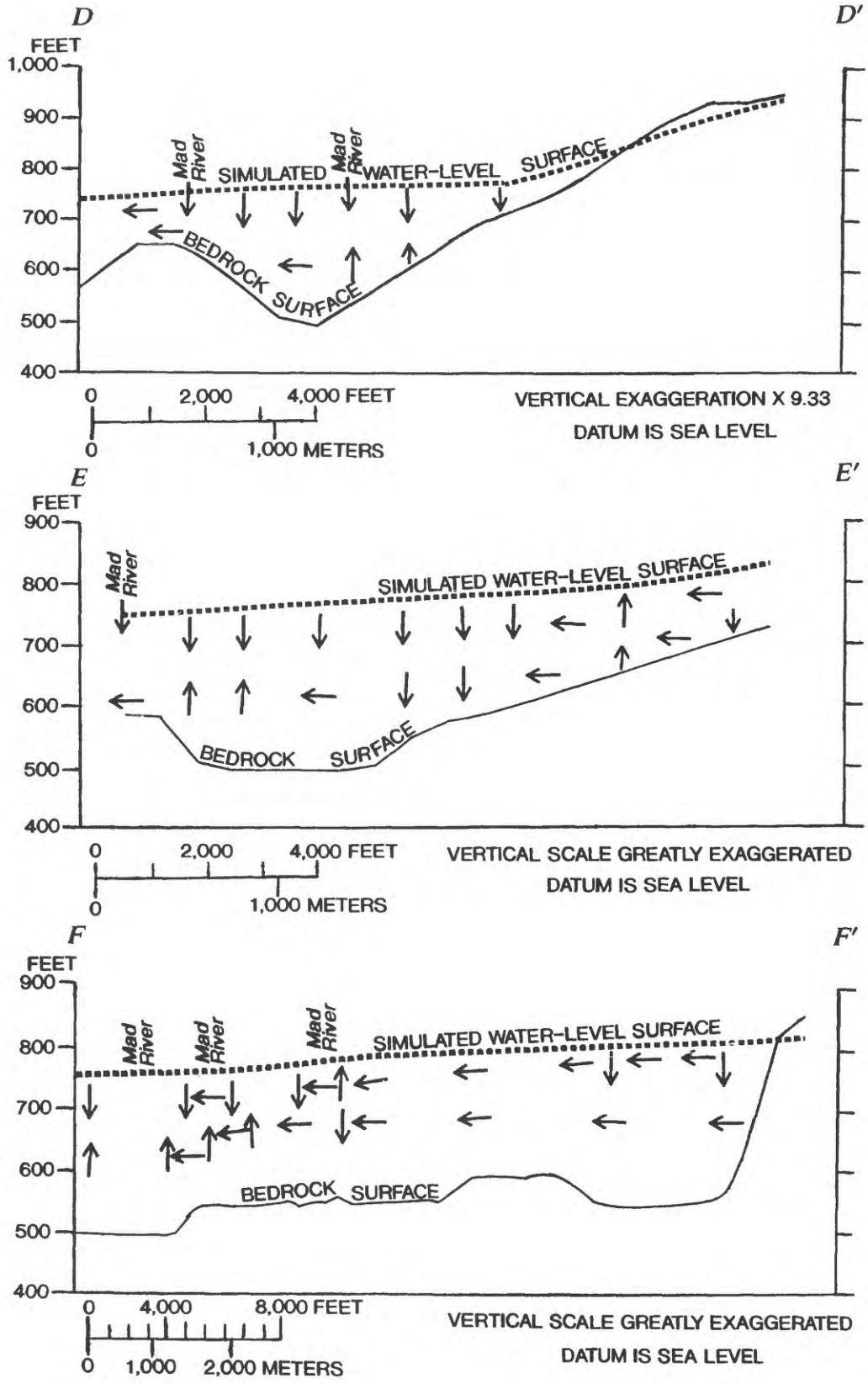

Figure 41.--Vertical-section ground-water flow nets derived from model results. (Arrows show flow direction based on head values in model cells. Location of section shown in figure 40.)--Continued.

scale. Large-scale changes, such as a 50-percent increase in pumping at Mad River well field, can be simulated with relative assurance of accuracy. Small changes, however, such as changing pumping from one well to another nearby, cannot be simulated accurately.

The effects of discrete sampling in space and time limit the accuracy of a model. Grid structure, boundary definitions, and calibration data all rely on hydrogeologic knowledge, which can never be complete. The modeler should not accept blindly the results of the model simulations, but should evaluate them in the light of ever-increasing hydrogeologic understanding of the study area.

GROUND-WATER QUALITY

The water-quality-sampling program was designed to provide a general assessment of current water quality at WPAFB and to assess the effects of recharge on ground-water quality in the shallow, intermediate, and deep parts of the glacial drift aquifer. An additional goal was to examine geochemical controls on major- and minor-element chemistry in the aquifer and to estimate the amount of ground water contributed to the glacial drift aquifer by flow through the bedrock valley walls. The amount of ground water contributed to the glacial drift aquifer by bedrock deposits was estimated by use of a chemical-mass approach in which boron was used as a conservative constituent.

Water samples were collected in June and July 1991 from 21 wells completed in the unconsolidated deposits and from 8 wells completed in bedrock (fig. 42). The samples were analyzed for pH, dissolved oxygen (DO), specific conductance, dissolved solids (DS), major and minor cations and anions, and dissolved organic carbon (DOC). Oxygen-18/oxygen-16 ($^{18}O/^{16}O$) and deuterium/hydrogen (D/H) isotope ratios, and tritium (^{3}H) concentration of ground water also were determined. A list of all water-quality characteristics determined for this study is given in table 13. This list includes current Ohio drinking-water standards for each property or constituent and discusses selected properties of each property or constituent in terms of implications for human health, domestic water use, and ground-water geochemistry. The water-quality characteristics listed in table 13 were chosen to provide a general assessment of water quality and ground-water geochemistry in the glacial aquifer that underlies WPAFB. Therefore, the list does not follow the Target Analyte List or Target Compound List that is associated with remediation activities at the Base. Results of analyses of the ground-water samples collected from the 29 wells are listed in table 14.

Median ground-water temperature at WPAFB was approximately 15oC (table 14). This temperature is probably not representative of the ground-water temperature at depth. Monthly average temperatures recorded in four deep wells (GR-319, GR-322, GR-324, GR-332) equipped with in-hole temperature sensors ranged from 12.0 to 13.2°C; the median temperature was 12.4°C. (See section on "Temporal Variability of Water Quality in Selected Wells".) Temperature recorded in a shallow well (GR-330) ranged from 13.8 to 13.2°C and was similar to the average ground-water temperature for the Dayton area reported by Norris and Spieker (1966) and Evans (1977) (14.1°C and 13.5°C, respectively). Water temperatures recorded in the flowthrough cell during sampling of the five wells ranged from 13.8 to 15.5°C. These temperatures were about 2.0°C higher than the monthly average temperatures recorded by the in-hole temperature probes.

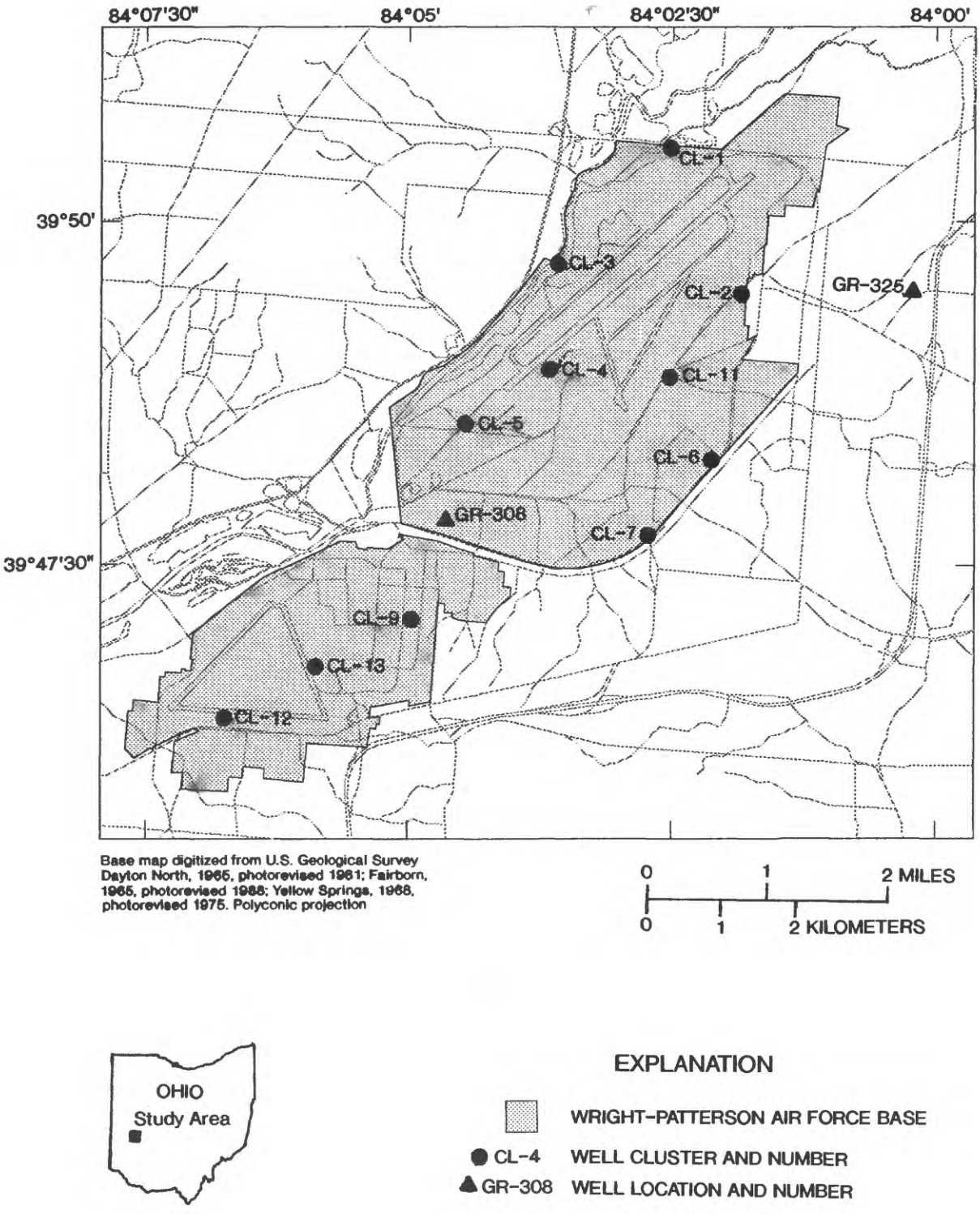

Figure 42.--Locations of water-quality sampling sites.

Table 13. — Concentration limits defined by Ohio Primary and Secondary Public Drinking-Water Regulations and implications for domestic water use and ground-water geochemistry for selected properties and chemical constituents in water samples collected at Wright-Patterson Air Force Base, Ohio

[OEPA, Ohio Environmental Protection Agency; MCL, Maximum contaminant level; SMCL, Secondary maximum contaminant level; mg/L, milligrams per liter; µS/cm, microsiemens per centimeter; $CaCO_3$, calcium carbonate; MCL's are established on the basis of health effects; SMCL's are established on the basis of aesthetic effects. MCL's and SMCL's are based on Ohio drinking water standards set by the Ohio Environmental Protection Agency (OEPA, 1991). Geochemical implications of each water property as they relate to this study are based on results given in the text and the discussion of natural water chemistry given by Hem (1989).]

Constituent or property	Concentration limits and water use implications	Implications for ground-water geochemistry
Temperature, °C (Celsius)	Regulatory standards not established.	Needed for speciation and saturation-state calculations. Can be used to identify recharge-discharge zones.
Specific conductance, µS/cm	Regulatory standards not established.	Proportional to total ionic concentration in solutions and can be used to indicate relative concentrations of ionic solutes between different water samples.
Solids, residue at 180°C, mg/L	Aesthetic—SMCL is 500 mg/L. Concentrations greater than 1,000 mg/L may cause objectionable tastes and laxative effects. May also cause foaming or may corrode some metals.	Proportional to dissolved ion concentrations. Like specific conductance, may be used to distinguish between different water types in an aquifer.
Dissolved oxygen, mg/L	Regulatory standards not established with respect to drinking water although concentration limits for surface-water bodies (streams and rivers) may have been set by OEPA.	Atmospheric oxygen dissolves in shallow ground water, and its presence at concentration exceeding reporting limits indicates highly oxidizing conditions. Oxygen reacts with organic matter, ferrous iron, or sulfide-bearing minerals and is quickly removed from the aquifer. The presence of dissolved oxygen in deep parts of an aquifer indicates rapid recharge rates or a lack of oxidizable material (organic matter, sulfide minerals) in aquifer rocks and sediments.
pH, standard units	Aesthetic—SMCL standard requires values between 7.0 and 10.5. Values outside of this range indicate to corrosive water.	General measure of the acidity or alkalinity of a water sample. One of the most important properties with respect to regulating the transport of metals, organics, and other dissolved constituents in ground water. Also controls dissolution-precipitation reactions in the aqui fer.
Hardness mg/L, as $CaCO_3$	Aesthetic—Upon heating and evaporation, hard water precipitates carbonate mineral deposits, scale, and crusts on pipes, hot water heaters, boilers, and cooking utensils. Also causes increased soap consumption. Public-water supplies with hardness concentrations greater than 100 mg/L are typically softened.	Hardness is caused by high concentrations of calcium, magnesium, and to a lesser extent, strontium. Waters with hardness values greater than 200 or 300 mg/L are usually associated with carbonate- or gypsum-bearing aquifers.
Calcium, dissolved mg/L	Aesthetic—Regulatory standards not established. Major contributor to hardness and scale formation.	In carbonate-bearing aquifers, is derived from the dissolution of calcite or dolomite and in some instances, gypsum. Concentrations of calcium are usually regulated by equilibria with carbonate minerals such as calcite. Carbonate equilibria are, in turn, largely controlled by pH and pCO_2.

Table 13.—Concentration limits defined by Ohio Primary and Secondary Public Drinking-Water Regulations and implications for domestic water use and ground-water geochemistry for selected properties and chemical constituents in water samples collected at Wright-Patterson Air Force Base, Ohio—Continued

Constituent or property	Concentration limits and water use implications	Implications for ground-water geochemistry
Magnesium, dissolved mg/L	Aesthetic—Regulatory standards not established. Contributes to hardness and scale formation. At high concentrations (> 125 mg/L) may cause laxative effects, especially to transient users.	In carbonate-bearing aquifers, is derived from the dissolution of magnesium-bearing calcite or dolomite.
Sodium, dissolved mg/L	Health—Health advisory level is 20 mg/L for persons with medical reasons for moderating dietary intakes of sodium. Otherwise, sodium in water is not dangerous to human health.	May be derived from the dissolution of sodium-bearing aluminosilicate minerals (such as albitic feldspar) or halite (NaCl) present in evaporite deposits. In carbonate aquifers, high sodium concentrations are often indicative of the effects of human activities such as road deicing or leaking septic tanks. At WPAFB elevated sodium concentrations were associated with shallow glacial waters and with highly saline sodium chloride waters collected from bedrock shale of Ordivician age.
Potassium, dissolved	Regulatory standards not established. No health or aesthetic implications for the range of concentrations found in this study.	Typically derived from the dissolution of potassium-bearing aluminosilicate minerals such as potassic feldspar or micas. Concentrations are typically low because of the low reactivity of the potassium-bearing silicate minerals and the incorporation of potassium in clay minerals such asillite (a common mineral in glacial-till deposits).
Alkalinity, mg/L as $CaCO_3$	Regulatory standards not established. No health or aesthetic implications for the range of concentrations found in this study. Alkalinity is a measure of the capacity of a water to neutralize acid.	In carbonate-bearing aquifers, almost all alkalinity is due to the presence of the bicarbonate ion (HCO_3^-) which is derived from the dissolution of carbonates by CO_2-based carbonic acid (H_2CO_3). Minor contributors to alkalinity include the carbonate (CO_3^{2-}) and hydroxide (OH^-) ions.
Chloride, dissolved mg/L	Aesthetic—SMCL is 250 mg/L. At concentrations greater than 250 to 400 mg/L imparts a salty taste to water depending on individual tolerance. High concentrations are corrosive to most metals.	Derived from the dissolution of halite. Is a rare constituent of non-evaporitic rocks. High concentrations imply inputs of saline brines of natural origin or anthropogenic sources such as road salt. Major constituent of sodium chloride waters found in bedrock shales at WPAFB.

Table 13.—Concentration limits defined by Ohio Primary and Secondary Public Drinking-Water Regulations and implications for domestic water use and ground-water geochemistry for selected properties and chemical constituents in water samples collected at Wright-Patterson Air Force Base, Ohio—Continued

Constituent or property	Concentration limits and water use implications	Implications for ground-water geochemistry
Sulfate, dissolved mg/L	Aesthetic—SMCL is 250 mg/L. Combines with calcium to form scale in water heaters and boilers. At concentrations exceeding 500-600 mg/L, imparts a bitter taste and may cause laxative effects in some individuals.	Derived from dissolution of gypsum ($CaSO_4 \cdot 2H_2O$) or the oxidation of sulfide minerals such as pyrite (FeS_2). Stable under oxidizing conditions; howver, under reducing conditions can be converted to H_2S.
Fluoride, dissolved mg/L	Health—MCL is 4.0 mg/L. SMCL is 2.0 mg/L. Beneficial to development and health of children's teeth at concentrations below 2.0 mg/L. At higher concentrations causes mottling of tooth enamel and skeletal fluorosis.	Major source is the mineral fluorite (CaF_2). Fluoride is also derived from flouride-bearing micas and phos phate minerals. Concentrations often regulated by ion equilibria, although control by fluorite equilibria is possible. At WPAFB, elevated concentrations were observed in sodium chloride waters of bedrock shales.
Nitrate, dissolved mg/L	Health—MCL is 44.0 mg/L as NO_3^-. Concentrations exceeding the MCL may cause methemoglobinemia (blue-baby syndrome) in bottle fed infants.	Presence of nitrate indicates oxidizing conditions in the aquifer. Elevated concentrations (>0.50 mg/L) are indicative of anthropogenic sources of nitrate (fertilizer, septic tank leakage) and indicate that the aquifer is vulnerable to infiltration of surface drainage.
Orthophosphate, dissolved mg/L as PO_4^{3-}	No health or aesthetic implications for the range of concentrations determined in this study.	Although a common minor element in most rocks, readily soluble forms are rare. Major component of sewage and industrial cleaning wastes; elevated concent rations indicate that the aquifer is vulnerable to infiltration of surface drainage.
Iron, dissolved	Aesthetic—SMCL is 0.30 mg/L. At concentrations exceeding the SMCL iron contributes to a metallic taste and staining of fixtures, utensils, and laundry. Higher concentrations form reddish-brown sediment and water-line deposits.	General redox indicator. Dissolved-iron concentrations are below detection limits in oxygenated waters at near neutral pH conditions. Under more reducing conditions, dissolved iron concentrations may exceed several milli grams per liter.
Manganese, dissolved, mg/L	Aesthetic—SMCL is 0.10 mg/L. At concentrations exceeding the SMCL, manganese may cause dark-brown or black staining of laundry and utensils.	Concentrations controlled by various oxide and oxy-hydroxide equilibria. Dissolution of manganese-oxide coatings on glacial aquifer material under reducing con ditions is a likely source of dissolved manganese.

Table 13.—Concentration limits defined by Ohio Primary and Secondary Public Drinking-Water Regulations and implications for domestic water use and ground-water geochemistry for selected properties and chemical constituents in water samples collected at Wright-Patterson Air Force Base, Ohio—Continued

Constituent or property	Concentration limits and water use implications	Implications for ground-water geochemistry
Silica, dissolved mg/L	No health or aesthetic implications for the range of concentrations determined in this study.	Used to evaluate controls on silica concentration.
Boron, dissolved	Regulatory limits not established. No human health or aesthetic implications for the range of concentrations found in this study. Boron is essential for plant nutrition and is toxic to some plants at high concentrations.	Concentration of boron is not affected by adsorption, precipitation or dissolution reactions. It can therefore be used as a chemical tracer. Notably elevated boron concentrations are found at WPAFB in sodium chloride waters of the bedrock shales. Boron concentrations were used to assess bedrock contribution to the glacial aquifer. Boron is present in high concentrations in most landfill leachate.
Dissolved organic carbon, mg/L	Regulatory limits not established. No health or aesthetic implications for the range of concentrations found in this study.	Concentrations greater than 3-4 mg/L are unusual for ground water and may indicate the presence of hydrocarbon compounds derived from human activities and vulnerability of the aquifer to surface drainage. Present at high concentrations in landfill leachate and in ground water affected by petroleum spills or leaks.
δD and $\delta^{18}O$ stable isotopes in per mil	Not applicable.	Used to evaluate sources of water and geochemical processes (mixing, isotopic exchange with aquifer materials). See text for further details.
Tritium (^{3}H), tritium units	Regulatory limits not established. No health or aesthetic implications for the range of concentrations found in this study.	Radioactive isotope of hydrogen introduced into the atmosphere in large quantities during the period of atomic bomb testing in early 1950's and 1960's. Used to estimate approximate recharge age of ground water; to examine ground-water-flow paths in the glacial aquifer; and examine contributions of bedrock aquifer ground water to the glacial aquifer.

Table 14.—Results of chemical analyses of ground water at Wright-Patterson Air Force Base

[µS/cm, microsiemens per centimeter at 25 degrees Celsius; mg/L, milligrams per liter; TU, tritium units; --, data not obtained or not applicable. ND, not detected or below reporting level; S, shallow glacial well (<60 feet in depth); I, intermediate-depth glacial well (100 to 150 feet in depth); D, deep glacial well (80 to 240 feet in depth, depending on depth to bedrock); B, well finished in bedrock; B (Brass), well partially or totally finished in Brassfield Limestone. Reporting limits from Enseco Inc. (1991). Ohio drinking-water standards from Ohio Environmental Protection Agency (1991); (MCL), Maximum Contaminant Level; (SMCL), Secondary Maximum Contaminant Level. Median values were not calculated if the total number of samples was less than four]

Well number	Date of sampling	Depth (S,I,D,B)	Site number (in fig. 42)	Temperature (degrees Celsius)	Specific conductance (µS/cm)	Solids residue at 180° C dissolved (mg/L)	Oxygen dissolved (mg/L)	pH, field (standard units)	pH, laboratory (standard units)
GR-314	6/21/91	B	CL-2	14.5	2,480	1,400	<0.5	7.3	7.4
GR-303	6/24/91	B	CL-3	16.6	3,610	1,930	<.5	7.9	8.3
GR-305	6/20/91	B	CL-5	14.7	1,780	1,380	<.5	8.0	8.0
GR-304	6/19/91	B	CL-4	17.5	4,690	3,070	<.5	7.5	7.6
GR-313	6/27/91	B	CL-13	18.5	6,820	4,280	<.5	7.1	7.4
GR-308	6/24/91	B	CL-8	--	1,560	884	--	7.5	8.2
GR-309	7/01/91	B (Brass)	CL-9	14.8	698	459	<.5	7.2	7.4
GR-325	6/26/91	B (Brass)	GR-325	13.8	775	467	6.6	7.3	7.9
GR-324	6/20/91	D	CL-5	13.8	638	358	<.5	7.4	7.6
GR-328	6/25/91	D	CL-7	--	--	359	--	7.3	8.1
GR-332	6/27/91	D	CL-6	14.0	657	377	<.5	7.4	7.8
GR-322	6/19/91	D	CL-4	14.1	765	442	<.5	7.3	7.7
GR-335	6/26/91	D	CL-11	15.4	626	366	<.5	7.4	7.9
MT-153	6/28/91	D	CL-12	15.2	748	439	<.5	7.1	7.5
GR-317	6/18/91	D	CL-1	13.8	591	328	<.5	7.5	7.6
GR-319	6/21/91	D	CL-2	15.0	914	481	<.5	7.2	7.4
GR-327	6/25/91	I	CL-7	14.4	619	351	<.5	7.4	8.1
GR-334	6/26/91	I	CL-11	16.1	750	437	<.5	7.3	7.6
GR-331	6/26/91	I	CL-6	13.9	690	400	<.5	7.3	7.8
GR-323	6/20/91	S	CL-5	14.1	899	536	<.5	7.3	7.5
GR-329	6/27/91	S	CL-13	15.0	868	529	5.3	7.1	7.4
GR-333	6/26/91	S	CL-11	16.6	989	575	5.0	7.2	7.7
GR-326	6/25/91	S	CL-7	14.3	842	472	.7	7.3	7.8
GR-316	6/18/91	S	CL-1	15.6	609	356	<.5	7.5	7.7
GR-318	6/21/91	S	CL-2	15.0	832	482	<.5	7.2	7.3
GR-321	6/19/91	S	CL-4	14.7	779	454	<.5	7.2	7.6
GR-330	6/27/91	S	CL-6	15.5	965	571	3.0	7.1	7.4
GR-320	6/24/91	S	CL-3	14.8	629	348	<.5	7.6	8.1
MT-152	6/28/91	S	CL-12	14.7	933	572	<.5	7.2	7.4
Median bedrock		--	--	14.8	2,130	1,390	--	7.4	7.8
Median deep glacial		--	--	14.1	657	372	--	7.3	7.7
Median shallow glacial		--	--	14.9	855	506	--	7.2	7.6
Median all glacial		--	--	14.7	772	439	--	7.3	7.6
Reporting limit		--	--	--	--	10	.5	--	--
Ohio drinking water standard		--	--	--	--	500 (SMCL)	--	7.0 - 10.5 (SMCL)	

Table 14.—Results of water-quality analyses of ground water at Wright-Patterson Air Force Base—Continued

Well number	Depth (S,I,D,B)	Hardness, (mg/L as $CaCO_3$)	Calcium, dissolved (mg/L)	Magnesium, dissolved (mg/L)	Sodium, dissolved (mg/L)	Potassium, dissolved (mg/L)	Alkalinity, field (mg/L as $CaCO_3$)	Alkalinity, laboratory (mg/L as $CaCO_3$)	Chloride, dissolved (mg/L)	Sulfate, dissolved (mg/L)	Fluoride, dissolved (mg/L)
GR-314	B	592	142	58	237	8.4	149	138	724	1.1	1.8
GR-303	B	148	34	16	649	27.9	338	247	984	58.6	3.8
GR-305	B	83	18	9	315	21.5	345	299	362	1.0	3.7
GR-304	B	1,080	228	124	407	33.7	128	117	1,500	1.4	3.4
GR-313	B	1,230	284	126	895	45.8	199	185	2,270	29.0	3.8
GR-308	B	365	71	46	155	24.1	383	273	224	163	1.4
GR-309	B (Brass)	328	86	39	5.4	ND	312	282	7.0	78.4	ND
GR-325	B (Brass)	333	86	29	34.3	ND	245	227	62.1	73.2	ND
GR-324	D	333	79	33	ND	ND	298	272	11.1	36.3	ND
GR-328	D	323	76	33	7.9	ND	359	323	5.1	13.9	ND
GR-332	D	354	88	33	5.2	ND	375	333	2.0	8.7	ND
GR-322	D	392	93	39	5.4	ND	306	280	49.9	50.0	ND
GR-335	D	328	78	32	5.8	ND	313	279	8.1	30.4	ND
MT-153	D	389	96	37	9.8	ND	364	329	15.7	48.9	ND
GR-317	D	311	74	31	ND	ND	298	275	4.0	33.7	ND
GR-319	D	442	106	43	12.1	ND	302	277	94.8	41.2	ND
GR-327	I	321	77	31	ND	ND	316	287	3.8	30.5	ND
GR-334	I	386	91	39	7.2	ND	296	278	26.4	74.3	ND
GR-331	I	372	93	34	6.0	ND	391	343	3.2	13.0	ND
GR-323	S	416	107	36	23.6	ND	310	284	56.0	98.6	ND
GR-329	S	460	114	43	7.7	ND	332	306	38.6	89.0	ND
GR-333	S	379	97	33	56.8	ND	295	270	98.8	59.9	ND
GR-326	S	365	98	29	31.3	ND	269	242	86.4	51.9	ND
GR-316	S	289	64	31	12.4	ND	222	203	25.2	78.1	ND
GR-318	S	378	96	34	25.0	ND	312	286	49.2	59.4	ND
GR-321	S	391	94	38	8.1	ND	303	280	51.3	55.2	ND
GR-330	S	456	114	42	32.2	ND	377	351	74.4	46.2	ND
GR-320	S	300	72	29	11.2	ND	255	241	22.9	52.0	ND
MT-152	S	443	110	41	26.4	ND	347	347	62.6	87.0	ND
Median bedrock		349	86	42	276	26	279	237	540	43.8	3.6
Median deep glacial		345	83	33	6.9	--	310	280	9.6	35.0	--
Median shallow glacial		385	97	35	24.3	--	306	282	53.7	59.7	--
Median all glacial		378	93	34	10.5	--	310	280	26.4	50.0	--
Reporting limit		1.4	0.2	0.2	5.0	5.0	10.0	5.0	0.5	0.5	0.5
Ohio drinking water standard		--	--	--	--	--	--	--	250 (SMCL)	250 (SMCL)	4.0 (MCL)

Table 14.—Results of water-quality analyses of ground water at Wright-Patterson Air Force Base—Continued

Well number	Depth (S,I,D,B)	Nitrate, dissolved (mg/L)	Ortho-phosphate (mg/L as P)	Iron, dissolved (mg/L)	Manganese, dissolved (mg/L)	Silica, dissolved (mg/L)	Boron, dissolved (mg/L)	Dissolved organic carbon (mg/L)	δD, stable-isotope ratio (per mil)	$\delta^{18}O$, stable-isotope ratio (per mil)	Tritium ^{3}H (TU)
GR-314	B	ND	ND	1.10	0.11	7.9	1.70	1.2	-47.0	-7.70	< .3
GR-303	B	0.53	ND	ND	.04	7.0	4.70	1.5	-46.5	-7.60	< .3
GR-305	B	ND	ND	0.06	.05	7.4	4.20	1.0	-45.0	-7.55	< .3
GR-304	B	ND	ND	3.30	.19	6.7	3.80	1.1	-47.0	-7.70	< .3
GR-313	B	ND	ND	1.20	.10	7.4	3.00	.8	-44.5	-7.65	.6
GR-308	B	ND	ND	ND	.06	5.5	2.80	3.6	-45.0	-7.60	< .3
GR-309	B (Brass)	.26	ND	1.50	.18	15.7	ND	2.0	-43.5	-7.50	40.1
GR-325	B (Brass)	.52	ND	ND	ND	8.2	.04	1.1	-39.0	-6.60	16.7
GR-324	D	ND	ND	1.40	.12	16.1	ND	.7	-48.0	-7.75	21.3
GR-328	D	ND	ND	1.40	.07	18.5	.05	2.3	-47.0	-7.90	< .3
GR-332	D	ND	ND	1.90	.05	21.6	ND	1.2	-50.0	-8.05	< .3
GR-322	D	ND	ND	1.70	.08	13.6	ND	1.2	-46.5	-7.65	36.7
GR-335	D	ND	ND	.66	.08	16.9	ND	.9	-47.0	-7.65	< .3
MT-153	D	ND	ND	.55	.03	16.8	ND	.9	-47.0	-7.80	< .3
GR-317	D	ND	ND	.66	.20	15.7	ND	1.0	-47.0	-7.70	7.1
GR-319	D	.89	ND	2.40	.17	16.7	.03	5.6	-47.0	-7.65	8.6
GR-327	I	ND	ND	1.20	.09	16.4	ND	2.7	-47.5	-7.85	10.2
GR-334	I	ND	ND	2.10	.08	17.0	ND	.8	-46.5	-7.75	49.4
GR-331	I	ND	ND	2.10	.05	21.8	ND	1.2	-50.0	-8.15	.6
GR-323	S	ND	ND	.72	.06	13.9	.04	1.3	-41.0	-7.65	18.8
GR-329	S	2.90	ND	ND	ND	14.6	ND	1.2	-45.0	-7.60	37.0
GR-333	S	ND	ND	ND	ND	10.6	.08	1.1	-44.0	-7.30	20.7
GR-326	S	.95	ND	.22	ND	11.0	.04	2.3	-45.0	-7.55	21.6
GR-316	S	ND	0.80	ND	.01	8.4	.04	1.5	-41.0	-6.65	21.6
GR-318	S	4.10	ND	ND	ND	11.2	.04	1.1	-44.5	-7.45	17.3
GR-321	S	ND	ND	ND	ND	12.1	ND	1.0	-47.0	-7.60	33.3
GR-330	S	3.90	ND	ND	ND	17.0	.05	1.0	-45.5	-7.70	21.9
GR-320	S	1.40	ND	ND	.11	10.5	.06	2.2	-42.5	-6.95	29.6
MT-152	S	ND	ND	.11	.02	14.4	ND	1.4	-45.5	-7.45	21.6
Median bedrock		--	--	1.20	0.10	7.4	3.00	1.2	-45.0	-7.60	< .3
Median deep glacial		--	--	1.40	.08	16.8	--	1.1	-47.0	-7.70	3.5
Median shallow glacial		--	--	--	--	11.7	.04	1.3	-44.8	-7.50	21.6
Median all glacial		--	--	--	--	15.7	--	1.2	-46.5	-7.65	20.7
Reporting limit		0.2	0.5	0.04	0.01	0.30	0.03	0.50	--	--	--
Ohio drinking water standard		44.0 (MCL)	--	.30 (SMCL)	.05 (SMCL)	--	--	--	--	--	--

The positive error in temperature is attributed to heating of the ground water as it flowed through exposed hose and tubing that connected the pump outlet to the measurement point in the flowthrough cell. Variations in surface air temperature and the length of tubing used to connect the pump outlet to the flowthrough cell probably accounts for the large range of ground-water temperatures (13.8 to 18.5°C) recorded during sampling. It should be noted that air temperature during late June and early July was about 30°C.

General Overview of Water Quality

Ground water at WPAFB can be divided into two compositional groups on the basis of major cation and anion concentrations: calcium magnesium bicarbonate (Ca-Mg-HCO_3) waters and sodium chloride (Na-Cl) waters. Water collected from the unconsolidated deposits is exclusively of the calcium magnesium bicarbonate type. Water collected from bedrock is compositionally variable. Wells completed in the Brassfield Limestone yield calcium magnesium bicarbonate waters, whereas wells completed in bedrock shales yield waters whose major-ion compositions range from sodium chloride (Na-Cl) to sodium calcium chloride (Na-Ca-Cl) waters.

Unconsolidated Deposits

Water collected from wells completed in the unconsolidated glacial-drift deposits had a median field pH of 7.3 and a median specific conductance of 772 µS/cm (table 14). The dominant cations were calcium and magnesium, with median concentrations of 93 and 34 mg/L, respectively. As a result, glacial-drift ground water at WPAFB is considered to be very hard (median hardness was 378 mg/L as $CaCO_3$) (Durfor and Becker, 1964; Hem, 1989). The median sodium concentration for ground water in the glacial drift was 10.5 mg/L, whereas potassium concentration was consistently below the reporting limit (5.0 mg/L, table 14). Alkalinity determinations indicate that bicarbonate was the dominant anion (median alkalinity determined in the field was 280 mg/L as $CaCO_3$). Chloride and sulfate concentrations were highly variable, ranging from 2.0 to 99 mg/L Cl and 8.7 to 99 mg/L SO_4. Nitrate, fluoride, phosphate, and boron concentrations were generally below reporting limits, although some samples from shallow wells contained measurable concentrations of boron and nitrate (table 14).

Iron and manganese concentrations ranged widely, iron from below reporting limits to 2.4 mg/L and manganese from below reporting limits to 0.20 mg/L (table 14). Water from 12 wells completed in the unconsolidated deposits equalled or exceeded the secondary maximum contaminant level (SMCL) of 0.3 mg/L for iron and 0.05 mg/L for manganese set by the Ohio Environmental Protection Agency (OEPA) (1991). SMCL's are non-enforceable recommended standards for water quality based on aesthetic criteria (color, taste, odor, staining potential) related to the public's acceptance of drinking water (table 13). Concentrations of DOC ranged from 0.7 to 5.6 mg/L; the median concentration was 1.2 mg/L. Most ground-water samples from the unconsolidated deposits did not contain measurable concentrations of DO.

For comparative purposes, water samples collected from well clusters completed in the unconsolidated deposits are subdivided into shallow, intermediate, and deep waters. This subdivision is based on the presence or absence of less transmissive layers that may locally retard vertical flow between sand and gravel bodies. In general, shallow wells are screened at depths less than 60 ft, whereas deep wells, because of the large variation in depth to bedrock throughout the study area, are screened at depths ranging from 80 to 240 ft. Intermediate wells were drilled only in the thickest parts of the glacial aquifer (total aquifer thickness > 200 ft). These wells, which were completed in sand and gravel layers located between less transmissive silt and clay layers, are screened at depths between 100 and 150 ft (Dumouchelle and de Roche, 1991).

It was hypothesized that each depth subgroup would have distinct chemical or isotopic characteristics that would facilitate identification of recharge effects at various depths in the aquifer. On the basis of major-ion chemistry, however, waters of the three subgroups cannot be clearly distinguished from one another. This is illustrated on a trilinear diagram (fig. 43), which graphically groups water types on the basis of the milliequivalent percentages of major cations and anions in the water. Water samples from the three subgroups plot in relatively tight, overlapping clusters in the calcium-magnesium-bicarbonate part of the diagram. Some separation between the shallow and deep waters is noted, particularly with respect to the anion composition of these waters. In contrast, most bedrock samples plot in locations on the diagram indicating predominately sodium-chloride or sodium-calcium-chloride compositions.

Upon closer examination, subtle chemical variations are noted, especially between the shallow and deep sample groups. The small number of intermediate-depth samples (3) precludes meaningful statistical comparisons with the other groups, although the compositional characteristics of the intermediate-depth waters generally are similar to those of the deep waters (table 14). Ground water collected from shallow wells was higher in mean temperature, specific conductance, and DS concentrations than waters from deep wells (table 14). Median sodium and chloride concentrations of the shallow waters were notably higher than those of the deep waters (table 14). The largest number of samples containing measurable nitrate and boron concentrations was found in the shallow subgroup. In addition, the shallow subgroup was the only sample group whose waters had measurable DO concentrations. The presence of oxygenated waters in the shallow part of the aquifer is correlated with uniformly low iron and manganese concentrations. Elevated iron and manganese concentrations were associated with anoxic waters collected from sand and gravel units in the intermediate and deep parts of the aquifer.

Results of the current study can be compared with historical water-quality data collected from supply wells at WPAFB (fig. 44). More than 250 analyses of water collected from 17 shallow wells during 1954-73 have been compiled (W.L. Cunningham, U.S. Geological Survey, written commun., 1992). All of the wells were completed in the unconsolidated deposits and were screened at depths of less than 80 ft. Although differences in sample-collection procedures and analytical methods preclude direct comparison of the historical and current water-quality data sets, it is noted that the median properties and constituent concentrations samples of the historical group (table 15) are similar to the compositions of waters collected in 1991 from shallow parts of the unconsolidated aquifer. On a trilinear plot, the historical data plot in a tight cluster in the calcium

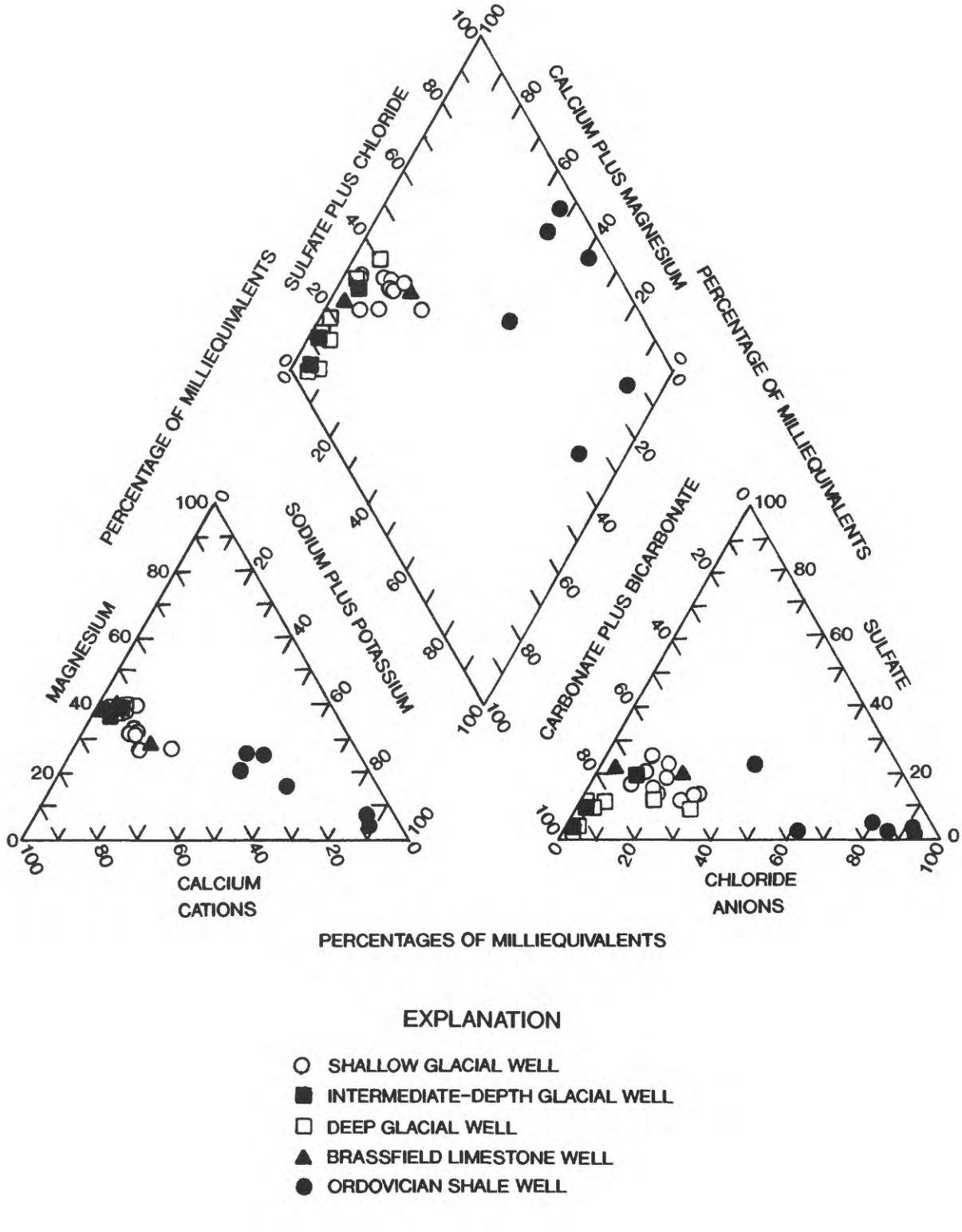

Figure 43.--Trilinear plot of major cation and anion percentages of ground-water samples collected at Wright-Patterson Air Force Base in June-July 1991.

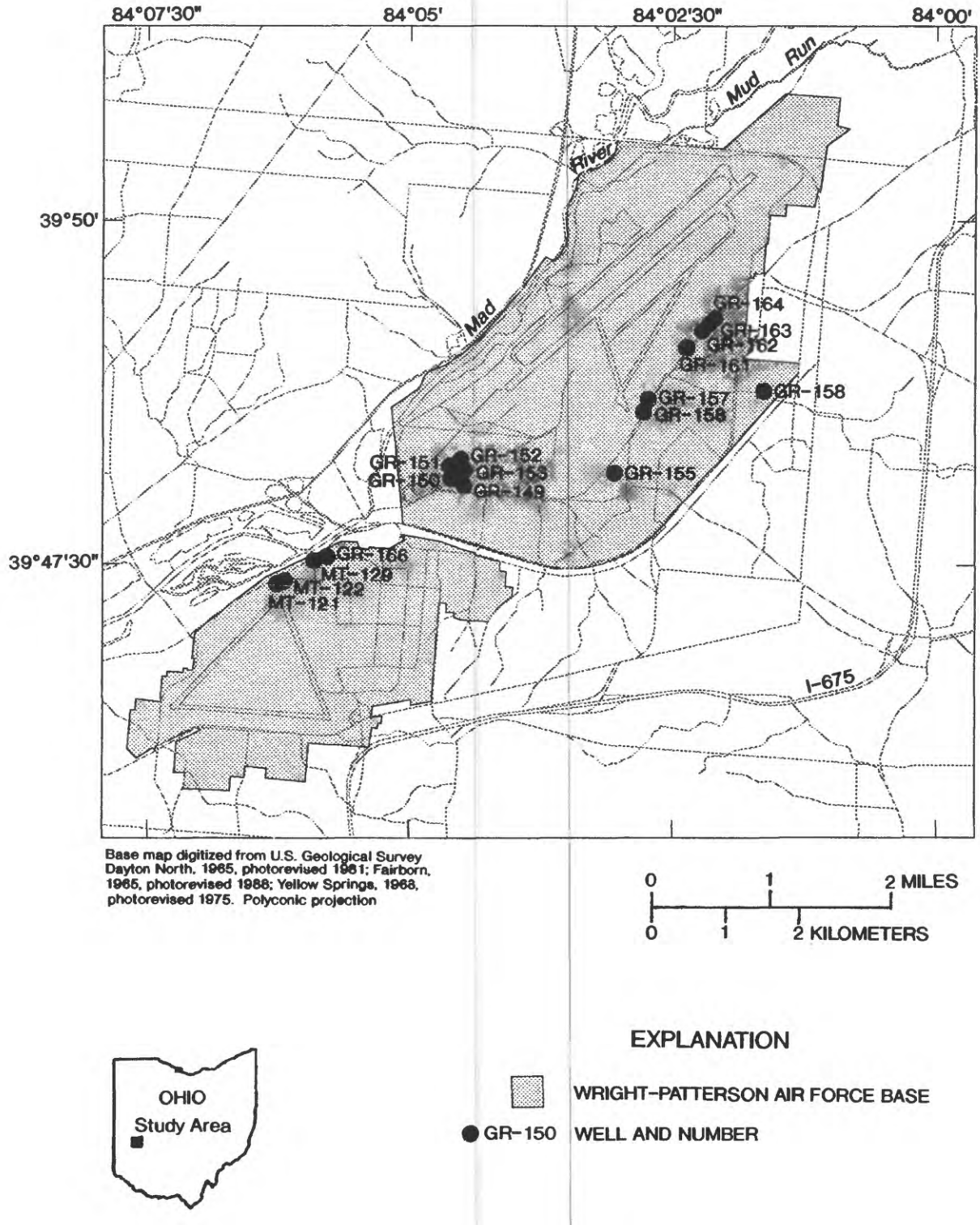

Figure 44.--Locations of previous (1954-73) water-quality sampling sites.

Table 15.—Median values for selected properties and constituents of ground-water samples collected at Wright-Patterson Air Force Base, 1954-73

[µS/cm, microsiemens per centimeter at 25 degress Celsius; mg/L, milligrams per liter. Data source: W.L. Cunningham, U.S. Geological Survey, written commun., 1992]

Well number	Number of samples	Well depth (feet)	Specific conductance (mS/cm)	Solids, residue at 180° C, dissolved (mg/L)	pH, laboratory	Hardness (mg/L as $CaCO_3$)	Calcium, dissolved (mg/L)	Magnesium, dissolved (mg/L)	Sodium, dissolved (mg/L)
GR-150	14	85	992	655	7.4	505	131	49	21.5
GR-152	14	79	1,009	658	7.3	530	132	48	24.5
GR-151	11	88	1,070	706	7.5	560	140	48	32.0
GR-153	14	81	954	620	7.4	500	122	49	18.0
GR-163	15	60	812	483	7.5	410	101	39	20.0
GR-164	17	60	834	524	7.5	420	106	40	20.0
GR-162	15	64	916	606	7.4	396	107	37	25.0
GR-155	15	59	894	569	7.4	440	110	40	18.0
GR-158	14	52	812	514	7.6	420	102	36	22.0
GR-161	15	59	1,040	652	7.4	450	122	43	50.0
GR-156	16	58	907	553	7.5	420	107	38	33.0
GR-157	15	61	853	528	7.4	410	103	38	25.0
GR-166	15	57	827	537	7.5	410	98	38	17.0
GR-149	16	79	922	606	7.5	490	123	46	17.0
MT-121	16	52	743	454	7.6	370	94	34	14.5
MT-122	14	61	729	470	7.5	380	96	36	16.5
MT-123	16	71	836	547	7.5	420	104	40	18.5
Median of all samples	15	60	894	553	7.5	420	107	40	20.0

Table 15.—Median values for selected properties and constituents of ground-water samples collected at Wright-Patterson Air Force Base, 1954-73—Continued

Well number	Potassium, dissolved (mg/L)	Alkalinity, laboratory (mg/L as $CaCO_3$)	Chloride, dissolved (mg/L)	Sulfate, dissolved (mg/L)	Fluoride, dissolved (mg/L)	Nitrate, dissolved (mg/L)	Iron, dissolved (mg/L)	Manganese, dissolved (mg/L)	Silica, dissolved (mg/L)
GR-150	2.0	321	48	168	0.20	< 0.1	1.40	0.06	13.0
GR-152	2.1	337	62	158	.20	< .1	1.50	.08	14.0
GR-151	2.2	336	76	185	.20	< .1	1.00	.07	13.0
GR-153	1.8	340	48	130	.20	.1	.76	.09	15.0
GR-163	2.1	310	42	89	.20	13.0	.02	.01	12.0
GR-164	2.2	285	46	91	.20	13.0	.06	.01	12..0
GR-162	2.9	325	62	96	.20	7.7	.13	.03	13.0
GR-155	2.0	312	63	80	.20	10.0	.03	.01	14.0
GR-158	3.5	304	46	83	.10	15.0	.06	< .01	12.0
GR-161	3.1	323	80	114	.20	7.1	.05	.03	13.0
GR-156	2.6	314	70	72	.10	9.3	.03	.01	12.0
GR-157	2.8	310	65	72	.10	10.0	.03	< .01	13.0
GR-166	2.1	274	40	113	.20	1.6	.07	.04	10.0
GR-149	1.7	325	38	151	.20	.5	.23	.08	12.0
MT-121	2.1	267	25	90	.20	6.6	.06	.01	11.0
MT-122	2.2	267	29	93	.20	4.3	.05	.03	11.0
MT-123	2.1	274	41	126	.20	1.7	.09	.03	11.5
Median of all samples	2.1	312	48	96	0.20	6.6	0.06	0.03	12.0

magnesium bicarbonate field (fig. 45); however, the samples collected during 1954-73 generally contained higher concentrations of sulfate than did the shallow well waters collected during the current study.

Consolidated Deposits

Waters collected from wells completed in consolidated deposits can be subdivided into two groups. Wells that are partly or wholly completed in the Brassfield Limestone (GR-309 and GR-325) yield calcium magnesium bicarbonate waters whose pH, specific conductance, and overall solute compositions were compositionally similar to the waters collected from the unconsolidated deposits. In contrast, the waters collected from the six wells completed solely in the Ordovician shales were sodium chloride (or sodium calcium chloride) waters whose concentrations of calcium, magnesium and bicarbonate (table 14) were highly variable. The sodium chloride waters were very hard; median field pH was 7.4, and median specific conductance was 3,490 µS/cm. The degree of salinity of the sodium chloride waters was highly variable, with sodium and chloride concentrations ranging from 155 to 895 mg/L and 224 to 2,270 mg/L, respectively. The maximum DS concentration was 4,280 mg/L. Median sodium and chloride concentrations of the sodium chloride waters were 276 and 540 mg/L, respectively. Total concentrations of lesser cations and anions were also highly variable (table 14).

Sodium chloride waters were notably enriched in boron and fluoride, with median dissolved boron and fluoride concentrations of 3.0 and 3.6 mg/L respectively (table 14). The fluoride concentration of these waters exceeded the SMCL set for fluoride by OEPA (2.0 mg/L) in four out of six wells. Currently, no drinking-water standards pertain to boron. Iron and manganese concentrations ranged from < 0.04 to 3.3 mg/L, and < 0.04 to 0.19 mg/L, respectively. The SMCL for iron (0.30 mg/L) was exceeded in waters from three out of six wells, and the SMCL for manganese (0.05 mg/L) was equaled or exceeded in waters from four out of six wells. The SMCL for chloride (250 mg/L) was exceeded in five out of six samples collected from wells completed in the bedrock shales, whereas all samples exceeded the SMCL for DS (500 mg/L).

Geochemical Controls on Ground-Water Quality

Ground-water quality reflects the net sum of all geochemical, hydrologic, and biological processes that have modified the solute composition of recharge water since it entered the aquifer. Important processes that affect water quality include water-gas-rock reactions, mixing of different water types, the effects of human activities, and various biological processes. Among these general categories, the first process can be evaluated quantitatively with equilibrium thermodynamic models, whereas the second and third processes can be evaluated qualitatively by use of available chemical data. The influence of biological processes, because of their inherent complexity and variability, are much more difficult to evaluate and are not considered in this report.

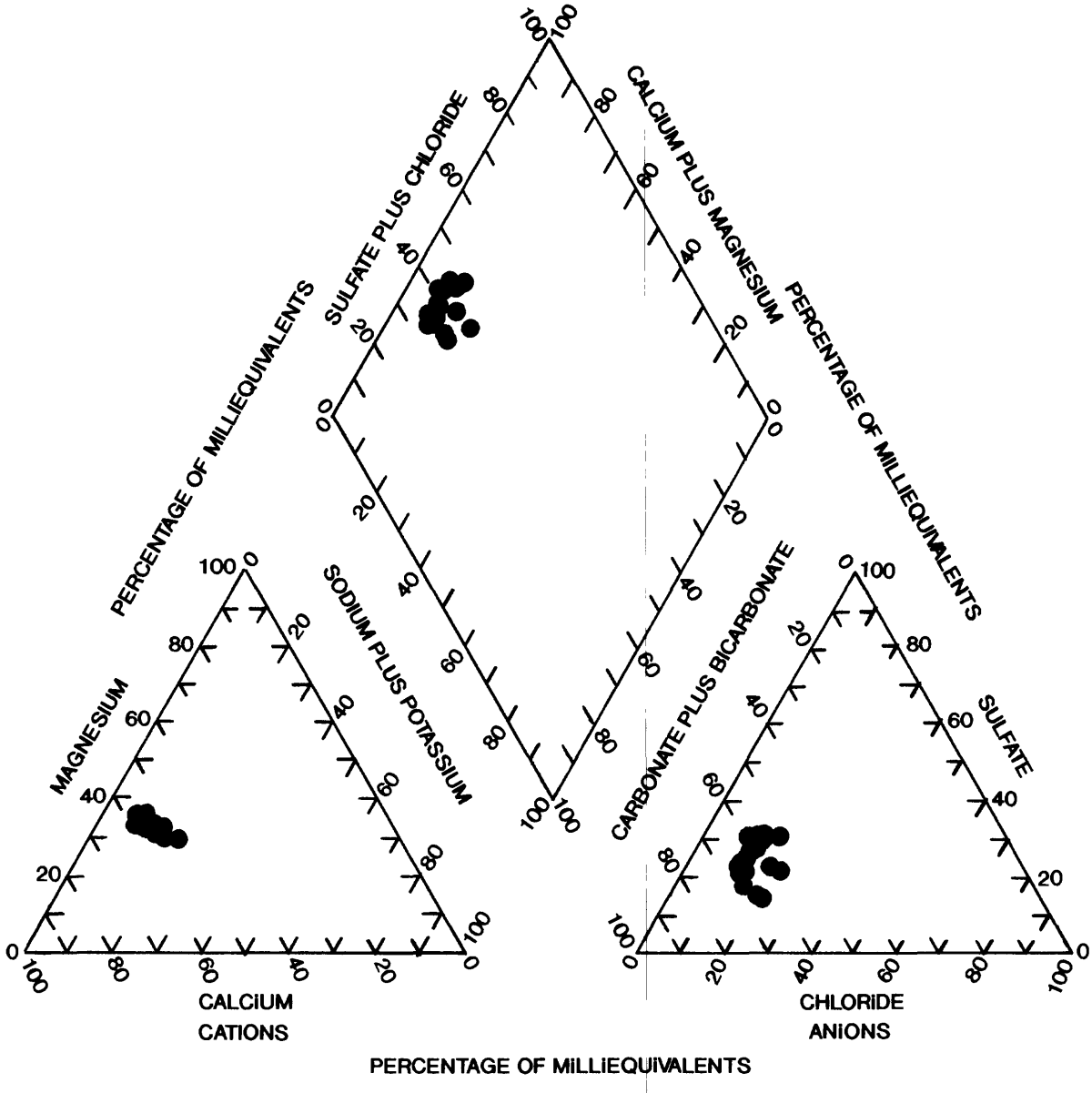

Figure 45.--Trilinear plot of major cation and anion percentages based on median properties and constituent concentrations of ground-water samples collected at Wright-Patterson Air Force Base, Ohio, 1954-73.

Water-Mineral Equilibria

The chemistry of ground water is partly controlled by reactions between the ground water and reactive minerals present in the aquifer. To investigate thermodynamic controls on water composition and quality, investigators evaluated the equilibrium speciation of each water sample by entering the analytical data of tables 14 and 15 into the equilibrium thermodynamic model WATEQ4F (Ball and Nordstrom, 1991). The model calculates the aqueous speciation of a given water analysis and the saturation index (SI) of reactive minerals that may be precipitating or dissolving in the system. The SI of a mineral is defined as

$$SI = \text{Log } IAP/K_T , \qquad (5)$$

where IAP is the ion activity product of the mineral and K_T is the thermodynamic equilibrium constant evaluated at the temperature of the water sample. If the SI value is greater than zero, the water is supersaturated with respect to the particular mineral, and precipitation of the mineral in the aquifer is possible. If the SI value is less than zero, the water is undersaturated with respect to the given mineral, and dissolution of the mineral is possible. SI values equal to zero indicate equilibrium between the ground water and mineral.

Water analyses from the current and historical data sets (tables 14 and 15) were evaluated with WATEQ4F. Historical water samples were evaluated to see if any major changes in water quality had occurred. Results of the WATEQ4F calculations included calculation of the SI's for calcite ($CaCO_3$), dolomite ($CaMg(CO_3)_2$), gypsum ($CaSO_4 \cdot 2H_2O$), quartz and chalcedony (both SiO_2), fluorite (CaF_2), and siderite ($FeCO_3$) (tables 16 and 17). These minerals were selected because they are common, relatively reactive minerals that may have a role in regulating the concentration of several major and minor elements in ground water. The equilibrium log pCO_2 (partial pressure of carbon dioxide) also was calculated. The partial pressure of CO_2 is calculated from the pH and alkalinity data and is used to evaluate reactions involving carbonate minerals and the oxidation of organic matter. To calculate the saturation index for siderite, it was assumed that all dissolved iron in the water was present as ferrous (Fe^{2+}) iron (tables 16 and 17). This assumption is based on the fact that, at neutral pH, ferric hydroxide ($Fe(OH)_3$) solubility will not allow dissolved ferric iron (Fe^{3+}) concentrations to rise above the reporting limit given in table 14 (Hem, 1989). The median fluoride concentration of the historical data set (0.2 mg/L) was used to evaluate the saturation index of fluoride for all samples of ground water collected from the glacial drift aquifer in 1991. The saturation indices of aluminosilicate phases (feldspars, clays) could not be evaluated because of the absence of dissolved aluminum data.

The speciation and SI calculations discussed above are subject to a combined uncertainty that is caused by several unrelated factors. These factors include errors in the thermodynamic data set used by WATEQ4F, analytical error associated with individual cation and anion analyses, and errors in pH measurement. For waters whose cation-anion charge balance is less than 10 percent, the effect of analytical error is minimal, and the bulk of the error can be attributed to experimental error associated with the measurement of the equilibrium constant. Uncertainty in the thermodynamic data lead to overall uncertainties of ± 0.1 in the SI's for calcite and gypsum; ± 0.2 for dolomite, fluorite, quartz, and chalcedony; and ± 0.5 for siderite (Nordstrom and Ball, 1989; Busby and others, 1991). Calculated SI's that are within the quoted uncertainties indicate water compositions in equilibrium with the given mineral.

Table 16.—Log of the partial pressure of carbon dioxide (pCO_2) and saturation indices for selected mineral phases for ground-water samples collected at Wright-Patterson Air Force Base and Fairborn in June and July 1991

[SI, saturation index of the mineral; --, data not obtained or not applicable; S, shallow glacial well; I, intermediate depth glacial well; D, deep glacial well; B, well completed in bedrock; B (Brass), well completed in the Brassfield Limestone]

Well number	Depth (S,I,D,B)	Log pCO_2	Calcite	Dolomite	Siderite	Gypsum	Fluorite	Chalcedony	Quartz
GR-314	B	-2.17	-0.05	-0.32	0.01	-3.46	-0.22	-0.18	0.29
GR-303	B	-2.35	.18	.32	.31	-2.06	--	.11	.58
GR-305	B	-2.43	.12	.11	-.32	-4.23	-.37	-.22	.25
GR-304	B	-2.45	.19	.29	.52	-3.32	.39	-.25	.22
GR-313	B	-1.85	.03	-.11	-.19	-2.01	.51	-.20	.27
GR-308	B	-1.91	.23	.45	--	-1.53	-.71	-.34	.13
GR-309B	(Brass)	-1.70	.01	-.15	.36	-1.67	--	.11	.58
GR-325B	(Brass)	-1.91	.01	-.28	--	-1.69	--	-.17	.30
GR-324	D	-1.92	.18	.15	.53	-.20	--	.13	.59
GR-328	D	-1.74	.14	.09	.49	-2.44	-1.17	.19	.65
GR-332	D	-1.81	.31	.37	.71	-2.59	--	.25	.72
GR-322	D	-1.82	.15	.09	.52	-1.84	--	.05	.52
GR-335	D	-1.88	.18	.14	.20	-2.09	--	.15	.51
MT-153	D	-1.55	.03	-.17	-.12	-1.84	--	.14	.61
GR-317	D	-2.03	.26	.32	.31	-2.06	--	.11	.58
GR-319	D	-1.75	.11	.01	.58	-1.89	--	-.03	.44
GR-327	I	-1.86	.17	.11	.45	-2.09	--	.13	.60
GR-334	I	-1.78	.07	-.05	.55	-1.57	--	.14	.62
GR-331	I	-1.68	.22	.19	.65	-2.40	--	.26	.72
GR-323	S	-1.77	.14	-.01	.83	-1.51	--	.06	.53
GR-329	S	-1.57	.03	-.20	--	-1.55	--	.08	.55
GR-333	S	-1.70	.00	-.21	--	-1.76	--	-.06	.41
GR-326	S	-1.90	.14	-.08	-.39	-1.80	--	-.14	.42
GR-316	S	-2.18	.09	.03	--	-1.76	--	-.16	.31
GR-318	S	-1.74	.10	-.09	--	-1.75	--	-.03	.44
GR-321	S	-1.76	.08	-.06	--	-1.77	--	.00	.46
GR-330	S	-1.53	.10	-.07	--	-1.82	--	.15	.62
GR-320	S	-2.24	.32	.42	--	-1.88	--	-.06	.41
MT-152	S	-1.63	.11	-.04	-.79	-1.57	--	.08	.55
Error[1]	--	.20	.10	.20	.50	.10	.20	.20	.20

[1] Combined uncertainty of the mineral equilibrium constant and analytical error.

Table 17.—Logarithm of the partial pressure of carbon dioxide (pCO2)and saturation indices for selected mineral phases based on median composition of ground water sampled at Wright-Patterson Air-Force Base, 1954-73

[SI, saturation index of the mineral; --, data not obtained or not applicable; S, shallow glacial well; I, intermediate depth glacial well; D, deep glacial well; B, well completed in bedrock; B (Brass),well completed in the Brassfield Limestone]

Well number	Depth (S,I,D,B)	Log pCO_2	Calcite	Dolomite	Siderite	Gypsum	Fluorite	Chalcedony	Quartz
GR-150	S	-1.91	0.36	0.47	0.50	-1.25	-2.12	0.03	0.50
GR-152	S	-1.79	.28	.31	.45	-1.27	-2.11	.07	.53
GR-151	S	-1.99	.50	.71	.46	-1.19	-2.10	.03	.50
GR-153	S	-1.88	.37	.51	.26	-1.37	-2.14	.10	.56
GR-163	S	-2.02	.37	.50	-1.21	-1.58	-2.18	.00	.47
GR-164	S	-2.06	.38	.46	-.78	-1.55	-2.16	.00	.47
GR-162	S	-1.99	.31	.31	-.50	-1.53	-2.16	.06	.53
GR-155	S	-1.92	.31	.36	-1.15	-1.59	-2.15	.06	.53
GR-158	S	-2.13	.47	.66	-.67	-1.60	-2.17	.00	.47
GR-161	S	-1.91	.35	.42	-.94	-1.43	-2.13	.03	.50
GR-156	S	-2.02	.40	.53	-1.06	-1.65	-2.16	.00	.47
GR-157	S	-2.02	.38	.51	-1.05	-1.66	-2.17	.03	.50
GR-166	S	-2.07	.30	.37	.73	-1.48	-2.19	-.08	.39
GR-149	S	-2.08	.45	.65	-.18	-1.31	-2.13	.00	.47
MT-121	S	-2.18	.39	.51	-.70	-1.58	-2.19	-.04	.43
MT-122	S	-2.08	.29	.34	.89	-1.56	-2.19	-.04	.43
MT-123	S	-2.07	.32	.40	.62	-1.42	-2.18	-.02	.45
Error[1]	--	.20	.10	.20	.50	.10	.20	.20	.20

[1] Combined uncertainty of the mineral equilibrium constant and analytical error.

Further error in the calculated saturation indices is introduced by uncertainty in the in-place temperature of the ground water at depth. The average annual temperature for ground water as indicated by data collected from the five wells with in-hole temperature probes is 12.8°C. Norris and Spieker (1966) report that ground-water temperature in the Dayton area generally ranges from 11 to about 13.5°C. Therefore, to eliminate uncertainty due to variable temperature, speciation calculations for current and historical ground-water samples were based on a temperature of 13°C. It is likely that actual ground-water temperatures at the time of sample collection are within ± 2°C of 13°C. Resulting uncertainties in the calculated SI values due to the temperature uncertainty of ± 2°C are, with the exception of dolomite, less than 0.1 log units (± 0.05). For dolomite, the uncertainty in the calculated SI value is approximately 0.2 log units (± 0.1)

Unconsolidated Deposits

Results of the WATEQ4F calculations indicate that water collected from the unconsolidated deposits at WPAFB in 1991 generally was in equilibrium with calcite, dolomite, and chalcedony (tables 16 and 17, figs. 46 and 47). The waters were undersaturated with respect to gypsum and fluorite, but were supersaturated with respect to quartz. Calculated SI's for siderite are highly variable, representing conditions ranging from moderately undersaturated to slightly supersaturated. Calculated partial pressures of CO_2 ranged from $10^{-1.5}$ to $10^{-2.5}$ atmospheres and are similar to those reported for other glacial drift aquifers in Ohio (Breen, 1988).

SI's for calcite and dolomite calculated for the set of historical data (table 17) indicate a relatively constant degree of supersaturation that is probably related to errors in the laboratory pH measurements caused by the degassing of CO_2. Field pH measurements of the June 1991 samples measured in the closed, flowthrough cell were, on average, approximately 0.4 pH units lower than pH values measured in the laboratory. The increase in pH is caused by degassing of CO_2, which shifts the following equilibria to the right

$$H^+ + HCO_3^- \leftrightarrow H_2CO_3 \leftrightarrow H_2O + CO_{2(g)}\uparrow , \qquad (6)$$

resulting in an increase in pH and a decrease in the concentration bicarbonate. Clear evidence for degassing of the samples is provided in table 14, which shows increases in pH and decreases in HCO_3^- between the lab and field measurements of these characteristics. Because the IAP for calcite is based on the equilibria

$$CaCO_{3(s)} + H^+ \leftrightarrow Ca^{2+} + HCO_3^- , \qquad (7)$$

the saturation index of calcite is directly proportional to pH of the sample and will decrease one log unit for each unit increase in pH. Application of the average 0.4 pH-unit difference between the field and laboratory pH for the June 1991 data set to the average pH reported for the historical data set results in a decrease of the calcite SI by 0.4 log units. The same 0.4-log-unit shift applies to the SI of siderite; for dolomite, the SI shift is twice the pH difference (0.8 log units) because two hydrogen ions are required to dissolve dolomite. The shift in SI is applied to the historical

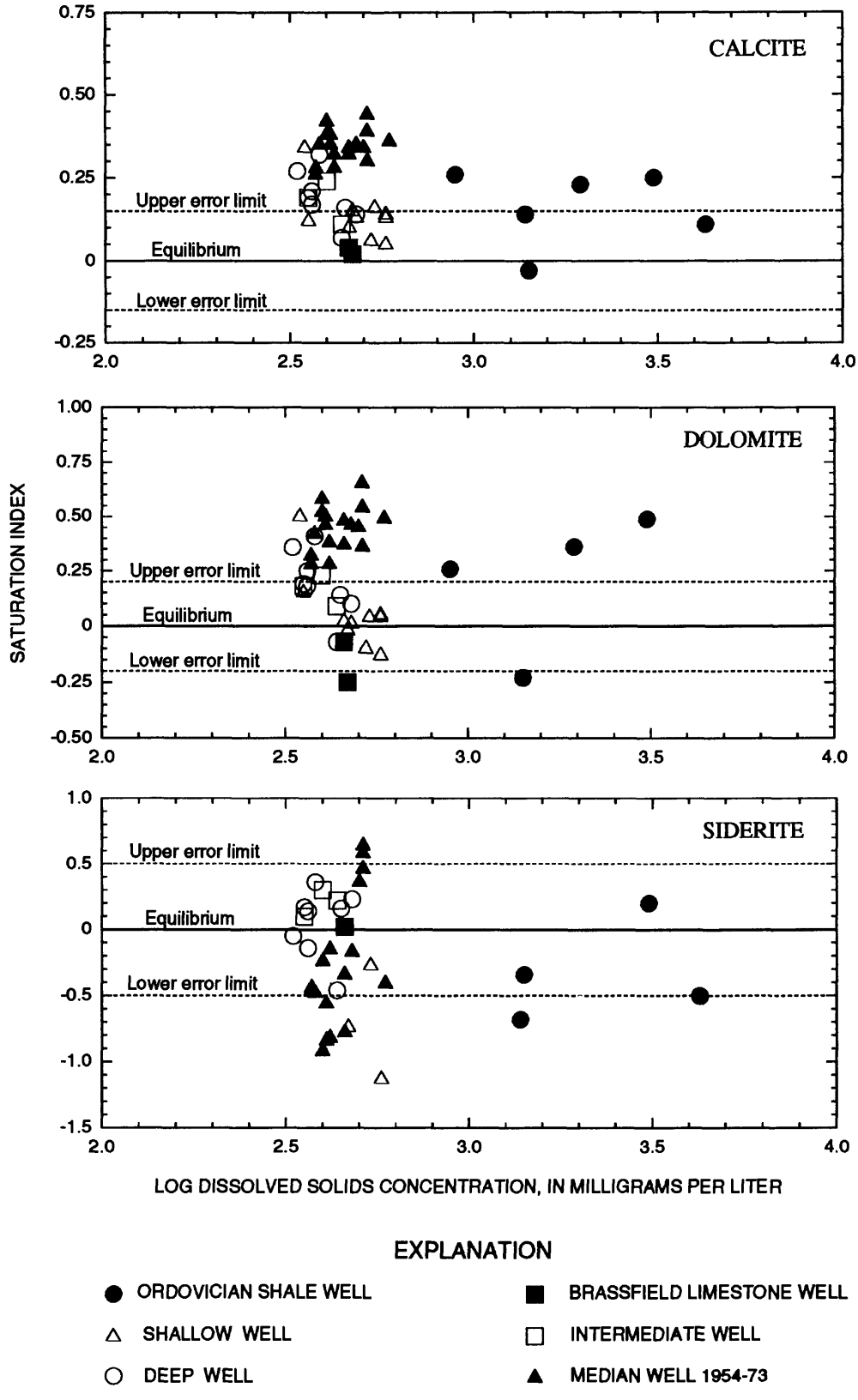

Figure 46.--Saturation index as a function of the log of dissolved-solids concentrations for calcite, dolomite, and siderite for ground-water samples collected at Wright-Patterson Air Force Base. (Error limits are due to analytical and thermodynamic data uncertainties. Points plotting with these lines are considered to be in equilibrium with the given mineral.)

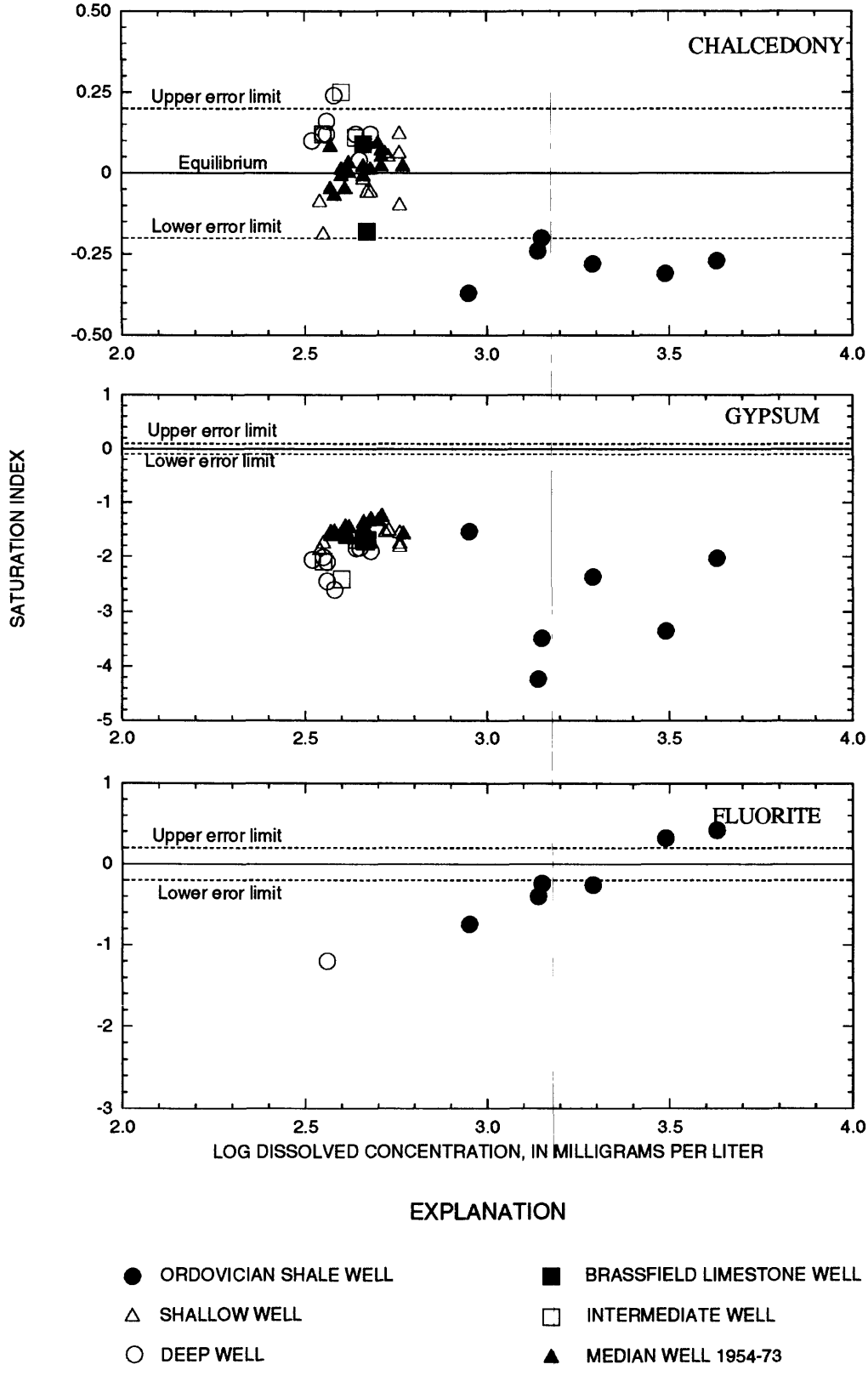

Figure 47.--Saturation index as a function of the log of dissolved-solids concentrations for chalcedony, gypsum, and fluorite for ground-water samples collected at Wright-Patterson Air Force Base. (Error limits are due to analytical and thermodynamic data uncertainties. Points plotting within these lines are considered to be in equilibrium with the given mineral.)

data set to reflect in-place conditions more accurately. The results indicate that, under in-place conditions, the median historical ground-water samples were saturated with respect to calcite, were saturated to slightly undersaturated with respect to dolomite, and were generally undersaturated with respect to siderite.

Taken together, results of WATEQ4F calculations for the June 1991 sample set and the 1954-73 average data set indicate that calcium, magnesium, and bicarbonate concentrations in the glacial drift aquifer are controlled by dissolution of carbonate minerals. These results are consistent with the known mineralogy of the glacial drift-deposits of northwestern Ohio that consist largely of dolomitic carbonates of Devonian and Silurian age eroded and deposited during Pleistocene glaciation (Stout, 1941; Norris and Spieker, 1966).

Dissolved-silica concentrations are probably controlled by equilibrium with chalcedony, a common minor component of carbonate rocks in the midwestern United States (Weiner and Koster Van Groos, 1976). Additional controls on dissolved-silica concentrations are the formation of clays (kaolinite, illite) and adsorption reactions (Hem, 1989). Although the ground waters are supersaturated with respect to quartz, precipitation of quartz at such low temperatures is unlikely.

The wide range of SI's for siderite indicates that siderite is not a control for dissolved ferrous iron concentrations. In shallow parts of the aquifer, dissolved-iron concentrations are likely to be regulated by the precipitation of ferrihydroxide ($Fe(OH)_3$). Coatings and cements of ferrihydrite are commonly found in glacial sediments in the shallow, oxygenated parts of glacial drift aquifers. Ferrihydrite will precipitate rapidly at neutral or alkaline pH when dissolved ferrous iron is oxidized by dissolved oxygen in recharging meteoric waters (Breen, 1988). In deeper, anoxic parts of the aquifer, variations in dissolved-iron concentrations probably reflect the relative abundance of reactive iron minerals in the unconsolidated deposits and (or) the presence of hydrogen sulfide (H_2S).

The dominant geochemical process responsible for the formation of the calcium magnesium bicarbonate waters is the dissolution of carbonate minerals by carbonic acid. For dolomite, this reaction can be written as follows:

$$CaMg(CO_3)_{2(s)} + 2H_2O + 2CO_2 \leftrightarrow Ca^{2+} + Mg^{2+} + 4HCO_3^- \quad . \qquad (8)$$

If dissolved calcium, magnesium, and bicarbonate are added to the ground water solely through this mechanism, then a plot of the molar concentrations [Ca+Mg] as a function of [HCO_3] yields a linear relation with a slope of 0.5. A plot of data (fig. 48) from tables 14 and 15 reveals no obvious correlation between [Ca+Mg] and [HCO_3] for waters collected from the unconsolidated deposits. A linear regression of the data yields a best fit line with a slope of 0.11 and a correlation coefficient (r^2) of 0.02, indicating an extremely weak relation to the simple carbonate-dissolution model in equation 8.

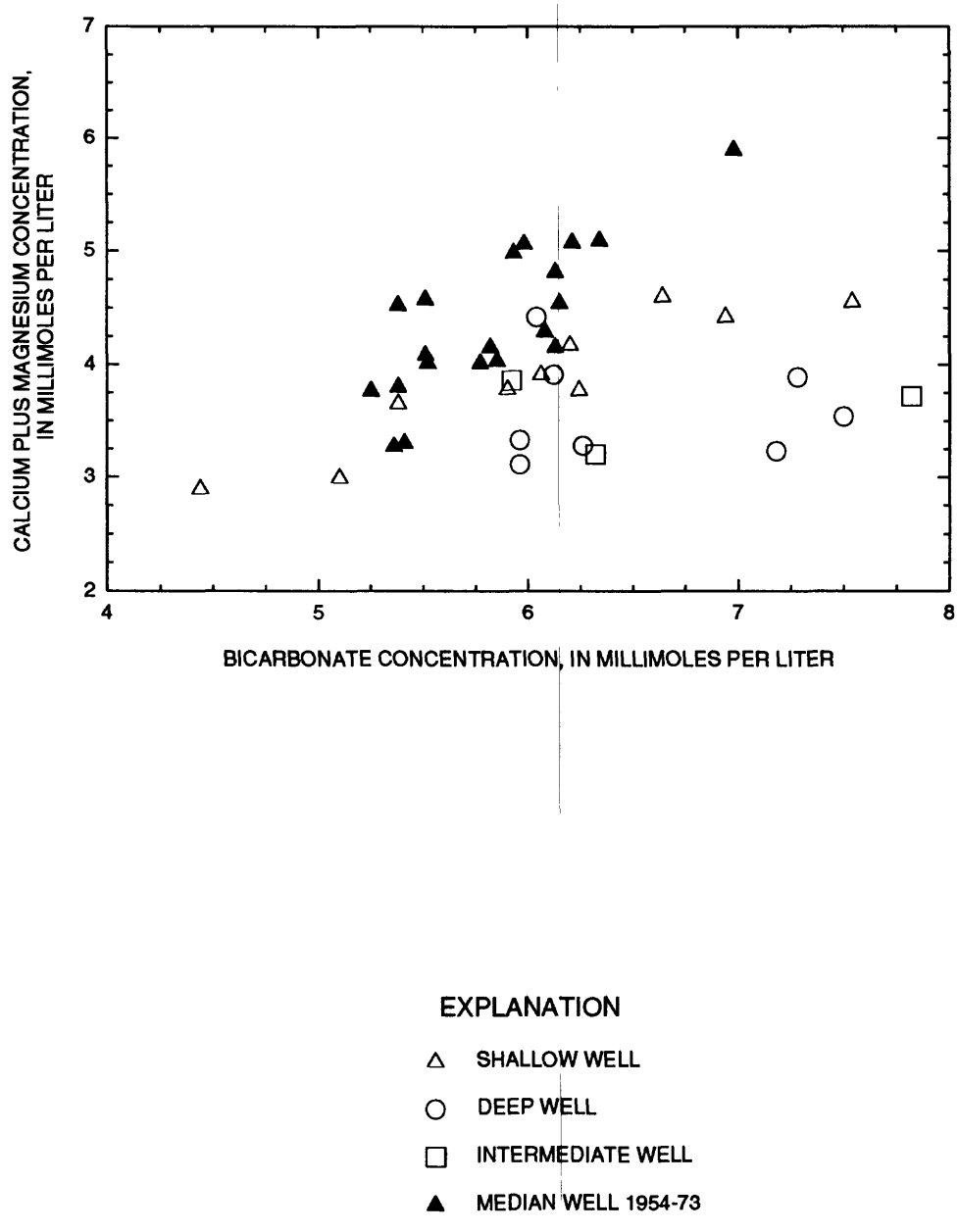

Figure 48.--Concentration of calcium plus magnesium as a function of concentration of bicarbonate for ground-water samples collected from wells completed in glacial deposits at Wright-Patterson Air Force Base.

The weak relation to the carbonate dissolution model indicates that other geochemical processes are affecting the ratio of [Ca+Mg] to [HCO_3]. Geochemical studies of carbonate aquifers by Back and others (1983) and Busby and others (1991) indicate that dedolomitization may be important. Dedolomitization occurs in response to the dissolution of gypsum or anhydrite in aquifer rocks after equilibrium with calcite and dolomite has been reached. Continued dissolution of gypsum or anhydrite releases additional calcium (and sulfate) into solution, eventually resulting in the precipitation of secondary calcite and the selective dissolution of the dolomitic component of the rock. The overall reaction can be written as

$$CaMg(CO_3)_{2(s)} + CaSO_4 \cdot 2H_2O_{(s)} + H_2CO_3 \leftrightarrow CaCO_{3(s)}$$

$$+ Ca^{2+} + Mg^{2+} + SO_4^{2-} + 2HCO_3^- + 2H_2O.$$

As the reaction proceeds, Ca:Mg ratios in the solution decrease, and the sulfate concentration of the ground water increases with increasing reaction progress. On a plot of [Ca+Mg] as a function of [$SO_4 + 0.5HCO_3$], this reaction will yield a line with a slope of 1. A plot of data from tables 16 and 17 yields a line regression with a slope of 1.09 and a correlation coefficient of 0.81, indicating a relatively strong correlation between the dedolomitization model and the field data (fig. 49).

An alternative to the dedolomitization model involves dissolution of dolomitic carbonates by sulfuric acid (H_2SO_4) produced by the oxidation of pyrite (FeS_2):

$$FeS_2 + 7/2O_2 \leftrightarrow Fe(OH)_{3(s)} + H_2SO_4 \qquad (9)$$

(Nordstrom and others, 1979). The sulfuric acid then reacts with dolomite, yielding

$$CaMg(CO_3)_{2(s)} + H_2SO_4 \leftrightarrow Ca^{2+} + Mg^{2+} + SO_4^{2-} + 2HCO_3^-. \qquad (10)$$

The overall reaction yields a stoichiometry identical to that of the dedolomitization reaction. This reaction will occur rapidly in shallow, oxygenated parts of the aquifer where sufficient dissolved oxygen is available to drive the reaction. Alternatively, experimental work by Moses and others (1987) has shown that small amounts of pyrite can be oxidized by ferric iron under the anoxic, near-neutral pH conditions that characterize deeper parts of the glacial drift aquifer. Pyrite is a common minor constituent (< 0.5 weight percent) of many of the Devonian and Silurian carbonates and shales which, along with various igneous and metamorphic rocks of glacial origin, compose the bulk of material in the glacial drift (Stout, 1941). Gypsum is also a minor constituent of these rocks and is especially common in the upper Devonian carbonate sequences (Stout, 1941). Because gypsum is moderately soluble, however, it is very likely that erosion and transport processes associated with the Pleistocene glaciation caused dissolution of all gypsum originally present so that little, or no gypsum remains in the present-day aquifer sediments. Unfortunately, detailed petrographic data on the bulk mineralogic composition of the tills and outwash deposits in the vicinity of WPAFB are unavailable. Sulfur-isotope data for dissolved sulfate would be required to determine the source of sulfate in the ground water and to decide which model best represents the geochemical processes actually occurring in the glacial aquifer.

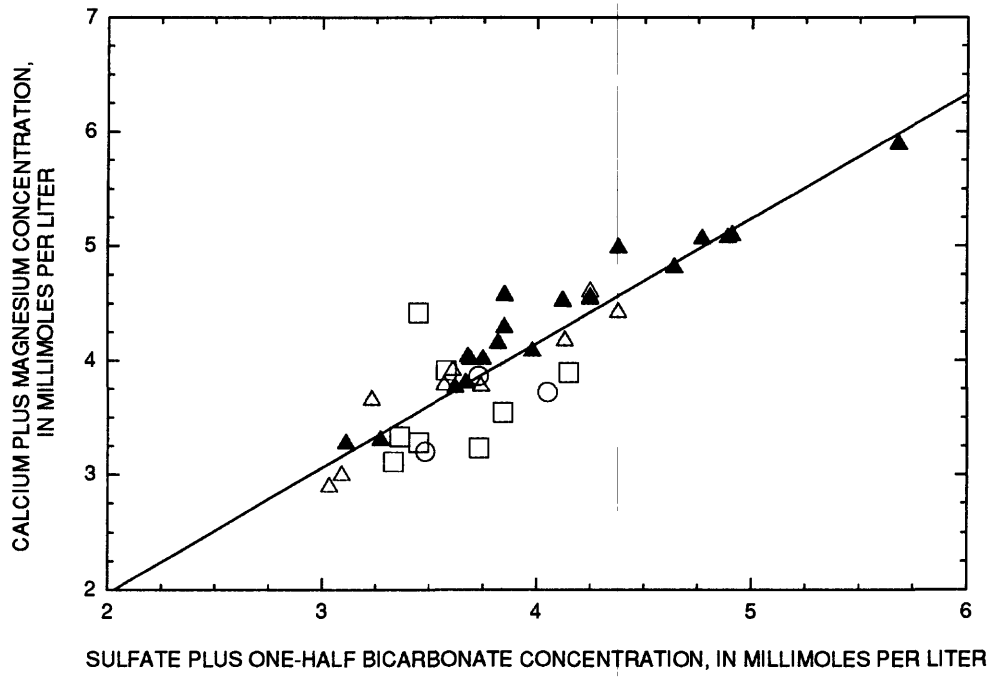

Figure 49.--Concentration of calcium plus magnesium as a function of concentration of sulfate plus one-half bicarbonate for ground-water samples from wells completed in glacial deposits at Wright-Patterson Air Force Base.

Consolidated Deposits

Water samples collected from wells completed partly or wholly in the Brassfield Limestone were in equilibrium with calcite but were slightly undersaturated with respect to dolomite (fig. 46). These results are consistent with the mineralogy of the Brassfield, which is predominately limestone with a minor dolomitic component (Stout, 1941). The Ordovician rocks are composed primarily of calcareous shales that include variable amounts of thinly bedded, siliceous limestone (Stout, 1941). Water collected from wells completed in the bedrock shales was slightly supersaturated with respect to calcite and generally saturated with respect to dolomite and siderite (fig. 46). Undersaturation of the waters with respect to chalcedony indicate that silica concentrations may be regulated by equilibrium with clays such as illite or kaolinite present in shale-rich parts of the Ordovician rocks. Extreme undersaturation of the waters with respect to gypsum reflects the generally low sulfate contents of the samples. A trend towards supersaturation with respect to fluorite with increasing DS is noted (fig. 47); however, the fact that the trend does not level off at SI = 0 indicates that fluorite precipitation is not an important control on fluoride concentrations.

Effects of Surface Recharge

Sand and gravel units of the unconsolidated deposits, because of their high transmissivities, are susceptible to contamination by surface water that has been affected by human activities. At WPAFB, waters from shallow wells have markedly higher median nitrate, sulfate, sodium, and chloride concentrations (table 14) than do waters from intermediate depth and deep wells. Median sodium and chloride concentrations of the shallow waters are similar to those of the median historical data set (table 15), which consists of samples collected from shallow supply wells screened at depths no greater than 80 ft. The historical data include even higher mean concentrations of nitrate and sulfate. Elevated nitrate concentrations in the current and historical data are probably related to either application of nitrogen-based fertilizers or leakage of nitrate-rich waste from septic tanks or waste-disposal sites. Superphosphate and ammonium sulfate fertilizers (both of which contain sulfate) applied on or near the Base or leakage of leachate from septic tanks or waste-disposal sites may be responsible for the elevated sulfate concentrations found in the current shallow-water and historical data sets (Langmuir, 1971).

Sodium chloride is the predominant road-deicing salt used in western Ohio. ($CaCl_2$ also is used in small quantities.) Elevated sodium and chloride concentrations in shallow ground-water samples are attributed to deicing salt that dissolves in rainwater and enters shallow parts of the glacial aquifer. The influence of road-deicing practices on shallow ground water in the study area is illustrated on a plot of sodium as a function of chloride. Dissolution of sodium chloride salt yields one mole of sodium and one mole of chloride. Thus, if sodium and chloride are added to shallow ground water by the addition of Na-Cl-rich deicing salt, then a plot of sodium and chloride concentrations on a moles per liter basis should yield a linear trend with a slope near one. The compositional data for the shallow and 1954-73 median ground-water samples (the latter of which are all from shallow wells) define a clear, linear trend (fig. 50). Linear regression analysis of the shallow and median 1954-73 compositional data yields a line with a slope of 0.81 and correlation coefficient of 0.79. Deviation of the slope from unity could be due in part to the use

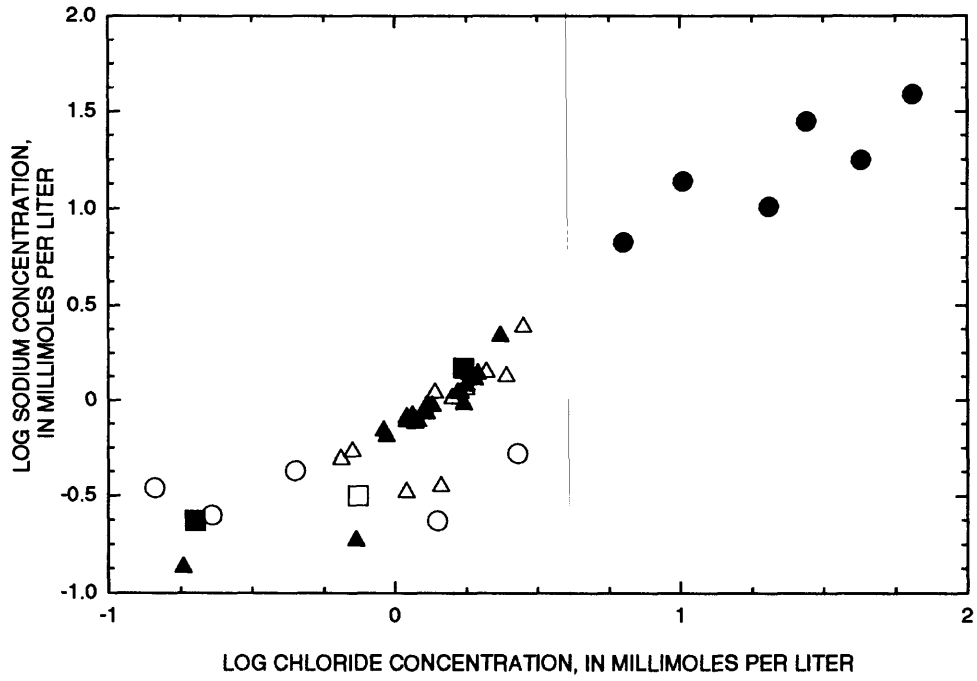

EXPLANATION

- BRASSFIELD LIMESTONE WELL
- ORDOVICIAN SHALE WELL
- SHALLOW WELL
- DEEP WELL
- INTERMEDIATE WELL
- MEDIAN WELL 1954-73

Figure 50.--Log sodium as a function of log chloride for ground-water samples at Wright-Patterson Air Force Base.

of deicing salts containing a small amount of calcium chloride (addition of 10 mole percent $CaCl_2$ will shift the sodium-chloride ratio of 0.82). The lack of a better correlation could be caused by several factors, including well locations, variations in recharge rates and salt-application rates, and clay contents of local sediments (ion exchange of Na for Ca).

Most of the deep and intermediate-depth samples do not fall on the linear trend, suggesting that these wells are hydrologically isolated from shallow ground waters that are affected by road deicing salt. The presence of less transmissive silt and clay layers in the glacial drift aquifer may be responsible for this phenomenon. Nevertheless, sodium and chloride concentrations in ground-water samples collected from wells completed in the Ordovician shales plot on a linear trend defined by the shallow samples, suggesting that recharge from the shales may be influencing water quality in parts of the unconsolidated aquifer. This possibility is evaluated in the following section.

Ground-Water Mixing Between Glacial Drift and Bedrock Waters

The Brassfield Limestone is moderately transmissive, due mainly to fracture permeability (Norris and Spieker, 1966), and flow through fractures in the Brassfield likely contributes some recharge water to the glacial drift aquifer in higher elevation sections of the buried valley. However, quantifying the amount of recharge received by the unconsolidated glacial deposits from the Brassfield Limestone is extremely difficult to assess by use of compositional data because the calcium magnesium bicarbonate composition of Brassfield ground water is virtually identical to that of ground water collected from the unconsolidated deposits (table 14, figs. 43 and 45). Application of stable isotope data is also inconclusive. (See section on "Oxygen and Hydrogen Stable Isotopes".)

The bulk of the unconsolidated deposits in the study area are in contact with, or are underlain by, Ordovician strata that are predominately shales. According to Norris and Spieker (1966), the mixed shale and argillaceous limestone sequences of these rocks are poorly permeable and, consequently, produce little water. This observation was confirmed by the current study, as most wells completed in the bedrock yielded shales little, if any, water. Although appreciable recharge from the bedrock shales to the unconsolidated deposits is considered unlikely, some recharge of brackish water to the unconsolidated deposits could be derived by flow through fractured or weathered parts of the bedrock.

Because of the relatively low concentrations of sodium and chloride in the deep parts of the glacial drift aquifer, significant inputs of sodium chloride water from the Ordovician shale would result in noticeable changes in the chemistry of ground water in the unconsolidated deposits. However, despite the fact that most sodium chloride waters from the Ordovician shale plot near the linear trend defined by shallow ground-water samples shown on figure 50, few of the deep glacial drift samples plot on the mixing trend. This difference indicates that little saline water is being contributed to the unconsolidated deposits by leakage from the underlying bedrock shale.

Additional evidence for a minimal recharge through bedrock shale can be found in the boron and fluoride concentrations of the deep glacial drift waters. None of the deep glacial drift waters contain elevated concentrations of these elements, despite notably high concentrations of fluoride and boron in the bedrock-shale waters (table 14). If significant amounts of sodium chloride water were being recharged through the bedrock shales, then concentrations of boron and fluoride should be elevated in the deep glacial drift waters (if both constituents are assumed to be conservative). Boron should be relatively unaffected by precipitation or ion-exchange reactions in the unconsolidated deposits and should be conservative in the glacial drift aquifer. Concentrations of boron in the bedrock-shale waters range from 1.7 to 4.7 mg/L (table 14). Water from only one well had a boron concentration significantly above the report limit for boron (0.03 mg/L). This was well GR-333, which yielded water with a boron concentration of 0.08 mg/L. Simple mass--balance calculations indicate that this water would result from a mixture composed of 95 percent glacial drift water ([B] = 0.03 mg/L) and 5 percent dilute bedrock-shale water ([B]= 1.7 mg/L, the lowest concentration among the bedrock-shale samples). Well GR-333 is near the edge of the buried-valley wall (CL-1, fig. 42) and could be influenced by ground-water flow from the walls of the buried valley. The intermediate and deep wells in the same cluster, however, do not have detectable concentrations of boron (< 0.03 mg/L); it is, therefore, probable that the elevated boron concentration at this well is caused by human activity, perhaps by leakage from a septic tank or waste-disposal site.

In light of the general lack of boron in intermediate or deep wells completed in unconsolidated deposits and the low Na and Cl concentrations in deep parts of the glacial aquifer, it is concluded that significant recharge to the glacial aquifer (as a whole) is not occurring along the glacial drift/bedrock contact. It is possible, however, that rates of recharge are locally higher in fractured or weathered parts of the bedrock shales. Because of the elevated permeability of these zones, and, consequently, the higher water flux through these areas, geochemical features of Ordovician shale pore waters (high Na, B, F, and Cl concentrations) may not be preserved. Thus recharge from the bedrock would not be identified by use of the conservative ion tracers considered in this study. Alternatively, if small amounts of mildly saline sodium chloride brine are entering the aquifer through valley-wall seepage, the high transmissivity and rapid ground-water velocities of the unconsolidated glacial deposits would quickly dilute conservative dissolved constituents to background levels.

Isotope Geochemistry

The ratios of the stable isotopes of oxygen and hydrogen in water were calculated to provide an independent means of distinguishing water types and sources in the aquifer. Oxygen and hydrogen stable-isotope ratios behave conservatively and can be used as hydrologic tracers of fluid flow in the ground-water system. Tritium concentrations were used to assess the relative ages of ground water in different parts of the aquifer, thus providing further information on flow in the aquifer.

Oxygen and Hydrogen Stable Isotopes

Water samples were collected for analysis of $^{18}O/^{16}O$ and deuterium/hydrogen ($^{2}H/^{1}H$) stable isotope ratios from all 29 wells sampled during June and July 1991 (table 14). Oxygen and hydrogen isotope data given in table 14 are reported in delta (δ) notation relative to the international water standard VSMOW (Vienna Standard Mean Ocean Water) in units of parts per thousand (permil) where

$$\delta^{18}O \text{ (in permil)} = \{[(^{18}O/^{16}O)_{sample} / (^{18}O/^{16}O)_{VSMOW}]-1\} \times 1000$$

and

$$\delta D \text{ (in permil)} = \{[(D/H)_{sample} / (D/H)_{VSMOW}]-1\} \times 1{,}000 .$$

Values of δD and $\delta^{18}O$ can be positive, negative, or zero (equivalent to VSMOW). Positive values indicate enrichments in ^{18}O or deuterium relative to VSMOW, whereas negative values indicate depletion relative to VSMOW. Waters enriched in the heavy isotope are described as being isotopically heavy; depleted samples are described as isotopically light. Analytical uncertainty of the δD and $\delta^{18}O$ reported in table 14 are $\pm$ 1.5 and $\pm$ 0.1 permil, respectively.

Variation in the δD and $\delta^{18}O$ of natural water samples results from isotopic fractionation that occurs during various physical processes and chemical reactions. For meteoric water, deviations from the mean isotopic composition of sea water are due to isotopic fractionation accompanying the evaporation and subsequent condensation of water vapor during precipitation events. Because water vapor is preferentially enriched in the lighter isotopes during evaporation and condensation, almost all meteoric water samples are isotopically depleted relative to sea water. Analysis of thousands of meteoric water samples collected at various latitudes has revealed a linear relation between δD and $\delta^{18}O$ values defined by the equation

$$\delta D = 8\delta^{18}O + 10 .$$

This line is known as the Meteoric Water Line (MWL) (Craig, 1961). Because the fractionation factor between vapor and liquid increases with decreasing temperature, precipitation at higher latitudes (or elevations) is isotopically depleted relative to precipitation falling at lower latitudes or elevations. In addition, changes in air temperature and storm tracks can produce marked seasonal shifts in the isotopic composition of precipitation. However, all rain water and most surface waters will plot on or near the local meteoric water line.

Stable-isotope analyses were done to determine if ground water from different parts of the buried-valley aquifer and the underlying bedrock could be distinguished by their stable-isotope composition. Median δD and $\delta^{18}O$ values for the shallow glacial ground waters are slightly heavier than median δD and $\delta^{18}O$ values of the deep glacial drift waters and bedrock waters (table 14). The difference between the medians is slight, however, and is insignificant given the analytical uncertainties and small size of the sample groups. A δD - $\delta^{18}O$ plot (fig. 51) shows that waters of each subgroup cannot be clearly distinguished by their oxygen and hydrogen isotope ratios. Values of δD and $\delta^{18}O$ for a couple of the shallow glacial drift samples and for water collected from well GR-325 (completed in the Brassfield Limestone) are slightly heavier than those for the other samples. These samples could represent recent or isotopically distinctive recharge events; however, temporal isotopic data to evaluate such a hypothesis are not available.

Ground-water samples collected during this study plot above the global MWL defined by Craig (1961) and slightly above a local meteoric water line defined by isotopic data for ground water collected from a shallow dolomite aquifer in northwestern Ohio (de Roche and Breen, 1989) (fig. 51). Samples collected during this study are isotopically heavier than the ground water from dolomite sampled by de Roche and Breen (1989) (fig. 51). The isotopic composition of the ground water collected during this study, however, is similar to that of ground-water samples collected from glacial outwash and till deposits in central and northeastern Ohio as part of the Midwestern Basin and Arch Regional Aquifer-Systems Analysis project (L.L. Lesney, U.S. Geological Survey, written commun., 1992). The range of δD and $\delta^{18}O$ in this study is similar to the range of δD and $\delta^{18}O$ recorded for ground water in the Killbuck Creek glacial drift aquifer near Wooster, Ohio (Dysart, 1988) (fig. 51).

Tritium

Tritium, ^{3}H, is a radioactive isotope of hydrogen that is extensively used as a hydrologic tracer and age-dating tool (International Atomic Energy Agency, 1981). Tritium gas is rapidly oxidized, yielding tritiated water (HTO) that enters the hydrologic cycle. Although produced naturally at low levels by reactions between cosmic rays and water in the upper atmosphere, the use of tritium as a tracer in hydrologic studies is due almost entirely to the introduction of large quantities of tritium into the atmosphere following the initiation of large-scale atmospheric testing of nuclear bombs in late 1952. Tritium concentrations in precipitation increased 2 to 3 orders of magnitude above their "pre-bomb" levels. Highest concentrations are found in the northern hemisphere (Michel, 1989). With the signing of the nuclear test ban treaty in the late 1960's, levels of tritium in the atmosphere generally have been declining. Levels in present-day (1993) precipitation are approaching the pre-bomb levels of 2 to 10 tritium units (TU; 1 TU is equal to 1 tritium atom in 10^{18} hydrogen atoms or 3.24 picocuries per liter, pCi/L) estimated by Thatcher (1962). The time-dependent nature of the tritium input function, combined with its short half life ($\tau_{1/2}$ = 12.43 years; International Atomic Energy Agency, 1981), makes tritium an excellent hydrologic tracer for use in ground-water systems in which the ground water is less than 100 years old. As a rule, tritium can be used only to obtain qualitative estimates of the age of the water. If detectable quantities of tritium ($\geq$ 1 TU) are measured in the water, it is certain that some fraction of that water must have entered the aquifer since the beginning of nuclear testing. The presence of tritium in ground water, therefore, is a useful indicator of post-1953 recharge to an aquifer.

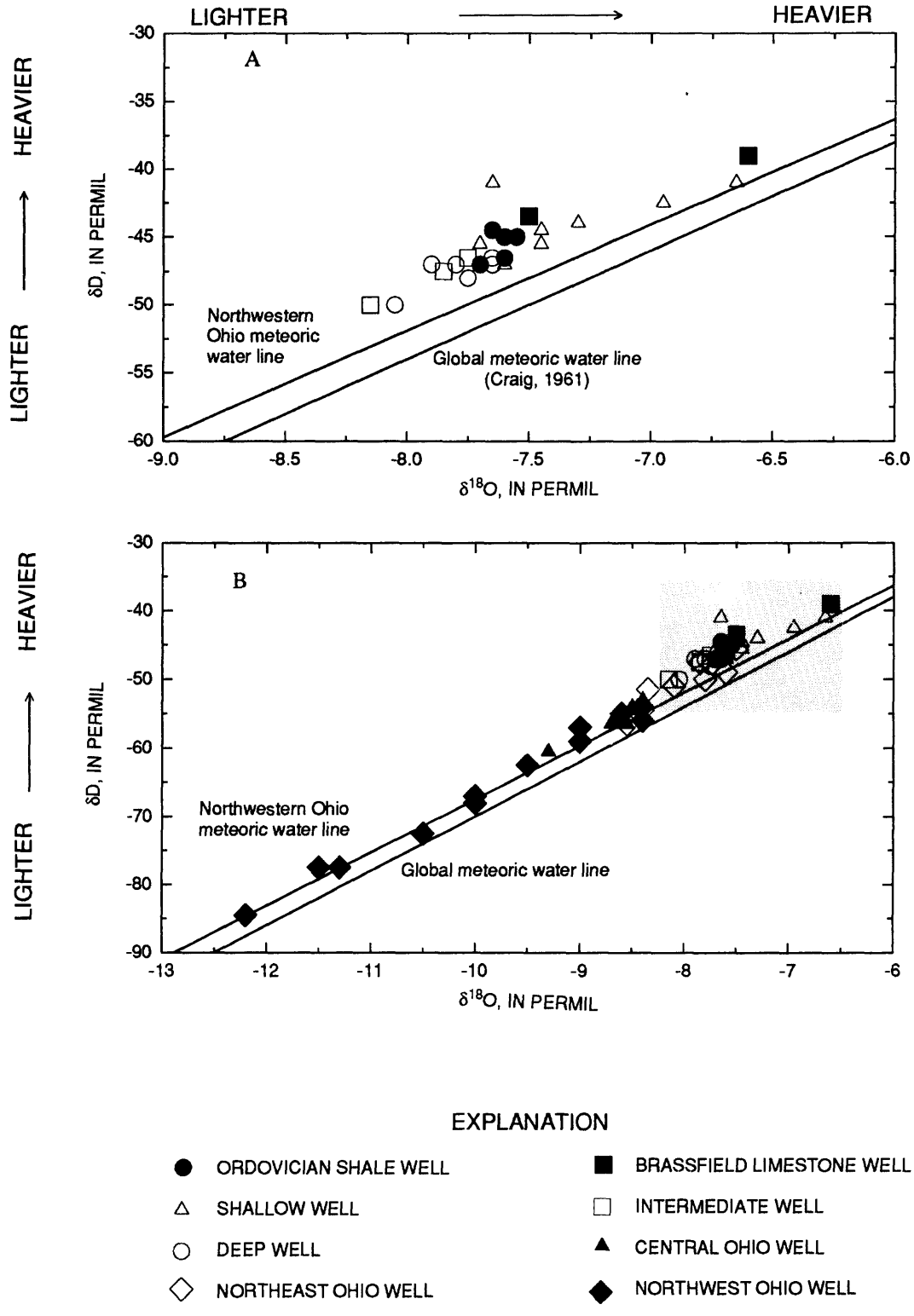

Figure 51.--Relations between stable isotopes of hydrogen (δD) and oxygen ($\delta^{18}O$) for (A) ground-water samples collected at Wright-Patterson Air Force Base and (B) other glacial and carbonate ground-water samples collected in Ohio. (Shaded box of (B) represents range of isotopic compositions shown in (A). Data for (B) compiled from Dysart (1988), deRoche and Breen (1989), and L. Lesney (U.S. Geological Survey, written commun., 1992).

To derive constraints on the recharge age of the ground water, one must know or estimate the tritium input function for precipitation falling on southwestern Ohio. Data for deriving the tritium-input function comes from several locations across North America. The most complete data set currently available was measured at Ottawa, Ont., and contains data from 1953 through the mid-1980's (International Atomic Energy Agency, 1981). The USGS began measuring tritium concentrations at several locations in the United States in 1960 (Michel, 1989). Data from these stations were combined with the Ottawa data set to estimate the weighted annual tritium deposition for the continental United States for the period 1953-83. Results reported by Michel (1989) indicate a strong north-south gradient in tritium deposition in the continental United States, with the highest tritium deposition occurring in the north. High concentrations of tritium also were noted at stations in the mid-continent and on the east coast. Because of nuclear bomb testing, nearly 60 percent of total tritium deposition in the continental United States occurred during the period 1961-65 (Michel, 1989).

The tritium-input curve for Ohio for the period 1953-83, corrected for radioactive decay up to the time of sample collection (June 1991), is shown in figure 52. This curve was derived from the tritium-deposition estimates for central Ohio given by Michel (1989). Also shown are the decay-corrected tritium input functions for USGS stations at Washington, D.C., and St. Louis, Mo. Data sets for these stations, which are at a latitude similar to that of southwestern Ohio, are reasonably complete through 1989. The data from these two stations are therefore used to estimate the tritium-input function for southwestern Ohio for the period 1984-89. The most notable feature of the tritium-input curve is the bomb-related spike in tritium concentration; ground water entering the aquifer in the early 1960's and sampled in June 1991 would contain several hundred tritium units (fig. 52) if no mixing with older ground water had occurred since the water entered the aquifer.

The tritium-input curve can be used to estimate the recharge age of waters in which tritium is present at greater than 1.0 TU (waters containing < 1.0 TU recharged the aquifer at some unknown date before 1953 or are highly mixed with pre-1953 waters). The age estimates are derived from the assumption that the tritium data used to derive the curve in figure 52 are a reasonable approximation of the actual tritium concentration of rain falling on the study area over the time period considered. Minimum ages are derived from the assumption that waters containing elevated tritium concentrations could not have entered the subsurface after the decay-corrected tritium input curve falls below the tritium concentration of the sample. For example, water collected from well GR-334, which contains 49.4 TU, could not have entered the aquifer after 1969. The maximum age of water in well GR-334 is derived from the knowledge that recharge water capable of producing the observed 1991 tritium concentration of 49.4 TU could not have entered the aquifer before 1958 (table 18). The decay-corrected tritium-input curves given in figure 52 indicate that waters with tritium concentrations greater than 32 TU entered the aquifer between 1958 and 1972, whereas waters containing 7 to 32 TU could have entered the aquifer any time between 1954 and 1989. The most precise constraints on recharge age for waters collected during this study can be placed on ground water that has tritium concentrations in excess of 45 TU. As discussed above, such waters must have entered the ground sometime between 1958 and 1969.

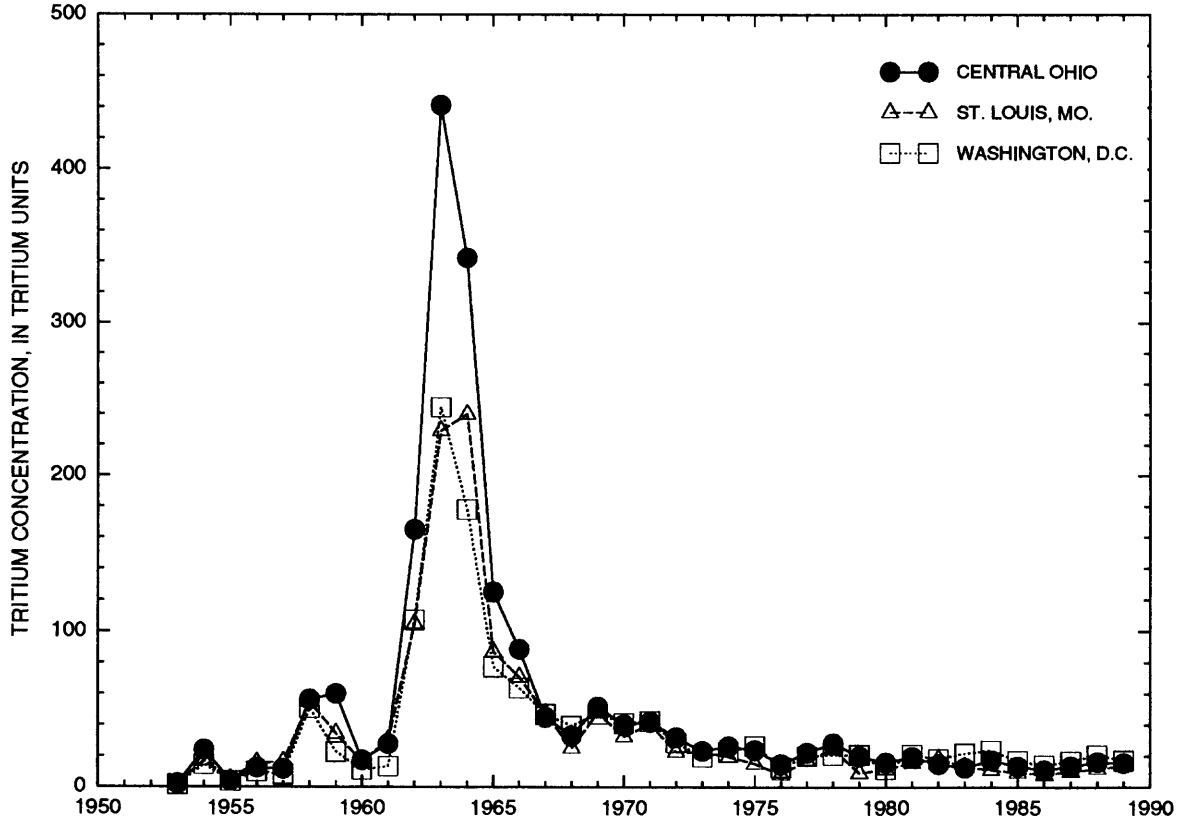

Figure 52.--Tritium-input functions for central Ohio, St. Louis, Mo., and Washington, D.C., for 1953-89. (Tritium concentrations in rain water used to generate the input functions are from Michel (1989) and R. Michel (U.S. Geological Survey, written commun., 1992). All data were corrected from radioactive decay up to June, 1991.)

Table 18.—Depth to screened interval and tritium-based minimum and maximum recharge ages for ground water at Wright-Patterson Air Force Base and Fairborn, Ohio

[--, data not obtained or not applicable; S, shallow glacial well; I, intermediate depth glacial well; D, deep glacial well; B, well completed in bedrock; B (Brass), well completed in the Brassfield Limestone; TU, tritium units; ND, no data]

Well number	Site number in figure 42	Depth[1] (S,I,D,B (feet))	Tritium (TU)	Maximum age[2]	Minimum age[3]
GR-314	CL 2	B (232)	< 0.3	--	< 1953
GR-303	CL 3	B (51)	< .3	--	< 1953
GR-305	CL 5	B (147)	< .3	--	< 1953
GR-304	CL 4	B (215)	< .3	--	< 1953
GR-313	CL 13	B (84)	.6	--	< 1953
GR-308	GR-308 (Brass)	B (10.6)	< .3	--	< 1953
GR-309	CL 9	B (44)	40.1	1958	< 1971
GR-325	GR-325 (Brass)	B (ND))	16.7	1954	< 1989
GR-324	CL 5	D (117)	21.3	1954	< 1989
GR-328	CL 7	D (240)	< .3	--	< 1953
GR-332	CL 6	D (185)	< .3	--	< 1953
GR-322	CL 4	D (137)	36.7	1954	< 1989
GR-335	CL 11	D (225)	< .3	--	< 1953
MT-153	CL 12	D (80)	< .3	--	< 1953
GR-317	CL 1	D (126)	7.1	1954	< 1989
GR-319	CL 2	D (150)	8.6	1954	< 1989
GR-327	CL 7	I (144)	10.2	1954	< 1989
GR-334	CL 11	I (145)	49.4	1958	< 1969
GR-331	CL 6	I (105)	.6	--	< 1953
GR-323	CL 5	S (46)	18.8	1954	< 1989
GR-329	CL 13	S (45)	37.0	1958	< 1971
GR-333	CL 11	S (25)	20.7	1954	< 1989
GR-326	CL 7	S (34)	21.6	1954	< 1989
GR-316	CL 1	S (48)	21.6	1954	< 1989
GR-318	CL 2	S (43)	17.3	1954	< 1989
GR-321	CL 4	S (38)	33.3	1954	< 1972
GR-330	CL 6	S (40)	21.9	1954	< 1989
GR-320	CL 3	S (17)	29.6	1954	< 1978
MT-152	CL 12	S (26)	21.6	1954	< 1989

[1] Depth, in feet, to top of screened interval. Screened interval thickness between 5 and 15 feet.
[2] Earliest possible year that recharge water could have entered the aquifer.
[3] Most recent year water could have entered the aquifer.

In the study area, tritium concentrations in ground water range from below detection limits (0.3 TU) to 49.4 TU (table 18, fig. 53). Water collected from wells completed in shale-rich Ordovician strata contain less than 1.0 TU, indicating no post-1953 recharge water in these rocks. This observation is consistent with the geochemical and hydrologic evidence discussed previously, and indicates that little or no ground-water flow occurs through the poorly permeable Ordovician shale. In contrast, the two bedrock wells believed to be recharged by ground water from the Brassfield Limestone (GR-309, GR-325) contain a significant component of post-1953 recharge, as evidenced by tritium concentrations of 17 and 40.1 TU (table 18).

In the unconsolidated deposits, tritium concentrations range from less than 0.3 TU in wells completed in deeper parts of the outwash deposits to nearly 49 TU in intermediate parts of the aquifer (table 18, fig. 53). Water collected from the deepest parts of the aquifer (>180 ft) sampled during this study contains no measurable tritium, whereas ground water sampled at intermediate depths (100-160 ft) contains from 0.6 to 49 TU. Water collected from wells completed in the shallow parts of the unconsolidated deposits typically contains from 17 to 37 TU (table 18, fig. 53). Because of the limitations of this age-dating method, the year during the recharge ages of ground water in shallow parts of the glacial drift aquifers can be estimated only as later than 1954 and prior to 1989.

Because of the lack of precision, the tritium age estimates cannot be used to identify recharge and discharge areas, to derive estimates of ground-water velocity along flow paths, or to estimate rates of recharge to the unconsolidated aquifer. However, the pre- and post-1953 age estimates defined by the presence or absence of measurable tritium in the ground-water provide invaluable qualitative information about vertical and horizontal age relations in the aquifer. The data indicate that recharge water requires at least 40 years to reach the deepest wells (> 180 ft) completed in the glacial aquifer (GR-328, GR-332, GR-335); however, the presence of measurable tritium (> 7.0 TU) in several deep and intermediate-depth wells (GR-324, GR-322, GR-317, GR-319; table 18, fig. 54) near the center of the glacial valley indicates that some parts of the aquifer have received significant amounts of recharge since 1953. The tritium data indicate that these parts of the aquifer are subject to the entry of surface and shallow ground-water-borne contaminants at time scales of a few years to a few decades.

Interestingly, a deep well containing "young" water (GR-324 in cluster 5) was noted downgradient from a well containing "old" water (GR-328 in cluster 7) along a predicted ground-water-flow path. This observation is in apparent disagreement with results of the flow net analysis and predictions of the ground-water-flow model, indicating that waters should get older as ground water flows west from the eastern border of WPAFB in the vicinity of cluster 7 towards the center of the glacial valley (cluster 5) (fig. 54). Nevertheless, this anomaly is consistent with the complex and highly heterogeneous nature of the glacial-drift deposits. Such geologic and hydrologic complexity, which produces distinct, highly localized, variations in aquifer properties, results in multiple, small-scale flow paths in the aquifer. The flow rate and directions of these local flow paths may or may not reflect ground-water flow on a regional scale. In addition, because of differences in rates and directions of flow, the ages of recharge water along the local-scale flow paths are likely to differ from the ages of recharge water along the regional flow paths. Thus, the complex hydrogeology of the glacial drift aquifer provides a likely explanation for the apparent contradiction in recharge ages discussed above.

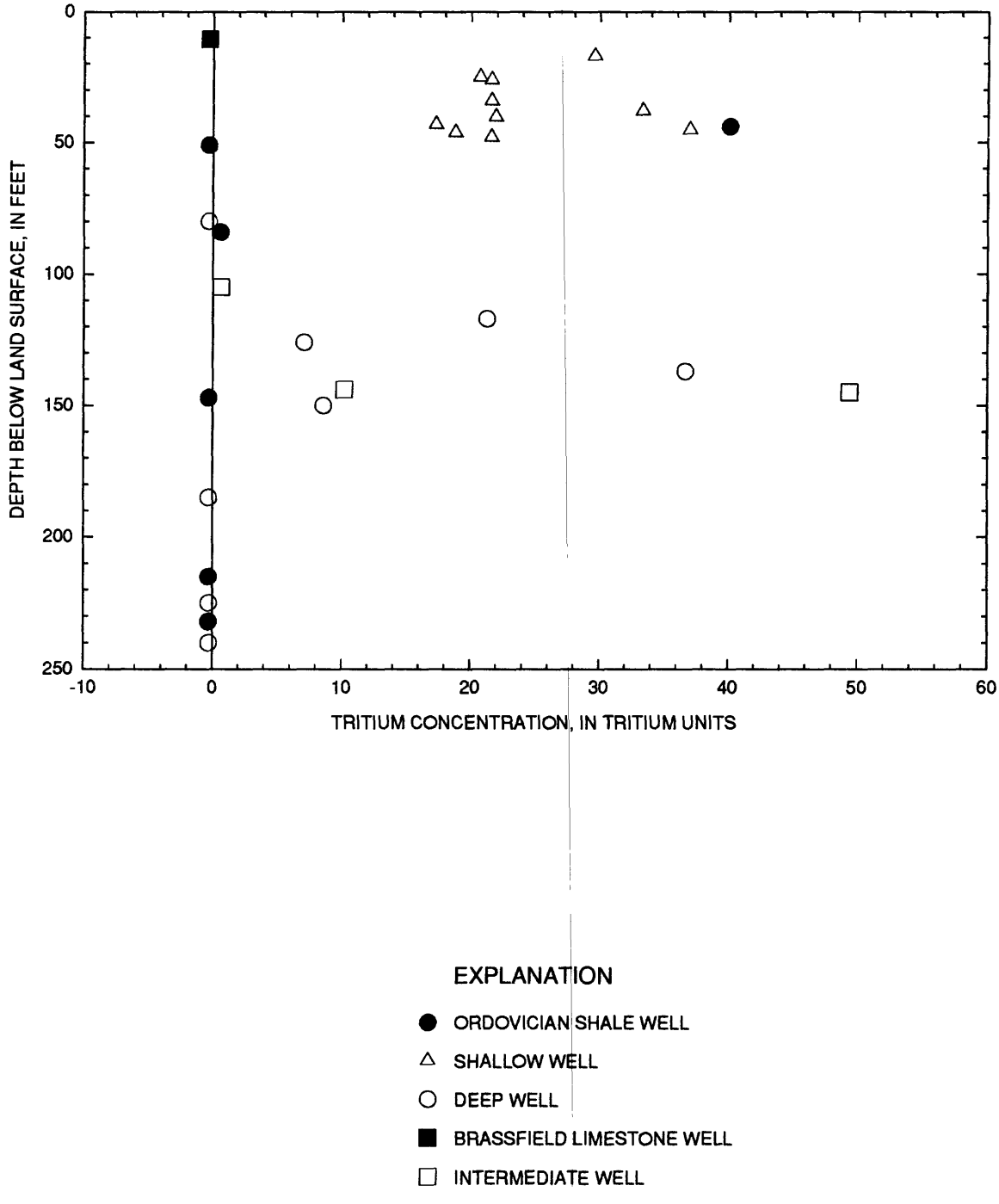

Figure 53.--Tritium concentrations as a function of depth for ground-water samples collected at Wright-Patterson Air Force Base in June-July 1991.

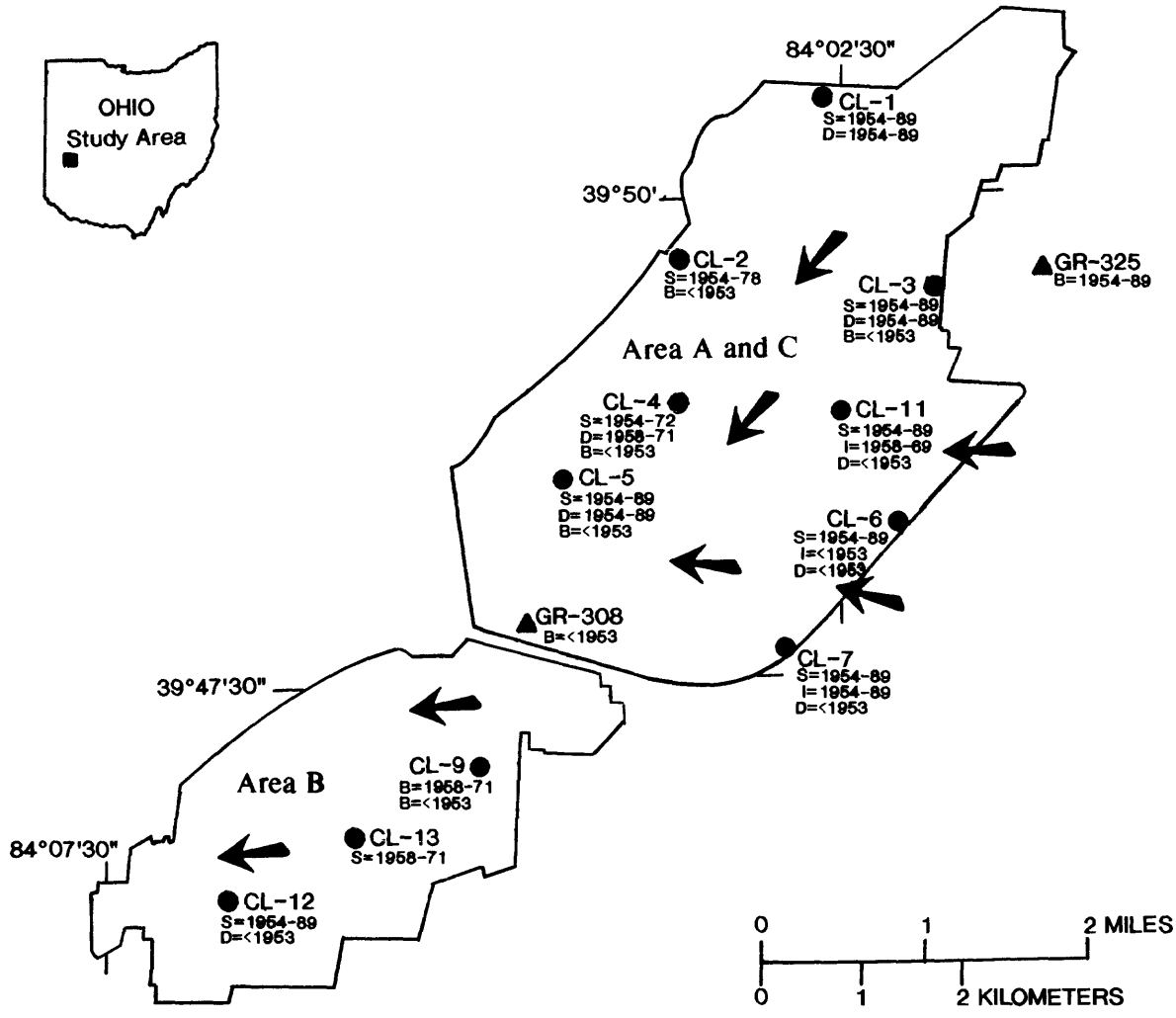

EXPLANATION

———	WRIGHT-PATTERSON AIR FORCE BASE BOUNDARY
←	REGIONAL GROUND-WATER FLOW PATHS
● CL-3	WELL CLUSTER AND NUMBER
▲ GR-308	WELL AND NUMBER
S=1954-89	ESTIMATED AGE RANGE FOR SPECIFIED DEPTH--S, shallow-depth glacial well; I, intermediate-depth glacial well; D, deep glacial well; B, bedrock well

Figure 54.--Regional ground-water-flow paths and estimated tritium ages for ground-water samples collected at Wright-Patterson Air Force Base, April 1991-April 1992.

The presence of elevated concentrations of tritium in all of the shallow wells indicates that the upper parts of the glacial drift aquifer are being recharged by precipitation at a relatively rapid (but unknown) rate. Because of the transient nature of the tritium-input function, a single sample set cannot be used to calculate accurate recharge rates for shallow parts of the glacial drift aquifer. Multiple data sets that define temporal trends in tritium concentration in the aquifer would be required to obtain the more precise age estimates needed for accurate estimation of recharge rates.

Temporal Variability of Water Quality at Selected Wells

To examine temporal variations in water quality and surface-water/ground-water interactions in the glacial drift aquifer, data recorders were installed at several wells at WPAFB. The earliest recorder data were obtained from well GR-320, a shallow well adjacent to the Mad River (site CL-3 on fig. 42). Specific conductance, pH, temperature, and concentrations of DO were measured hourly from August 22, 1989 to September 7, 1989 by means of sensors connected to a digital data recorder. Measured pH and specific conductance (7.1 and 650 µS/cm, respectively) were similar to those recorded during water-quality sampling in June and July 1991 (7.6 and 629 µS/cm, respectively; table 14) and remained constant during the recording period despite a significant rainfall event (0.63 in. during a 3-hour period on August 24, 1989). Temperature fluctuated only slightly ($\pm$ 0.1°C) throughout the 2-week recording period. The most notable difference between the 1989 recorder data and the June-July 1991 water-quality data was with respect to the DO concentration, which averaged nearly 7 mg/L during the 2-week recording period. This value is near saturation with respect to atmospheric oxygen at this temperature and is significantly higher than the <0.5 mg/L recorded during pumping of the well for water-quality sampling. The high concentration probably reflects diffusion of atmospheric oxygen into standing water of the well. Fluctuations of DO concentration and pH were steady, and minor fluctuations were within the precision of the instruments. As with the specific conductance and temperature data, however, no variations in pH or DO that could be related to precipitation events were noted over the recording period.

Recorders were installed at five observation wells in April 1991 to acquire information about the effects of recharge to shallow parts of the unconsolidated aquifer and (or) recharge from bedrock-valley walls on a seasonal and annual basis. Temperature and specific conductance were monitored at five wells; water levels were measured with calibrated pressure transducers in two of the five instrumented wells. The types of data collected at each location are given in the following table:

Well number	Cluster	Depth (feet)	Data collected		
			Temperature	Specific conductance	Water level
GR-332	6	195	X	X	X
GR-330	6	49.5	X	X	X
GR-324	5	128	X	X	
GR-322	4	147	X	X	
GR-319	2	160	X	X	

The sensors and recorders were installed April 16-18, 1991; plots of temperature and specific conductance recorded through April 30, 1992, for each of the five wells are shown in figures 55 and 56, respectively. Gaps in the line plots on figure 55 indicate periods of no data, whereas the distinct square and triangle-shaped spikes (particularly notable in the records for GR-319 and GR-332) are instrument-induced variations of unknown cause.

Temperature data for the four deep wells (clusters 2, 4, 5, and 6) do not display any significant trends and are constant within the precision of the temperature probe ($\pm 0.2^{o}C$) at 13.2, 12.4, 12.0, and 12.4°C, respectively (fig. 55). In contrast, water temperatures in the shallow well (GR-330) appeared to respond to seasonal variations in air temperature; peak mean daily temperatures (13.8°C) recorded from April to August declined steadily to 13.2°C by early January and then rose to 13.4°C in April 1992. As noted in the methods section, the average ground-water temperature recorded by the downhole sensors at each of the five wells is approximately 2.0 degrees lower than temperatures recorded at the surface during water-quality sampling. This difference is attributed to heating of the polypropylene tubing used to connect the pump outlet to the flowthrough cell in which temperature was measured.

Specific-conductance data for two of the deep wells (GR-322, GR-324) are constant over the entire recording period within the accuracy of the specific-conductance sensors (accuracy of the specific conductance sensors is estimated at ± 3 percent, which yields an uncertainty of ± 20 µS/cm if specific conductance of ground water is 650 µS/cm). Sharp rises (spikes) in specific conductance followed by declines to a relatively constant specific conductance (near 650 µS/cm) were noted in well GR-319 after initial emplacement of the sensor in April 1991 and after water-quality sampling in June 1991 (fig. 56). The cause of the large spikes is unknown, but these spikes (and similar but smaller spikes in GR-330) may be related to the effects of ground-water sampling activities on the specific-conductance sensor. A gradual increase from approximately 630 µS/cm in January 1992 to 670 µS/cm at the end of April 1992 may be related to the intrusion of more concentrated winter recharge waters at this depth in the aquifer; however, additional data would be required to confirm this hypothesis. Specific conductance declined in the shallow well (GR-330) by approximately 100 µS/cm from April 1991 to February 1992 in conjunction with declining temperature and water levels. This decline may represent a lag effect of approximately 4 to 5 months between introduction of road-salt-contaminated recharge water and transport to this location in the aquifer. However, water-quality data are insufficient to test this hypothesis.

Water-level data for the shallow and deep wells of cluster 6 (GR-330 and GR-332) indicate generally declining water levels from April 1991 through April 1992 (fig 57). The water-level decline for both wells was approximately 4 ft, and the head difference between the two wells remained relatively constant at approximately 2.5 ± 0.25 ft. Water levels in the wells appear not to have responded to major recharge events. The hydraulic gradient inferred from the water-level data at these two wells indicates that ground-water flow in the vicinity of cluster 6 is upwards. The observed upward hydraulic gradient may be caused by recharge from the adjacent bedrock topographic highs to the deep part of the aquifer, perhaps through a localized fracture zone.

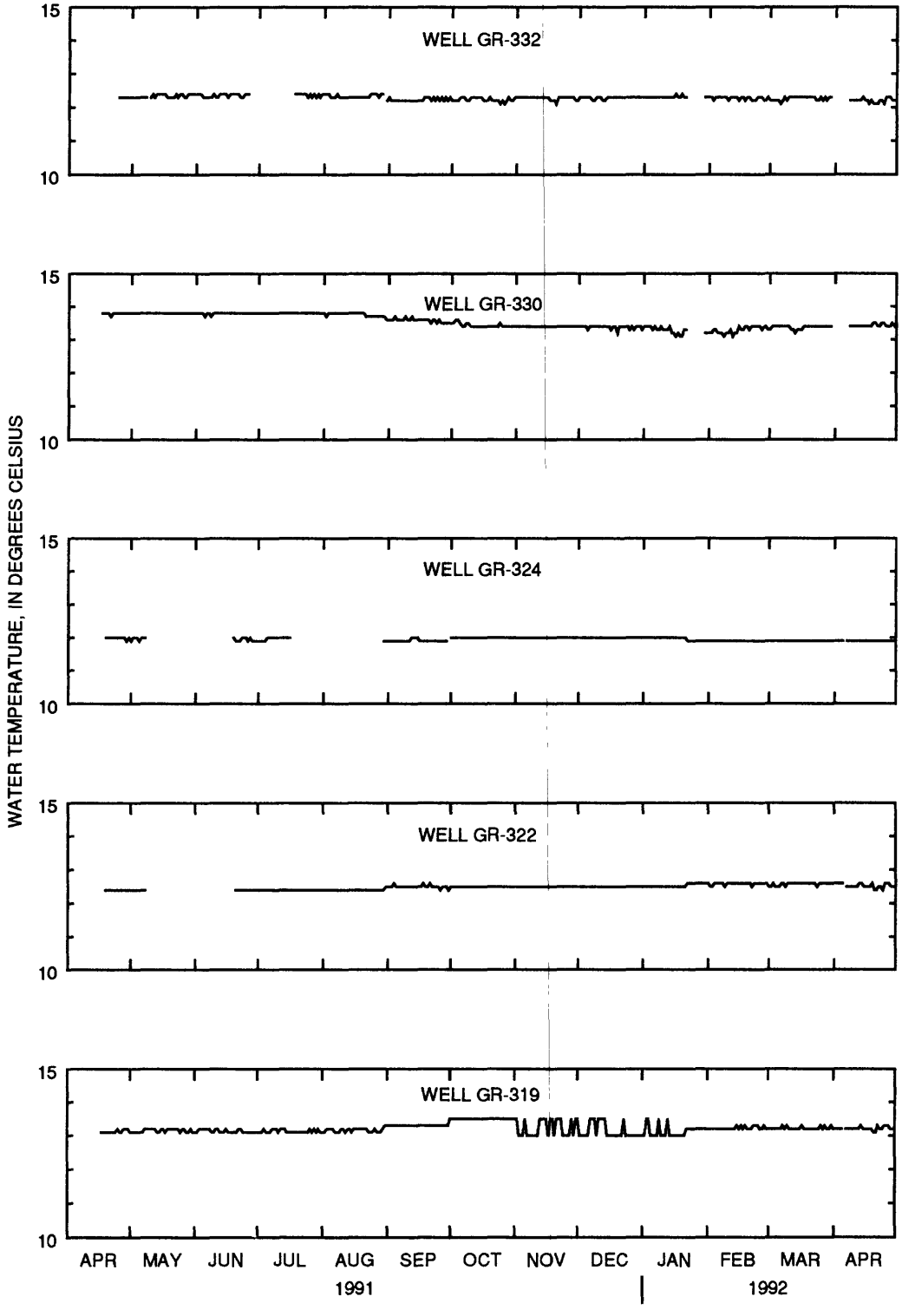

Figure 55.--Temperature of ground water in selected wells at Wright-Patterson Air Force Base, April 1991-April 1992.

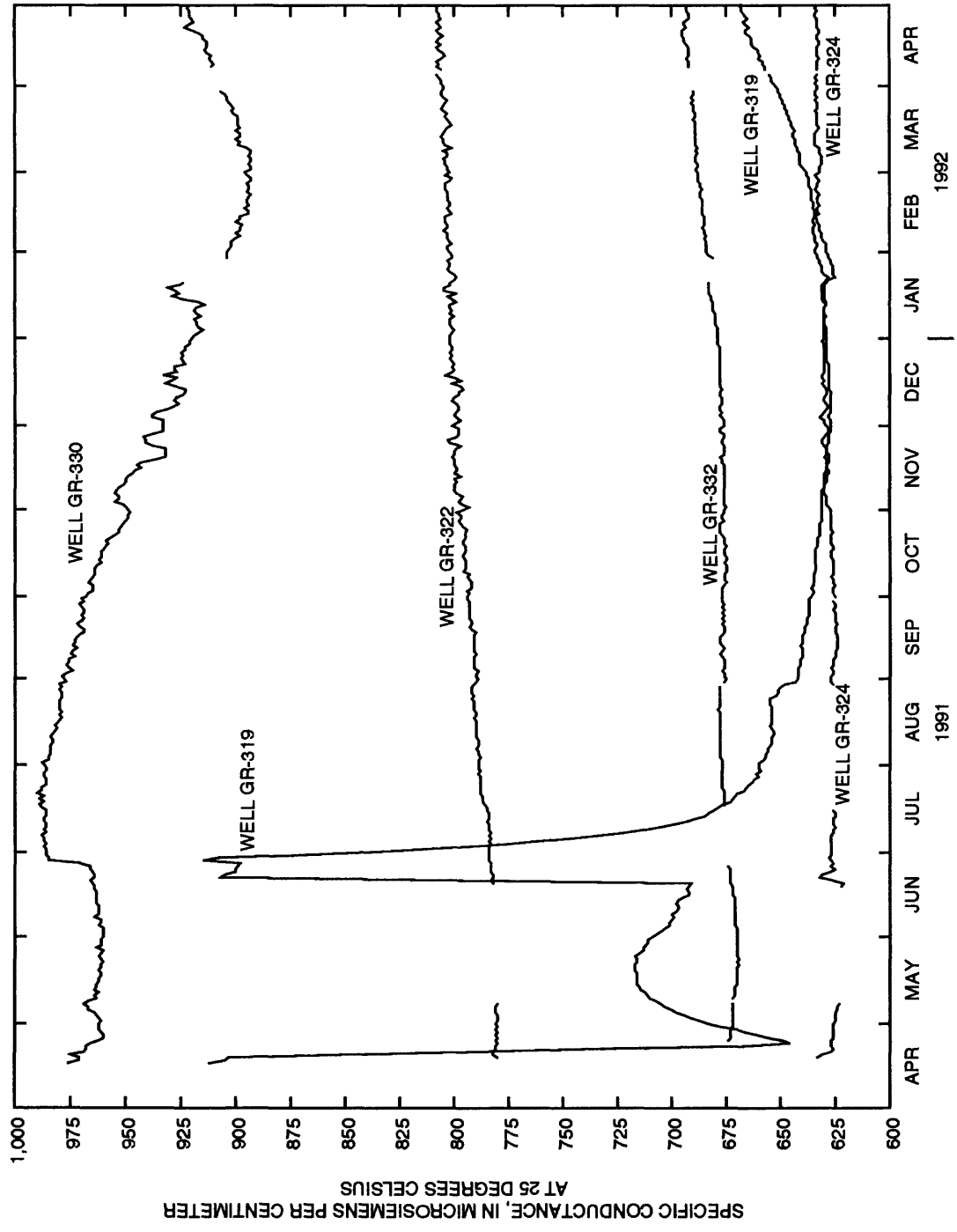

Figure 56.--Specific conductance of ground water in selected wells at Wright-Patterson Air Force Base, April 1991-April 1992.

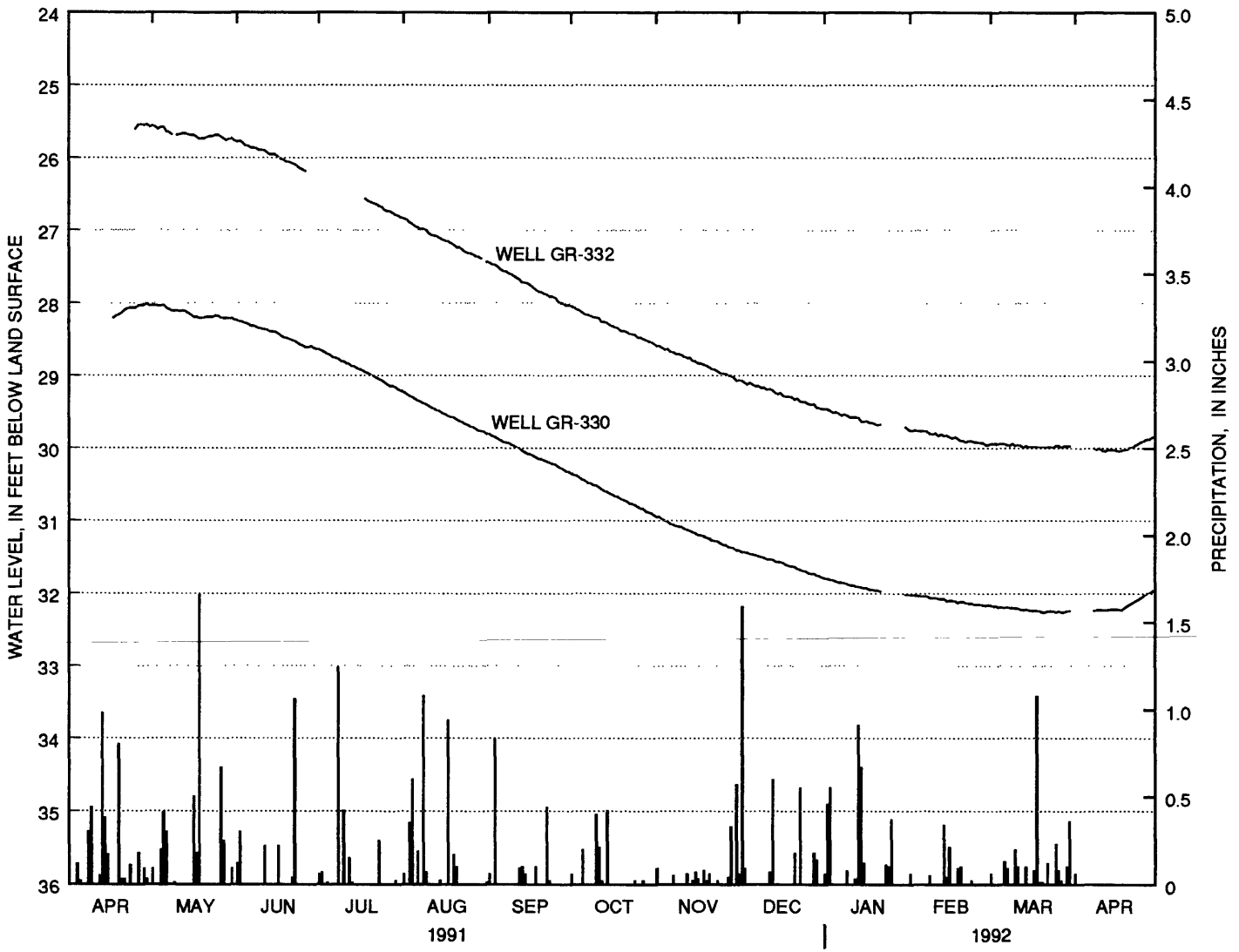

Figure 57.--Water-level data for wells GR-332 and GR-330 and precipitation data at Wright-Patterson Air Force Base, April 1991-April 1992.

SUMMARY AND CONCLUSIONS

Ground water is the primary source of water in Clark, Greene, and Montgomery Counties. Wright-Patterson Air Force Base (WPAFB), located along the Mad River Valley where the three counties join, overlies an aquifer that consists of valley-train deposits (glacial sands and gravels) that fill a buried bedrock-valley system.

Most of the consolidated rocks in the region consist of poorly permeable shales, although in part of the upland areas, the moderately permeable Brassfield Limestone is present. Before the Pleistocene Epoch, the bedrock in the region was extensively eroded, and many valleys formed. During the Pleistocene Epoch, these valleys were filled with Wisconsinan glacial sediments. These glacial deposits consist of clay-rich tills and coarse-grained outwash deposits. Although the tills are poorly permeable, the sands and gravels of the outwash deposits are the most productive aquifers in the region, yielding as much as 2,000 gal/min to wells.

Hydraulic conductivities reported from pumped-well aquifer tests in the unconsolidated deposits range from less than 1 to 2,500 ft/d; corresponding transmissivities range from 2,140 to 37,400 ft^2/d. Hydraulic conductivities determined from slug tests on wells in the sands and gravels at WPAFB range from less than 1 to more than 1,000 ft/d. Estimates of the hydraulic conductivity of the bedrock from slug tests on wells at WPAFB range from 0.0016 to 12 ft/d.

Ground water flows from the uplands towards the valleys and the major rivers in the region, the Great Miami and the Mad Rivers. In the valleys, ground water flows towards the rivers and downgradient through the valleys. In the Fairborn area, east of WPAFB, flow in the valley is towards the Mad River and Huffman Dam. Southeast of the dam, ground-water flow is toward either the Mad or the Great Miami River and southeast through the valley or to well fields. Hydraulic-head data indicate that flow may occur between the bedrock and unconsolidated deposits. The direction of this flow varies from site to site; however, the volume is negligible compared to the flow within the unconsolidated deposits.

Data from a gain/loss study (a series of discharge measurements) of the Mad River and selected tributaries reveal that streams within the study area are either gaining or losing water. The data, although not conclusive, suggest that the Mad River is gaining water from I-70 to Huffman Dam. The greatest loss of water occurred on the Mad River between Huffman Dam and Harshman Road, the reach that flows past the well field at Rohrer's Island. Hebble Creek lost water along its whole length.

Water-level data from four wells on the Base, near the Mad River, show consistent upward gradients, indicating that the area is a discharge area for the aquifer. In this area, the shale bedrock is probably within 10 ft of the riverbed. One of the four wells is completed in the shale. The hydrograph for this well is similar to that for a nearby shallow well completed in the sands and gravels. The similarity in water-level records indicates that, in this area, the bedrock may be fractured or weathered enough to respond hydrologically in the same manner as do the glacial deposits.

A steady-state, three-dimensional, 3-layer flow model of the ground-water system beneath WPAFB and vicinity was constructed to help understand the flow system and to determine horizontal directions of flow in the region. The modeled area encompasses about 100 mi^2 and is centered on WPAFB. Model boundaries, designated as no-flow or constant-flux, were designed to coincide with natural hydrologic boundaries near the edges of the study area. Spatial variations in transmissivity, recharge, and pumping were incorporated into the model.

The model simulates steady-state conditions, based on water levels and hydraulic gradients measured from October to December 1987 and river discharges measured in 1991. The RMSE between simulated and observed heads in layer 1 was 9.4 ft, and AAHD was 7.5 ft. Simulated discharges to streams in the study area were in general agreement with measured discharges. Simulated head gradients approximated observed gradients in recharge (downward flux) and discharge (upward flux) areas in the valley-train deposits. The simulated mass-balance error in the modeled area was zero. Ground water enters the modeled area primarily by river leakage (52 percent), boundary flux (29 percent), and precipitation (19 percent); ground water exits the modeled area primarily by boundary flux (45 percent), production wells (35 percent), and river leakage (20 percent). An analysis involving systematic changes of hydrologic parameters in the model indicated that simulated hydraulic heads are most sensitive to decreases in riverbed conductance and vertical conductance and are also highly sensitive to changes in the hydraulic conductivity of layer 1. The sensitivity analysis also indicates that the contribution of water to the buried-valley aquifer from the bedrock that forms the valley walls is about 2 to 4 percent of the total ground-water flow in the modeled area.

Ground-water in the vicinity of Wright-Patterson Air Force Base is classified into two compositional groups based on dominant cation and anion concentrations: (1) calcium magnesium bicarbonate waters and (2) sodium chloride waters. Calcium magnesium bicarbonate-type waters are found in wells completed in the unconsolidated glacial deposits and in the Brassfield Limestone, whereas sodium chloride waters are exclusively associated with shale-rich bedrock strata.

The calcium magnesium bicarbonate-type waters are slightly alkaline, very hard, and commonly anoxic. Concentrations of dissolved iron and manganese in sampled waters commonly exceeded OEPA SMCL's set for iron and manganese. Equilibrium speciation calculations indicate that ground water of the glacial drift aquifer is in equilibrium with calcite, dolomite, and chalcedony, but is undersaturated with respect to gypsum and fluorite. Siderite equilibria does not appear to control dissolved-iron concentrations in the glacial drift aquifer.

Samples of shallow ground water from the glacial drift aquifer contained elevated concentrations of sodium, chloride, sulfate, and nitrate that are related to human activities that alter the composition of precipitation-derived recharge and shallow ground water. Significantly lower median sodium and chloride concentrations in water from deeper parts of the glacial aquifer indicates that recharge to these parts of the aquifer occurs relatively slowly.

Wells completed in the shale bedrock yield sodium chloride waters. Dissolved solids concentrations in these moderately saline waters exceeded OEPA SMCL's and concentrations of iron, manganese and fluoride generally exceeded the SCML's. Sodium chloride waters also contained elevated boron concentrations. These waters were slightly supersaturated with respect to calcite, dolomite, and siderite but were undersaturated with respect to chalcedony. Fluorite does not appear to control fluoride concentrations. Simple mass-balance calculations treating boron as a conservative species indicate that little (< 5 percent) or no recharge from the shale bedrock to the glacial drift aquifer is occurring.

Stable-isotope data for hydrogen and oxygen indicate a meteoric origin for all ground water beneath WPAFB, but the data were inconclusive with respect to identification of distinct isotopic differences between ground water collected from the glacial drift and bedrock aquifers. Tritium concentrations, used to distinguish waters having a pre- and post-1953 recharge component, indicate that most water entered the glacial drift aquifer after 1953. This finding indicates that recharge from shallow to deep parts of the aquifer occurs over time intervals of a few years or decades. However, the fact that some deep parts of the glacial aquifer did not contain measurable tritium indicates that ground-water flow from recharge zones to these parts of the aquifer takes decades or longer. Ground water collected from wells screened in the Brassfield formation did contain tritium; therefore, indicating that recharge to the Brassfield strata probably occurred over a time scale of a few years to a few decades. The absence of tritium in ground water collected from wells completed in the Ordovician shales indicates very slow recharge rates, an observation consistent with the inferred low permeability of the shale bedrock.

REFERENCES CITED

Ball, J.W., and Nordstrom, D.K., 1991, User's manual for WATEQ4F, with revised thermodynamic data base and tese cases for calculating speciation of major, trace, and redox elements in natural waters: U.S. Geological Survey Open-File Report 91-183, 189 p.

Back, W., Hanshaw, B.B., Plummer, L.N., Rahn, P.H., Rightmire, C.T., and Rubin, M., 1983, Process and rate of dedolomitization-mass transfer and ^{14}C dating in a regional carbonate aquifer: Geological Society of America Bulletin, v. 94, p. 1415-1429.

Bouwer, Herman, 1978, Groundwater hydrology: New York, McGraw-Hill, p. 38.

Bouwer, Herman, and Rice, R.C., 1976, A slug test of determining hydraulic conductivity of unconfined aquifers with completely or partially penetrating wells: Water Resources Research, v. 12, no. 3, p. 423-428.

Bradbury, K.R., and Muldoon, M.A., 1990, hydraulic conductivity determinations in unlithified glacial and fluvial materials; in Nielsen, D.M., and Johnson, A.I., eds., Ground water and vadose zone monitoring: Philadelphia, American Society for Testing and Materials, ASTM STP 1053, p. 138-151.

Breen, K.J., 1988, Geochemistry of the stratified-drift aquifer in Killbuck Creek Valley, west of Wooster, Ohio, *in* Randall, A.D., and Johnson, A.I., eds., Regional aquifer systems of the United States—the northeast glacial aquifers: American Water Resources Association Monograph Series, no. 11, p. 105-131.

Busby, J.F., Plummer, L.N., Lee, R.W., and Hanshaw, B.B., 1991, Geochemical evolution of water in the Madison aquifer in parts of Montana, South Dakota, and Wyoming: U.S. Geological Survey Professional Paper 1273-F, 89 p.

Craig, H., 1961, Isotopic variations in meteoric waters: Science, v. 133, p. 1702-1703.

Cross, W.P., and Feulner, A.J., 1964, Anomalous streamflow–ground-water regimen in the Mad River basin, near Springfield, Ohio: Article 166 *in* U.S. Geological Survey Professional Paper 475-D, p. D198-D201.

Cunningham, W.L., 1992, Hydrogeology and simulation of ground-water flow at the South Well Field, Columbus, Ohio: Columbus, Ohio, The Ohio State University, Master's thesis, 154 p.

Dames & Moore, Incorporated, 1986a, Installation Restoration Program report, site investigation report—landfills 8 and 10: Prepared for Wright-Patterson Air Force Base [variously paginated].

——— 1986b, Installation Restoration Program report, site investigation report—landfill 12. Prepared for Wright-Patterson Air Force Base [variously paginated].

Davis, P.E., Lerch, Norbert, Tornes, Larry, Steiger, Joseph, Smeck, Neil, Andrus, Howard, Trimmer, John, and Bottrell, George, 1976, Soil survey of Montgomery County, Ohio: U.S. Department of Agriculture, 107 p., 83 sheets, scale 1:15,840.

de Roche, J.T., and Breen, K.J., 1989, Hydrogeology and water quality near a solid- and hazardous-waste landfill, Northwood, Ohio: U.S. Geological Survey Water-Resources Investigations Report 88-4093, 76 p.

Dumouchelle, D.H., 1992, Altitude of top of bedrock in the vicinity of Wright-Patterson Air Force Base, Ohio: U.S. Geological Survey Water-Resources Investigations Report 92-4072, 1 sheet, scale 1:53,300.

Dumouchelle, D.H., and de Roche, J.T., 1991, Lithologic, natural-gamma, grain-size, and well-construction data for Wright-Patterson Air Force Base, Ohio: U.S. Geological Survey, Open-File Report 91-181, 94 p.

Durfor, C.N., and Becker, Edith, 1964, Public water supplies of the 100 largest cities in the United States, 1962: U.S. Geological Survey Water-Supply Paper 1812, 364 p.

Dysart, Joel., 1988, Use of oxygen-18 and deuterium mass-balance analysis to evaluate induced recharge to stratified-drift aquifers, *in* Randall, A.D., and Johnson, A.I., eds., Regional aquifer systems of the United States—the northeast glacial aquifers: American Water Resources Association Monograph Series, no. 11, p. 133-156.

Engineering-Science, Incorporated, 1982, Installation Restoration Program report, Phase 1—records search: Prepared for Wright-Patterson Air Force Base [variously paginated].

———1991, Standard operating procedures for ground-water sampling at Wright-Patterson Air Force Base: [variously paginated].

Enseco Incorporated, 1991, Analytical results for U.S. Geological Survey Enseco-RMAL: Arvada, Colo., analyses 015512, 015540, 015550, 015571, 015623, 015640, and 015675, issued July 8-18, 1991.

Environmental Research Systems Institute, 1987, ARC/INFO users guide: Redlands, Calif., Environment Research Systems Institute, [variosly paginated].

Evans, K.F., 1977, Water quality of the glacial-outwash aquifer in the Great Miami River Basin, Ohio: U.S. Geological Survey Water-Resources Investigations 77-76, 2 sheets.

Fenneman, N.M., 1938, Physiography of Eastern United States: New York, McGraw-Hill, p. 449-536.

Fetter, C.W., 1988, Applied hydrogeology (2nd ed): Merrill Publishing Company, Columbus, Ohio, 592 p.

Fidler, R.E., 1975, Digital model simulation of the glacial-outwash aquifer at Dayton, Ohio: U.S. Geological Survey Water-Resources Investigations 18-75, 25 p.

Franke, O.L., Reilly, T.E., and Bennett, G.D., 1987, Definition of boundary and initial conditions in the analysis of saturated ground-water flow systems—an introduction: U.S. Geological Survey Techniques of Water-Resources Investigations, book 3, chap. B5, 15 p.

Freeze, R.A., and Cherry, J.A., 1979, Groundwater: Englewood Cliffs, N.J., Prentice-Hall, 604 p.

Gale Research Company, 1989, Climate of the States—National Oceanic and Atmospheric Administration narrative summaries: Detroit, Mich., Gale Research Companty, p. 868.

Garner, D.E., Ritchie, A., and Siegenthaler, V.L., 1978, Soil survey of Greene County, Ohio: U.S. Department of Agriculture, 105 p., 53 sheets, scale 1:15,840.

Geraghty & Miller, Incorporated, 1987, Mad River well field assessment: Prepared for the City of Dayton [variously paginated].

Harstine, L.J., 1991, Hydrologic Atlas for Ohio—average annual precipitation, temperature, streamflow, and water loss for 50-year period, 1931-1980: Ohio Department of Natural Resources, Division of Water, Water Inventory Report 28, 12 p., 4 sheets.

Hazen, A., 1911, Discussion—dams and sand foundations: Transactions, American Society of Civil Engineers, 73, 199 p.

Hem, J.D., 1989, Study and interpretation of the chemical characteristics of natural waters (3d ed.), U.S. Geological Survey Water-Supply Paper 2254, 263 p.

Hoffman, M.S, ed., 1990, The World almanac and book of facts, 1991: New York, Pharos Books, p. 602.

International Atomic Energy Agency, 1981, Statistical treatment of environmental isotope data in precipitation: Technical Report Series, no. 206, 256 p.

IT Corporation, 1990, Installation Restoration Program report, environmental investigation of ground-water contamination at Wright-Patterson Air Force Base, Ohio: Dayton, Ohio, Battelle Environmental Management Operations, prepared for Wright-Patterson Air Force Base [variously paginated].

Langmuir, D., 1971, The geochemistry of some carbonate ground waters in central Pennslyvania: Geochimica et Cosmochimica Acta, v. 35, p. 1023-1045.

Lehman, S.F., and Bottrell, G.D., 1978, Soil survey of Miami County, Ohio: U.S. Department of Agriculture, 100 p., 59 sheets, scale 1:15,840.

Masch, F.E., and Denny, K.J., 1966, Grain size distribution and its effect on the permeability of unconsolidated sands: Water Resources Research, v. 2, no. 4, p. 665-677.

McDonald, M.G., and Harbaugh, A.W., 1988, A modular three-dimensional finite-difference ground-water flow model: U.S. Geological Survey Techniques of Water-Resources Investigations, book 6, chap. A1 [variously paginated].

Michel, R. L., 1989, Tritium deposition in the continental United States, 1953-1983: U.S. Geological Survey Water-Resources Investigations Report 89-4072, 46 p.

Moses C.O., Nordstrom, D.K., Herman, J.S., and Mills, A.L., 1987, Aqueous pyrite oxidation by dissolved oxygen and by ferric iron: Geochimica et Cosmochimica Acta, v. 51, p. 1561-1571.

National Oceanic and Atmospheric Administration, 1982, Monthly normals of temperature, precipitation, and heating and cooling degree days, 1951-80, Ohio: Asheville, N.C., National Climatic Center, Climatography of the United States 81, 16 p.

Nordstrom, D.K., Jenne, E.A., and Ball, J.W., 1979, Redox equilibria of iron in acid mine waters *in*: Jenne, E.A., ed., Chemical modeling of aqueous systems—Speciation, sorption, solubility, and kinetics: American Chemical Society Symposium Series 93, p. 51-79.

Nordstrom, D.K., and Ball, J.W., 1989, Mineral saturation states in natural waters and their sensitivity to thermodynamic and analytic errors: Scientific Geological Bulletin v. 42, no. 4, p. 269-280.

Norris, S.E., and Spieker, A.M., 1966, Ground-water resources of the Dayton area, Ohio: U.S. Geological Survey Water-Supply Paper 1808, 167 p.

Norris, S.E., Cross, W.P., and Goldthwait, R.P., 1948, The water resources of Montgomery County Ohio: Ohio Water Resources Board Bulletin no.12, 83 p.

———1950, The water resources of Greene County, Ohio: Ohio Department of Natural Resources, Division of Water Bulletin 19, 52 p.

Norris, S.E., Cross, W.P., Goldthwait, R.P., and Sanderson, E.E., 1952, The water resources of Clark County, Ohio: Ohio Department of Natural Resources, Division of Water Bulletin 22, 82 p.

Ohio Environmental Protection Agency, 1991, Rules and regulations, public water systems, 3745-81, primary contaminant control; 3745-82, secondary contaminant standards: Ohio Environmental Protection Agency [variously paginated].

Ohio Soil Survey, 1969, Supplement to the soil survey of Clark County, Ohio: U.S. Department of Agriculture, 27 p.

Petro, J.H., 1958, Soil survey of Clark County, Ohio: U.S. Department of Agriculture, 139 p., 6 sheets, scale 1:24,000.

Rantz, S.E., and others, 1982, Measurement and computation of streamflow—volume 1 measurement of stage and discharge: U.S. Geological Survey Water-Supply Paper 2175, p. 79-183.

Schalk, C. W., 1992, Ground-water levels and flow in the vicinity of Wright-Patterson Air Force Base, Ohio, October-December, 1987: U.S. Geological Survey Water-Resources Investigations Report 92-4022, 1 sheet, scale 1:46,980.

Shindel, H.L., Klingler, J.H., Mangus, J.P., and Trimble, L.E., 1989, Water resources data, Ohio, water year 1988: U.S. Geological Survey Water-Data Report OH-88-2, 204 p.

——— 1990, Water resources data, Ohio, water year 1989: U.S. Geological Survey Water-Data Report OH-89-2, 226 p.

——— 1991, Water resources data, Ohio, water year 1990: U.S. Geological Survey Water-Data Report OH-90-2, 281 p.

———1992, Water resources data, Ohio, water year 1991: U.S. Geological Survey Water-Data Report OH-91-2, 430 p.

Stout, Wilbur, 1941, Dolomites and limestones of western Ohio: Geological Survey of Ohio, Bulletin 42, 468 p.

Thatcher, L.L., 1962, The distribution of tritium fallout in precipitation over North America: Bulletin of the International Association of Scientific Hydrology, v. 7, no. 2, p. 48-58.

Veley, R.J., 1993, Estimated water use in Ohio, 1993—public-supply data: U.S. Geological Survey Open-File Report 93-72 (Water Fact Sheet), 2 p.

Walton, W.C., and Scudder, G.D., 1960, Ground-water resources of the valley-train deposits in the Fairborn area, Ohio: Ohio Department of Natural Resources, Division of Water Technical Report 3, 57 p.

Wang, H.F., and Anderson, M.P., 1982, Introduction to groundwater modeling: New York, W.H. Freeman and Company, 237 p.

Weiner, W.F., and Koster Van Groos, A.F., 1976, Petrographic and geochemical study of the formation of chert around the Thornton reef complex, Illinois: Geological Society of America Bulletin, v. 87, p. 310-318.

Weston, Roy F., Incorporated, 1983, Installation Restoration Program report, Phase II—problem confirmation and quantification study: Prepared for Wright-Patterson Air Force Base [variously paginated].

——— 1985, Installation Restoration Program report, Phase II—Stage 1 study: Prepared for Wright-Patterson Air Force Base [variously paginated].

——— 1989, Installation Restoration Program report, stage 2 report: Prepared for Wright-Patterson Air Force Base, 3 v. [variously paginated].